UNIVERSITAT DE BARCELONA

Cell-extrinsic barriers of cellular plasticity: contribution of natural killer cells, T lymphocytes and vitamin B12 to *in vivo* reprogramming

Elena Meléndez Esteban

CELL-EXTRINSIC BARRIERS OF CELLULAR PLASTICITY: CONTRIBUTION OF NATURAL KILLER CELLS, T LYMPHOCYTES AND VITAMIN B12 TO IN VIVO REPROGRAMMING

ELENA MELÉNDEZ ESTEBAN

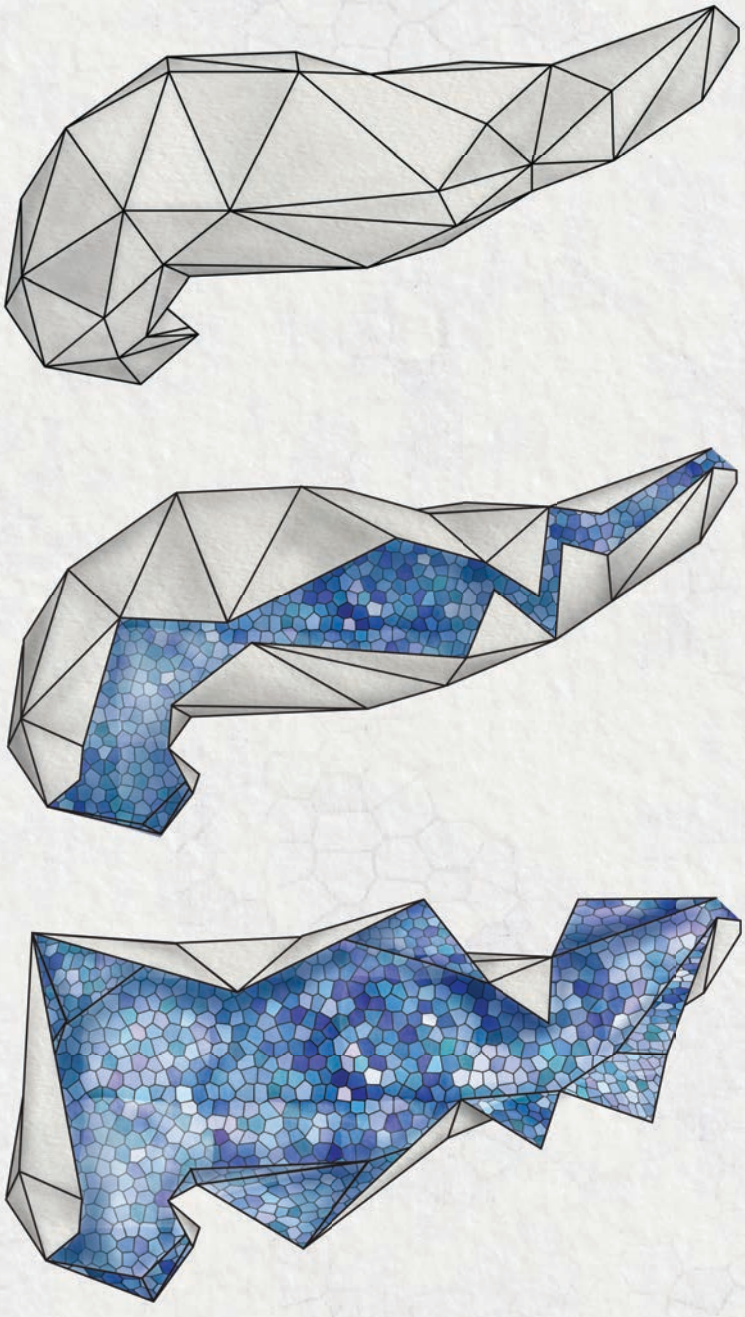

DOCTORAL THESIS

CELL-EXTRINSIC BARRIERS OF CELLULAR PLASTICITY: CONTRIBUTION OF NATURAL KILLER CELLS, T LYMPHOCYTES AND VITAMIN B12 TO *IN VIVO* REPROGRAMMING

DOCTORAL THESIS

Programa de Doctorat en Biomedicina

Memòria presentada per l'**Elena Meléndez Esteban** per optar al grau de doctora per la Universitat de Barcelona.

El treball presentat en aquesta tesi ha sigut realitzat al laboratori de Cellular Plasticity and Disease de l'Institut de Recerca Biomèdica de Barcelona, sota la direcció i supervisió del **Dr. Manuel Serrano Marugán**.

Barcelona, 2022

Dr. Manuel Serrano Marugán	**Dr. Antonio Zorzano Olarte**	**Elena Meléndez Esteban**
Thesis Director	Thesis Tutor	PhD student

Acknowledgments

I would like to thank Manuel Serrano for the opportunity to conduct this exciting research in his laboratory, for his support and encouragement, and for creating a fantastic laboratory environment in which to learn and grow as a researcher.

I would like to thank all of the Serrano lab members for their scientific insight, advice, assistance, and eagerness to gather at La Bolera for a cold beer every week. You have become part of my family, thanks!

I would like to thank all of the fantastic core facilities at the IRB Barcelona I have had the pleasure to work with throughout the years, specially the Histopathology Facility, the Mass Cytometry Facility and the Animal Facility.

Last but not least, I would also like to thank my family and my friends for their love and constant support.

THANK YOU

Summary

The ectopic expression of transcription factors Oct4, Sox2, Klf4 and Myc (OSKM) enables the conversion of differentiated cells into pluripotent stem cells, a process known as "reprogramming". Methods based on *in vivo* reprogramming are a promising strategy for tissue regeneration and rejuvenation. However, this process is inefficient, and little is known about the barriers that limit reprogramming in an *in vivo* context.

Here we have explored how the immune system affects cellular reprogramming. We report that natural killer (NK) cells significantly limit reprogramming. Cells in the process of reprogramming upregulate the expression of NK-activating ligands, such as *Mult1*, *Icam1* and *Cd155.* NK cells recognize and kill cells undergoing reprogramming in a degranulation-dependent manner that is partially blocked by antibodies against the NK-activating receptor NKG2D. In mice, transient depletion of NK cells using antibodies significantly improves the efficiency of reprogramming, as determined by the emergence of dysplastic cells and $NANOG^+$ cells. Finally, organoids derived from NK-depleted reprogrammed pancreata are remarkably large, suggesting that NK cells preferentially target those cells with high organoid-formation capacity. Other cell types from the innate immune system also contribute to the modulation of *in vivo* reprogramming efficiency. In particular, $Gr1^+$ cells, which include neutrophils and myeloid-derived suppressor cells (MDSCs), favour reprogramming, which is in contrast to the negative effect of NK cells. We have also explored the adaptive immune system. Interestingly, $CD4^+$ and $CD8^+$ T cells restrict reprogramming, thereby suggesting that reprogramming elicits an antigenic response to self-antigens. As a first step to study this notion, we have obtained the MHC-I immunopeptidome of partially reprogrammed fibroblasts. Intriguingly, we have found novel peptides not known to be presented by normal cells and tissues and, therefore, with the potential to be self-antigenic. We have also studied the role of vitamin B12 in reprogramming. Genomic analysis of stool bacteria led us to identify vitamin B12 as a limiting metabolite for reprogramming. Remarkably, vitamin B12 supplementation significantly improves the efficiency of the process both *in vivo* and *in vitro*. This finding has led us to uncover the limiting role of the one-carbon metabolism during reprogramming.

We conclude that NK cells are a main barrier for *in vivo* reprogramming, and their transient depletion facilitates the generation of cells with progenitor properties. Partial reprogramming elicits an adaptive immune response that may involve the presentation of peptides that are not presented by normal cells and tissues. Furthermore, vitamin B12 can act as a safe and easily administered metabolite to improve *in vivo* reprogramming. Our current findings may apply to other contexts of tissue regeneration.

Table of contents

Abbreviations

1C	One Carbon
5,10-methyl-THF	5,10-methylenetetrahydrofolate
5-methyl-THF	5-methyltetrahydrofolate
AA	Amino Acid
AAV	Adeno-Associated Viruses
ADCC	Antibody-Dependent Cell-mediated Cytotoxicity
ADM	Acinar-to-Ductal Metaplasia
Ag	Antigen
AHCY	Adenosylhomocysteine
AP	Alkaline Phophatase
APC	Antigen-Presenting Cell
ASC	Adult Stem Cell
BM	Bone Marrow
BrdU	BromodeoxyUridine or 5-Bromo-2'-deoxyUridine
CD107a/LAMP-1	Lysosomal-Associated Membrane Protein-1
CDK	Cyclin-Dependent Kinase
CER	Caerulein
CLP	Common Lymphoid Progenitor
CMP	Common Myeloid Progenitor
ConA	Concanamycin A
CPA1	Carboxypeptidase 1
CpG	C-phosphate-G
D	Day
DAMP	Damage Associated Molecular Patterns
DAPI	4 ',6-diamidino-2-fenilindol
DC	Dendritic Cell
DCLK1	Doublecortin-Like Kinase-1
DDA	Data-Dependent Acquisition
DMEM	Dulbecco's Modified Eagle's Medium
DNA	Deoxyribonucleic acid
DNAM-1	DNAX Accessory Molecule-1
DOX	Doxycycline
E	Embryonic Day
E:T	Effector:Target
E-cadherin	E-cadherin
EGC	Embryonic Germ Cell
EGFP	Enhanced Green Fluorescent Protein
EMT	Epithelial-to-Mesenchymal Transition
EPI	Epiblast
ER	Endoplasmic Reticulum
ESCs	Embryonic Stem Cells
F-class	Fuzzy-class of pluripotent cells
FCS	Fetal Calf Serum

FDR	False Discovery Rate
GAPDH	Glyceraldehyde-3-Phosphate Dehydrogenase
GSEA	Gene Set Enrichment Analysis
GSK3β	Glycogen Synthase Kinase 3 β
h	Hour
H2	Histocompatibility Antigen-2
H3K4me3	Tri-methylation at the 4th lysine residue of the histone H3 protein
H60	Histocompatibility 60
HA	Hemagglutinin
HE	Hematoxylin and Eosin
HNF1β	Hepatocyte Nuclear Factor 1 β
HSC	Hematopoietic Stem Cell
Hsp70	70 kilodalton heat shock protein
i4F	Induced 4 Factors
ICAM-1	Intracellular Adhesion Molecule 1
ICM	Inner Cell Mass
IFNγ	Interferon γ
IL-15	Interleukin 15
IL-2	Interleukin 2
IL-6	Interleukin 6
IL-9	Interleukin 9
ILC	Innate Lymphoid Cell
iPSCs	Induced Pluripotent Stem Cells
KEGG	Kyoto Encyclopedia of Genes and Genomes
Klf2	Kruppel-like factor 2
Klf4	Kruppel-like factor 4
Klf5	Kruppel-like factor 5
KLRG1	Killer cell Lectin-like Receptor G1
KRT19	Keratin, Type I cytoskeletal 19
KSR	Knockout Serum Replacement
LC-MS	Liquid Chromatography-Mass Spectrometry
LFA-1	Leukocyte Function-associated Antigen-1
LIF	Leukemia Inhibitory Factor
LMPP	Lymphoid-primed Multipotent Progenitor
LN	Lymph Node
LP	Liposomes
M157	Cytomegalovirus-encoded ligand 157
MAT2A	Methionine adenosyltrasnferase 2A
MDSC	Myeloid-Derived Suppressor Cell
MEF	Mouse Embryonic Fibroblast
mer	Number of residues in the peptide
MET	Mesenchymal-to-Epithelial Transition
Met	Methionine

mg	milligrams
MHC-I	Major Histocompatibility Complex class I
MHC-II	Major Histocompatibility Complex class II
min	Minutes
ml	Millilitres
mm	Millimeters
mM	Millimolar
mRNA	MessengeR-RNA
MS	Methionine Synthetase
MSC	Mesenchymal Stem Sells
MT	Methyltransferases
MULT	Murine UL16-binding Protein-Like Transcript 1
MUT	Methylmalonyl-CoA mutase
Myc	Myelocytomatosis viral oncogene
MyoD	Myoblast determination protein 1
Mϕ	Macrophage
NES	Normalized Enrichment Score
Neto2	Neuropilin and Tolloid like 2
Ngn3	Neurogenin 3
NK	Natural killer
NKG2D	Natural-killer receptor group2, member D
NON-B	Non-binder
NT	Neutrophil
OCT4	Octamer-binding Transcription Factor 4
OSKM	Oct4-Sox2-Klf4-cMyc
p21	Cyclin-dependent kinase inhibitor 1a
p53	Tumour protein p53
PAMP	Pathogen Associated Molecular Patterns
PCA	Principal Component Analysis
Pcae	acyl-alkyl-phosphatidylcholines
Pdx1	Pancreatic Duodenal Transcription Factor 1
PE	Primitive Endoderm
PGC	Primordial Germ Cells
POU	Pituitary Octamer Unc-86
Pparg	Peroxisome Proliferator-Activated Receptor gamma
PSC	Pluripotent Stem Cell
PTF1a	Pancreas Associated Transcription Factor 1a
qRT-PCR	Quantitave Reverse Transcription PCR
RAE1	Retinoic Acid Early Inducible-1
RNA	RiboNucleic Acid
RT	Room Temperature
rtTA	Reverse tetracycline-controlled transactivator
SAH	S-adenosylhomocysteine

SAM	S-adenosylmethionine
SASP	Senescence-Associated Secretory Phenotype
SB	Strong Binder
SCNT	Somatic Cell Nuclear Transfer
scRNAseq	Single cell RNA sequencing
Sen	Senescent
SOX2	Sex determining region Y-box 2
SOX9	Sex determining region Y-box 9
SSEA-1	Stage-Specific Embryonic Antigen-1
STAT3	Signal Transducer and Activator of Transcription 3
STMN1	Stathmin-1
T reg	T regulatory cell
TAP	Transporter associated with Antigen Processing
TCR	T-Cell Receptor
TE	Trophoectoderm
tetO	Tetracycline-Controlled Transcriptional Activation
TF	Transcription Factor
Tg	Transgenic
TNF	Tumor Necrosis Factor
TRAIL	TNF-Related Apoptosis-Inducing Ligand
TW	Transwell
U	Units
UMAP	Uniform Manifold Approximation and Projection
Wnt	Wingless-related integration site
WT	Wild-Type
βgal	β-galactosidase
µg	Micrograms
µl	Microlitres
µm	Micrometers
µM	Micromolar

Introduction

1. Cell potency throughout development

The mammalian development is a unidirectional process that comprises the formation of an adult organism from a single fertilized cell, the zygote. Achieving this requires a complex network of cellular decisions supervised by multiple regulatory layers (Leung and Zernicka-Goetz, 2015). Along development, cell potency, the capacity of a cell to differentiate into other cell types, progressively decreases. More than 60 years ago, Conrad Waddington proposed the model of "epigenetic landscape" to illustrate cell differentiation during development (Waddington, 1957). Using a metaphor, stem cells situated on top of a hill roll down segregating into different groves in the slope towards their final fate (**Figure 1**). Thus, zygote and their cleaved-cell products, the blastomeres, are placed on top of the hill as totipotent cells. While rolling down, they differentiate into both embryonic and extraembryonic lineages.

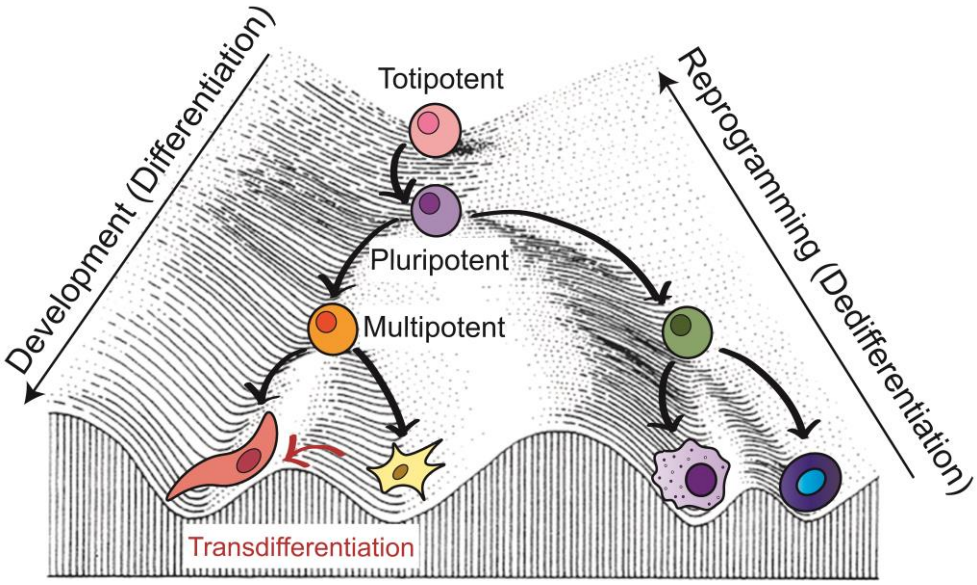

Figure 1 | Schematic representation of Waddington's epigenetic landscape model. During embryonic development, a totipotent cell "rolls" down to a landscape that is divided into different groves on a slope. Depending on the groove in which the cells falls, it will acquire different cell fates. During cellular reprogramming, a differentiated cell "rolls" from the bottom to the top of the hill, acquiring again pluripotent capacity. At this stage, it can be redifferentiated into another somatic cell type. During direct cell fate conversion, a tissue-specific cell converts into a related tissue-specific cells without going through a stable intermediate pluripotent state in a process called cell transdifferentiation.

The first cell fate decision of development occurs in the eight-cell stage, when blastomeres polarize within the morula leading to the formation of 2 different cell fates: the inner cell mass (ICM) and the trophectoderm (TE) (**Figure 2**). At embryonic stage E3.5,

the second cell fate decision occurs within the ICM, setting apart the primitive endoderm (PE) and the epiblast (EPI). The PE will develop into the extraembryonic yolk sac (Kunath *et al.*, 2005), and the EPI will give rise to the three germ layers of the embryo (endoderm, mesoderm and ectoderm) (Martin, 1981). The TE will generate the extraembryonic placenta (Tanaka *et al.*, 1998). At E4.5, the PE cells move to the cavity side of the ICM following the maturation of the blastocyst prior to implantation. Embryonic stem cells (ESCs) are obtained from the ICM cells of the blastocyst at E4.5 and are able to self-renew and to differentiate in the presence of different stimuli (Yamanaka *et al.*, 2006). After implantation, the crosstalk between embryonic and extraembryonic cells leads to the establishment of the anterior and posterior domains. The EPI grows into a cup-shaped epithelial tissue that flanks a luminal space, which gives rise to an elongated structure covered by the PE (Shahbazi and Zernicka-Goetz, 2018). From this moment, gastrulation is initiated and posterior EPI cells undergo epithelial-to-mesenchymal transition (EMT) to form the mesoderm, the endoderm and the primordial germ cells.

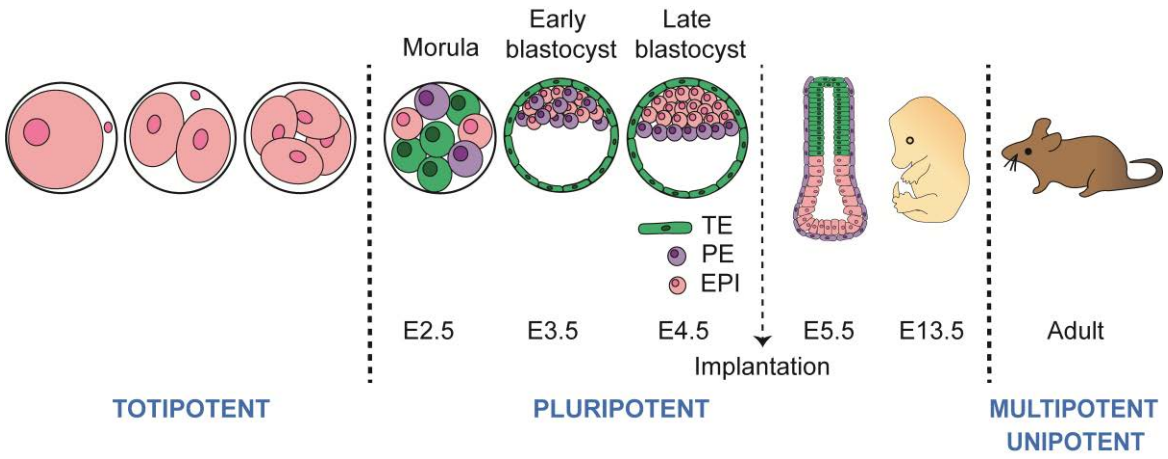

Figure 2 | Overview of mouse embryonic development. Representation of the different stages of the embryo development in mouse, from the totipotent stage to the adult organism. The first fate decision takes place at the eight-cell stage (E2.5), when the inner cell mas (ICM) and the trophectoderm (TE) are formed. At the early blastocyst stage (E3.5), the primitive endoderm (PE) and the epiblast (EPI) are generated from the ICM. After implantation (E5.5), the anterior and the posterior domains of the embryo are formed in the gastrulation process. Development continues until the formation of the adult organism, which contains multipotent or unipotent adult stem cells (ASCs), depending on their potential.

In the adult organism, cell potency is dramatically reduced and tissues are mainly formed by terminally differentiated and specialized cells. Nevertheless, some tissues are composed by cells with different degrees of differentiation potential, being adult stem cells (ASCs) at the top of the hierarchy of lineage commitment. ASCs self-renew and are

classified as either multipotent, if they differentiate into cells of a specific tissue, or unipotent, if they give rise to a single cell type (Snippert and Clevers, 2011). Upon terminal differentiation, cells loss their developmental potential and acquire specific functions that constitute the main core of adult tissues.

2. Induction of pluripotency: cellular reprogramming

Hallmark studies in the last years have further expanded the boundaries of cell plasticity. Somatic cells can be reprogrammed to pluripotency in a process called cellular reprogramming. Moreover, cell fates can be converted between related lineages within the same germ layer in the process of cellular transdifferentiation (**Figure 1**). These advances have given rise to a non-hierarchical model of cell fate transition in which cell fates have multiple possible directions (Moris, Pina and Arias, 2016).

2.1. History of cellular reprogramming

The milestones of cellular reprogramming were set up more than 70 years ago, when Robert Briggs and Thomas King described the technique of somatic cell nuclear transfer (SCNT) (Briggs and King, 1952) (**Figure 3**). Using this method in the Northern leopard frog (*Rana pipiens*), the authors were able to generate tadpoles by replacing the nuclei of enucleated oocytes with the nuclei of blastomeres. Similarly, in 1958, John Gurdon used the African clawed frog (*Xenopus laevis*) to prove that the nuclei of differentiated somatic cells, such as the ones from tadpoles just before hatching, could give rise to adult frogs when introduced in an enucleated oocyte (Gurdon, 1962b, 1962a). All the generated adult organisms were genetically identical to the donor of the original parental cell. This experiment proved that nuclei of differentiated cells retain the capacity to coordinate the formation of a fully functioning organism, thus suggesting that the restriction in cell potency that occurs during development is imposed by reversible epigenetic mechanisms. In the following years to that experiment, the transfer of the nucleus of an adult epithelial cell to an enucleated oocyte was used to generate Dolly the sheep, the first evidence of SCNT in mammals (Campbell *et al.*, 1996). In 1983, cell fusion of a mouse muscle cell with a human ammiocyte (fetal cell present in the amniotic fluid) induced in the re-expression of silenced human muscle-specific genes. The resulting cell was called heterokaryon and contained both human and mouse nuclei (Blau, Chiu and Webster, 1983) (**Figure 3**). Others reported that fusion of pluripotent stem cells (PSCs), such as embryonic germ cells (EGCs) (Tada *et al.*, 1997) or ESCs (Tada *et al.*, 2001), with somatic differentiated cells resulted in the epigenetic reprogramming of the latest. This suggested

the existence of key factors produced in pluripotent cells that were able to direct cell fate by regulating gene expression in somatic cells.

Further evidence of the existence of reprogramming factors came from a study in 1987 in which mouse fibroblasts were converted into myoblasts by introducing a single transcription factor (TF), the myoblast determination protein (MyoD) (Davis, Weintraub and Lassar, 1987). Years later, similar transdifferentiation processes were achieved: *Gata1* overexpression converted myeloblasts in megakaryocyte and erythrocyte precursors (Kulessa, Frampton and Graf, 1995), *C/EBPα* overexpression transformed B lymphocytes to macrophages (Xie *et al.*, 2004), and *MafA*, *Ngn3* and *Pdx1*genes expression converted acinar cells into pancreatic β-cells (Zhou *et al.*, 2008). Furthermore, fibroblasts have been transdifferentiated to cardiomyocytes (Ieda *et al.*, 2010), neurons (Vierbuchen *et al.*, 2010) and hepatocytes (Huang *et al.*, 2011) using specific TFs. All these studies provided strong evidence that TFs are master regulators of cell identity.

The confluence of the knowledge derived from all these works led to a breakthrough discovery in 2006, when Takahashi and Yamanaka demonstrated that terminally differentiated cells could be converted into PSCs by the ectopic expression of 4 *bona fide* reprogramming factors: octamer-binding transcription factor 4 (OCT4), sex determining region Y-box2 (SOX2), Krüppel-like factor 4 (KLF4) and c-MYC (hereafter referred to as OSKM or 4 Yamanaka factors) (Takahashi and Yamanaka, 2006). These resulting cells had ES-like properties and were named induced pluripotent stem cells (iPSCs) (**Figure 3**). The initial experiment was performed using fibroblasts as cells of origin. However, in the last years, many other cell types have been converted to iPSCs (Aasen *et al.*, 2008; Aoi *et al.*, 2008; Eminli *et al.*, 2008; Hanna *et al.*, 2008; Stadtfeld, Brennand and Hochedlinger, 2008). Moreover, OSKM successfully induces iPSCs in cells from different species, such as human (Takahashi *et al.*, 2007), monkey (Liu *et al.*, 2008) and rat (Liao *et al.*, 2009). These experiments proved that iPSCs can be obtained regardless of the cell type or specie of origin, which demonstrates the highly conserved nature of the pluripotency transcriptional network. The recent genome-editing technology CRISPR/Cas9 has also been used to achieve successful *in vitro* reprogramming (**Figure 3**). The targeting and activation of endogenous *Oct4* and *Sox2* gene locus in MEFs was sufficient to induce full pluripotency (Liu *et al.*, 2018).

Due to the oncogenic nature of some of the reprogramming TFs together with the ethical concerns that genome editing arise in society, several studies have focused on finding small molecules that replace the four Yamanaka factors (**Figure 3**). In 2013, the first example of fully chemical reprogramming was published (Hou *et al.*, 2013; Zhao *et al.*, 2015). Small molecules have the advantages of being cell permeable, easy to manipulate and they do not integrate into the genome. However, the reprogramming

process using this combination of drugs is slower and more inefficient than when using the OSKM method.

Nowadays, the different methods aimed to obtain iPSCs are considered valuable tools for treatments in regenerative medicine. The possibility of obtaining patient-specific iPSCs-derived cells to regenerate damaged tissues and organs is being extensively exploited, as it would overcome the immune-related rejections that occur upon allogenic transplants.

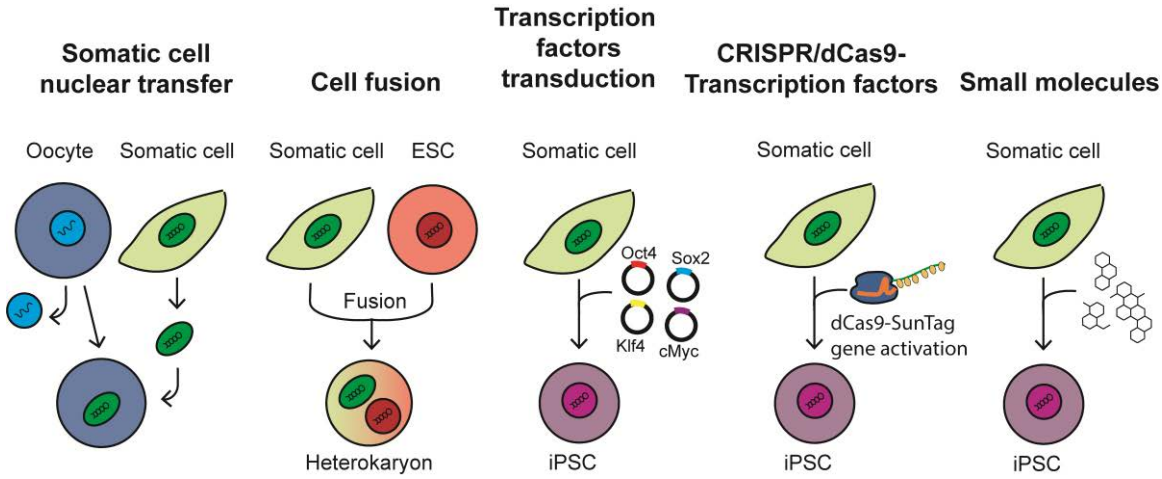

Figure 3 | Overview of current reprogramming approaches. A somatic nucleus can be reprogrammed to an embryonic state through different methods: somatic cell nuclear transfer, cell fusion, ectopic transcription factor expression, endogenous pluripotent gene activation by synthetic CRISPR/dCas9 and addition of small molecules (direct reprogramming). Embryonic stem cell (ESC); induced pluripotent stem cell (iPSC).

2.2. The four Yamanaka reprogramming factors

The unique cocktail of TFs described by Takahashi and Yamanaka in 2006 was obtained after studying possible combinations of genes that were essential for ES maintenance and self-renewal. The OSKM factors were the minimal possible combination capable of originating iPSCs colonies *in vitro* (Takahashi and Yamanaka, 2006).

OCT4, encoded by the gene *Pou5f1*, is a member of the POU (Pituitary Octamer Unc-86) family of DNA binding-proteins. In cooperation with the pluripotency gene *Nanog* and *Sox2*, *Oct4* activates a network of genes and non-coding RNAs that are necessary for pluripotency (Tomioka *et al.*, 2002; Ruairi, Sjaak Van Der and Patrick J., 2005; Jaenisch and Young, 2008). At the same time, *Oct4* limits cell differentiation by repressing lineage-specific TFs. In the first fate decision of embryonic development, *Oct4* expression is

maintained high in the ICM cells (Pesce and Schöler, 2001; Kehler *et al.*, 2004), where it represses the transcription of *Cdx2*, a TF that is essential for TE specification (Niwa *et al.*, 2005). Later, in the blastocyst stage, *Oct4* is required for the formation of the pluripotent EPI cells and the restriction of the formation of the PE (**Figure 1**). In adults, *Oct4* expression is restricted to spermatogonial stem cells (Greder *et al.*, 2012). In the context of cancer, *Oct4* is known to be essential for the survival of tumour-initiating cells and it enhances tumour invasion (Abubaker *et al.*, 2014; Koo *et al.*, 2015).

SOX2 is part of the SOXB1 family of TFs. As mentioned before, *Sox2* is essential for maintaining pluripotency and for repressing the transcription of genes that induce differentiation by interacting with *Oct4* and *Nanog* (Tomioka *et al.*, 2002; Ruairi, Sjaak Van Der and Patrick J., 2005; Jaenisch and Young, 2008). During embryonic development, it is detected in the ICM and, later, in the EPI. Underscoring a critical role in pluripotency regulation, *Sox2* depletion in the zygote stage induces malformation of the EPI, which results in embryonic lethality (Avilion *et al.*, 2003). In later stages, its expression is maintained in lineage committed progenitor cells mostly of epithelial and neuronal fate (Feng and Wen, 2015). In adulthood, *Sox2* expression marks tissue-resident ASCs and progenitor cells in various organs (Taranova *et al.*, 2006; Okubo, Clark and Hogan, 2009; Que *et al.*, 2009; Tompkins *et al.*, 2009; Arnold *et al.*, 2011). Its key role in adult tissue homeostasis was showed in an inducible *Sox2* KO mouse model, in which enhanced tissue cell apoptosis and onset of lethality was observed two weeks after *Sox2* depletion (Arnold *et al.*, 2011). Moreover, *Sox2* has been described as an oncogene in various cancer types, mainly of epithelial and neuronal origin (Bass *et al.*, 2009; Lengerke *et al.*, 2011; Maier *et al.*, 2011; Leis *et al.*, 2012; Bareiss *et al.*, 2013; Pham *et al.*, 2013; Schröck *et al.*, 2013, 2014). In some cases, *Sox2* overexpression in cancer stem cells is a related to chemotherapy resistance (Yin *et al.*, 2019) and promotion of clonogenicity (Wahl and Spike, 2017).

KLF4 belongs to the family of zinc finger containing TFs. *Klf4*, together with *Klf2* and *Klf5*, are important for ES cells maintenance, and their expression is reduced upon cell differentiation (Bourillot *et al.*, 2009). Although these three TFs bind to the promoters of *Oct4, Sox2* and *Nanog* (Jiang *et al.*, 2008), each one also regulates the expression of specific genes of the pluripotency network (Parisi *et al.*, 2008; Aksoy *et al.*, 2014). *Klf4* is a downstream target of the LIF-JAK/STAT3 pathway, which induces transcription of the main pluripotent genes (Hall *et al.*, 2009; Zhang *et al.*, 2010). *Klf4* expression during development is detected as early as the two-cell stage and its knockdown induces ES differentiation to extraembryonic endoderm (Bourillot *et al.*, 2009). In the later stages of development, *Klf4* is involved in the development of organs belonging to the three primary germ layers (Ohnishi *et al.*, 2000; Yoshida *et al.*, 2010; Qin *et al.*, 2011; Kurotaki *et al.*, 2013). In the adult organism, it plays important roles in both homeostasis and damage. For

example, it regulates spermatogenesis (Sze, Lee and Lui, 2008), differentiation of goblet cells in the colon (Michael R. *et al.*, 2002) and monocytes (Kurotaki *et al.*, 2013), and proliferation of corneal epithelial cells (Swamynathan, Davis and Piatigorsky, 2008) and B cells (Klaewsongkram *et al.*, 2007). Upon irradiation-induced DNA damage, p53 induces *Klf4* expression, which in turn promotes cell cycle arrest (Yoon and Yang, 2004; Yoon *et al.*, 2005). In the case of the irradiated intestine, for example, *Klf4* contributes to crypt regeneration (Talmasov *et al.*, 2015; Kuruvilla *et al.*, 2016). The role of *Klf4* in cancer is also context-dependent, as it can act as a tumour-suppressor gene or as an oncogene (Rowland and Peeper, 2006).

C-MYC is a member of the MYC family of basic helix-loop-helix-leucine zipper (bHLH-*ZIP*) proteins, which also includes *N-Myc* and *L-Myc.* It is a well-known oncogene regulated by the LIF-JAK/STAT3 pathway that promotes cell proliferation and survival (Cartwright et al., 2005). In development, *c-Myc* and *N-Myc* maintain the pluripotency state of cells by inhibiting differentiation through the expression of microRNAs (Lin *et al.*, 2009). *c-Myc* also coordinates with BMP4, a protein that belongs to the TFGβ superfamily of proteins, to inhibit MAPK signalling and, therefore, blocking differentiation (Hishida *et al.*, 2011; Zhongwei *et al.*, 2012; Chappell *et al.*, 2013). Thus, the simultaneous depletion of the three members of the MYC family leads to differentiation towards endoderm and mesoderm (Smith, Singh and Dalton, 2010). In reprogramming, iPSC colonies can be obtained without using *c-Myc*, but the efficiency of the process is much lower. In the context of cancer, *c-Myc* overexpression occurs in many different types of tumours, which confers cell metabolic advantages for survival (Miller *et al.*, 2012).

2.3. Phases of cellular reprogramming

Fibroblast have been the main somatic cell model used for reprogramming studies. Based on extensive transcriptomic analysis in this cell type, the process has been classified in three sequential waves: initiation, maturation and stabilization (Samavarchi-Tehrani *et al.*, 2010) (**Figure 4**).

In the **initiation phase**, the four OSKM factors bind to several genomic locations in a stochastic way. *C-Myc* is especially important in this first stage, as it enhances OSK factors binding to inaccessible chromatin, by promoting the formation of euchromatin (Sridharan *et al.*, 2009; Buganim *et al.*, 2012; Soufi, Donahue and Zaret, 2012). This early period is characterized by changes in morphology, in which fibroblasts undergo mesenchymal-to-epithelial transition (MET), and increase their proliferation rate. Mesenchymal genes are initially repressed by *Oct4* and *Sox2* (Sridharan *et al.*, 2009; Wang

et al., 2013), and *c-Myc* enhances the cell cycle (Smith *et al.*, 2010). After that, the epithelial gene expression programs are partially induced by *Klf4*. In order to cope with the energy demand, there is also a metabolic switch from oxidative phosphorylation to glycolysis, as it happens in cancer cells (Folmes *et al.*, 2011; Panopoulos *et al.*, 2012; Mathieu *et al.*, 2014). Molecularly, there is loss of somatic identity conducted by repression of key identity genes and upregulation of early pluripotent-associated markers, such as SSEA-1 and alkaline phosphatase (Samavarchi-Tehrani *et al.*, 2010; Hansson *et al.*, 2012; Polo *et al.*, 2012). These events result in the appearance of partially reprogrammed cells that will enter the maturation phase in a transgene-dependent manner. This transition is a major bottleneck for reprogramming as only a small percentage of cells that initiate reprogramming is able to progress to the maturation phase (Polo *et al.*, 2012). The exact sequence of events required for the cells to complete the initiation phase is not yet fully understood. A single-cell analysis suggested that, in a stochastic manner, the path taken is not deterministic as long as all the initiation phase-associated modifications are acquired (Buganim *et al.*, 2012).

The **maturation phase** is characterized by the gradual activation of more pluripotency-associated genes. The first markers expressed are *Fbxo15*, *Sall4* and the endogenous *Oct4*. Later, *Nanog* and *Essrb* can be detected, followed by *Sox2* and *Dppa4* (Stadtfeld, Maherali, *et al.*, 2008; Samavarchi-Tehrani *et al.*, 2010; Buganim *et al.*, 2012; Golipour *et al.*, 2012). The expression of cell surface marker intracellular adhesion molecule 1 (ICAM-1) also starts to be expressed in committed-cell populations at this stage reprogramming (O'Malley *et al.*, 2013). Of note, although the expression of these markers are good indicators of the different sub-stages of the maturation phase, cells that express them do not necessary achieve complete reprogramming (Buganim *et al.*, 2012; Golipour *et al.*, 2012). A hierarchical sequence of events must occur at the late stage of maturation for the cells to stabilize in a pluripotency state. One of the most determinant ones is the silencing of the OSKM transgene, which provides cells with the capacity to self-renew independently of the four Yamanaka factors. Moreover, inactive DNA regions coding for pluripotency-associated genes must be converted into poised regions through a series of DNA methylation changes (Polo *et al.*, 2012).

The **stabilization phase** englobes the molecular changes that occur in cells once they have acquired functional pluripotency, including the establishment of bivalent domains at CpG island-containing promoters of developmental genes. This way, pluripotent cells suppress developmental pathways at the same time that they preserve their capacity to respond to specific differentiation cues. Moreover, there is silencing of retroviral vectors, reactivation of the inactive X chromosome in female mouse iPSCs,

telomeres elongation and insensitivity to loss of global repressors, such as DNA methylation (Maherali *et al.*, 2007; Stadtfeld, Maherali, *et al.*, 2008).

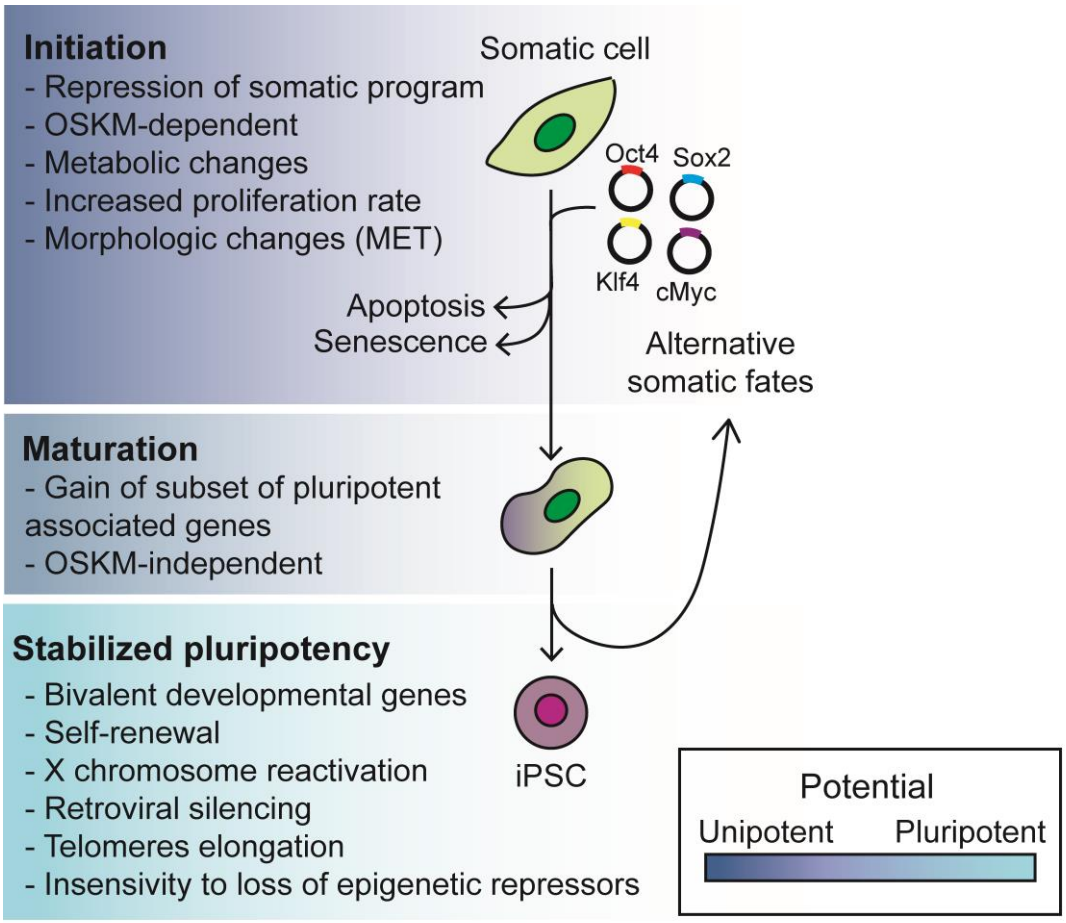

Figure 4 | Summary of the roadmap of *in vitro* reprogramming. Initially, OSKM expression induces unstable modulation of the somatic state. Mesenchymal genes are repressed by OCT4 and SOX2, the cell cycle is accelerated by c-MYC and the epithelial gene expression program is sustained, in part, by KLF4. Mesenchymal-to-epithelial transition (MET) also induces morphological changes. In this phase, some cells die and others senesce. In the maturation phase, epigenetic changes do not depend on OSKM expression anymore. Stabilized pluripotency is achieved when a sufficient number of key regulator genes are active. In this last phase, cells acquire many features specific of pluripotency, such as establishment of bivalent domains at promoters of developmental genes, silencing of retroviral vectors, telomeres elongation, insensitivity to loss of epigenetic repressors (e.g. DNA methylation) and X chromosome reactivation in females. Alternative somatic fates can be induced, but require transient passage through pluripotency. Adapted from (Zachary D. Smith, Sindhu and Meissner, 2016).

The complex cascade of epigenetic and molecular changes required for cellular reprogramming makes it an inefficient process, with less than 3% of OSKM-expressing cells converting to iPSCs (Hanna *et al.*, 2009). The majority of cells that do not complete

reprogramming die by apoptosis mainly triggered by *c-Myc* induction (Kim *et al.*, 2018), or enter a non-proliferative state called senescence due to the activation of tumour suppressor pathways INK4A/ARF and p53 (Banito *et al.*, 2009; Hong *et al.*, 2009; Kawamura *et al.*, 2009; Li *et al.*, 2009; Marión *et al.*, 2009; Utikal *et al.*, 2009; Rasmussen *et al.*, 2014) (**Figure 4**). Cells can also stay in an intermediate stage due to incomplete chromatin remodelling, therefore failing to achieve pluripotency (Mikkelsen *et al.*, 2008; Chen *et al.*, 2013). Alternative somatic fates can also be induced, such as cells with placenta-like and neural-like identities (Schiebinger *et al.*, 2017). These cell types are generated after transiently passing through pluripotency and are OSKM-dependent. Similarly, a pluripotent state epigenetically and transcriptionally distinct to iPSCs, the called F-class cells, has been characterized (Benevento *et al.*, 2014; Clancy *et al.*, 2014; Hussein *et al.*, 2014; Tonge *et al.*, 2014). All these possible non-successful fates demonstrate that cellular reprogramming is not simply a reversion of the differentiation process that occurs during development, but a much more complex process.

2.4. Modulation of in vitro reprogramming efficiency

Reprogramming somatic cells to iPSCs is an inefficient process (Hanna *et al.*, 2009). Therefore, efforts have been focused on studying signalling and epigenomic modulators of the efficiency of this process. On the one hand, cell-intrinsic barriers such as the oncogene *p53*, and the tumour suppressor proteins $p16^{INK4A}$ and $p21^{CIP1}$ are known to limit the efficiency of the process. Consequently, inactivation of the $p16^{INK4A}$ pathway or inhibition of p53 increase *in vitro* reprogramming efficiency (Banito *et al.*, 2009; Hong *et al.*, 2009; Kawamura *et al.*, 2009; Li *et al.*, 2009; Marión *et al.*, 2009; Utikal *et al.*, 2009; Rasmussen *et al.*, 2014). On the other hand, the forced expression of cell-cycle enhancers, such as the GTP-binding protein REM2 or cyclin D1 improves the reprogramming efficiency (Edel *et al.*, 2010; Tanabe *et al.*, 2013). Moreover, the ectopic expression of highly expressed genes in ES cells, like *Utf1*, *Lin28*, *Esrrβ*, *Trim71* or *Tbx3* improves reprogramming (Zhao *et al.*, 2008; Feng *et al.*, 2009; Han *et al.*, 2010; Worringer *et al.*, 2014).

Regarding epigenetic modulators of reprogramming, molecules that regulate post-transcriptional modifications of histones can affect the transcription of pluripotent-associated and somatic genes, thereby modulating cell fate. For example, suppression of H3K79 histone methyltransferase DOT1L accelerates reprogramming (Onder *et al.*, 2012). Ascorbic acid (Vitamin C) added to the culture medium has also been described to improve reprogramming efficiency by promoting the activity of the histone demethylases JHDM1a/1b (Wang *et al.*, 2011). A combination of ascorbic acid, DOT1L and a cocktail called 2i (inhibitors to mitogen-activated protein kinase [MAPK] and glycogen synthetase

kinase 3 [GSK-3]) was proven to increase even more the efficiency of the process (Tran *et al.*, 2019). Additionally, depletion of *Mbd3*, a member of the Mbd3/NuRD (chromatin remodelling and histone deacetylation) repressor complex, induces reprogramming of near 100% of the cultured cells (Rais *et al.*, 2013). Similarly, CCAAT/enhancer binding protein-α (C/EBPα) expression followed by OSKM activation induces a 100-fold increase in iPSCs formation (Di Stefano *et al.*, 2014). On the contrary, inhibition of the core components of the polycomb repressive complex 1 and 2, such as the H3K27 methyltransferase EZH2, lessens the efficiency of the process.

Activation of inflammatory pathways also modulates the efficiency of *in vitro* reprogramming. The cytokine IL-6, which is secreted in response to tissue damage, activates pluripotent pathways that improves reprogramming (Mosteiro *et al.*, 2016; Mahmoudi *et al.*, 2019). Similarly, activation of the Toll-like receptor 3 (TLR3) in OSKM-expressing fibroblasts enables epigenetic changes that accelerates and enhances iPSCs formation (Lee *et al.*, 2012).

2.5. Models of *in vivo* reprogramming

Full reprogramming has also been achieved *in vivo* in the context of an adult organism. The first two models in *in vivo* reprograming were published in 2013. The first study used DNA plasmids encoding for OCT3/4, SOX2, KLF4 and c-MYC injected intravenously in Balb/C adult mice. These plasmids were highly expressed in the liver and they induced loss of hepatic markers within 24-48h of injection. Although $NANOG^{+}$ cells were observed, no teratomas (tumour produced by pluripotent cells) were formed after 120 days of injection (Yilmazer *et al.*, 2013). In the second study, mice that transiently expressed the OSKM factors under the control of doxycycline administration were generated (Abad *et al.*, 2013). OSKM activation for one week led to loss of cellular identity and acquisition of pluripotency markers (e.g. NANOG). Upon doxycycline withdrawal, mice developed three germ layers-containing teratomas in various organs. Despite the systemic expression of the four factors, some tissues, such as the pancreas, stomach, intestine and the kidney presented more incidence of teratomas than other organs. Of note, iPSCs isolated from the blood of these mice displayed a gene expression profile closer to that of ES cells compared to the *in vitro* generated ones. Furthermore, *in vivo* iPSCs could give rise to trophectodermal cells, suggesting that they achieve a more primitive state than ES cells. Finally, they were able to generate embryo-like structures that expressed embryonic and extraembryonic markers when injected intraperitoneally back into the mice, which revealed their totipotent-like state. In 2014, a similar OSKM-inducible mouse model was generated by Yamanaka and

Yamada (Ohnishi *et al.*, 2014). In both mouse models, there was a direct relationship between the appearance of teratomas and the duration of the expression of the 4 factors. Ohnishi *et al*, for instance, showed that after a short pulse of OSKM induction dedifferentiated pancreatic cells reacquired their mature phenotype and physiological function within days.

3. Cellular plasticity in tissue damage and regeneration

The term of cellular plasticity infers the capacity of cells to switch to new identities. By definition, it is a *bona fide* characteristic of embryonic and PSCs (Wang, 2019). However, some differentiated cells can also acquire cellular plasticity after injury in order to promote tissue regeneration (Jessen, Mirsky and Arthur-Farraj, 2015).

Plasticity has been widely studied in lower vertebrates, as they present a remarkable ability to regenerate. These studies have shown a strong correlation between regeneration and dedifferentiation. For instance, in axolotls, limb injury triggers the formation of proliferating blastemal cells, which retain memory of their tissue of origin and re-differentiate to regenerate the missing limb (Kragl *et al.*, 2009). Dedifferentiation has also been described to occur during heart (Poss, Wilson and Keating, 2002; Raya *et al.*, 2003) and liver (He *et al.*, 2014) regeneration in zebrafish.

Mammals, however, have a more restricted capacity to regenerate their tissues. Generally, tissues with high cellular turnover contain resident ASCs or progenitor cells that are activated upon damage and repair the tissue. This is seen for instance in the blood (Seita and Weissman, 2010), the hair follicles (Morita *et al.*, 2021), the skeletal muscle (Masaki *et al.*, 2013) and the gut (Barker *et al.*, 2007). Nevertheless, tissues that lack ASCs depend on other strategies to regenerate. Some of them rely on proliferation or transdifferentiation of terminally differentiated cells to repopulate the damaged area. In the respiratory epithelium, for example, ciliated and club cells can transdifferentiate into distinct epithelial cell types in order to replenish the lost cell mass (Park *et al.*, 2006; Tata *et al.*, 2013). In the case of the liver, remaining hepatocytes can proliferate to re-establish the normal hepatic functions, or they can transdifferentiate into biliary cells (Yanger *et al.*, 2013; Sekiya and Suzuki, 2014). Finally, in other organs, remaining somatic cells dedifferentiate, proliferate and then re-differentiate in order to replace lost cells. Some example are the kidney (Kusaba *et al.*, 2014), the liver (Yanger *et al.*, 2013), the heart (Ubil *et al.*, 2014) and the Schwann cells (Masaki *et al.*, 2013).

A key player in the regeneration process is the presence of non-proliferative cells called senescent cells in the tissue microenvironment. Senescent cells are generated as a protective mechanism to avoid uncontrolled cell division upon damage (Campisi and d'Adda di Fagagna, 2007). Through their senescence-secretory associated phenotype (SASP), senescence cells promote tissue regeneration by activating tissue resident progenitor cells (Ritschka *et al.*, 2017). Some studies showed that IL-6, a member of the SASP, promotes liver regeneration (Cressman *et al.*, 1996; Nechemia-Arbely *et al.*, 2011), wound healing (Lin *et al.*, 2003; McFarland-Mancini *et al.*, 2010) and damaged heart recovery (Kubin *et al.*, 2011). Another key player in the process of regeneration is the immune system. Tissue damage resulting from mechanical injury or exposure to infectious/toxic agents promotes the release of damage associated molecular patterns (DAMPs) from damaged cells and pathogen associated molecular patterns (PAMPs) from pathogens, which activates immune cells (Janeway and Medzhitov, 2002). Their recruitment to the site of damage determine the outcome of the regeneration process, as they provide appropriate signals for proliferation of SCs or dedifferentiation of somatic cells, depending of the tissue. Immune cells also eliminate damaged cells and clean cellular debris (Abnave and Ghigo, 2019).

During cellular reprogramming, somatic differentiated cells also acquire certain degree of cellular plasticity. Interestingly, recent reports show that transient OSKM expression improves tissue regeneration in models of muscle injury (De-Lázaro *et al.*, 2014; Chiche *et al.*, 2017), retinal degeneration and optic nerve crush injury (Lu *et al.*, 2020), myocardial infarction (Y. Chen *et al.*, 2021), β-cell damage (Ocampo *et al.*, 2016) and skin wound (Doeser, Schöler and Wu, 2018; Kurita *et al.*, 2018). Similarly to the context of physiological damage, IL-6 is a critical factor in promoting cellular reprogramming, thus enhancing regeneration (Mosteiro *et al.*, 2016, 2018; Chiche *et al.*, 2017). Cellular reprogramming also contributes to the amelioration of age-related phenotypes. *In vitro,* reprogramming of human cells from old people followed by their consequent re-differentiation gave rise to fully rejuvenated cells (Lapasset *et al.*, 2011; Sarkar *et al.*, 2020). *In vivo*, Ocampo *et al.* showed that short-term cyclic expression of OSKM improves physiological parameters and extends the lifespan in a model of premature aging without risk of teratoma formation (Ocampo *et al.*, 2016).

4. The pancreas in homeostasis and disease

The pancreas is a glandular organ derived from the endoderm composed by both exocrine and endocrine cell types (**Figure 5**). The exocrine pancreas (95%) comprised by acinar and

ductal cells is responsible for nutrient digestion. Acinar cells are arranged into clusters called acini that secrete amylase, lipase, and peptidases from their apical poles into the ducts (Whitcomb and Lowe, 2007). Ductal cells secrete bicarbonate that neutralizes gastric acid and drains acinar digestive enzymes towards de duodenum. The other 5% of the pancreas is formed by 5 types of endocrine cells, which produce hormones that regulate glucose homeostasis: α-cells (glucagon), β-cells (insulin), δ-cells (somatostatin), ε-cells (ghrelin) and γ-cells (pancreatic polypeptide). Endocrine cells are clustered in the islets of Langerhans (Pan and Wright, 2011). Centroacinar cells and terminal duct cells have been proposed as progenitor cells located at the junction between acinar cells and the adjacent terminal ductal epithelium (Rovira *et al.*, 2010). Finally, the pancreas is also composed by blood vessels, nerve fibres and stroma cells, which together maintain the fine-tune homeostasis of the pancreas (Walker, 2018).

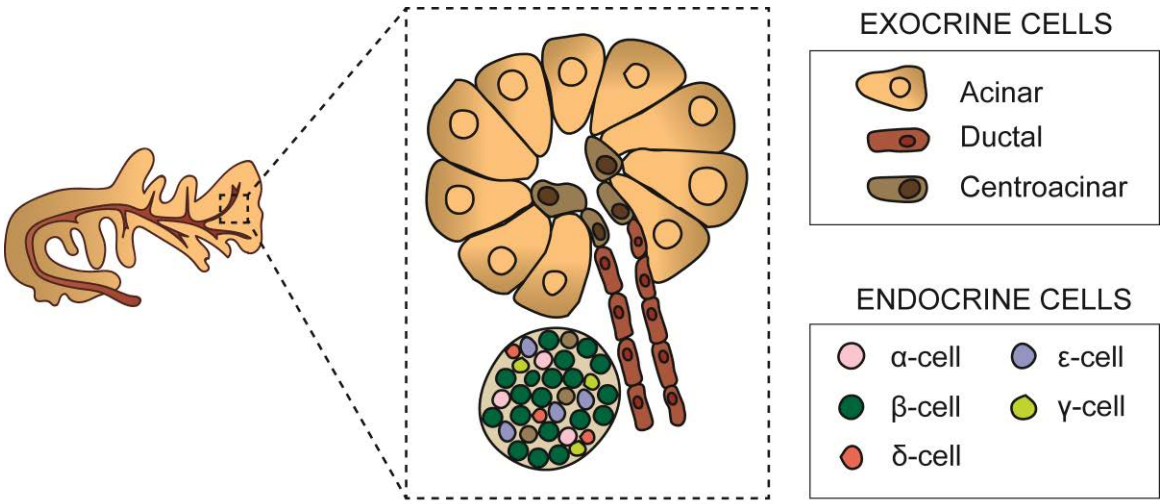

Figure 5 | Adult mouse pancreas. The pancreas is composed of two functional distinct compartments: the exocrine (acinar and ductal cells) and the endocrine (Islets of Langerhans) pancreas. The Islets of Langerhans consist of five different types of cells that secrete hormones: α-, β-, δ-, ε- and γ-cells.

Despite the fact that acinar cells are described as a single pool of cells, they are heterogeneous in terms of proliferation. Most acinar cells have low proliferative capacity or are binuclear and unable to divide. However, a minor subset of acinar cells (around 1%) expressing stathmin-1 (STMN1) retain high proliferative activity long term (Wollny *et al.*, 2016).

The capacity of the adult pancreas to regenerate is limited and it declines with age (Teta *et al.*, 2005; Watanabe *et al.*, 2005; Takahashi *et al.*, 2012). In physiological conditions, both exocrine and endocrine cells are able to maintain their compartments by self-duplication in a unipotent lineage restricted manner (Herrera, 2000; Dor *et al.*, 2004;

Desai *et al.*, 2007; Teta *et al.*, 2007). However, upon injury, different cell types have been described to orchestrate pancreas regeneration depending on the experimental model. The most common procedure to induce acute inflammation of the pancreas (acute pancreatitis or AP) is the administration of caerulein, a mouse analogue of the hormone cholecystokinin, which leads to the release of digestive enzymes by damaged acinar cells. As consequence, most acinar cells die by apoptosis or necrosis, and some others lose their granules and undergo morphological and transcriptional changes to resemble ductal cells in a process termed acinar-to-ductal metaplasia (ADM) (Strobel *et al.*, 2007). This process involves dedifferentiation of acinar cells, which is associated with repression of acinar markers (e.g. *Ptf1a*), and acquisition of some ductal markers (e.g. *Hnf6*) (Prévot *et al.*, 2012). Within a week after caerulein treatment, the pancreas recovers its homeostatic morphology and functions. Regeneration of acinar cells occurs through the proliferation of surviving acinar cells (Desai *et al.*, 2007; Strobel *et al.*, 2007; Blaine *et al.*, 2010), being most of them positive for the above mentioned marker STMN1 (Wollny *et al.*, 2016). A subpopulation of doublecortin-like kinase-1 (DCLK1)-positive cells, which are quiescent in homeostatic conditions, have also been described to start proliferating upon damage to regenerate the pancreas (Westphalen *et al.*, 2016). Also, *Hnf1b*$^{+}$ ductal cells were described to promote recovery after AP, as their ablation prevents regeneration of the tissue (Westphalen *et al.*, 2016). However, whether cells that undergo ADM after caerulein administration are able to reverse their phenotype contributing to regeneration of the tissue is still under debate.

Other cell types are involved in regeneration after different pancreatic damages. In the model of duct ligation, for instance, lineage tracing showed that surviving acinar cells converted to progenitor-like cells in order to re-differentiate into acinar, ductal and endocrine cells 60 days after the damage (Pan *et al.*, 2013). Moreover, diphtheria toxin-mediated cell ablation of acinar and endocrine cells demonstrated that pancreatic regeneration was promoted by surviving ductal cells, in a process that resembles pancreatic development (Criscimanna *et al.*, 2011). Regarding the endocrine compartment, severe β-cell loss is recovered by conversion of α- or δ-cells, depending on the mice age (Thorel *et al.*, 2010; Chera *et al.*, 2014). Finally, centroacinar cells and terminal duct cells highly proliferate upon damage (Leeson and Leeson, 1986; Gasslander, Ihse and Smeds, 1992; Nagasao *et al.*, 2003), although, so far, there are not models of lineage tracing that show their direct contribution to tissue regeneration. From these studies, one can conclude that various cell types play a key role in pancreatic regeneration depending on the target cell affected and the severity of the injury of each experimental model.

Immune cells play an important role in the pathogenesis of AP and determine the severity of the disease (Zheng *et al.*, 2013). Upon caerulein administration, acinar cells

upregulate ICAM-1, which promote neutrophil infiltration at the early phase of the inflammation. Neutrophil depletion leads to reduction in AP severity (Frossard *et al.*, 1999), which demonstrates their key contribution to the progression of the damage. Monocytes, macrophages and T lymphocytes also promote inflammation and ADM by liberating cytokines and chemokines (McKay, Imrie and Baxter, 1996; Geou-Yarh *et al.*, 2013). Accordingly, depletion of macrophages via injection of clodronate liposomes, or T cell depletion via antibodies prevented caerulein-mediated AP in mice (Demols *et al.*, 2000; Saeki *et al.*, 2012).

5. The immune system

The immune system consists of different organs, tissues and cell types connected through the blood and the lymphatic vessels. The main role of the immune system is to detect pathogens and infected cells, as well as transformed cells, to further eliminate them (Day and Schultz, 2010). Functionally, the immune system is classified into two categories: the innate and the adaptive immune system. Although innate and adaptive immune responses are often considered as sequential, there is now increasing evidence that there is an overlap between the two, both mechanistically and in timelines (Petrus-Reurer *et al.*, 2021).

Immune cells are generated from hematopoietic stem cells (HSCs) in the bone marrow (BM), where most of them also mature (**Figure 6**). According to the classical model for adult HSC lineage commitment, HSCs give rise to common myeloid progenitors (CMPs) and common lymphoid progenitors (CLPs) upon stimulation. On the one hand, CMP cells further differentiate into megakaryocytes, which produce platelets, erythrocytes (red blood cells that carry oxygen) and leukocytes (white blood cells). On the other hand, CLP cells commit to become T and B lymphocytes, and natural killer (NK) cells. The leukocytes that derive from CMP are the monocytes, the mast cells, the myeloid-derived suppressor cells (MDSC) and the neutrophils, eosinophils and basophils. The latter three are known as granulocytes because of their cytoplasmic granules. They circulate in blood and are recruited at sites of inflammation and infection. Neutrophils mainly phagocyte bacteria or damaged cells, whereas eosinophils and basophils are related to allergic inflammation and elimination of parasites. Monocytes enter tissues where they differentiate into macrophages, which are phagocytic cells, or into dendritic cells (DC), which present antigens to T lymphocytes in the lymphoid tissues. Mast cells are important for allergic responses. Under pathological conditions, MDSCs act as the main immunosuppressive cell type in order to avoid detrimental effects of inflammation in tissues (Veglia, Perego and Gabrilovich, 2018). Regarding the cells derived from the CLP branch, B cells differentiate into antibody-producing plasma cells when they encounter antigens, whereas naïve T

lymphocytes give rise to NKT cells, CD4 naive T cells, CD8 naive T cells, T regulatory cells (T reg) and γδ T cells upon specific activating signals (Day and Schultz, 2010).

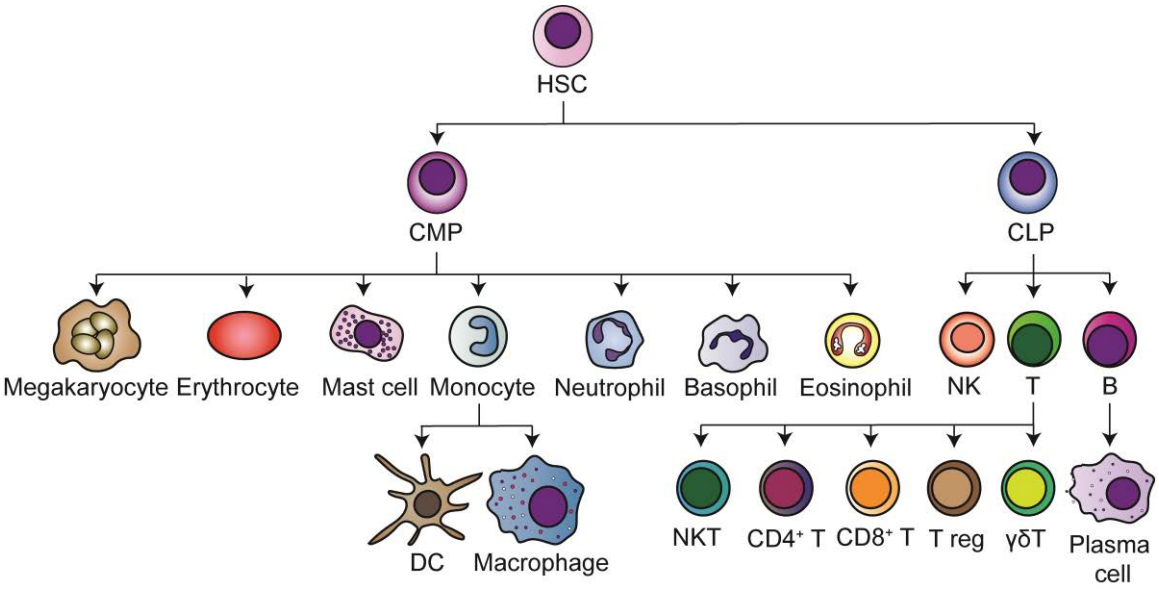

Figure 6 | Immune system cells arise from hematopoietic stem cells (HSC) in the bone marrow (BM). In the classical model, pluripotent HSCs differentiate to produce a common myeloid progenitor (CMP) and a common lymphoid progenitor (CLP). CMP give rise to different types of leukocytes, erythrocytes and megakariocytes, whereas CLP give rise to T, B and NK lymphocytes. The leukocytes that derive from CMP are the monocytes, the mast cells and the neutrophils, basophils and eosinophils. Monocytes can further differentiate into macrophages and DCs in the tissues. After encountering antigens, B cells differentiate into plasma cells, and T cells can differentiate into NKT, CD4 naïve T cells, CD8 naïve T cells, T regulatory cells (T reg) and γδ T cells. Note: this illustration is a simplification of the immune cell subsets that exist.

5.1. Innate immune system

The innate immune system is form by physical barriers, mucus layers, soluble proteins, bioactive molecules and different cell types. Such cells have membrane receptors that bind PAMPs and DAMPs expressed on the surface of invading pathogens or infected cells. They are also able to recognize activating ligands or the absence of inhibitory ligands in the surface of damaged or transformed cells. They exert fast (0-96h) and usually non-specific immune responses with no immunological memory. The cells that constitute the innate immune system are DCs, monocytes, macrophages, mast cells, megakaryocytes, NK cells and granulocytes (neutrophils, basophils and eosinophils).

5.1.1. Natural killer cells

In the earlier 1960s, a lymphocyte population with innate cytotoxic properties was described for the first time. These cells received the name of NK cells (Smith, 1966). NK cells constitute around 2-5% of total lymphocytes in the mouse spleen and BMs of inbred laboratory mice (Jiao *et al.*, 2016) and their turnover in blood is around 2 weeks (Jamieson *et al.*, 2004; Walzer *et al.*, 2007). NK cells respond to inflammatory stimuli and are well-known for their roles in anti-viral immunity and tumour immunosurveillance (Abel *et al.*, 2018). Recent studies have also demonstrated that NK cells regulate anti-inflammatory processes, such as tissue repair (Jewett, Man and Tseng, 2013; Kumar *et al.*, 2013).

NK cells originate primarily in the BM, but also in secondary lymphoid tissues including tonsil, spleen and lymph nodes (LNs) (Scoville, Freud and Caligiuri, 2017). They classically belong to the group of innate lymphoid cells (ILCs) type 1, as they produce interferon-gamma (IFNγ) and tumour necrosis factor (TNF)-α upon stimulation. However, they have cytolytic functions similar to those of $CD8^+$ T cells, which differentiates them from the rest of ILCs type 1 (Zhang and Huang, 2017). As consequence of being functionally quite different, a new classification of ILCs was proposed in 2018, in which NK cells were considered as an independent group from ILC1s (Vivier *et al.*, 2018).

The intermediate populations that give rise to mature NK (mNK) cells in mice are defined by the differential expression of surface markers. The expression of the activating receptor natural-killer receptor group2, member D (NKG2D) marks the transition from NK progenitor cells to immature NK (iNK) cells, followed by the acquisition of the activating receptors NK1.1 (Klrb1c/CD161) and NCR1(NKp46) (Huntington, 2017). Finally, terminally mNK cells are identified based on the expression of CD43 (Leukosialin), CD11b (Mac-1), Killer cell Lectin-like Receptor G1 (KLRG1) and Ly49s receptors (Kim *et al.*, 2002; Ito *et al.*, 2006; Huntington *et al.*, 2007). These last ones can be activating (Ly49D and Ly49H) or inhibitory (Ly49A, Ly49C/I and Ly49G) receptors (Schenkel, Kingry and Slayden, 2013). During the immature phases, NK cells also express CD27, a marker that is lost in mNKs, and its absence is also used to identify the last stage of NK maturation (Abel *et al.*, 2018). mNK cells are then fully functional and migrate into peripheral blood, lymph nodes, spleen and several organs as resting NK cells in homeostatic conditions (Peng and Tian, 2017). Resting NK cells have poor cytotoxic potential and they require “priming” in order to be activated. The main interleukins involved in NK cell priming include IL-2, IL-15 and IL-21 (Long, 2007; Lucas *et al.*, 2007). Whereas IL-2 controls NK cell proliferation and production of lytic molecules (Gasteiger *et al.*, 2013), IL-15 is required for their maturation and survival (Lodolce *et al.*, 1998; Kennedy *et al.*, 2000; Gilmour *et al.*, 2001). IL-21 synergies with IL-2 to increase the expression of cytotoxic receptors in the surface

(Brady *et al.*, 2004). Most of these ILs are secreted by other immune cell types, such as macrophages, DC and T cells (Long, 2007), which makes them modulators of NK cells activity. Upon activation, NK cells migrate toward specific inflammation sites attracted by chemokines (Maghazachi, 2010).

NK cells conduct immunosurveillance by probing cells *via* their inhibitory receptors to check whether the major histocompatibility complex class I (MHC-I) (histocompatibility antigen-2 (H2) in mouse) is expressed in order to ensure tolerance against healthy cells (**Figure 7A**). The decision whether or not an NK cell will kill a target cell depends on the balance of signals transmitted from activating or inhibitory ligands to NK surface receptors. Thus, NK cell activation can be triggered in many ways: in some cases, stressed cells downregulate MHC-I, which ablates the inhibitory signal in NK cells. This phenomenon called "missing-self" induces NK cells activation and target cell lysis (**Figure 7B**). Stressed cells can also express high levels of activating ligands that overcome MHC-I-mediated inhibitory signalling. This "induced-self" phenomenon also results in NK cell activation and killing of target cells (**Figure 7C**). Thirdly, expression of allogeneic MHC-I by donor transplanted tissue is recognized by NK cells as "non-self", which triggers target cell death (**Figure 7D**). Activation of NK cell-cytotoxic activity by any of the mentioned mechanisms induces the release of cytotoxic granules containing perforin and granzymes that promotes caspase-dependent apoptosis in the target cells. NK cells, however, are protected from the lytic activity of these granules by expressing the molecule lysosomal-associated membrane protein-1 (CD107a/LAMP-1) in their plasma membranes, which inhibits the binding of perforin to their cell surface (Cohnen *et al.*, 2013) (**Figure 8**). Another mechanism by which NK cells get activated occurs when they detect the presence death receptors situated at the membrane of damaged cells, leading to their death-receptor mediated apoptosis. Concretely, NK cells express the ligands TNF-related apoptosis-inducing ligand (TRAIL) and Fas ligand (FasL or CD95L), which bind to TNF-related apoptosis-inducing ligand-receptor (TRAIL-R) and Fas (CD95), respectively, situated at the target cell membrane (Smyth, Cretney, *et al.*, 2005). Finally, NK cells exert a third effector function based on IFNγ production. Upon stimulation, NK cells release IFNγ that, together with the formation of channels that promote osmotic perturbation, induces cell death called pyroptosis (Zhou *et al.*, 2020). This last mechanism has been particularly studied in virally-infected cells (Zeromski *et al.*, 2011).

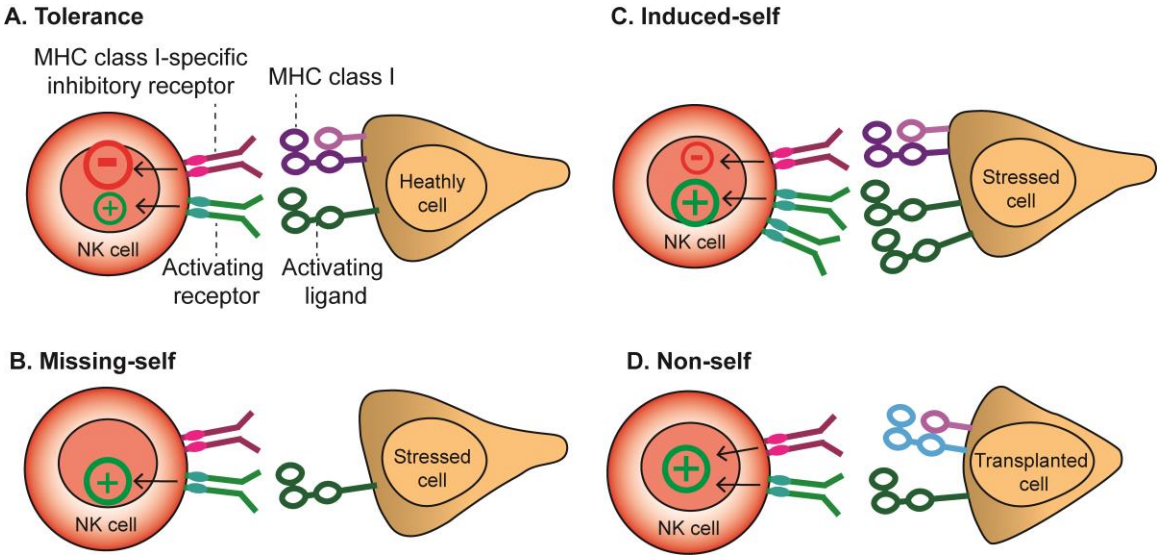

Figure 7 | Mechanisms of target cell recognition by NK cells that induce granule-mediated cytotoxicity. NK cells rely on activating and inhibitory receptors to recognize potential target cells. **A**. Tolerance: recognition of autologous major histocompatibility complex class I (MHC-I) by specific inhibitory receptors in NK cells prevents their activation. **B**. Missing-self: recognition of stressed cells that either do not express MHC-I or reduce them below optimal levels induce NK cells activation. **C**. Induced-self: stressed cells that express high levels of activating ligands overcome MHC-I-mediated inhibitory signalling, which results in NK cell activation. **D**. Non-self: NK cells recognise and eliminate transplanted cells that express allogeneic MHC-I.

NK cells express receptors that can detect multiple activating and inhibitory ligands in the surface of possible target cells. (**Figure 8**). Among the inhibitory receptors, there are three subtypes of lectin-like Ly49 dimers (A, C/I and G2) and the CD94/NKG2A heterodimers, which recognize the molecules MHC-Ia (haplotype H2-Kb for Ly49C/I and haplotype H2-Kd for Ly49A and G2) and MHC-1b (Qa1b in mouse and HLA-E in humans), respectively (Yokoyama and Plougastel, 2003). Of note, in C57BL/6 mice, Ly49G2 and Ly49A are expressed, but are non-functional, as their ligand, MHC-I (haplotype H2-Kd), is not present in this strain (Hanke *et al.*, 1999). NK cells also express activating receptors, such as Ly49D and leukocyte function-associated antigen-1 (LFA-1), which bind to MHC-Ia and ICAM-1, respectively. Another major activating receptor is the NKG2D, which have three possible ligands in mouse target cells: retinoic acid early inducible-1 (RAE1), murine UL16-binding protein-like transcript 1 (MULT1) and histocompatibility 60 (H60). Similarly, the receptor DNAX accessory molecule-1 (DNAM-1) binds to CD112 (NECTIN-2) and CD155 (PVR) in the surface of target cells (de Andrade, Smyth and Martinet, 2014). Moreover, the activating receptor Ly49H, present only in mice of C57BL/6 background, recognizes the murine cytomegalovirus-encoded ligand 157 (m157) (Adams *et al.*, 2007), and NKp46 (NCR1) interacts with hemagglutinins

(HAs) derived from influenza and parainfluenza viruses, among other ligands (Mandelboim and Porgador, 2001). Of note, NK cells also mediate antibody-dependent cell-mediated cytotoxicity (ADCC) through the FcγRIIIA (CD16) receptor by target cells coated with antibodies (Wang *et al.*, 2015). The most relevant receptors and ligands for this thesis are illustrated in **Figure 8.**

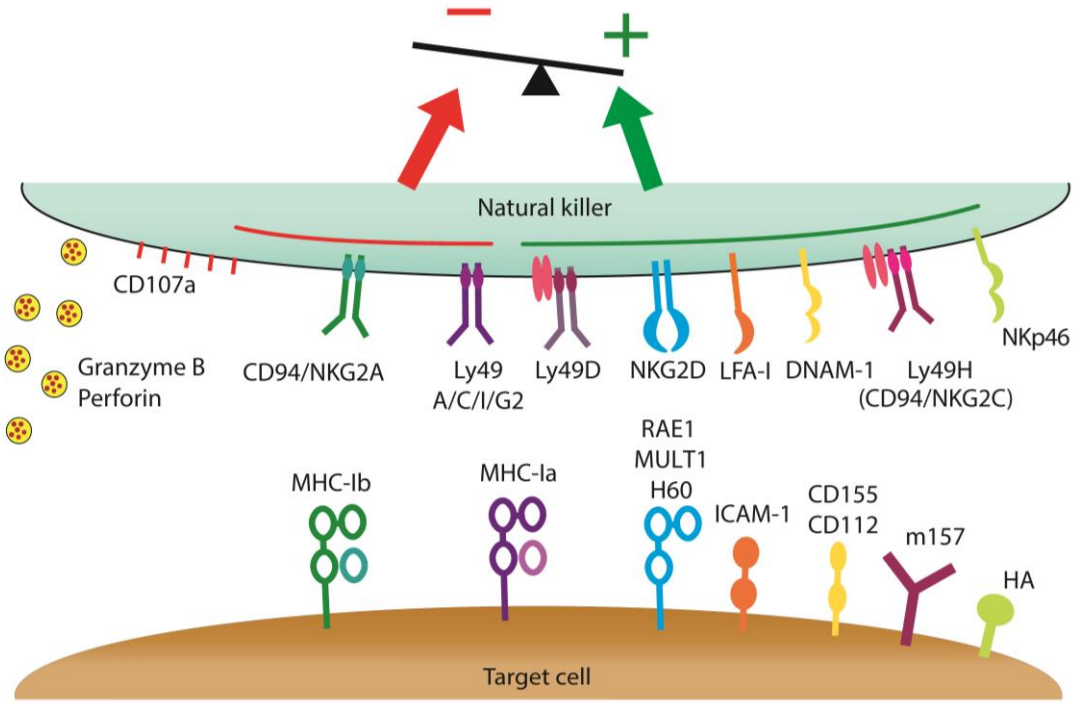

Figure 8 | Major inhibitory and activating NK cell receptors and their cognate ligands on target cells. The balance of signals from activating and inhibitory receptors determine whether NK cells kill target cells. Upon activation, NK cells release cytotoxic granules containing granzymes (e.g. granzyme B) and perforin, which induce apoptotic cell death in the target cell. The expression CD107a/LAMP-1 in the plasma membrane of NK cells inhibits the binding of perforin to their cell surface, protecting them from lysis. Major histocompatibility complex class Ia (MHCI-a); Major histocompatibility complex class Ib (MHC-Ib); natural-killer receptor group2, member D (NKG2D); leukocyte function-associated antigen-1 (LFA-1); influenza virus hemagglutinin (HA); murine cytomegalovirus-encoded ligand 157 (m157); receptor DNAX accessory molecule-1 (DNAM-1); retinoic acid early inducible-1 (RAE1); murine UL16-binding protein-like transcript 1 (MULT1); histocompatibility 60 (H60); intracellular adhesion molecule 1 (ICAM-1). Note: this figure is a simplification of the receptors and ligands related to NK activity.

Regarding markers to classify NK cells, the NK1.1 surface molecule is widely used in mice of C57BL/6 and SJL/J backgrounds (Carlyle *et al.*, 2006). It is important to mention that NK1.1 is also expressed in $CD3^+$ cells, such as NKT cells (Bendelac *et al.*, 1997) and

a subset of T cells (Vicari and Zlotnik, 1996). Thus, distinction between CD3- cells (NK) and $CD3^+$ (NKT and T) cells is required when identifying NK, NKT and T cells that express the marker NK1.1. NKp46 (NCR1) is also an NK cell marker, although it is also expressed in a subset of T cells (Walzer *et al.*, 2007).

As mentioned above, many studies have demonstrated the importance of NK cells in tumour clearance. Concretely, the receptor NKG2D has a prominent role in tumour surveillance, as it detects ligands that are normally over-expressed upon cellular distress (e.g. DNA damage response) (Raulet and Guerra, 2009). Ectopic expression of NKG2D ligands is sufficient to induce tumour rejection in syngeneic mice (Cerwenka, Baron and Lanier, 2001; Diefenbach *et al.*, 2001). Moreover, NKG2D blocking with antibodies promoted significantly formation of tumours compared with animals that received isotype control antibody (Smyth, Swann, *et al.*, 2005). Similarly, NKG2D-deficient mice were more susceptible to tumour growth (Guerra *et al.*, 2008). Another study showed that chemotherapeutic compounds that induce senescence in cancer cells also increase the expression of NKG2D ligands, making them more susceptible to NK-mediated clearance (Soriani *et al.*, 2009). It is important to mention that persistent exposure to NKG2D ligands in target cells causes decrease of NKG2D surface expression. NKG2D is internalized and it signals from the endosomal compartment, leading to NK activation (Molfetta *et al.*, 2016a, 2017). Similarly, high amounts of IFNγ also decrease NKG2D expression (Zhang *et al.*, 2005). Thus, NKG2D expression in the cell surface does not necessarily correlate with the levels of NK cell activation. Moreover, it is worth mentioning that NK cell responses are tilted towards inhibition when both inhibitory and activating ligands are engaged, so full activation of NK cells requires the co-engagement of at least two different activating receptors (e.g. NKG2D and NKp46 or NKG2D and LFA-1) to overcome the inhibitory signal (Abdool *et al.*, 2006; Bryceson, Ljunggren and Long, 2009). This requirement for a synergetic combination of at least two activating receptors may prevent unrestrained activation of NK cells. A recent study, however, showed that engagement of NK cells *in vitro* with NKG2D alone was sufficient to activate them (Wu *et al.*, 2021). Numerous studies have shown that cancer cells are also targeted by NK cells due to the lack or downregulation of MHC-I levels (Raulet and Guerra, 2009).

Importantly, activated NK cells produce inflammatory cytokines and chemokines that can shape the functions of other immune cell types. For instance, NK cells can meet DCs in the peripheral tissues and in the secondary lymphoid organs, and act on them in two possible ways: they either kill immature DCs (Hayakawa *et al.*, 2004) or they promote their maturation by secretion of IFNγ and TNF, which leads to enhanced antigen presentation to T cells (Moretta *et al.*, 2006). NK cells can also promote the priming of $CD4^+$ T helper type I (T_{H1}) by secreting IFNγ (Martín-Fontecha *et al.*, 2004) and eliminate activated T cells that

do not express sufficient amounts of MHC-I molecules (Lu *et al.*, 2007). NK cells also produce chemokines, such as CCL3 (MIP-1α), CCL4 (MIP-1β), CCL5 (RANTES) and CXCL8 (IL-8), which attract effector T cells and myeloid cells to inflamed tissues. Finally, NK cells also bind and eliminate damaged endothelial cells through the CX3CR1/CX3CL1 axis in order to avoid possible vasculopathies (Yoneda *et al.*, 2000).

5.2. Adaptive immune system

The adaptive immune system gives a delayed and more complex response than the innate immune system. It constitutes the base of the immune memory, which protects against future exposures to the same activating agents. The main components of the adaptive immune system are B and T cells. Although NK cells have been widely described as part of the innate immune system, recent findings show that they can be long-lived and are capable of rapid recall responses, which would include them as a bridge between innate and adaptive immune system (Sun, Beilke and Lanier, 2010; Vivier *et al.*, 2011). However, the underlying mechanisms for the generation of NK memory are still unknown.

One of the most studied components of the adaptive immune system are T cells. This cell type reacts against bacterial and viral infections and also mediate surveillance of transformed and foreign tissues (Koch and Radtke, 2011). They originate in the BM and then they travel to the thymus, where they differentiate and finally mature into functional T cells. During this period, T cells undergo somatic recombination to generate T cell clones with unique T-cell receptors (TCRs). These TCRs bind and recognize antigens presented by other cells on MHC proteins. It is vitally important that TCRs produced by somatic recombination distinguish between self-antigens, presented in the MHC complexes of normal cells, and non-self antigens, produced by foreign or abnormal cells. This process is called positive and negative selection. In positive selection, T cells in the thymus, referred as thymocytes, bind moderately to MHC complexes of antigen-presenting cells (APCs) and receive survival signals. However, thymocytes whose TCRs bind too strongly to MHC complexes are considered self-reactive and are eliminated in the process of negative selection (Klein *et al.*, 2014).

MHC molecules are very polymorphic and are encoded by H-2 genes in mice and HLA genes in human (Vivier *et al.*, 2018). They can be divided in two categories: (1) MHC-I molecules are expressed on nearly all somatic cells and present endogenous antigens to $CD8^+$ cytotoxic T cells and (2) MHC-II molecules, which are abundantly expressed in APCs and present exogenous peptides to $CD4^+$ helper T cells (Rock, Reits and Neefjes, 2016) (**Figure 9**).

All cells in homeostatic conditions express endogenous peptides through MHC-I, which allows $CD8^+$ T cells to sample the intracellular environment continuously. In the case of healthy cells, $CD8^+$ T cells are tolerant to autologous peptides presented in their MHC-I molecules. However, when cells are expressing mutant sequences (e.g. cancer cells), microbial genes (e.g. from infections) or foreign polymorphic genes (e.g. transplants), $CD8^+$ T cells recognize these "non-self" antigens as immunogenic. The repertoire of peptides presented by MHC-I to a specific set of cells is called immunopeptidome (Schuster *et al.*, 2018). Presentation of endogenous peptides starts with degradation of endogenous proteins and defective ribosomal products by the proteasome (Michalek *et al.*, 1993; Rock *et al.*, 1994) (**Figure 9**). The majority of those peptides are further eliminated in the cytosol by peptidases, but some of them escape to the endoplasmic reticulum (ER) lumen through the transporter associated with antigen processing (TAP). Inside the ER, empty MHC-I molecules start binding peptides in a slow off rate until a peptide with appropriate anchor residues is bound (Garstka *et al.*, 2015). These are peptides with a length of 8-12 amino acids (AAs). Different fragments from a specific antigen can be presented by different MHC-I molecules, as the MHC peptide-binding grooves (commonly known as "pockets") are very polymorphic.

The most studied type of neoepitopes are those derived from tumour-specific mutations in coding regions. However, it is important to mention that many antigenic epitopes of cancer cells do not correspond to mutated peptides (Lee *et al.*, 2020). It is now well-established that stressed and infected cells can have defective translation, which generates peptides with non-mutated amino acid sequences that are recognized as neoepitopes. Furthermore, stressed cells may alter their signalling, resulting in altered phosphoproteome (Meyer *et al.*, 2009), acetylome or glycome (Haurum *et al.*, 1999) or other post-translational modifications (Zarling *et al.*, 2000; Mohammed *et al.*, 2008). The resulting peptides can be antigenic and again do not have a mutated amino acid sequence. In the last years, it has been demonstrated that MHC-I can also present exogenous antigens in a process known as cross-presentation (Ulmer, Donnelly and Liu, 1994). This pathway operates in DCs and other phagocytic cells and allow them to acquire antigens from infected or malignant cells and then report their presence to $CD8^+$ T cells in lymphoid organs (Segura and Amigorena, 2015).

MHC-II molecules are expressed by immune cells, such as DCs, B cells, monocytes and macrophages. The MHC-II-associated peptides are 10-25 AAs in length and are derived from extracellular proteins mainly, but it can also present self-proteins that are degraded in the endosomal pathway (Suri, Lovitch and Unanue, 2006) (**Figure 9**). MHC-II molecules are assembled in the ER, and then move to a compartment while being bound

to a low-affinity invariant chain fragment called CLIP. This CLIP fragment is then exchanged for high-affinity peptides (Denzin and Cresswell, 1995), which originate from proteins taken up by endocytosis or phagocytosis that haven been cut by endosomal proteases. Finally, MHC-II molecules move to the plasma membrane, where they present the peptides to naïve $CD4^+$ T cells.

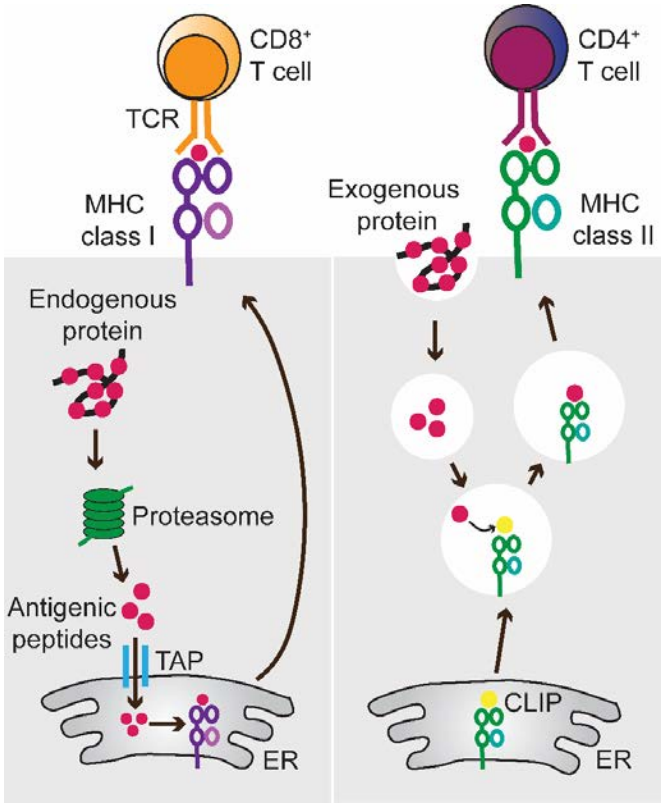

Figure 9 | MHC-I and MHC-II antigen presentation pathways. Endogenous antigens are degraded by the proteasome to produce peptide fragments (left). These peptides translocate to the endoplasmic reticulum (ER) lumen through the transporter associated with antigen processing (TAP), where MHC-I molecules await to be loaded with the appropriate antigens. Only MHC-I with optimal high-affinity peptides leave the ER to present the peptide to $CD8^+$ T cells at the cell surface. In the case of exogenous peptides or peptides derived from proteins degraded in the endosomal compartment, they are presented by MHC-II molecules (right). MHC-II are assembled in the ER, where they bind to a peptide sequence called CLIP and then move to late endosomal compartments. There, CLIP is exchanged by high-affinity peptides, previously cut by endosomal proteases. Finally, MHC-II moves to the cell surface, where it presents the antigens to $CD4^+$ T cells.

5.3. Immune system and cellular reprogramming

The capacity of the innate and adaptive immune system to recognize and target PSCs for elimination has been previously demonstrated. For instance, NK cells (Frenzel *et al.*, 2009;

Dressel *et al.*, 2010) and the complement system (Koch, Jordan and Platt, 2006) have been described to play a role in the rejection of SCs *in vitro* and *in vivo* after transplantation. NK cells also limit teratoma formation after subcutaneous injection of mouse ESCs, iPSCs and maGSCs (Dressel *et al.*, 2008) or human iPSCs (Benabdallah *et al.*, 2019). The sensitivity of PSCs to NK-mediated clearance has been ascribed to the downregulation of MHC-I on the surface of PSCs ("missing self") and to the upregulation of NK-activating ligands (Dressel *et al.*, 2008, 2009, 2010; Frenzel *et al.*, 2009). Indeed, both ESCs and iPSCs have been shown to express very low levels of MHC-I molecules (Drukker and Benvenisty, 2004). In principle, this property should confer them immune privilege properties in front of $CD8^+$ T cells. However, it is known that activated $CD8^+$ T lymphocytes are indeed able to kill PSCs, including multipotent adult germ-line stem cells (maGSCs), ESCs and iPSCs, in a peptide-dependent manner despite low expression of MHC-I molecules (Dressel *et al.*, 2009). Supporting this idea, two reports from the same group proposed that iPSCs share neo-antigens with cancer cells, which makes them suitable immunization agents to promote anti-tumor responses (Kooreman *et al.*, 2018; Ouyang *et al.*, 2021). Indeed, injection of irradiated iPSCs together with the adjuvant CpG prevented tumour growth after malignant cell injection or in a mouse model of pancreatic adenocarcinoma. In both studies, the common antigens identified in iPSCs and cancer cells stimulated cytotoxic $CD8^+$ T cell effector and memory responses. A more recent study obtained similar results when combining irradiated iPSCs with the histone deacetylase inhibitor valproic acid in tumours harbouring stemness features (Kishi *et al.*, 2021). Some studies stated that the DNA damage and the genomic instability that occurs during cellular reprogramming could be the source of these neo-antigens (Mayshar *et al.*, 2010; Ruiz *et al.*, 2015). Overall, literature support the idea that, despite expressing low levels of MHC-I, iPSCs are still able to present immunogenic antigens. Finally, it is important to mention that $CD8^+$ T cells express NKG2D and DNAM-1 receptors in their surface (Drukker and Benvenisty, 2004; Prajapati *et al.*, 2018), which are another source of iPSCs recognition (Dressel *et al.*, 2008, 2009, 2010; Frenzel *et al.*, 2009).

5.4. Immune system and senescence

Cellular senescence is an irreversible arrest of proliferation in damaged or stressed cells maintained by two main pathways: one of them is regulated by p53 (transcriptional regulator) and 21 (cyclin-dependent kinase (CDK)), and the other one is governed by $p16^{INK4a}$ (CDK) and pRB (transcriptional regulator) (Muñoz-Espín and Serrano, 2014). Long-term accumulation of senescent cells occurs in aging and upon cellular damage, producing deleterious effects (van Deursen, 2014; Childs *et al.*, 2016; Farr *et al.*, 2017; Jeon *et al.*, 2017; Bussian *et al.*, 2018; Musi *et al.*, 2018). However, senescent cells also

have beneficial roles in development and reprogramming, by adjusting the plasticity of neighbouring cells (Mosteiro *et al.*, 2016; Ocampo *et al.*, 2016).

Senescent cells are known to interact extensively with the innate immune system (Kale *et al.*, 2020). Their secretion of SASP factors results in local inflammation and recruitment of innate immune cells. Macrophages, for instance, are known to eliminate senescent cells in different physiological and pathological contexts (Irvine *et al.*, 2014; Egashira *et al.*, 2017). SASP generally promotes the proliferation and polarization of macrophages to a pro-inflammatory M1 phenotype (Lujambio *et al.*, 2013). However, studies have shown that some components of the SASP can also induce the conversion to an anti-inflammatory M2 phenotype (Dimitrijević *et al.*, 2016). In response to inflammatory signals, NK cells can also be recruited to the sites of accumulation of senescent cells. Chemotherapy-induced senescence in multiple myeloma tumours induces the upregulation of NKG2D and DNAM-1 ligands, which triggers their elimination by NK cells (Soriani *et al.*, 2009; Antonangeli *et al.*, 2016, 2019). Similarly, in the context of liver fibrosis, senescent stellate cells upregulate NKG2D ligands, supporting NK cell engagement (Krizhanovsky *et al.*, 2008; Sagiv *et al.*, 2016). Nevertheless, some senescent cells acquire strategies to evade clearance by NK cells. For instance, human senescent fibroblasts upregulate HLA-E (Qa-1b in mouse), which interacts with NKG2A to inhibit NK cytotoxicity (Pereira *et al.*, 2019). Moreover, senescent cells can also shed MICA and MICB ligands, the human equivalents of mouse RAE1, by metalloprotease secretion as part of the SASP, which prevents NK cells to bind to senescent cells and kill them (Muñoz *et al.*, 2019). Finally, neutrophils, together with macrophages and NK cells, infiltrate senescent-induced tumours for their elimination. In fact, depletion of all three populations separately delayed tumour regression (Xue *et al.*, 2007).

Regarding the interaction of the adaptive immune system with senescent cells, it is still unknown whether senescent cells harbour specific T cells antigens and, if so, which T cell-mediated immunity is triggered. Nevertheless, it is known that oncogene-induced senescence in melanocytes induces $CD4^+$ T cell recruitment and proliferation (van Tuyn *et al.*, 2017). Similarly, pre-malignant senescent hepatocytes are subject to $CD4^+$ T cell-mediated clearance (Kang *et al.*, 2011). Moreover, it is known that human senescent cells upregulate MHC-I molecules (Pereira *et al.*, 2019). Thus, these studies suggest that T cells could have an important role in eliminating senescent cells.

6. Mouse microbiota and vitamin B12

The mouse gut microbiota is a complex ecosystem composed by thousands of microbial species that vary according to age, sex and mouse strain (J. Wang *et al.*, 2019). In rodents, the microbiota is an important source of B-vitamins. In the case of vitamin B12 (also known as cobalamin), ~20 genera of bacteria are known to produce it (Luczynski *et al.*, 2016). Vitamin B12 is incorporated into the stools of mice, which are later ingested by them, as mice are coprophages. Thus, part of the required vitamin B12 comes indirectly from the microbiota (Kelly *et al.*, 2019) and another considerable part derives from the diet.

6.1. Vitamin B12 in metabolism

In humans and mice, vitamin B12 is used as a cofactor by two enzymes, both of which are essential (Green *et al.*, 2017). The mitochondrial enzyme methylmalonyl-CoA mutase (MUT) is essential for the catabolism of branched-chain AAs via isomerization of methylmalonyl-CoA to succinyl-CoA (**Figure 10A**) (Green *et al.*, 2017). The other B12-dependent enzyme is methionine synthase (MS), which produces methionine from homocysteine in the methionine cycle (**Figure 10B**). Methionine is then converted to S-adenosylmethionine (SAM) by methionine adenosyltrasnferase 2A (MAT2A). Upon donation of SAM methyl group, this metabolite is converted to S-adenosyl-homocysteine (SAH) by methyltransferases (MTs). SAH is hydrolysed in order to generate homocysteine again, which can receive a methyl donation from the folate cycle and be converted back into methionine. The folate cycle, based on the use of vitamin B9 (also known as folate), is essential for the biosynthesis of purine and pyrimidines, which are necessary for DNA replication (Luczynski *et al.*, 2016). The methionine and folate cycles are the major components of the one carbon (1C) metabolism, which allows cells to generate 1C units (also known as methyl groups). Concretely, SAM is the universal methyl donor for all 1C reactions, including protein, DNA, and epigenetic methylation (Green *et al.*, 2017).

B12 deficiency in humans is mainly produced by low intake of B12-rich foods of animal origins, chemical inactivation or inherited disruption of B12 absorption. Without treatment, it can lead to neurological manifestations and haematological complications (Green *et al.*, 2017). Diagnosis is typically based on measurement of vitamin B12 levels. However, normal levels of vitamin B12 in serum can be accompanied by signs of deficiency if there are defects in tissue uptake and action of vitamin B12 at cellular level. Therefore, measurements of metabolites that accumulate as a result of vitamin B12 deficiency, such as methylmalonic acid and homocysteine, is the most accepted method nowadays (Vashi *et al.*, 2016). Vitamin B12 supplementation in diet is enough to reverse

its deficiency when there is not genetic cause, and moderate symptoms are reversible (Green *et al.*, 2017).

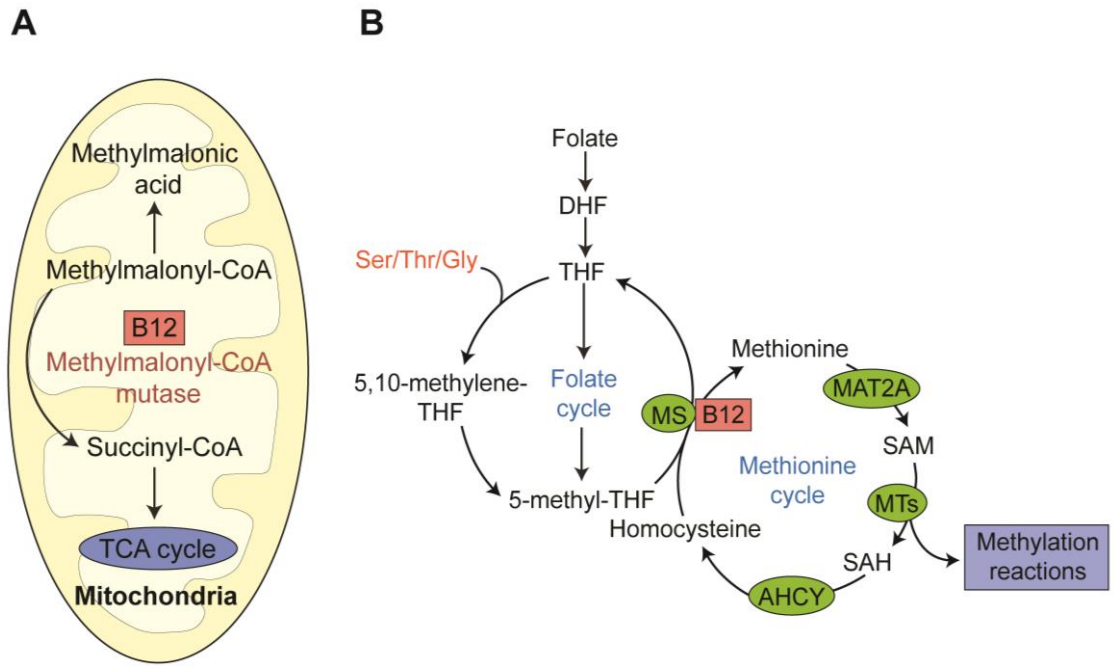

Figure 10 | Vitamin B12 and folate metabolism and functions. A. Schematic overview of methylmalonyl-coA mutase (MUT) enzymatic activity in the mitochondria. Isomerization of methylmalonyl-CoA by MUT with adenosyl-B12 as a cofactor generates succinyl-CoA, which is an intermediary of the tricarboxylic acid (TCA) cycle. This reaction produces methymalonic acid as product. **B**. Methionine is catabolized by methionine adenosyltrasnferase 2A (MAT2A), producing the methyl donor S-adenosylmethionine (SAM). Methyltransferases (MTs) use SAM as a source of methyl groups and generate S-adenosyl-homocysteine (SAH). SAH is then converted to homocysteine by adenosylhomocysteine (AHCY), which can be converted back to methionine by methionine synthetase (MS), thus completing the methionine cycle. MS receives a methyl group from 5-methyltetrahydrofolate (5-methyl-THF), which is part of the folate cycle. 5-methyl-THF is converted to THF, which is used to generate 5,10-methylenetetrahydrofolate (5,10-methylene-THF), the form required for the synthesis of pyrimidines and, later one, of purines. Enzymes are marked in green. Coenzyme vitamin B12 is marked in red. Adapted from Green *et al*., 2017.

6.2. Vitamin B12 in cancer and pluripotency

The 1C metabolism is required for the epigenetic reconfiguration that occurs during cell reprogramming, particularly with respect to the tri-methylation at the 4th lysine residue of the histone H3 protein (H3K4me3) (Ang *et al.*, 2011; Shyh-Chang *et al.*, 2013; Shiraki,

Ogaki and Kume, 2014a). This epigenetic modification is particularly important in bivalent chromatin domains, which is a well-established characteristic of SCs (Bernstein *et al.*, 2006), and for establishing cell identity via Hox gene activation (Bernstein *et al.*, 2006) H3K4me3 is also essential in maintaining the expression of cell identity genes (Bernstein *et al.*, 2006).

In the context of cancer, several studies have demonstrated evidence that tumour-initiating cells present high activity of enzymes related to methionine metabolism, most notably an upregulation of MAT2A activity (Z. Wang *et al.*, 2019). Accordingly, methionine restriction has shown antineoplastic effects in various mouse models (Guo *et al.*, 1993; Poirson-Bichat *et al.*, 1997; Strekalova *et al.*, 2015; Jeon *et al.*, 2016). It is known that many metabolic processes related to the methionine cycle, such as chromatin and acid nucleic methylation, and polyamines synthesis, are also related to cancer biology, creating a link between methionine availability and tumour growth. Currently, therapies targeting components of the methionine cycle, such as MAT2A, are being developed (Bernstein *et al.*, 2006).

Objectives

1- To determine markers of *in vivo* partial reprogramming

- Analysis of changes in histological markers during *in vivo* partial reprogramming
- Identification of cytokines and metabolites in serum during *in vivo* partial reprogramming

2- To decipher the interplay between immune system and *in vivo* reprogramming

- Analysis of immune cell infiltration during *in vivo* partial reprogramming at single-cell level
- Identification of immune populations that modulate the efficiency of *in vivo* reprogramming and characterize their mechanism of action

3- To investigate the metabolic requirements of *in vivo* reprogramming related to mouse intestinal microbiota

- Identification of microbial-derived metabolites required for *in vivo* reprogramming and characterization of their mechanism of action

Materials & Methods

1. Mouse experimentation

1.1. Animal procedures

All mice were bred and maintained at the animal facilities of the Barcelona Science Park in strict accordance with the Spanish and European Union regulations. Animal procedures were performed according to protocols approved by the Animal Care and Use Ethical Committee (IACUC) of Barcelona Science Park and the Catalan Government. Mice were housed at specific pathogen free (SPF) barrier area with access to *ad libitum* standard chow diet. Animal experiments were designed and conducted with consideration of the ARRIVE guidelines and mice were sacrificed when they presented signs of morbidity in accordance to the *Guidelines for Humane Endpoint for Animals Used in Biomedical Research* from the Council for International Organization of Medical Sciences (CIOMS). Experiments were performed with male and female mice of 8-16 weeks of age. All animals were sacrificed by cervical dislocation, unless blood extraction from the heart was performed. In that case, mice were sacrificed in a CO_2 chamber.

1.2. Mouse model

The reprogrammable *i4F* mouse strain was previously generated in the laboratory in a pure C57BL/6J.Ola.Hsd genetic background (Abad *et al.*, 2013). *i4F-B* strain contains an ubiquitous doxycycline-inducible transgene encoding for the four Yamanaka factors *Oct4, Sox2, Klf4* and *cMyc* (OSKM) inserted in the *Pparg* gene and the transcriptional activator (rtTA) within the *Rosa26* locus (Hochedlinger *et al.*, 2005). All mice included in this thesis were heterozygous for both OSKM and rtTA transgenes. Mice were genotyped at Transnetyx Enterprise (Cordova, TN, 38016).

1.3. Doxycycline treatment

Doxycycline hyclate BioChemica (PanReac, A2951) was administered in the drinking water (1 mg/ml) supplemented with 7.5% sucrose for 7 days. In the experiment of *in vivo* reprogramming using T cell-depleting antibodies, doxycycline at lower concentration (0.2 mg/ml) was administrated for 14 days.

1.4. Caerulein treatment

Mild acute pancreatitis was induced by seven intraperitoneal injections, given once per hour, of a pancreatic secretagogue cholecystokinin (CCK) analogue called caerulein (Bachem) at 100 µg/kg for two consecutive days. A second group of control animals received injections of PBS only. Mice were sacrificed at day 4 after the first injection.

1.5. Vitamin B12 treatment

Vitamin B12 (Sigma, V2876) supplementation was provided at 1.25 mg/l in the drinking water supplemented with 7.5% sucrose for 7 days concomitant with doxycycline (1 mg/ml) treatment.

1.6. scAAV8 injections

AAV8 virus were kindly provided by Dr. Dirk Grimm (Heidelberg University Hospital, Germany) and were produced as described elsewhere (Senís *et al.*, 2018). WT male mice were retro-orbitally injected with scAAV8 SFFV-hCO-O/K/S/M vectors at doses of $1x10^{11}$ vg/vector. A scAAV8 vector encoding GFP was added as tracer at the same concentrations. During the whole experiment, 200 µg of anti-NK1.1 (clone PK136, BioxCell) or its isotype control, IgG2a (clone C1.18.4, BioxCell), were injected intraperitoneally once a week until the end of the experiment. Mice were sacrificed when teratomas were palpable.

1.7. Depleting antibodies administration

Immune populations were depleted by intraperitoneal injection of 200 µg of anti-NK1.1 (clone PK136, BioxCell) or 200 µg of anti-Gr1 (clone RB6-8C5, BioxCell) at days -1, 3 and 5 of reprogramming. Isotypes control IgG2a (clone C1.18.4, BioxCell) and IgG2b (clone LTF-2, BioxCell) were used in control groups, respectively. For T lymphocyte depletion, 100 µg of anti-CD4 (clone GK1.5, BioxCell) and anti-CD8 (clone 2.43, BioxCell) were administrated at days -1 and 4 of reprogramming for the experiment of 7 day, and at day 11 additionally in the case of 14 days of reprogramming. The control group received 100 µg of IgG2b (clone, LTF-2, BioxCell). For the depletion of macrophages, mice received 200 µl of either clodronate or empty liposomes (Clodronate Liposomes) retroorbitally at days 1, 3 and 6 of reprogramming.

2. Cell culture techniques

2.1. Cell lines and culture conditions

Primary Mouse Embryonic Fibroblasts (MEFs) were obtained from *i4F* or WT embryos at E13.5 as previously described (Serrano *et al.*, 1997). MEFs were maintained in Dulbecco's modified Eagle's medium (DMEM) (Gibco) supplemented with 10% heat inactivated Fetal Bovine Serum (FBS) (Gibco) and penicillin-streptomycin (Gibco). MEFs undergoing reprogramming were cultured in "iPSC medium", composed by high glucose DMEM (Gibco) supplemented with 15% of KnockOut Serum Replacement (KSR) (Life

Technologies), LIF (1000 U/ml), non-essential amino acids, penicillin-streptomycin (Gibco) and 100 µM β-mercaptoethanol (Life Technologies, 31350010). Murine ES cells were cultured over gelatin-coated plates and maintained in iPSC medium. YAC-1 cells were cultured in RPMI-1640 media (Sigma, R8758) supplemented with 10% FBS at a density of $2x10^5$ - $2x10^6$ cells/mL. Cells were maintained in a humidified incubator at 37 °C with 5% CO_2. Cultures were routinely tested for mycoplasma and were always negative.

2.2. NK cell isolation and adoptive transfer

NK cells were enriched from the spleen of WT C57BL/6J mice via negative selection (Miltenyi Biotec NK cell isolation kit, 130-115-818) and treated with 100 ng/ml of IL-2 (Preprotech, 212-12) and 50 ng/ml of IL-15 (Preprotech, 210-15) for 24h in 96 well-plate ($1x10^5$ NK cells/well). NK cell culture medium was composed by RPMI-1640 (Sigma, R8758) supplemented with 10% FBS, 2mM L-glutamine, 100 µg/ml penicillin-streptomycin, 10mM HEPES, non-essential amino acids (all from Life Technologies), and 0.5 mM sodium pyruvate (Gibco). Next, day, 3.8×10^6 NK cells were injected retroorbitally into recipient mice in 150 µl of PBS at day 3 of *in vivo* reprogramming.

2.3. Isolation of pancreatic cells

To isolate all pancreatic cell types, tissue was digested using 1 mg/ml Collagenase P (Sigma, 11213865001), 2 U/ml Dispase II (Life Technologies, 17105041), 0.1 mg/ml Soybean Trypsin Inhibitor (Life Technologies, 17075-029) and 0.1 mg/ml DNase I (Sigma, D4513) in HBSS with Ca^{2+}/Mg^{2+} (Life Technologies, 14025050). Tissue dissociation was performed using the gentle MACS™ Octo Dissociator (Miltenyi Biotech) at 37°C for 40 min. The tissue was further digested with 0.05% Trypsin-EDTA (Life Technologies, 25300062) for 5 min at 37°C and erythrocytes were removed with red blood cell lysis buffer (Biolegend, 420301).

2.4. *In vitro* reprogramming assays

At passage one, $6x10^4$ MEFs were seeded in 12 well-plates (Corning) with Dulbecco's modified Eagle's medium (DMEM) (Gibco) supplemented with 10% heat inactivated Fetal Bovine Serum (FBS) (Gibco) and penicillin-streptomycin (Gibco). Next day, medium was washed away and "iPSC medium" supplemented with doxycycline (Sigma) at 1 µg/ml was used to induce OSKM-cassette expression. Medium was changed every other day until iPSC colonies appeared at day 11. Cells were then fixed with 4% paraformaldehyde (Aname S.L), washed with PBS and incubated from 30 minutes to 1 hour in Alkaline

Phosphatase staining solution (AP Blue Membrane Substrate Solution, Sigma). AP^+ colonies per well were scored to determine the efficiency of reprogramming.

For vitamin B12 effects on *in vitro* reprogramming, $3.6x10^5$ MEFs were seeded in 6 well-plates (Corning). Next day, iPSC medium with doxycycline (1 µg/ml) was added and the same reprogramming protocol was followed. MEFs were reprogrammed in the presence of vitamin B12 (2µM) (Sigma, V2876), MAT2A inhibitor PF-9366 (2µM) (MedChemExpress #HY-107778) or SAM (20µM) (Merck Life Science, A4377).

2.5. *In vitro* co-culture assays

For co-culture experiments, NK cells were isolated and activated *in vitro* as previously described. NK cells were co-cultured with MEFs from day 2 to day 6 of *in vitro* reprogramming in DMEM supplemented with 10% FBS (Life Technologies), LIF (1,000 U ml1) (Merck Chemicals), non-essential amino acids (Life Technologies), 10 mM HEPES penicillin-streptomycin (Gibco), 100 µM β-mercaptoethanol (Life Technologies), doxycycline (1 µg/ml, Sigma), 100 ng/ml of IL-2 (Preprotech, 212-12) and 50 ng/ml of IL-15 (Preprotech, 210-15). At day 6, NKs were removed and the culture was washed with PBS once before adding iPSC media. *In vitro* reprogramming continued until the appearance of iPSC colonies around day 11. AP^+ colonies per well were scored to determine the efficiency of reprogramming as previously described. E:T ratios were 0.5:1, 2,3:1 and 4,5:1. To test the mechanism of killing, NK:MEF co-coculture was performed in the presence of the granule exocytosis inhibitor Concanamycin A (100 nM, Merck Life Science S.L.U, 27689) at E:T ratio of 1:1. For the transwell experiment, NK cells were seeded on top of 12 mm Transwell® with 0.4 µm Pore Polycarbonate Membrane Insert (Corning, 3401) at day 2 of reprogramming (E:T ratio 1:1). Transwells were removed at day 6 of reprogramming. NKG2D receptor was blocked by adding mouse NKG2D/CD314 antibody (20 µg/ml) (Bio-Techne R&D Systems S.L, MAB1547-500) to the co-culture at days 2 and 4 of reprogramming (E:T ratio 1:1). For the cytotoxic assay, YAC-1 cells were kindly donated by Dr. Domingo Barber (CNB-CSIC). NK cells were isolated from *i4F* and WT mice treated with doxycycline for 5 days. They were primed *in vitro* with IL-2 and IL-15 in the presence of doxycycline (1 µg/ml) for 6 days, and they were co-cultured with YAC-1 cells for 4h. $DAPI^+$ YAC-1 cells were quantified by flow cytometry.

2.6. Pancreatic organoids

Pancreas were dissociated to the single cell level as described above. A total of $3x10^5$ cells were embedded in 200 µl growth factor reduced Matrigel droplets (Corning, 356231) in 6-well plates (Corning). Matrigel droplets were solidified at 37°C for 15 min. Pancreatic

organoid media, previously described elsewhere (Huch, Bonfanti, *et al.*, 2013), was composed by Advanced DMEM/F12 (Gibco,12634010) supplemented with 1.25 mM N-Acetylcysteine (Sigma), 10 nM gastrin (Sigma) B-27 without Vitamin A (Gibco) and the growth factors: 100 ng/ml FGF10 (Peprotech), 50 ng/ml EGF (Peprotech), 1 ug/ml R-spondin 1 (produced by Protein Expression Core Facility in IRB), 100 ng/ml Noggin (Peprotech) and 10 mM Nicotinamide (Sigma). Media was refreshed every 2 days and it was supplemented with doxycycline (1 µg/ml) to activate the OSKM cassette. At day 5 after seeding, 10 representative 4x fields per sample were taken to measure organoid size using Image J software (version 1.53g). At day 8, macroscopic pictures of the wells were taken with a camera to check the full formation of organoids. All analysis were conducted in a blinded way.

3. Molecular biology techniques

3.1. Flow cytometry

Blood to assess immune cells depletion was collected in EDTA-coated tubes (16.444, Microvette®) and incubated with red blood cell lysis buffer (Biolegend, 420301) for 5 min. Cells were then washed once with PBS and pre-incubated for 5 min with Mouse BD Fc Block™ containing purified anti-mouse CD16/CD32 mAb 2.4G2 at 1 µg/1 million cells in 100 µl (BD Biosciences, 553142) of FACS buffer (0.5% BSA and 5 mM EDTA in PBS) for 15 min at 4°C. After the washing step with FACS buffer, cells were incubated with the appropriate antibody for 40 min at 4°C (**Table 1**). After 3 more washes with FACS buffer, DAPI was added as marker of viability.

For the analysis of infiltrating cell populations, pancreas were digested as previously described and immune cell types were stained following the same protocol (**Table 1**), but keeping the samples at room temperature (RT). Cells were acquired by a Gallios Flow Cytometry System (Beckman Coulter) or in a FACSAria Fusion (BD Biosciences), depending on the experiment.

For the characterization of NK cell surface receptors, pancreatic cells were stained with the LIVE/DEAD™ Fixable Blue Dead Cell Stain Kit (Thermo Fisher Scientific, L23105) to evaluate viability during 15 min. After the washing step with PBS, cells were incubated for 20 min with a combination of anti-mouse antibodies (**Table 1**). Isotype control antibodies were used as negative controls. Cells were acquired by a BD LSRFortessa™ Flow Cytometer at Hospital Clinic (Barcelona). All data were analysed by FlowJo v10 software (BD Biosciences) and GraphPad Prism 9.0.1.

Table 1 | List of fluorescent antibodies used for cytometry analyses.

Antibody	Source	Identifier	Dilution
CD107a BV711	Biolegend	564348	1:100
CD11b A488	BioLegend	101219	1:200
CD11b PECy7	eBioscience	25-0112-82	1:300
CD11b PerCPCy5.5	eBioscience	45-0112-82	1:400
CD19-B220 APC-eF780	eBioscience	47-0452-80	1:200
CD3 AF700	eBioscience	56-0032-82	1:100
CD3 APC	eBiosciences	17-0032-80	1:300
CD3 FITC	Biolegend	100203	1:100
CD4 PE EF610	eBioscience	61-0042-80	1:400
CD45 PE	BD Biosciences	553081	1:400
CD45 PerCP	BioLegend	103130	1:200
CD8 FITC	eBioscience	11-0081-82	1:400
F4/80 AF647	BioLegend	123122	1:100
F4/80 APC	BioLegend	123115	1:100
Ly49CI BV421	BD Biosciences	744027	1:100
Ly6C FITC	BD Biosciences	561085	1:300
Ly6G PE	BD Biosciences	561104	1:300
NK1.1 APCCy7	BioLegend	108723	1:400
NKG2A/CD159A PECy7	Biolegend	142809	1:100
NKG2A/E/C FITC	BD Biosciences	550520	1:150
NKG2D/CD314 PE	Biolegend	130207	1:100

3.2. Determination of cytokine levels in serum

Serum was obtained from blood of *i4F* (n=4) or WT mice (n=5) treated with doxycycline (1 mg/ml) at the indicated time points. Whole blood was spun down for 10 minutes at 2500 g at 4°C and supernatant (serum) was separated, diluted 1:2 in PBS and stored at -80°C. Samples were analysed for cytokine and chemokine levels using the Mouse Cytokine 32-Plex Discovery Assay (Eve Technologies Corporation, Calgary, AB). Missing values correspond to extrapolated or out of range values.

3.3. Amylase and urea analysis

Serum was obtained from blood of WT (n=6) and *i4F* mice treated with isotype control (n=6) or anti-NK1.1 antibodies (n=6) at day 7 of doxycycline (1 mg/ml) administration in water. Whole blood was spun down for 10 minutes at 2500 g at 4°C and supernatant (serum) was separated and stored at -80°C. Samples were analysed with amylase and urea

kits (Spinreact, SP41201 and SP41041, respectively) following manufacturer's instructions in a Spinlab 100 (Spinreact, 9-9059) machine.

3.4. Vitamin B12 serum analysis

Mouse serum was diluted 1:20 in PBS and holotranscobalamin (holoTC) was measured using an ADVIA Centuar Immunoassay System (SIEMENS) with ADVIA Centuar Vitamin B12 Test Packs (07847260) according to manufacturer's instructions.

3.5. Metabolomics analysis

Mouse serum

Blood was harvested via cheek vein bleed (D0, 2, 4) or intracardiac puncture following deep CO_2 anesthetization (D7). Whole blood was spun down for 10 minutes at 6000 rpm at 4°C and supernatant (serum) was separated and stored at -80°C.

Standard and reagents

Acetonitrile (Sigma Aldrich), Isopropanol (Sigma Aldrich), Methanol (Sigma Aldrich), Chloroform (Sigma Aldrich), Acetic acid (Sigma Aldrich), Formic acid (Sigma Aldrich), Methoxyamine hydrochloride (Sigma Aldrich), MSTFA - N-Methyl-N-(trimethylsilyl) trifluoroacetamide (Sigma Aldrich), Pyridine (Sigma Aldrich), 3 nitrophenylhydrazine (Sigma Aldrich), *N*-(3-Dimethylaminopropyl)-*N*′-ethylcarbodiimide hydrochloride (EDC) (Sigma Aldrich), Sulfosalicylic acid (Sigma Aldrich) as previously described (Viltard *et al.*, 2019).

Sample preparation serum (lithium heparin)

A volume of 25 µL of serum were mixed with 250 µL a cold solvent mixture with ISTD (MeOH/Water/Chloroform, 9/1/1, -20°C), into 1.5 mL microtube, vortexed and centrifugated (10 min at 15000 g, 4°C). Upper phase of supernatant was split in three parts: 50 µL were used for GC-MS experiment in injection vial, 30 µL were used for the SCFA (Short Chain Fatty Acids) UHPLC-MS method, and 50 µL were used for others UHPLC-MS experimentations.

Widely-targeted analysis of intracellular metabolites gas chromatography (GC)

GC-MS/MS method was performed on a 7890B gas chromatography (Agilent Technologies, Waldbronn, Germany) coupled to a triple quadrupole 7000C (Agilent Technologies, Waldbronn, Germany) equipped with a High sensitivity electronic impact source (EI) operating in positive mode.

Targeted analysis of bile acids

Targeted analysis was performed on a RRLC 1260 system (Agilent Technologies, Waldbronn, Germany) coupled to a Triple Quadrupole 6410 (Agilent Technologies) equipped with an electrospray source operating in positive mode. Gas temperature was set to 325°C with a gas flow of 12 L/min. Capillary voltage was set to 4.5 kV.

Targeted analysis of polyamines

Targeted analysis was performed on a RRLC 1260 system (Agilent Technologies, Waldbronn, Germany) coupled to a Triple Quadrupole 6410 (Agilent Technologies) equipped with an electrospray source operating in positive mode. The gas temperature was set to 350°C with a gas flow of 12 l/min. The capillary voltage was set to 3.5 kV.

Targeted analysis of Short Chain Fatty Acid

Targeted analysis was performed on a RRLC 1260 system (Agilent Technologies, Waldbronn, Germany) coupled to a 6500+ QTRAP (Sciex, Darmstadt, Germany) equipped with an electrospray ion source.

Untargeted analysis of intracellular metabolites

The profiling experiment was performed with a Dionex Ultimate 3000 UHPLC system (Thermo Scientific) coupled to a Q-Exactive (Thermo Scientific) equipped with an electrospray source operating in both positive and negative mode and full scan mode from 100 to 1200 m/z. The Q-Exactive parameters were: sheath gas flow rate 55 au, auxiliary gas flow rate 15 au, spray voltage 3.3 kV, capillary temperature 300°C, S-Lens RF level 55 V. The mass spectrometer was calibrated with sodium acetate solution dedicated to low mass calibration.

MetaboAnalyst

The peak areas (corrected to quality control) corresponding to each annotated metabolite identified in the serum of wild type (WT) *versus* reprogrammable *i4F* mice (n=5/group) at day 7 after doxycycline treatment were converted to log2 values. Data were represented as log2 fold change (log2 FC) values to each mouse at day 0 (prior to doxycycline administration). Metabolic pathway impact was calculated by Global ANCOVA pathway enrichment and Outdegree Centrality Topology analysis through the MetaboAnalyst 4.0 software (Chong and Xia, 2020), using KEGG library as reference.

Differential expression of metabolites

Significantly changed metabolites were calculated using a moderated t-Test by empirical Bayes shrinkage, in which *i4F* mice were compared to WT mice at the different time points

studied (D0, D2, D4 and D7). Multiple contrasts adjustment was performed using Benjamini-Hoechberg false discovery rate (Benjamini and Hochberg, 1995).

3.6. RNA isolation and mRNA levels quantification

For *in vitro* experiments, total RNA was extracted from MEFs with Trizol (Invitrogen), following the providers recommendations. 1 µg of total RNA was retrotranscribed into cDNA using iScript cDNA Synthesis kit (BioRad, 170-8891). For pancreas samples, total RNA was isolated by acid guanidinium thiocyanate-phenol-chloroform extraction. Up to 5 µg of total RNA was reverse transcribed into cDNA using iScriptTM Advanced cDNA Synthesis Kit (BioRad, 172-5038). Quantitative real time-PCR was performed using Sybr Green Power PCR Master Mix (Promega Biotech, A6002) in a QuantStudio 6 Flex thermocycler (Applied Biosystem). CT value was normalized to *Gapdh*, using the ΔΔCt method. Primers used are listed in **Table 2**.

Table 2 | List of primers used for mRNA expression analyses.

Gene	Forward	Reverse
E2A-cMyc	GGCTGGAGATGTTGAGAGCAA	AAAGGAAATCCAGTGGCGC
Sox2-Klf4	ACTGCCCCTGTCGCACAT	CATGTCAGACTCGCCAGGTG
Nanog	AGGTCGGTGTGAACGGATTTG	TGTAGACCATGTAGTTGAGGTCA
Rae1	ACCCGAATGCAGACAGGAAGTTGA	GGACCTTGAGGTTGATCTTGGCTT
Mult1	CAATGTCTCTGTCCT CGGAA	CTGAACACGTCTCAGGCACT
Icam1	CTGTTTGAGCTGAGCGAGAT	AGGGTGAGGTCCTTGCCTAC
Fas	TATCAAGGAGGCCCATTTTGC	TGTTTCCACTTCTAAACCATGCT
CD155	CAACTGGTATGTTGGCCTCA	ATTGGTGACTTCGCACACAA
Gapdh	AGGTCGGTGTGAACGGATTTG	TGTAGACCATGTAGTTGAGGTCA

3.7. Single cell RNA sequencing

Single cell suspension of pancreatic cells was obtained as previously described, and DAPI-negative cells were selected by cell sorting using Flow Cytometry.

Libraries preparation and mRNA sequencing

Cells were loaded onto a 10x Chromium Single Cell Controller chip B (10x Genomics) as described in the manufacturer's protocol (Chromium Single Cell 3′ GEM, Library & Gel Bead Kit v3, PN-1000075). Generation of gel beads in emulsion (GEMs), barcoding, GEM-RT clean up, cDNA amplification and library construction were performed following the manufacturer recommendations. Libraries were loaded at a concentration of 1.8 pM and sequenced in an asymmetrical pair-end format in a NextSeq500 instrument (Illumina).

Data computational analysis

Cell Ranger matrix data (barcodes, features, and count matrix) were loaded onto the Seurat R package (version 3.1.0.). Each condition (WT, CER and *i4F*) was analysed separately as a merge from the corresponding replicates. Ambient RNA contamination was estimated and corrected using SoupX (Young and Behjati, 2020). Cells expressing < 150 genes and > 5% of mitochondrial genes were excluded, considered as low quality cells. Dimensionality of the datasets was set to the first 20 principal components based on the result of the JackStraw analysis and the stabilization of the elbow plot. Normalization and variance stabilization of filtered cells was carried out using negative binomial regression (SCTranform function) (Hafemeister and Satija, 2019). Cluster stability was visualized at different resolutions using clustree (Zappia and Oshlack, 2018). Resolution was set to 0.2 for the three datasets. Cell clusters were manually annotated based on the significant markers using FindAllMarkers function. Immune cells for each dataset were extracted as raw counts and merged together for the immune combined analysis. Normalization, dimensionality reduction, clustering and cell annotation was carried out in the immune dataset as mentioned before. All the datasets were visualized using UMAP projection (Becht *et al.*, 2019).

3.8. Immunopeptidome

WT and *i4F* MEFs were cultured *in vitro* in the presence of iPSC media (see above) and doxycycline (1 µg/ml, Sigma) for 5 days (n=4 for i4F group and n=3 for WT group). Senescent MEFs were obtained after treating them with doxorubicin (100 nM) for 10 days. Cells were then trypsinized, counted (100 x 10^6 cells/condition), washed twice with PBS and frozen at -80℃ for further analysis (**Figure 11**).

Upon arrival to CHU Sainte-Justine Research Center (Montreal), cell pellets were thawed and resuspended in 0.5 ml of cold PBS. The equivalent volume of 2x cell lysis buffer, prepared as previously described (Kovalchik *et al.*, 2020), was added to the cells in PBS and cell lysates were rotated (20 rpm) for 1 hour at 4℃. Cell lysates were then harvested 20 min at 17927 g at 4℃. Supernatants were transferred into new 2.0 ml tubes and kept on ice. Samples were solubilized in 5% ACN-4% formic acid (FA). Next, sepharose-CNBr activated beads were coupled with 1 mg of monoclonal antibodies anti-mouse MHC-I: H2-Kb (Y-3, BE0172, BioxCell) and H2-Db (B22-249.R1, MA5-17992, ThermoFisher). Sepharose antibody-coupled beads were incubated overnight with the cell lysate in a Bio-Rad column at 4℃ using a slow rotating wheel (22 rpm). MHC-I-ligand complexes were eluted from the beads with 2 x 300 µl of 1% trifluoroacetic acid (TFA) and kept on ice. Peptides were further eluted with 3 x 200 ul of 28%ACN-0.1%TFA. The flowthrough containing the eluted peptides was stored at -20℃. Data acquisition was done

by different liquid chromatography coupled to a triple quadrupole mass spectrometry (LC-MS/MS) systems in data-dependent acquisition (DDA) mode, as previously described (Schuster *et al.*, 2018). The identified peptides were clustered (GibbsCluster v.1), classified by length and predicted MHC-I binding affinity (NetMHCpan4.0). The final list of MHC-I-associated peptides (non-binders, weak-binders and strong-binders) were annotated in high-quality H2Db- and H2Kb-specific peptide spectral and assay libraries. Analysis of the number of common peptides between conditions was performed using Venn's diagrams (Venny 2.1.0).

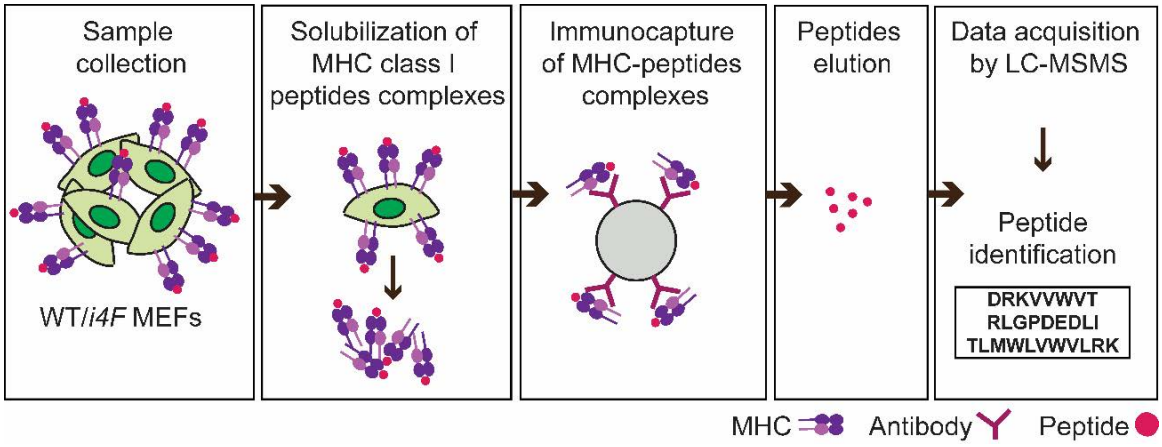

Figure 11 | Schematic overview of MHC-I-associated peptides isolation. MEFs were collected and MHC-I-peptide complexes were solubilized. Then, isolation of H2-Db and H2-Kb-associated peptides was done separately by immunoaffinity purification using monoclonal anti-mouse MHC-I antibodies (B22-249.R1 and Y-3, respectively). Acid-eluted peptides were identified by different liquid chromatography coupled to a triple quadrupole mass spectrometry (LC-MS/MS) systems in data-dependent acquisition (DDA) mode. Binding predictions for these subsets were made using NetMHCpan4.0.

4. Immunohistochemistry

4.1. Senescence-associated β-galactosidase staining of histological sections

Pancreas were isolated and quickly embedded in O.C.T^{TM} Compound Containing (Tissue-Tek, 4583). Samples were frozen in an isopentane-cointaining bucket surrounded by liquid nitrogen for 10 min. Then, tissue cryosections of 7 µm were cut in a rotary microtome cryostat (Leyca) and fixed in fixing solution, composed by 5 nM EGTA, 2 mM $MgCl_2$, 0.2% glutaraldehyde in 0.1 M phosphate buffer for 10 min. Then, slices were washed once with PBS and stained in staining solution overnight at 37°C. Staining solution contained citric acid (40 mM), potassium cyanoferrate (II) and (III) (5mM), sodium chloride (150

mM) and magnesium chloride (2 mM) dissolved in 0.1M phosphate buffer, plus X-gal (100mg/mL) (Melford, B71800) previously dissolved in DMF (Sigma, D4551). Next day, sections were washed 3 times with PBS to remove the staining solution. Then, they were counterstained with nuclear fast red, dehydrated and mounted.

4.2. Immunohistochemistry of tissue samples

Samples were fixed overnight at 4ºC with neutral buffered formalin (HT501128-4L, Sigma-Aldrich). Paraffin-embedded tissue sections (2-3 µm) were dried at 60ºC over-night and dewaxed.

For haematoxylin and eosin (HE) staining, a standard protocol using CoverStainer (Dako-Agilent) was performed. For some antibodies, immunohistochemistry was performed using a Ventana discovery XT for 60 minutes (min): NANOG D2A3 (Cell Signaling, 8822) at 1:100 - 1:250, F4/80 (eBioscience, clone BM, 14-4801-85) at 1:100, CD45-B220 (BD Biosciences, 550286) at 1:200 and p21 clone HUGO 291H/B5 (CNIO) RTU for 60 min. For the rest of antibodies, immunohistochemistry was performed manually or with the Leica Bond RX platform: CD3 (Dako-Agilent, 11503) at 1:10 for 120min, CD4 (Sino Biological, 50134R001) at 1:2000 for 120 min, CD8α [EPR20305] (Abcam, ab209775) at 1:1000 for 120 min, KLRBL/CD161 (E6Y9G) (Cell Signalling, 39197S) at 1:500 for 120min, NE (Abcam, ab68672) at 1:1000 for 120min, FOXP3 (Cell Signalling, 12653) at 1:750 for 60min and e-cadherin Clone 36 (BD 610181, Becton Dickinson, S.A.) at 1:300 for 120 min.

Antigen retrieval for NANOG, CD45-B220 and p21 was performed with Cell Conditioning 1 (CC1) buffer (Roche, 950-124) and for F4/80 with proteinase K (Dako-Agilent, S3020) for 5 min at RT. Secondary antibodies used were the OmniMap anti-Rat HRP (Roche, 760-4457) or OmniMap™ anti-Rb HRP (Roche, 760-4311). Blocking was done with Casein (Roche, 760-219). Antigen-antibody complexes were revealed with ChromoMap DAB Kit (Roche, 760-159). For CD3, CD4, CD8α, NE, FOXP3, KLRBL/CD161 and e-cadherin antigen retrieval was performed with BOND Epitope Retrieval Solution 1 (AR9961, Leica Biosystems), with BOND Epitope Retrieval Solution 2 (Leica Biosystems, AR9640), with Envision FLEX Target retrieval Solution HIGH pH (Dako-Agilent, K8004) or with Trizma Base/EDTA pH 9.0 (T6066-1 Kg /E51345006). Blocking was performed with Peroxidase-Blocking Solution at RT (Agilent, S2023) and 5 % of goat normal serum (Life Technology, 16210064) mixed with 2.5 % BSA diluted in wash buffer for 10 and 60 min at RT. The secondary antibody used was the BrightVision poly HRP-Anti-Rabbit IgG, incubated for 45 min (ImmunoLogic, DPVR-110HRP) or the polyclonal Goat Anti-Mouse (Dako-Agilent, P0447). Antigen–antibody complexes were

revealed with 3-3′-diaminobenzidine (Leica Biosystems, RE7230-K). Sections were counterstained with hematoxylin (Dako-Agilent, CS700) and mounted with Mounting Medium, Toluene-Free (Agilent, CS705) using a Dako CoverStainer. CPA1 (R&D Systems, AF2765), PTF1a (CNIO, mad in house), KRT19 (CNIO Monoclonal Antibodies Core Unit, AM-TROMA III) and HNF1β (Cell Signalling Technology, 89670) staining were performed in the Histopathology Unit of CNIO according to their protocols.

Specificity of staining was confirmed by staining with a rat IgG (R&D Systems, Biotechne, 6-001-F), mouse IgG (Abcam, ab37355) or a Rabbit IgG (Abcam, ab27478) isotype controls. Brightfield images were acquired with a NanoZoomer-2.0 HT C9600 digital scanner (Hamamatsu) equipped with a 20x objective.

4.3. Image acquisition

Brightfield images were acquired with a NanoZoomer-2.0 HT C9600 digital scanner (Hamamatsu) equipped with a 20x objective. All images were visualized with a gamma correction set at 1.8 in the image control panel of the NDP.view 2 U12388-01 software (Hamamatsu, Photonics, France).

4.4. Histopathological evaluation

Brightfield images of immunohistochemistry were quantified in a blinded way using QuPath software 0.1.2 (Bankhead *et al.*, 2017) with standard DAB detection methods. Reprogramming efficiency in the pancreas was evaluated and quantified by histopathological assessment of dysplastic areas. The rest of the organs were evaluated by focusing on the appearance of hyperplastic and dysplastic changes of epithelial cells. The severity and extension of the lesions were measured using a semi-quantitative grading system. Multifocal areas of glandular (stomach) and intestinal (small and large) crypt epithelial cell hyperplasia/dysplasia were scored from 0 to 5, in which 0 = no lesion; 1 = very slight; 2 = slight, 3 = moderate; 4 = intense and 5 = very intense. Tubular dilatation in the renal cortex of the kidney and renal pelvis dilatation were also scored from 0 to 5 following the same criteria.

5. Statistical analysis

The data were analysed using GraphPad Prism v.9.0.1 software and represented as mean ± SD or mean ± SEM of independent biological replicates (mice or clones of MEFs). Statistical analyses were performed using an unpaired two-tailed Student's t-test to

compare the means between two different groups. Means of multiple groups were compared by one-way analysis of variance (ANOVA). Differences were considered significant based on the P value (*p<0.05; **p< 0.01; ***p< 0.001; ****p< 0.0001).

6. GSEA analysis

GSEA (Subramanian *et al.*, 2005) was used to perform a gene set enrichment analysis of the NK cell mediated cytotoxicity KEGG pathway (entry: mmu04650). Previously published RNA-sequencing data generated in our laboratory from the pancreas of *i4F* and *i4F*;*p53*-null mice was pre-ranked by statistic and it was run with 1000 permutations, setting 'gene set' as the permutation method.

Results

PART 1. Markers of *in vivo* dedifferentiation induced by the 4 Yamanaka factors

In the last decades, great efforts have been made in identifying characteristic markers of the different phases of cellular reprograming, as it is a very heterogeneous process in which cells at different stages co-exist in time. Most of our current knowledge derives from *in vitro* studies (Brambrink *et al.*, 2008; Stadtfeld, Nagaya, *et al.*, 2008; Samavarchi-Tehrani *et al.*, 2010; Buganim *et al.*, 2012; Polo *et al.*, 2012). However, *in vivo* reprogramming presents extra layers of complexity, including the tissue microenvironment, the interplay with the immune system and the availability of specific metabolites. On the other hand, deciphering *in vivo* reprogramming is essential for advancing into its potential clinical applications. For this reason, we focused on describing new markers of cellular reprogramming in an *in vivo* context.

We have used a mouse model generated in our lab that contains a single tetracycline-inducible lentiviral transgene with the OSKM TFs and a single copy of a reverse tetracycline transactivator (rtTA) in the *Rosa26* locus, which is ubiquitously expressed (Abad *et al.*, 2013) (**Figure 12**). The tetracycline-inducible polycistronic cassette encodes for the four murine OSKM TFs separated by 2A peptides and its activation results in a synchronized and stoichiometric expression of these four genes (Carey *et al.*, 2009). The cassette is located within an intron of the *Pparg* locus, in the same chromosome as the gene *Rosa26*. Thus, both genes co-segregate to the progeny. In the original paper, this mouse model was referred to as i4F-B line, standing for "inducible four factors", as 2 different mouse lines were generated (i4F-A and i4F-B) (Abad *et al.*, 2013). In this thesis, we will refer to i4F-B as reprogrammable or *i4F* mouse model for the sake of simplicity.

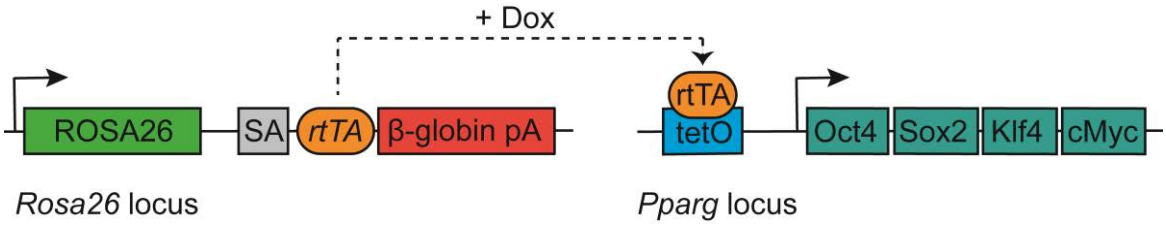

Figure 12 | Reprogrammable or *i4F* mouse model. Reprogrammable mice carry a tetracycline-inducible polycistronic transgene that encodes for four murine TFs (OCT4, SOX2, KLF4 and c-MYC) and a copy of a reverse tetracycline transactivator (rtTA) in the *Rosa26* locus. The transgene is integrated within an intron of the *Pparg* locus. Upon doxycycline (dox) administration, rtTA binds to the tetracycline operator (TetO) sequence and the four TFs are ubiquitously expressed.

In vivo reprogramming appears to be an asynchronous process, which is reflected in highly heterogeneous reprogramming efficiency among cells within the same tissue, as well as among *i4F* animals. Thus, in the first part of the thesis, we focused on identifying histological and serological markers of the early stages of *in vivo* reprogramming with the aim of better tracking this process.

1.1. OSKM activation leads to loss of differentiation markers

Our lab has previously demonstrated that short-term activation of OSKM *in vivo* leads to cellular dedifferentiation and tissue dysplasia, while long-term OSKM expression results in the generation of pluripotent cells that form teratomas (Abad *et al.*, 2013). We were particularly interested in finding markers of the first stages of reprogramming, as previous studies have shown therapeutic benefits in regeneration and rejuvenation after short-time expression of the OSKM factors (Ocampo *et al.*, 2016; Doeser, Schöler and Wu, 2018; Lu *et al.*, 2020; Y. Chen *et al.*, 2021). We first performed a timeline of *in vivo* reprogramming to better appreciate the dynamics of already described markers of reprogramming. We collected pancreas of WT and *i4F* mice at days 3, 6, 9 and 12 of OSKM induction, as it is the organ with the most severe phenotype (Abad *et al.*, 2013). We stained with HE to distinguish dysplastic areas, we performed immunohistochemistry for NANOG, which marks pluripotent cells, and for p21, to capture damaged and/or senescent cells, and we also stained for β-galactosidase, which visualises senescent cells (Abad *et al.*, 2013; Mosteiro *et al.*, 2016).

After 6 days of treatment, multiple focal dysplastic areas were observed in the HE staining (**Figure 13A**). These areas were progressively bigger and more abundant at days 9 and 12. $p21^+$ cells were present from day 6 and marked both dysplastic and non-dysplastic cells. Individual $NANOG^+$ cells were detectable from day 9, and at day 12 they formed isolated clusters of cells, probably reflecting the clonal expansion of individual successful reprogramming events. Interestingly, at day 12, we observed that clusters of $NANOG^+$ cells were not $p21^+$. As we were interested in characterizing the first steps of cellular dedifferentiation, when senescent cells ($p21^+$) and pluripotent cells ($NANOG^+$) are not very abundant, but still there is active cellular damage, we decided to set 7 days of OSKM activation as the time point for performing further analyses. This time point will be hereinafter referred to as "partial reprogramming". To further corroborate the dynamics of senescent cells in the pancreas up to 7 days of reprogramming, we stained for β-galactosidase (βgal) at days 0, 3, 5 and 7. At day 7, $βgal^+$ cells accounted for about 4.7±2.7% of the total tissue (**Figure 13B**), supporting our previous observation that cellular senescence is induced in a reduced subset of cells after one week of reprogramming.

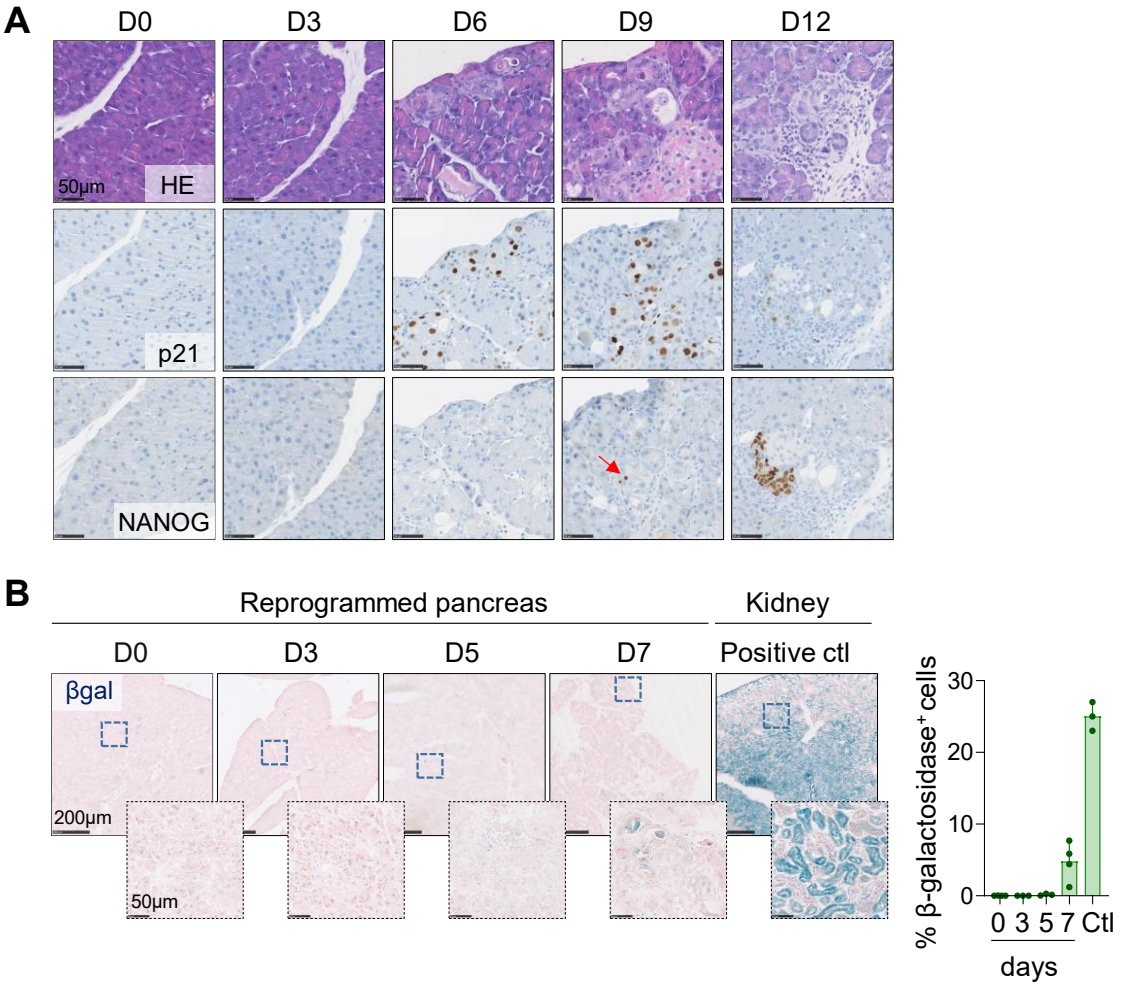

Figure 13 | Partially reprogrammed pancreas express senescence and pluripotency markers. A. Serial sections of haematoxylin and eosin (HE), p21 and NANOG staining of *i4F* pancreas from reprogrammed mice at days 0, 3, 6, 9 and 12 of doxycycline treatment in the drinking water (1 mg/ml) (*n*=3/ time point). **B**. β-galactosidase (βgal) staining (left) and quantification (right) of *i4F* pancreas from reprogrammed mice at days 0, 3, 5 and 7 of doxycycline treatment in the drinking water (1 mg/ml). Kidneys were used as positive control for the presence of βgal^+ cells (*n*=3).

Histologically, dysplastic areas in the pancreas resembled enlarged acini with a ductal-like morphology (**Figure 13A**), so we decided to check whether these regions conserved the expression of typical acinar markers. Pancreatic Carboxypeptidase (CPA1) and Pancreas Associated Transcription Factor (PTF1a) were lost in dysplastic areas, similarly to what has been reported in acinar-to-ductal metaplasia (ADM) lesions (Storz, 2017) (**Figure 14A**). At the same time, they expressed the ductal marker Keratin, Type I cytoskeletal 19 (KRT19). However, the transition to a ductal phenotype was not complete, as the dysplastic areas did not express another well-characterized ductal marker, the Hepatocyte Nuclear Factor 1-Beta (HNF1β) (**Figure 14B**). Of note, morphological alterations were neither observed in ductal exocrine cells, nor in the endocrine

compartment. Thus, we conclude that dysplastic areas, presumably of acinar origin, acquire an atypical ductal-like phenotype.

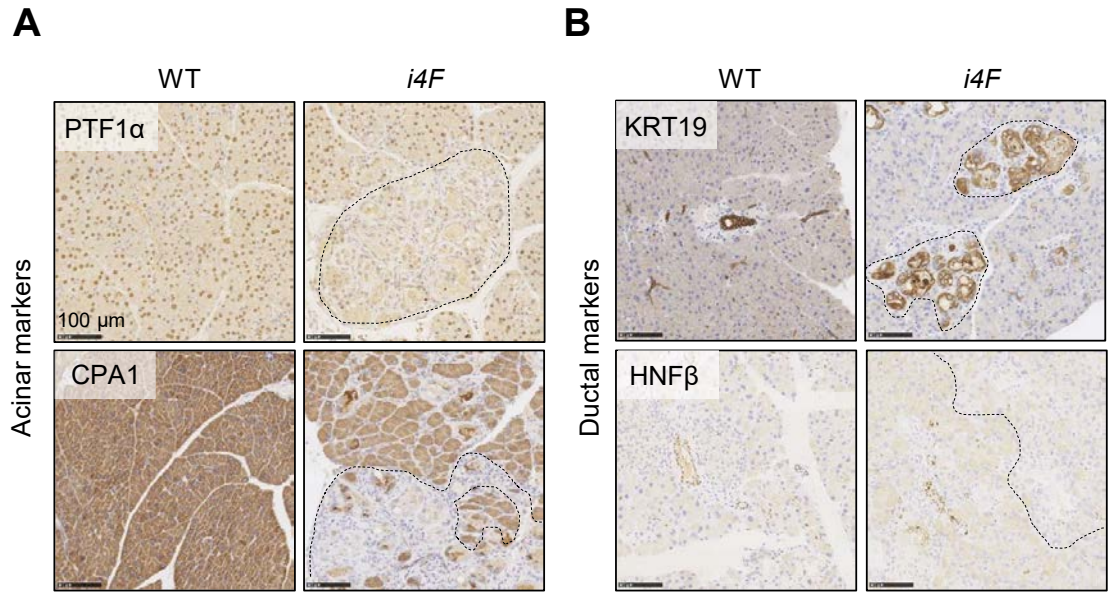

Figure 14 | Histological alterations in partially reprogrammed pancreas. A. Immunohistochemistry of the acinar markers Pancreas Associated Transcription Factor (PTF1a) and Pancreatic Carboxypeptidase (CPA1), as well as (**B**) of the ductal markers Keratin, Type I cytoskeletal 19 (KRT19) and Hepatocyte Nuclear Factor 1-Beta (HNF1β) in wild-type (WT) and *i4F* mice treated with doxycycline in water (1 mg/ml) for 7 days (*n*=3, non-serial sections).

After 7 days of reprogramming, dysplasia has also been observed in other organs such as the stomach, the colon and the kidney (Abad *et al.*, 2013). Indeed, reprogrammed kidneys presented dilatation of the renal pelvis, also known as hydronephrosis, due to the accumulation of urine (**Figure 15A, asterisk**). Similarly, the colon and the glandular part of the stomach presented several foci of dysplastic cells (**Figure 15B**). We decided to check whether these dysplastic areas had altered expression of well-described epithelial markers. In the case of the kidney, it is known that e-cadherin (e-cad) stains mainly the distal tubules (Jiang *et al.*, 2004). Although we could see complete loss of typical distal tubule morphology in *i4F* kidneys, e-cad staining was preserved in the dysplastic epithelial cells (**Figure 15A, right panel**). The epithelial pelvis urothelium also presented hyperplasia and dysplasia, but, similarly, e-cad staining was not lost in these areas (**Figure 15A, left panel, lower picture**). Interestingly, dysplastic cells in the colon and the stomach of *i4F* mice presented lower expression of KRT19, a marker of the gastroenteric tract (Jain *et al.*, 2010), than the non-dysplastic cells in the same tissue and the WT tissues.

Thus, we conclude that dysplastic cells in the pancreas, colon and stomach of reprogrammed mice lose expression of typical epithelial markers. The pancreatic dysplastic cells also acquire a ductal-like phenotype, as they start expressing KRT19. These results suggest onset of loss of epithelial identity in some organs during partial *in vivo* reprogramming.

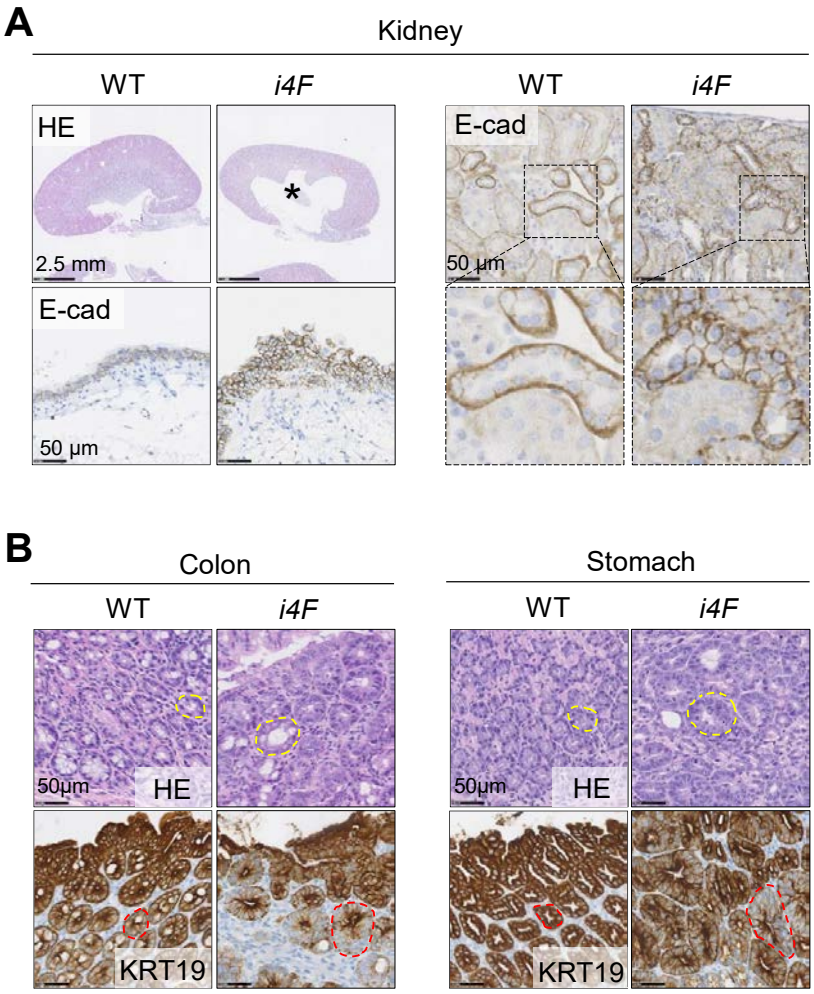

Figure 15 | Histological alterations in partially reprogrammed kidney, colon and stomach. A. Haematoxylin and eosin (HE) of wild-type (WT) versus *i4F* kidneys after doxycycline treatment (1 mg/ml) for 7 days (* = dilatation of the renal pelvis). E-cadherin (E-cad) staining of proximal (faint staining) and distal (intense staining) tubules in the renal cortex (right upper picture and magnification) and epithelial pelvis urothelium (left lower picture) (*n*=4, non-serial sections). **B**. HE and Keratin, Type I cytoskeletal 19 (KRT19) staining of WT versus *i4F* colons and glandular stomachs after doxycycline treatment (1 mg/ml) for 7 days (*n* =6, non-serial sections).

1.2. Serum markers associated to OSKM activation

Histological markers are useful to quantify the degree of reprogramming in post-mortem analysis. However, they do not allow to determine the degree of reprogramming in alive mice. Thus, we aimed to find serum markers to track the dynamics of reprogramming in an *in vivo* setting. Moreover, we wanted to know whether those markers could reflect the differences in the degree of reprogramming that exist among *i4F* animals. We first performed a cytokine array comparing serum from WT and *i4F* mice at days 0, 4 and 7 of reprogramming. Among the 33 analysed cytokines, four of them were significantly upregulated in *i4F* mice compared to WT animals at specific time points (**Figure 16**). Interleukin 15 (IL-15), for instance, was significantly upregulated at day 7 of reprogramming. IL-15 promotes activation and proliferation of immune cells, such as T cells and NK cells, in the context of cancer or autoimmune diseases (Allard-Chamard *et al.*, 2020; Fiore *et al.*, 2020). Similarly, the pro-inflammatory interleukin 6 (IL-6), which is known to promote reprogramming (Mosteiro *et al.*, 2016, 2018), was upregulated at day 7. Furthermore, interleukin 9 (IL-9), which is produced mainly by $CD4^+$ T helper cells, mast cells and lymphoid cells type 2 (ILC2), was highly upregulated at day 4 of OSKM induction. IL-9 has been described to have a context-dependent role, as it promotes inflammatory conditions, such as asthma, and it also promotes resolution of inflammation in contexts such as colitis (Chakraborty, Kubatzky and Mitra, 2019). Finally, IFNγ was significantly upregulated from day 4 in *i4F* mice. It is mainly produced by NK cells and $CD8^+$ T cells and promotes anti-tumour, anti-viral and anti-bacterial cytotoxicity (Schoenborn and Wilson, 2007).

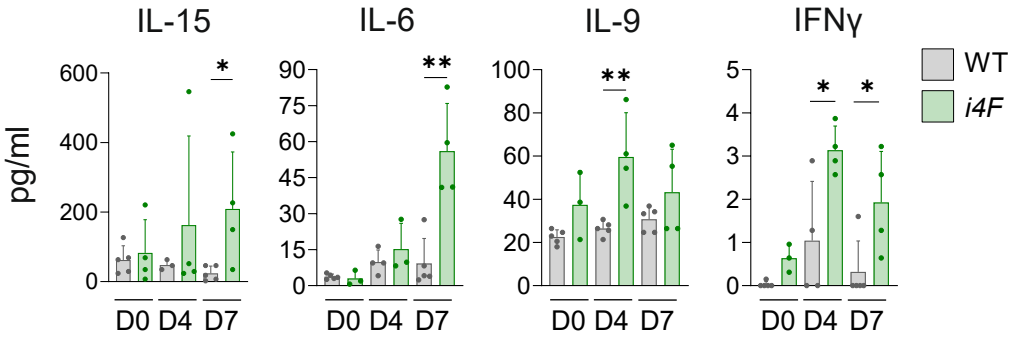

Figure 16 | Cytokine expression levels in serum change significantly upon partial reprogramming. Interleukin 15, 6 and 9 (IL-15, IL-6 and IL-9), together with interferon γ (IFNγ) were significantly upregulated at either day 4 (D4), day 7 (D7) or both days upon reprogramming with doxycycline (1 mg/ml) (n=5 for WT and n=4 for *i4F* mice). Graphs represent mean ± SD; *p<0.05, **p<0.01, and statistical significance was evaluated using two-tailed Student's t-test.

Overall, upregulation of serum cytokines depicts a general inflammatory signature upon reprogramming. IL-9 and IFNγ are the best markers to detect reprogramming at early time points, as they are significantly upregulated at day 4 after OSKM induction. From these two, IFNγ seems to be the more consistent one.

As we detected signs of inflammation in the serum of *i4F* mice (**Figure 16**), we wondered whether serum metabolites could also be good indicators of the levels of reprogramming. For that, we collected serum from WT and *i4F* mice at days 0, 3, 5 and 7 of reprogramming and we performed quantitative analysis of metabolites by mass spectrometry (MS) in collaboration with the team led by Guido Kroemer at the Gustave Roussy Metabolomics platform (France). We then selected those metabolites that were more significantly upregulated at days 5 and 7 of OSKM induction. Interestingly, a group of four acyl-alkyl-phosphatidylcholines (Pcae 18:1, Pcae20:1, Pcae20:2 and Pcae20:3) were significantly downregulated in *i4F* mice compared to WT mice at days 5 and 7 (**Figure 17A**). They are abbreviated as PCae *x*:*y*, where *x* represents the number of carbon atoms and *y* the number of double bonds. Phosphatidylcholines are a class of phospholipids, which are major components of cellular membranes. They influence trafficking of membrane proteins and have anti-inflammatory effects (Treede *et al.*, 2007; Furse and de Kroon, 2015). Furthermore, urea levels were particularly increased at days 5 and 7 (**Figure 17B**). Moreover, it can be routinely measured by commercial kits. Thus, we decided to validate the results of this last metabolite in serum samples previously collected from *i4F* mice. Indeed, urea levels were progressively upregulated in *i4F* mice, but not in WT mice treated with doxycycline (**Figure 17C**). In addition, there was a positive correlation between the concentration of urea in serum and the hyperplasia of the epithelial pelvic urothelium quantified at day 7 (**Figure 17D**), which is, as mentioned before, an histological alteration normally observed in the kidney upon reprogramming (**Figure 15A**).

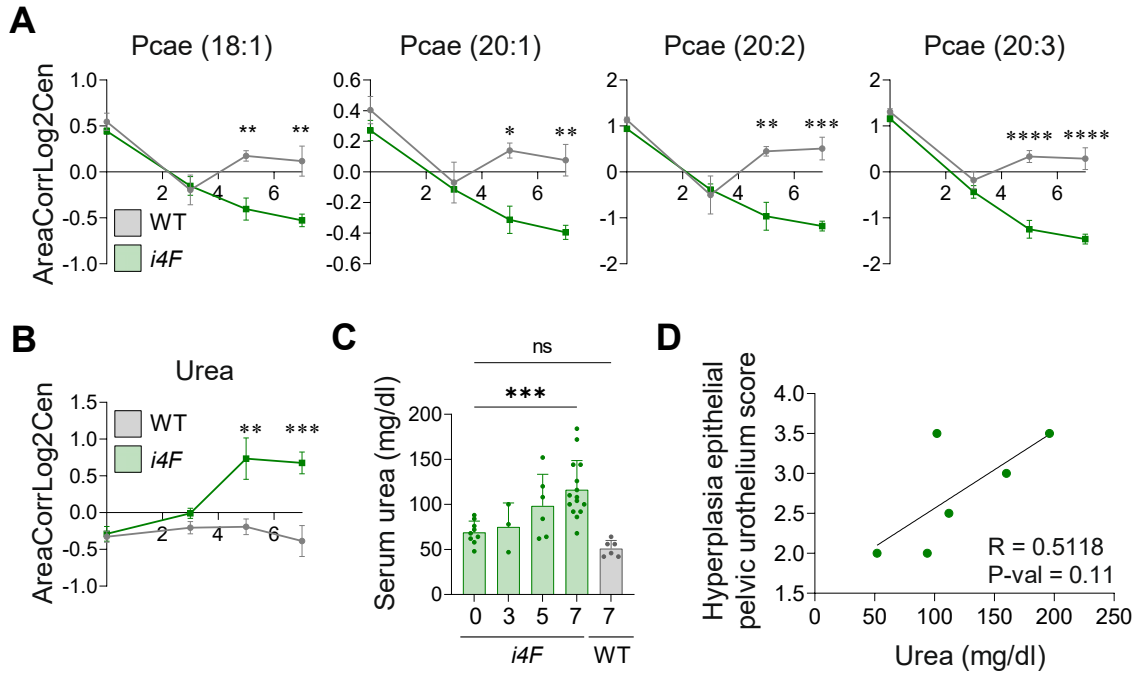

Figure 17 | Serum metabolites change in *i4F* mice compared to WT mice upon reprogramming. Serum from blood was obtained from WT and *i4F* mice at days 0, 2, 4 and 7 of reprogramming induced using doxycycline in water (1 mg/ml) for metabolomics analysis (n=5). **A**. Levels of acyl-alkyl-phosphatidylcholines (Pcae 18:1, Pcae20:1, Pcae20:2 and Pcae20:3) in serum. **B**. Urea levels in serum. **C**. Validation of urea levels in serum at days 0, 3, 5 and 7 (*i4F* mice) and day 7 (WT mice) (n=3-15). **D**. Correlation between concentration of urea in serum and hyperplasia of the epithelial pelvic urothelium at day 7 of reprogramming (n=6). For **A** and **B**, graphs were represented as areas corrected by means of quality controls, $\log^2$ transformed, and centred on the mean of the control sample. Moderated t-statistics by empirical Bayes shrinkage were used for significance; *p<0.05, **p<0.01, ***p<0.001, ****p<0.0001. For **C**, graph represents mean ± SD; ***p<0.001, and statistical significance was evaluated using one-way ANOVA. For **D**, statistical significance was evaluated using simple linear regression (p-val=0.11).

Hyperamylasaemia, or increased levels of amylase in serum, is a well-established marker of acute pancreatitis in humans (Quinlan, 2014; Rompianesi *et al.*, 2017). Thus, we wondered whether serum amylase levels increased upon reprogramming in our *i4F* mouse model. Indeed, amylase levels increased gradually, being significantly upregulated at day 7 compared to day 0 (**Figure 18A**). More noticeably, the levels of amylase in serum correlated with the levels of dysplasia measured in the pancreata of the same animals (**Figure 18B**).

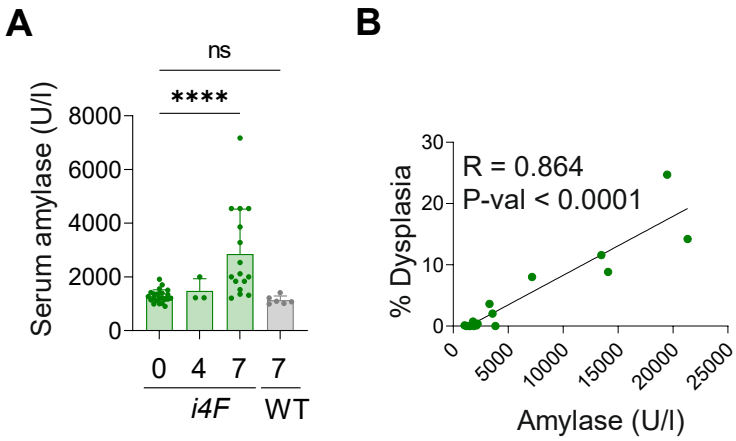

Figure 18 | Amylase levels in serum increase upon partial reprogramming. A. Levels of amylase in serum at day 0, 4 and 7 (*i4F* mice), and day 7 (WT mice) of mice treated with doxycycline (1 mg/ml) (*n*=3-23). Graph represents mean ± SD; ****p<0.0001, and statistical significance was evaluated using one-way ANOVA. **B**. Correlation between amylase in serum and percentage of dysplasia in pancreas of *i4F* mice at day 7 of reprogramming (*n*=12). Statistical significance was evaluated by simple lineal regression (p.val <0.0001).

Thus, we can conclude that both amylase and urea are useful markers of the degree of partial reprogramming in *i4F* mice, as their levels in serum correlate with the intensity of histological alterations previously described (**Figures 13A and 15A**). Not only they are easy to measure using commercial kits, but they allow to have an estimation of the efficiency of the process in mice previous to their sacrifice.

PART 2. Interplay between the immune system and cellular reprogramming

The upregulation of inflammatory cytokines in the serum of *i4F* mice suggested that immune cells may play a role during reprogramming. Although the elimination of PSCs by the immune system is a well-established phenomenon, nothing is known about its role in the early stages of reprogramming. It is currently unclear which immune subtypes infiltrate organs undergoing partial reprogramming, and to what extent they influence the outcome of *in vivo* reprogramming. Thus, in the second part of this thesis, we aimed to understand the interplay between the immune system and partial reprogramming.

2.1. Partial reprogramming elicits immune infiltration in the pancreas

To interrogate whether the immune system plays a role in *in vivo* reprogramming, we first explored the immune cell composition during partial reprogramming in the pancreas. We performed single-cell RNA sequencing (scRNAseq) of the pancreas of *i4F* (*n*=3) and WT (*n*=2) mice, all treated with doxycycline for one week. Mice in which acute pancreatitis was induced by treatment with the oligopeptide caerulein (CER) (seven injections at 1-hour intervals, for 2 days) were also included in the analysis (*n*=2) as a comparison to tissue damage (**Figure 19**).

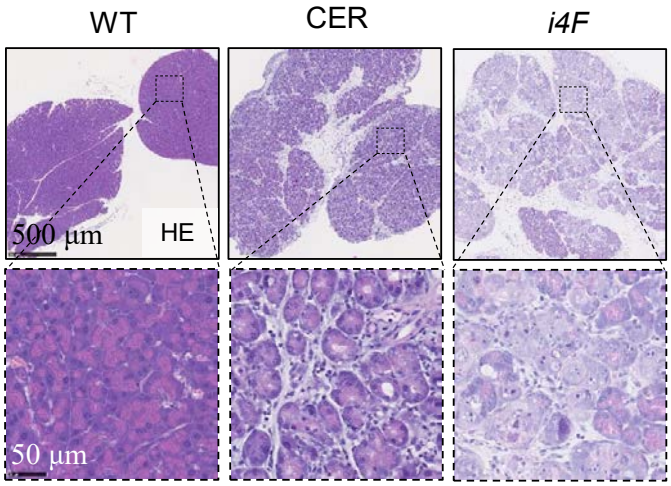

Figure 19 | Immunohistochemistry of samples used for single cell RNA-seq. Representative HE stainings of WT (*n*=2), caerulein-treated (CER) (*n*=2) and *i4F* (*n*=3) mice. WT and *i4F* mice were treated with doxycycline (1 mg/ml) for one week. Mice treated with caerulein to induce acute pancreatitis received seven injections in 1-hour intervals for 2 days.

Single cell suspensions of pancreata were sorted for live (DAPI$^-$) cells and sequenced using the 10x genomics system. In all the conditions, cells expressing < 150 genes and > 5% of mitochondrial genes were excluded. A preliminary classification of all the cell populations captured was done based on the expression of defined markers and EnrichR analysis (Kuleshov *et al.*, 2016).

Firstly, we processed and represented WT pancreata in a Uniform Manifold Approximation and Projection (UMAP) (**Figure 20A**). Clustering using Seurat function revealed 15 different clusters, in which all the main pancreatic populations described in the normal adult pancreas were detected (Baron *et al.*, 2016) (**Figure 20B**). Differentially expressed genes in each cluster, relative to the rest of clusters of the UMAP, were used to annotate the name of the populations. The top gene of the differentially expressed gene list for each cluster is shown in the individual UMAPs (**Figure 20C**).

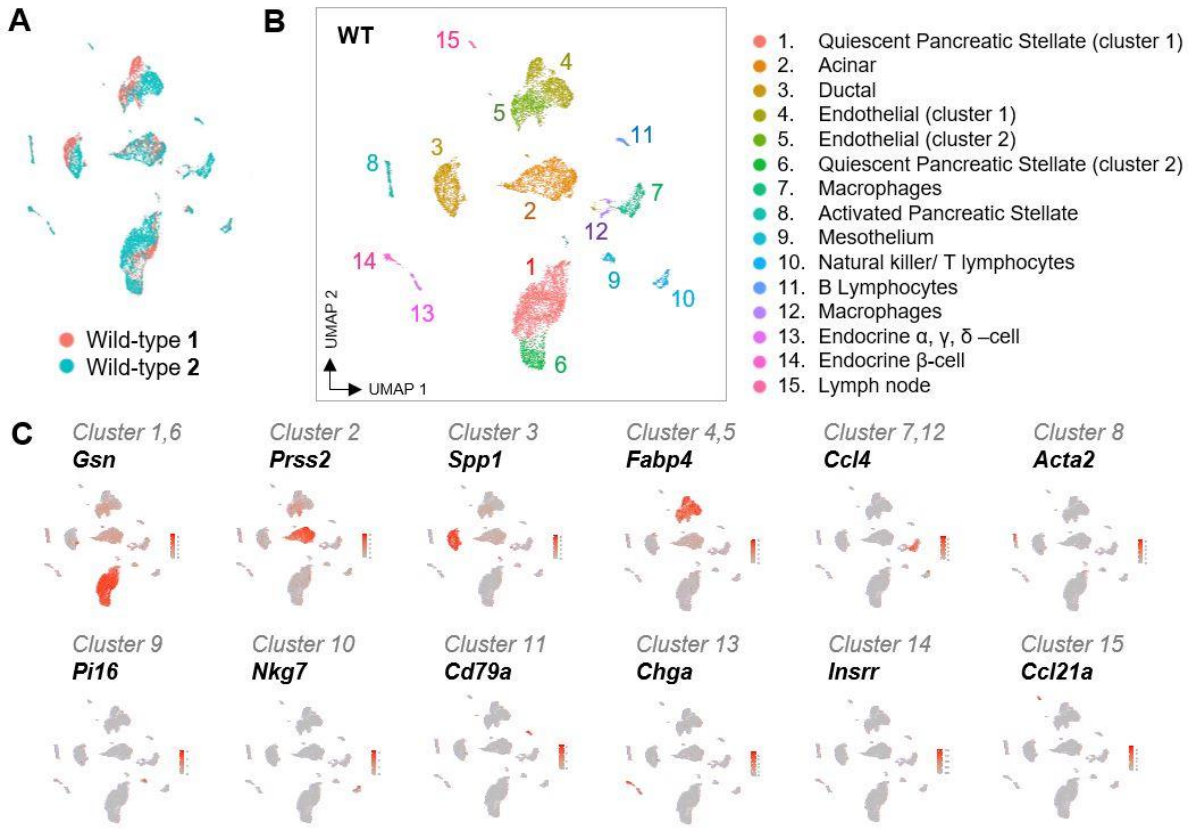

Figure 20 | Single cell RNAseq of WT pancreata. A. UMAP plot of two WT pancreata samples after merging. **B.** UMAP plot representing the 15 different clusters with the annotations of the corresponding cell populations. **C.** Top gene of the differentially expressed gene list for each cluster is represented in a UMAP plot.

Secondly, we represented in a UMAP the pancreata of the two mice treated with caerulein (CER) to induce acute pancreatitis. Similarly to the WT samples, the CER samples were well-overlapped **(Figure 21A)**, and we obtained 11 different clusters after using Seurat function **(Figure 21B)**. The top gene of the differentially expressed gene list for each cluster is shown in the individual UMAPs **(Figure 21C)**. In this case, we were also able to detect all the main populations described to coexist in the normal adult pancreas. Nevertheless, we could detect increased presence of immune cell types, as well as a cluster of activated pancreatic stellate cell. Both types of cell populations have been previously described to populate the pancreas upon acute pancreatitis (Mews *et al.*, 2002; Kylänpää, Repo and Puolakkainen, 2010; Zheng *et al.*, 2013; Habtezion, 2016).

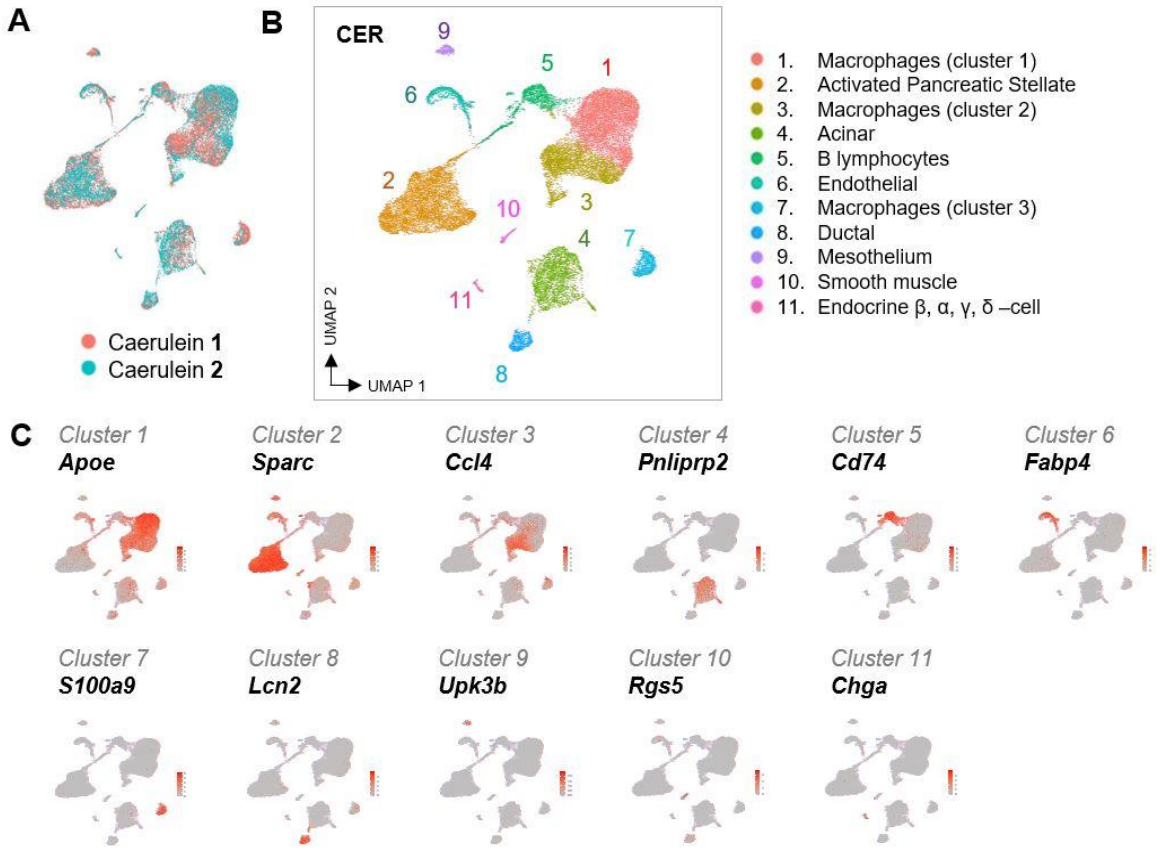

Figure 21 | Single cell RNAseq of caerulein-damaged pancreas. A. UMAP plot of two caerulein-damaged pancreata samples after merging. **B.** UMAP plot visualizing the 11 different clusters emerged, including the annotations of the clusters. **C.** Top gene of the differentially expressed gene list for each cluster is represented in a UMAP plot.

Finally, three *i4F* mice were treated with doxycycline (1mg/ml) for 7 days to induce partial reprogramming *in vivo*. Of note, two out of the three pancreas samples were highly reprogrammed, presenting 40% and 50% of dysplasia, respectively, while the third one was low reprogrammed, with 15% of dysplasia. Remarkably, the different degree of reprogramming is reflected at the UMAP (**Figure 22A**), as the cells of two highly reprogrammed (*i4F* 1 and 2) pancreata overlap, while the cells of *i4F* 3 pancreas are separated, possibly illustrating earlier intermediate cell fates. We obtained 14 different clusters after using Seurat function (**Figure 22B**) and the top gene of the differentially expressed gene list for each cluster is shown in the individual UMAPs (**Figure 22C**). Similarly, all main pancreatic cell types were identified, which is consistent with the fact that reprogramming only affects focal areas instead of the entire pancreas. Nevertheless, similar to caerulein-induced damage, there was abundant infiltration of immune cells and presence of activated pancreatic stellate cells due to, probably, the damage induced by OSKM.

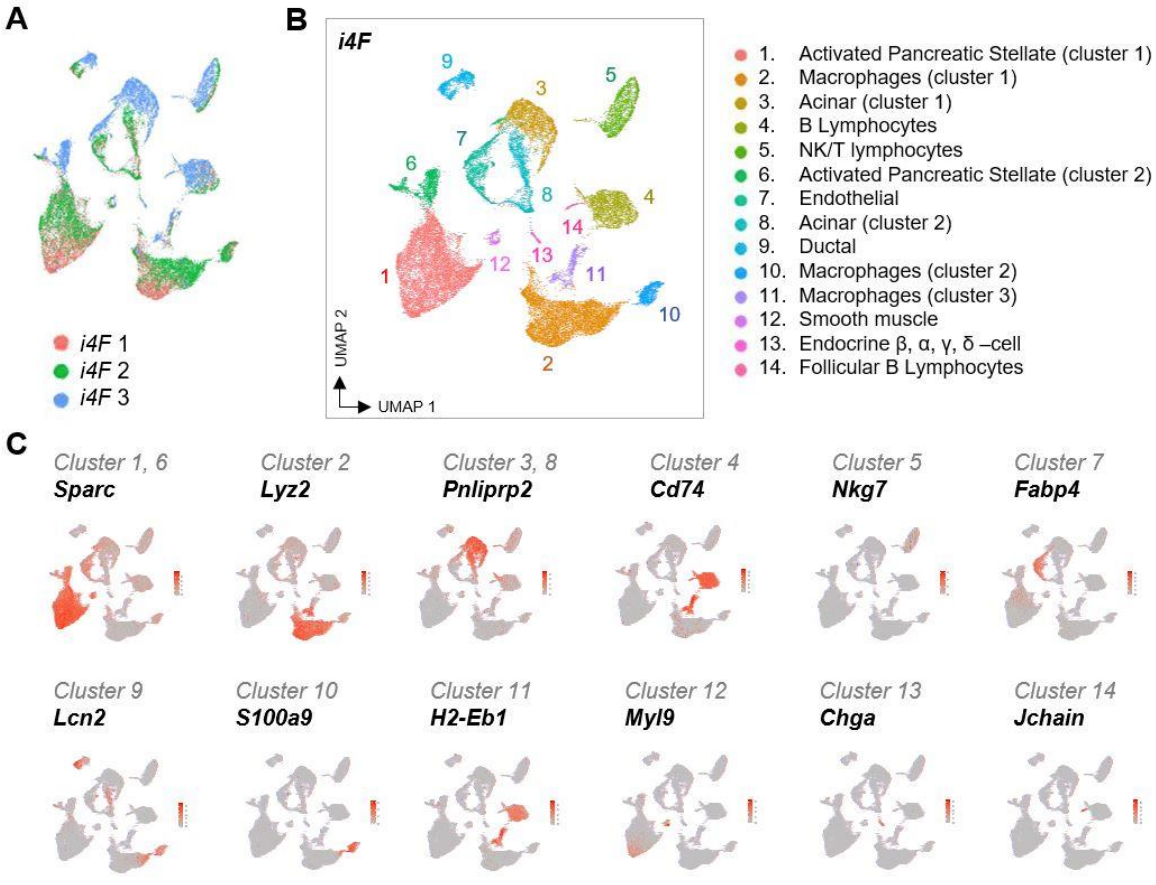

Figure 22 | Single cell RNAseq of *i4F* reprogrammed pancreata. A. UMAP plot of three partially reprogrammed pancreata samples after merging, which belong to *i4F* mice treated with doxycycline (1 mg/ml) for 7 days. **B.** UMAP plot representing the 14 different clusters with the annotations of the corresponding cell populations. **C.** Top gene of the differentially expressed gene list for each cluster is represented in a UMAP plot.

To further characterize the immune populations, we selected and merged the immune cells coming from all three conditions. UMAP representation showed an abundant infiltration of immune cells in response to reprogramming or caerulein, compared to WT animals (**Figure 23A**). We obtained 11 different clusters (**Figure 23B**) and the top gene of the differentially expressed gene list for each cluster is shown in the individual UMAPs (**Figure 23C**). Cluster annotation revealed treatment-specific patterns of immune cells infiltration in the pancreas. We found that NK cells, T cells, MDSCs and B cells were more abundant in the case of OSKM reprogramming, whereas macrophages (Mϕ) and DCs were over-represented in the context of caerulein-induced damage (**Figure 23B**). Of note, macrophages in caerulein-induced pancreatitis presented either pro-inflammatory (CD68 gene, M1 marker) or anti-inflammatory (CD206, M2 marker) signatures. Small clusters of mesenchymal-like cells, lymph nodes and follicular B cells were also detected coming from all three experimental conditions. Immune infiltration in *i4F* mice was further supported by immunohistochemistry analysis (**Figure 24**). Overall, it seems that immune cell types that infiltrate reprogrammed pancreata differ from the ones infiltrating the same organ in the context of acute pancreatitis.

FIGURE 9

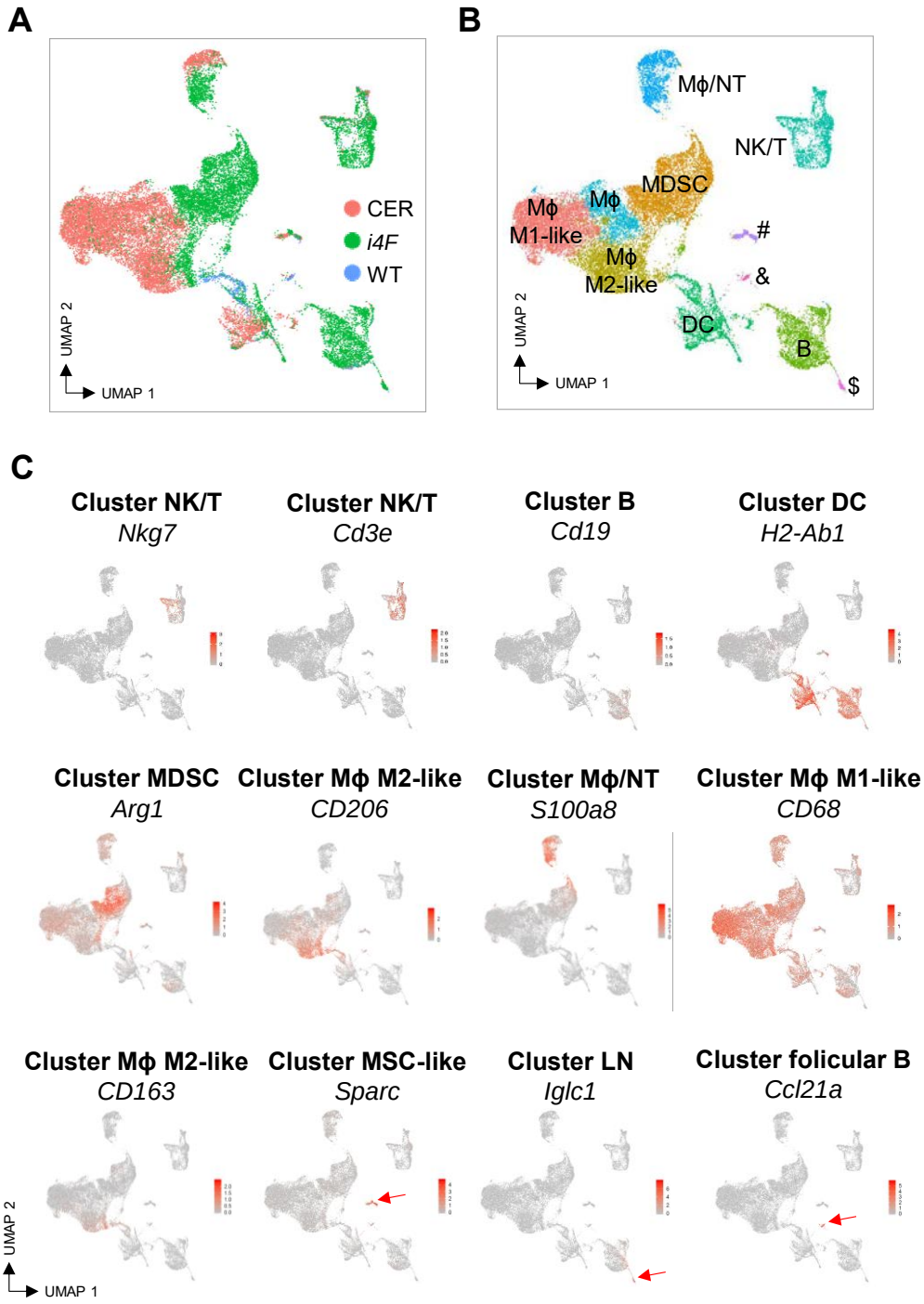

Figure 23 | Immune cell populations infiltrate the pancreas during *in vivo* reprogramming. A. UMAP plot visualizing immune cells infiltrated in the pancreas of WT (*n*=2), caerulein-treated (CER) (*n*=2) and *i4F* (*n*=3) mice. **B**. UMAP plot of immune cell populations based on gene expression. The minor clusters correspond to MSC-like cells (#), LN cells ($) and follicular B cells (&). **C.** Top markers of each cluster are represented in UMAPs plots. Mϕ = macrophages, NT = neutrophils, DC = dendritic cells, NK = natural killer cells, MDSC = myeloid-derived suppressor cells, T = T cells, B = B cells, LN = lymphoid nodes and MSC = mesenchymal stem cells.

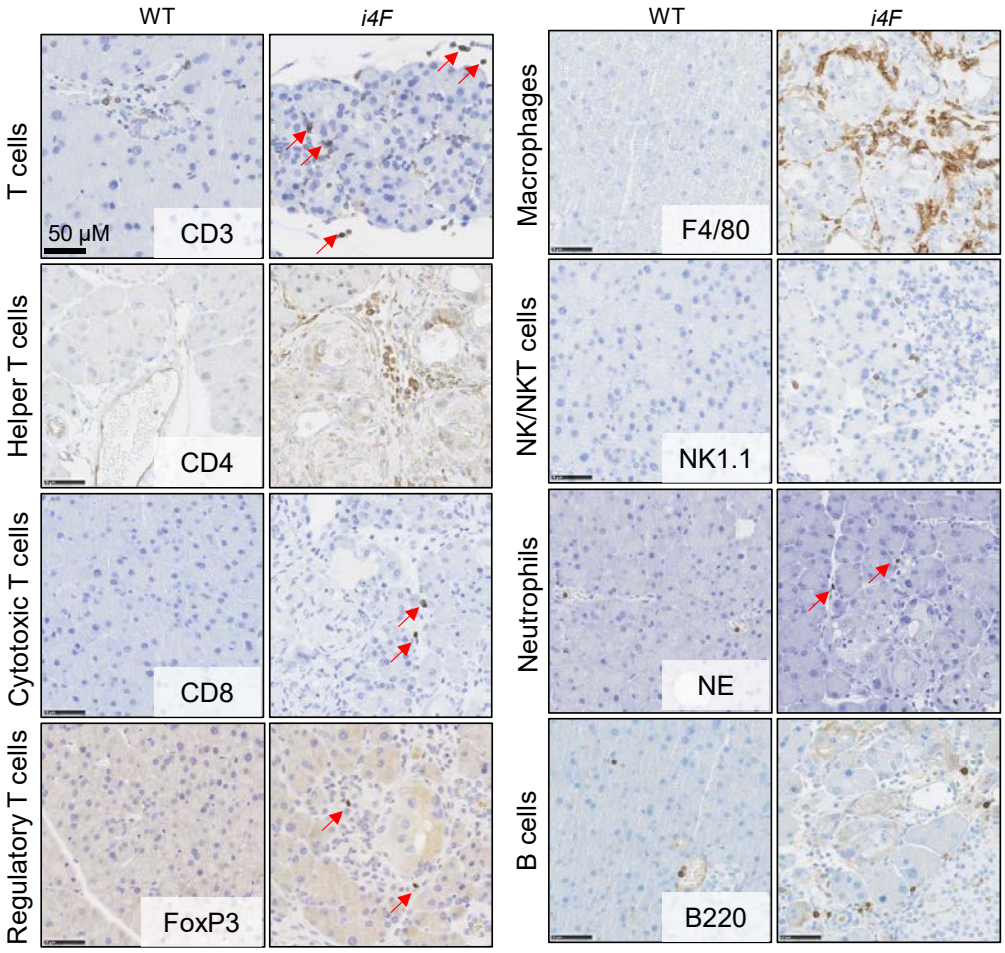

Figure 24 | Immune cells infiltrate partially reprogrammed pancreas. Representative images of reprogrammed pancreas at day 7 stained for the indicated immune cell markers (*n*=4, non-serial sections): CD3 (T cells), CD4 (helper T cells), CD8 (cytotoxic T cells), FoxP3 (regulatory T cells), F4/80 (macrophages), KLRB1c/CD161 or NK1.1 (NK/NKT cells), NE (neutrophil elastase, neutrophils) and B220 (B cells).

We next wondered whether the magnitude of immune infiltration could positively correlate with the extent of tissue dysplasia evoked by OSKM expression. As previously reported, *i4F;p53*-null mice are more prone to undergo reprogramming than *i4F* mice with functional p53 (Mosteiro *et al.*, 2016). Accordingly, we found by flow cytometry a higher proportion of $CD45^+$ immune cells in *i4F;p53*-null pancreata compared to their *i4F* counterparts, indicating that the degree of reprogramming correlates with the extent of immune cell infiltration (**Figure 25A**). The most abundant cell types infiltrating the reprogramming pancreas belong to the innate immune system, in particular, $F4/80^+$ and $CD11b^+$ cells (which mostly correspond to macrophages), $Gr1^+$ cells (which mostly correspond to neutrophils and MDSCs), and NK cells (**Figure 25A**). Of note, bulk transcriptomics analysis performed in the pancreas of *i4F;p53*-null mice revealed a

significant enrichment in NK cell cytotoxicity-associated genes (entry: mmu04650) compared to *i4F* mice (Mosteiro *et al.*, 2016) (**Figure 25B**). This result suggested that there might be an unknown association between NK cells and the efficacy of *in vivo* reprogramming. Thus, we decided to first explore the role of NK cells during partial reprogramming.

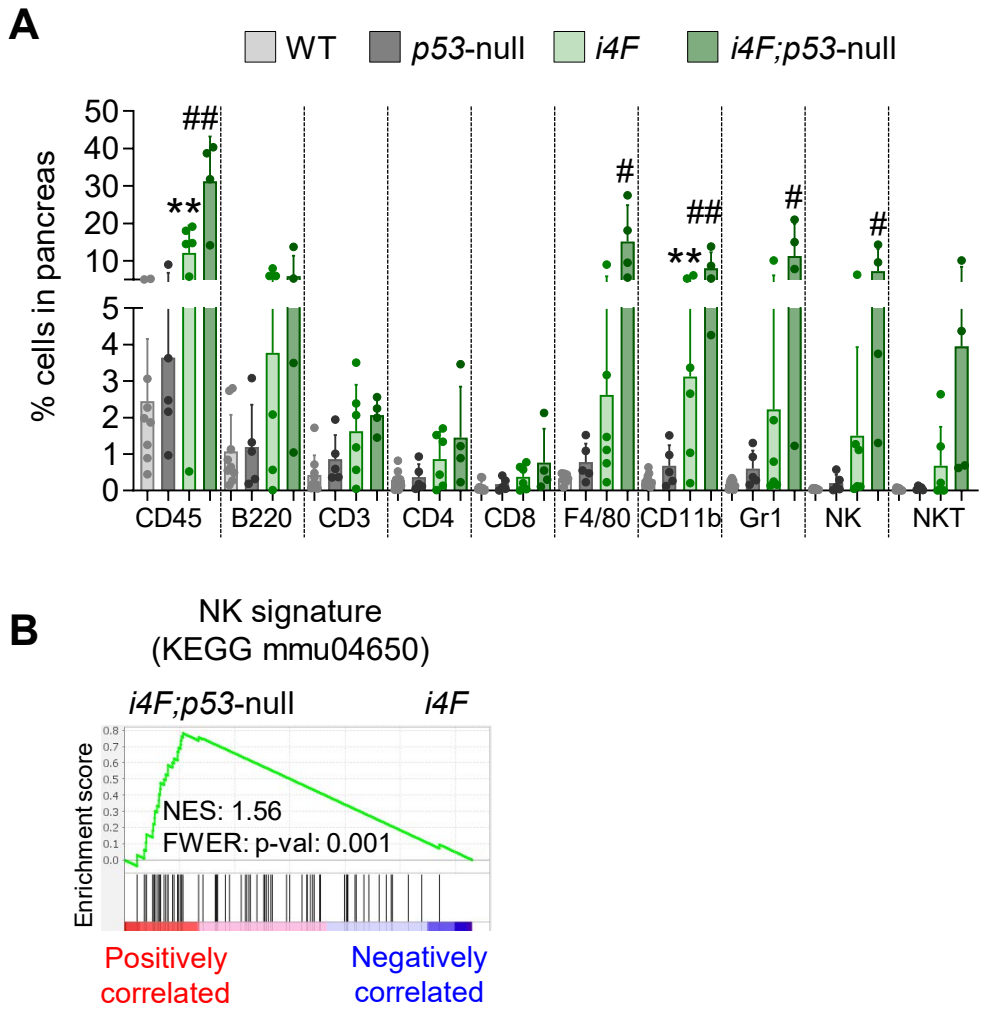

Figure 25 | Immune infiltration is proportional to the degree of reprogramming. A. Flow cytometry analysis of main immune populations infiltrating in the pancreas after WT (*n*=9), *p53*-null (*n*=5), *i4F* (*n*=6) and *i4F*;*p53*-null (*n*=4) mice were treated with doxycycline for 7 days. Cell were gated from $DAPI^{-}/CD45^{+}$ cells. Data are pooled from 2 independent experiments. Graph represents mean ± SEM; statistical significance was evaluated using the unpaired two-tailed Student's t test. ** p<0.01 (WT vs. *i4F*) and # p<0.05; ## p<0.01 (*i4F* vs. *i4F*;*p53*-null). **B.** Previously published RNA-sequencing data generated in our laboratory (Mosteiro *et al.*, 2016) from the pancreas of *i4F* and *i4F*;*p53*-null (high reprogramming) mice was used to perform gene set enrichment analysis (GSEA) against a published signature (entry: mmu04650) of NK cell mediated cytotoxicity (KEGG).

2.2. NK cells eliminate partially reprogrammed cells *in vitro*

To investigate whether NK cells can directly interfere with the early stages of reprogramming, we co-cultured primed splenic WT NK cells with *i4F* MEFs at different effector:target (E:T) ratios from day 2 to day 6 of *in vitro* reprogramming, when iPSC colonies are yet to be formed. At day 6, NK cells were removed from the culture and MEFs were allowed to transition to pluripotency (day 11) (**Figure 26A**). We observed that the number of alkaline phophatase-positive iPSC colonies was negatively correlated to the number of NK cells in the media (**Figure 26B and 26C**). Interestingly, by the end of the reprogramming assay (day 11), those plates co-cultured with the highest amount of NK cells (ratio 4.5:1) had no evidence of surviving MEFs, indicating a complete killing of the reprogrammed fibroblasts (**Figure 26C**). In contrast, non-reprogrammed fibroblasts co-cultured with the same amount of NK cells remained viable at the end of the experiment (**Figure 26C**). This result indicates that cells undergoing OSKM-induced reprogramming are targeted by NK cells for elimination.

NK ligands RAE1, MULT1 and H60 (which bind to the NKG2D receptor in mouse target cells), ICAM-1 (which interacts with LFA-1), and CD155 and CD122 (which bind to DNAM-1) have been described as major signalling molecules for NK activation (Abel *et al.*, 2018). We next evaluated the kinetics of expression of these ligands in reprogrammed MEFs. We observed a peak of expression of *Mult1* at day 6 of *in vitro* reprogramming. In line with previous observations by flow cytometry (Schwarz *et al.*, 2018), we detected a progressive upregulation of *Icam1* mRNA over the course of reprogramming, parallel to the upregulation of the pluripotency gene *Nanog*. We did not observe significant changes in the expression of *Rae1* or *CD155*, while *H60* and *CD122* were not detected. Taken together, these results show that fibroblasts undergoing reprogramming exhibit enhanced expression of a subset of NK stimulatory ligands, particularly *Mult1* and *Icam1*, at early stages of the process (**Figure 26C**).

To get mechanistic insights into the role of NK cells during *in vitro* reprogramming, we first asked whether NK cells require physical contact with partially reprogrammed target cells. To address this, we co-cultured primed NK cells with *i4F*-MEFs in transwell plates. We did not detect significant differences in the number of iPSC colonies between *i4F*-MEFs cultured with or without NK cells in transwells (**Figure 26D**). This suggests that the negative effect of NK cells on reprograming requires direct contact with the target cells. Indeed, the archetypical mechanism of cytotoxicity of NK cells requires direct contact between the above-mentioned ligands and receptors, followed by the release of cytotoxic granules from the NK cells. Degranulation involves the vacuolar type ATPase (V-ATPase) and this can be efficiently inhibited by Concanamycin A (ConA), which increases the pH

of the lytic granules and prevents their release abrogating the cytotoxic activity of NK cells. The presence of ConA abolished the inhibitory action of NK cells on iPSC formation (**Figure 26E**). Collectively, these data indicate that partially reprogrammed cells are lysed by NK cells in a process involving direct contact with their target cell and release of lytic granules.

To evaluate the implication of the NKG2D/ligand interaction in NK cell-mediated recognition and elimination of cells undergoing reprogramming, we co-cultured NK cells and *i4F*-MEFs with an NKG2D blocking antibody or with the corresponding isotype control. Prior to and during the co-culture, NK cells were primed with IL-2 and IL-15. Under this setting, we observed a tendency for the anti-NKG2D treatment to partially suppress the inhibitory effect of NK cells on reprogramming (**Figure 26F**). These data suggest that NK cells target partial reprogrammed cells, at least in part, via engagement of the NKG2D receptor.

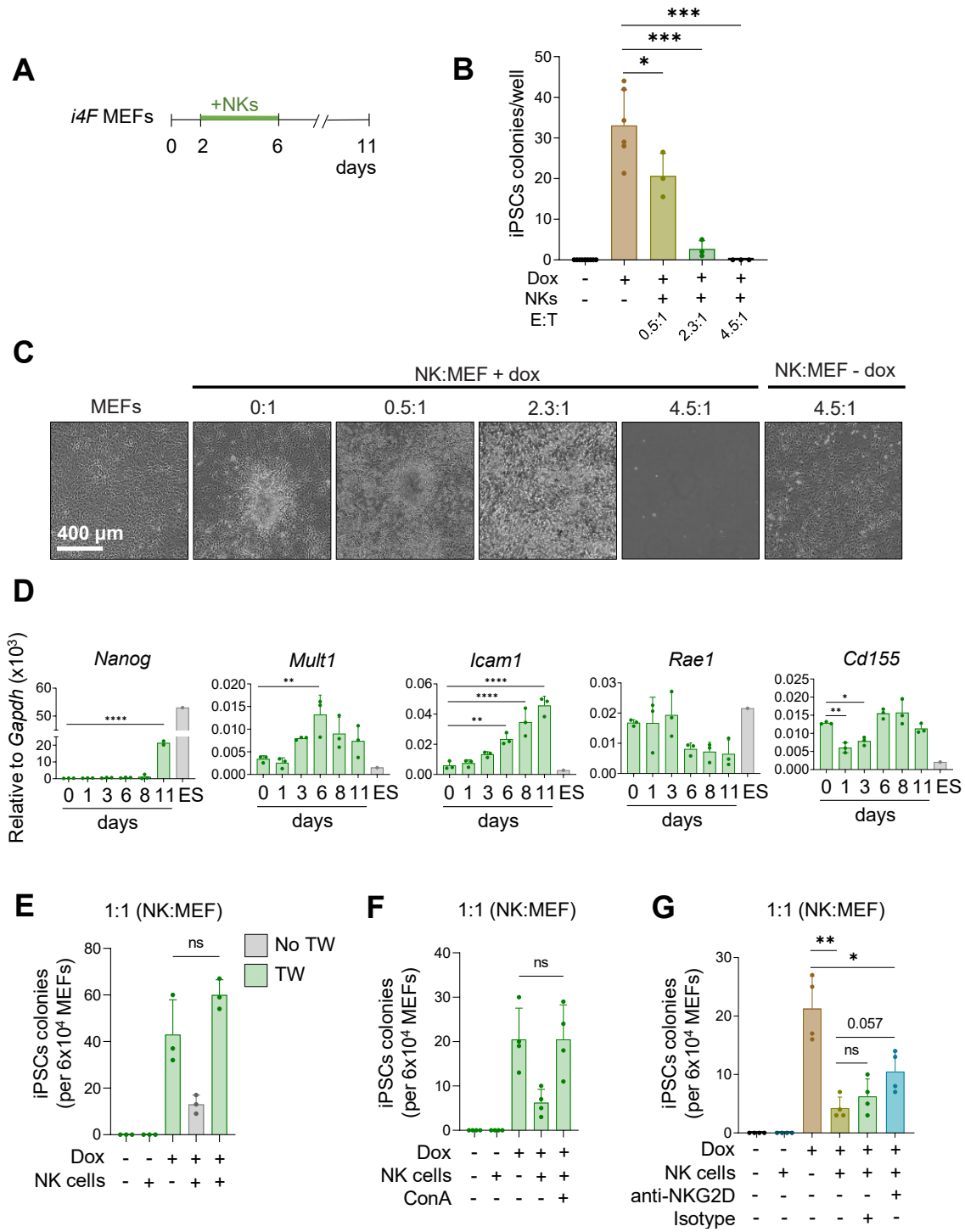

Figure 26 | NK cells eliminate partially reprogrammed cells *in vitro*. A. *i4F* MEFs were reprogrammed *in vitro* with doxycycline (1 µg/ml) for 11 days. From days 2 to 6, primed NK cells were added to the media and cells were co-cultured for 5 days. At day 11, iPSCs colonies were scored by alkaline phosphatase staining. **B**. Quantification and **C**. representative images of NK cells co-cultured with *i4F* MEFs at effector:target (NK:MEF) ratios of 0.5:1, 2.3:1 and 4.5:1. Data pooled from 2 independent experiments (*n*=3-6). **D**. *i4F* MEFs were reprogrammed with doxycycline (1 µg/ml) for 11 days. Changes in transcriptional expression of pluripotency gene *Nanog* and NK-activating ligands (*Rae1*,

Mult1, *Icam1* and *Cd155*) were assessed by RT-qPCR in MEFs and ES cells at different time points (n=3). **E.** Co-culture experiment in which primed NK cells were seeded in transwells (TW) at NK:MEF ratio of 1:1 to avoid cell-to-cell contact (n=3). **F.** Co-culture experiment using concanamycin A (ConA) to disrupt the function of lytic granules secreted by NK cells. NK:MEF ratio of 1:1 (n=4). **G**. Co-culture experiment using the blocking antibody anti-NKG2D, which was added to the media at days 2 and 4 of reprogramming. NK:MEF ratio of 1:1 (n=4). All graphs represent mean ± SD; *p<0.05, **p<0.001, ***p<0.001, ****p<0.0001 and statistical significance was evaluated using two-tailed Student's t-test (**D**, **E**, **F** and **G**) or one-way ANOVA (**B**).

2.3. NK cells activate and degranulate during *in vivo* reprogramming

To dissect the role of NK cells recruited to the pancreas during *in vivo* reprogramming, we analysed the expression of NK-activating ligands in the pancreata of *i4F* mice after 7 days of doxycycline treatment. In line with our *in vitro* observations, NK-activating ligands were transcriptionally upregulated in the pancreata of *i4F* mice compared to their WT counterparts. We found that the mRNA levels of *Icam1* and *Cd155* were significantly enhanced in the reprogrammed pancreas (**Figure 27A**). We surmise that the different behaviour of *Cd155* in pancreas *versus* cultured fibroblasts (**Figure 26D**) reflects cell type specific differences. This prompted us to examine the localization of infiltrating NK cells using the KLRB1c/ CD161 (E6Y9G) antibody, which represents the NK1.1 antigen, in the pancreata of mice undergoing reprogramming. Whereas NK1.1$^+$ cells were only detected within the lumen of blood vessels in the pancreata of WT animals, they were infiltrating dysplastic areas in the reprogrammed *i4F* pancreata (**Figure 27B**).

To infer additional information on the status of NK cells infiltrating the pancreata of *i4F* animals, we performed a NK profiling experiment in collaboration with José Alcamí and Núria Climent (Hospital Clínic, Barcelona). We used cell surface markers to characterise CD3$^-$/NK1.1$^+$ (NK) cells isolated from the pancreata of WT or *i4F* animals at different time points after doxycycline treatment (**Figure 27C**). We observed a transient, although modest, cell surface increased presence of NKG2D at day 3. The transient nature of NKG2D elevation in the cell surface is consistent with the idea that NKG2D engagement triggers its internalization, which is necessary for intracellular signalling (Quatrini *et al.*, 2015; Molfetta *et al.*, 2016b). Interestingly, as early as 5 days after doxycycline treatment, NK cells significantly upregulated the degranulation marker CD107a (also known as LAMP-1) (Alter, Malenfant and Altfeld, 2004). We also observed an upregulation of the inhibitory receptor Ly49C/I at day 3, followed by its downregulation. This result is consistent with a study in which NK cell activation in lung tumours led to shedding of Ly49C/I receptor, thus avoiding its upregulation in the cell surface (Shi *et al.*, 2018).

Finally, the gradual upregulation of the inhibitory receptor NKG2A could reflect a progressive NK cell exhaustion (Ablamunits *et al.*, 2011; Sun *et al.*, 2017; Zhang *et al.*, 2019). Notably, double positive $CD107a^+$ $NKG2A^+$ NK cells were progressively increased in time. Additionally, these two markers were highly correlated reflecting an association between degranulation and inhibition of NK cells. Collectively, these findings indicate that, upon infiltrating the reprogrammed pancreas, NK cells manifest sequentially the hallmarks of NK activation, namely, a transient upregulation of stimulatory receptors, degranulation and upregulation of inhibitory receptors.

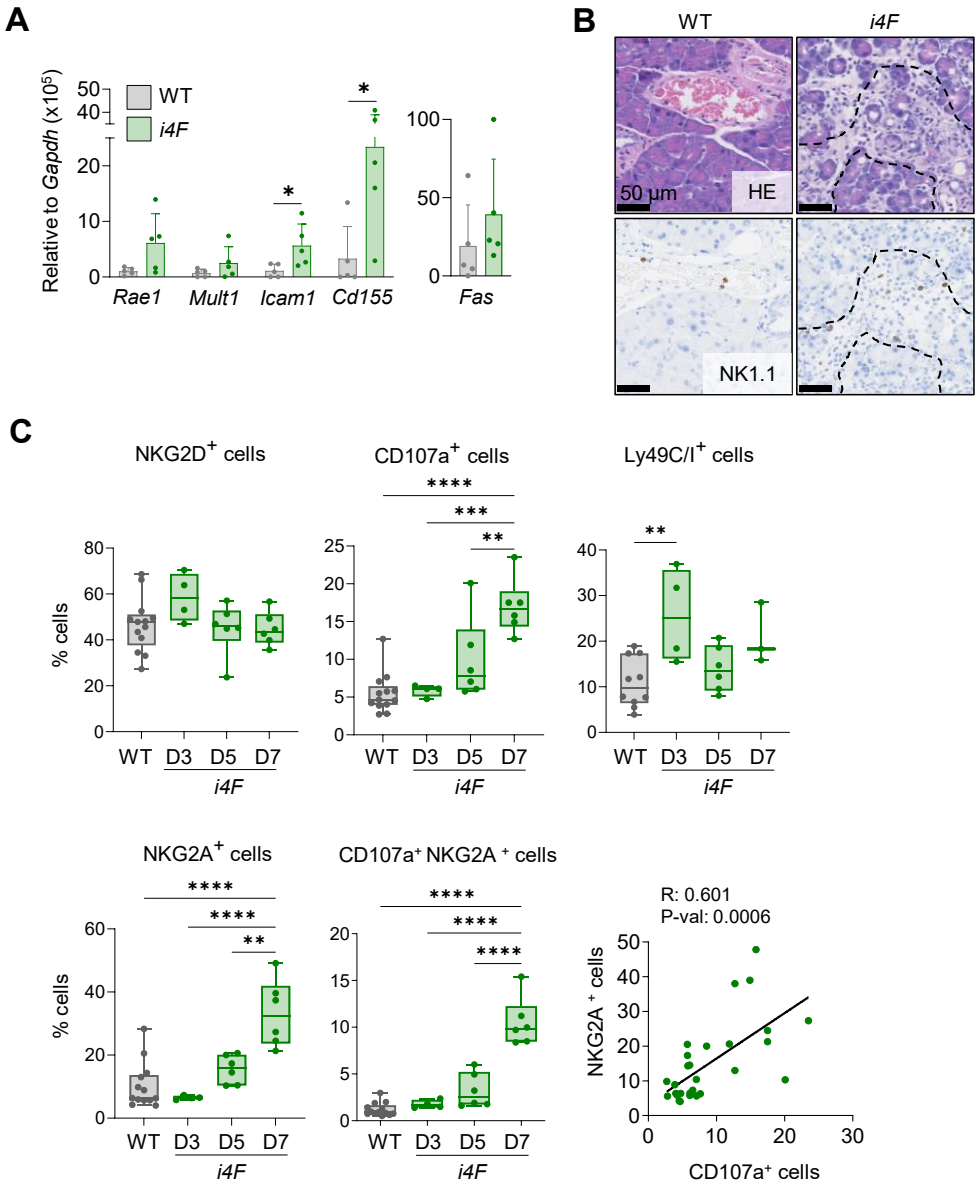

Figure 27 | NK cells recruited to the pancreas of *i4F* mice release lytic granules upon ligand-dependent activation. A. WT and *i4F* mice were treated with doxycycline (1 mg/ml) for 7 days and expression levels of NK-activating ligands (*Rae1, Mult1, Icam1*, *CD155* and *Fas*) in pancreatic tissue were assessed by RT-qPCR. Graphs represent mean ± SD. **p*<0.05 by two-tailed Student's t-test (*n*=5). **B.** Representative images of KLRB1c/CD161$^+$ cells in pancreas of WT and *i4F* mice treated with doxycycline for 7 days (*n*=5, serial sections). **C.** Subpopulations of infiltrating NK cells in pancreas undergoing reprogramming at days 3 (D3), 5 (D5) and 7 (D7) of doxycycline treatment. Cell populations were gated on CD3$^-$/NK1.1$^+$ cells and stained for the indicated activation, degranulation and inhibitory markers. Correlation of NKG2A$^+$ and CD107a$^+$ cells includes all time points. Graphs represent box with whiskers (min. to max); **p*<0.05, ***p*<0.01, ****p*<0.001, *****p*<0.0001 by one-way ANOVA (data pooled from 4 independent experiments). Statistical significance in the correlation between NKG2A$^+$ and CD107$^+$ cells was evaluated by simple lineal regression (p.val = 0.0006).

2.4. NK cells are a barrier for *in vivo* reprogramming in the pancreas

Based on the above findings, we hypothesized that NK cells might limit *in vivo* reprogramming. We first addressed the question of whether the activity of NK cells is affected by the activation of our transgenic OSKM allele, as it was shown that hematopoietic cells can be reprogrammed *in vivo* (Abad *et al.*, 2013). We first confirmed that the OSKM transgene is upregulated in splenic NK cells of *i4F* mice after 7 days of treatment with doxycycline (**Figure 28A**). We then isolated NK cells from the spleen of *i4F* and WT mice treated with doxycycline for 5 days *in vivo*. These NK cell isolates were then primed *in vitro* during 6 days with cytokines IL-2 and IL-15, while culturing them in the presence of doxycycline. Finally, NK activity was measured using YAC-1 as target cells, which are sensitive to NK clearance due to the lack of MHC-I expression (Cikes, Friberg Jr. and Klein, 1973). The percentage of dead ($DAPI^+$) YAC-1 cells did not vary between WT and *i4F* NK cells (**Figure 28B**). This result indicates that the expression of the OSKM cassette in NK cells does not alter their cytotoxic activity during the time frame of our *in vivo* reprogramming experiments.

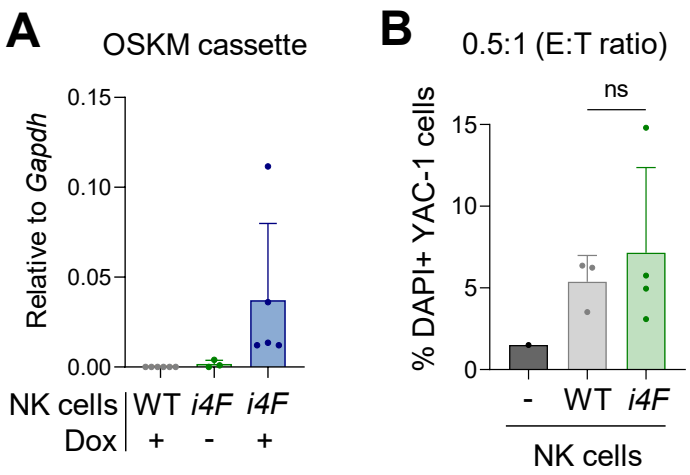

Figure 28 | NK cells maintain their cytotoxic activity upon OSKM induction. A. Spleens were harvested and NK cells were isolated on day 7 post-doxycycline (dox) initiation. Expression of the OSKM transgene was assessed by RT-qPCR (n=5 for WT+ dox and *i4F* + dox groups, and n=3 for *i4F* group). **B**. Percentage of $DAPI^+/NK1.1^-$ YAC-1 cells lysed by WT or *i4F* NK cells. Mice were reprogrammed *in vivo* for 5 days and NK cells were isolated from the spleen. NK cells were primed *in vitro* with IL-2 and IL-15 for 6 days in the presence of doxycycline (1 µg/ml). A cytotoxic assay using YAC-1 as target cells was done after 3 hours of co-culture. Cell death was assessed using DAPI (n=3 for WT and n=4 for *i4F* group).

Having established that NK cytotoxic activity is not affected by OSKM activation in our mouse model, we then addressed the effect of eliminating NK cells. We depleted

NK1.1$^+$ cells using a specific monoclonal antibody during reprogramming (**Figure 29A and 29B**). Remarkably, the absence of NK1.1$^+$ cells resulted in larger areas of pancreatic dysplasia and a significantly higher number of NANOG$^+$ cells, pointing into late stages of reprogramming (**Figure 29C**). Based on these results, we propose that NK cells hinder the process of *in vivo* reprogramming by eliminating emerging dysplastic cells. To further strengthen this hypothesis, we tested whether the adoptive transfer of exogenous NK cells could reduce the levels of reprogramming in the pancreas. Thus, NK cells from WT donor mice were injected at day 3 of reprogramming. Notably, exogenous transfer of NK cells dramatically reduced the efficiency of reprogramming, and no NANOG$^+$ cells were detected at day 7 of reprogramming (**Figure 29C**).

We next wondered whether NK cells could have a role in other models of tissue plasticity in the pancreas. In particular, we focused on caerulein-treatment, as ADM is a histological lesion that resembles to some extent OSKM-induced dysplasia (Shibata *et al.*, 2018). Importantly, NK1.1$^+$ cell ablation did not alter the amount of caerulein-induced ADM (**Figure 29D**). These results suggest that NK cell cytotoxic activity is specific of OSKM-induced *in vivo* reprogramming in the pancreas.

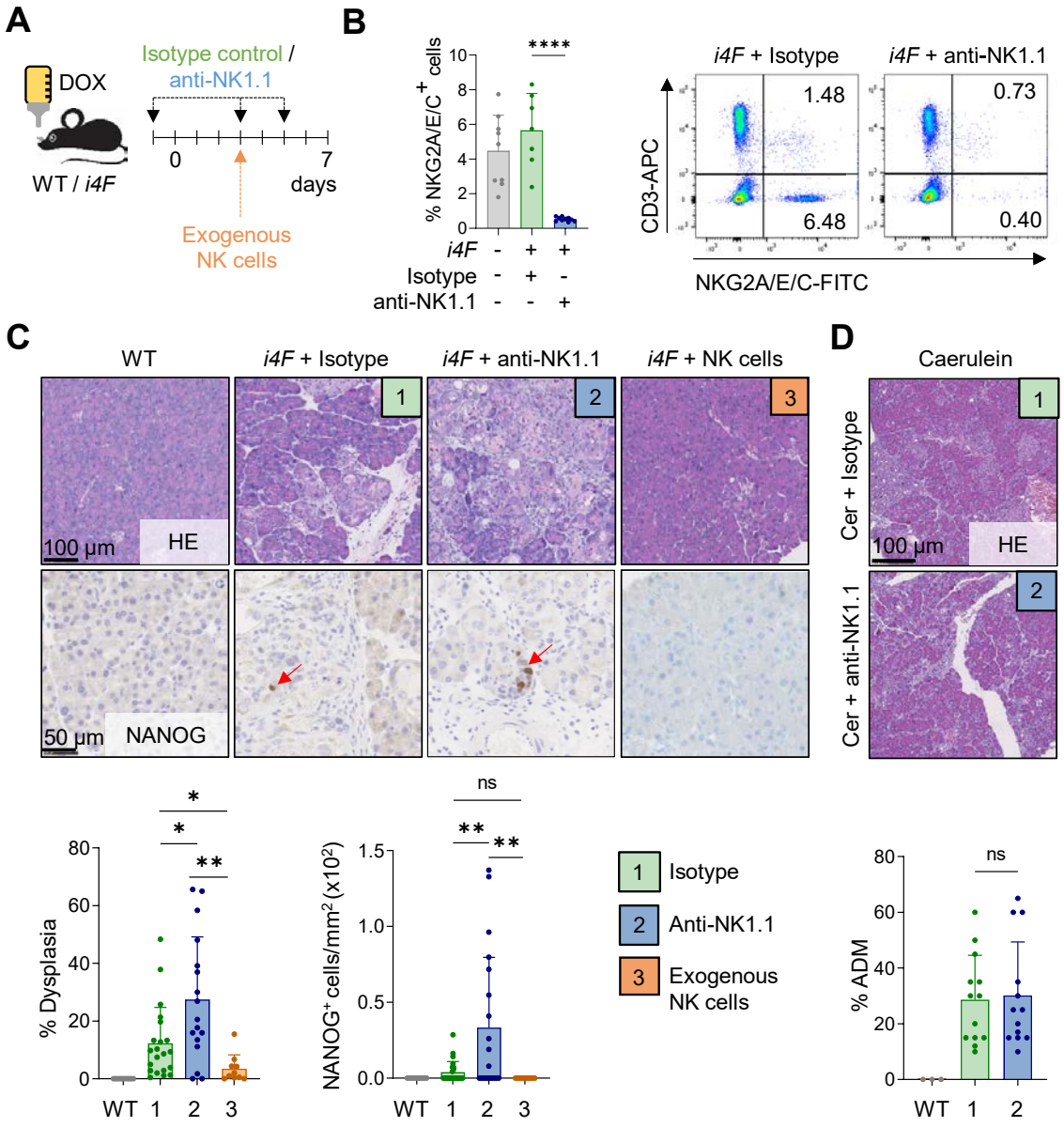

Figure 29 | NK cells are an extrinsic barrier for *in vivo* reprogramming in the pancreas. A. Flow cytometry analysis of NK cell depletion in blood at day 5 of reprogramming with doxycycline (1 mg/ml) after anti-NK1.1 or isotype control antibody administration (n=8-10). NK cells gated as $CD3^-/NKG2A/E/C^+$ cells. Data pooled from 4 independent experiments. **B.** Non-serial sections of representative HE and NANOG staining (upper) and quantification (lower) of WT (n=10) or *i4F* pancreata after 1 week of doxycycline. *i4F* mice were treated with either isotype control antibody (1) (n=21), anti-NK1.1 antibody at days -1, 3 and 5 of the treatment (2) (n=17) or received adoptive transfer of $3.8x10^6$ NK cells at day 3 of reprogramming (3) (n=10). Data pooled from five independent experiments in conditions 1 and 2, and from 2 independent experiments in condition 3. **C.** Representative HE images of caerulein-induced pancreatitis (100 mg/kg, 7 times/day) for 2 days with or without anti-NK1.1 treatment (n=13). Graphs represent mean ± SD; *p<0.05, **p<0.01, ****p<0.0001 and statistical significance was evaluated using two-tailed Student's t-test.

We next addressed whether the absence of NK cells could also alter the reprogramming efficiency in other organs (**Figure 30**). We measured several histological parameters after one week of doxycycline treatment: crypt epithelial hyperplasia and dysplasia (stomach and small intestine), crypt dysplasia (descending colon), and tubular dilatation and renal pelvis dilatation (kidney). Surprisingly, we could not see differences in the reprogramming scores between *i4F* animals treated with isotype control and anti-NK1.1. One possible interpretation for this observation is that NK cells limit reprogramming efficiency specifically in the pancreas and not in stomach, intestine, or kidney. However, it is important to remember that the kinetics of reprogramming are different in each tissue and that the pancreas is the most reprogrammed organ at day 7 of doxycycline treatment. Therefore, it is conceivable that, at this stage, the degree of reprogramming in stomach, small intestine, colon and kidney is still insufficient for the activation of NK recruiting signals.

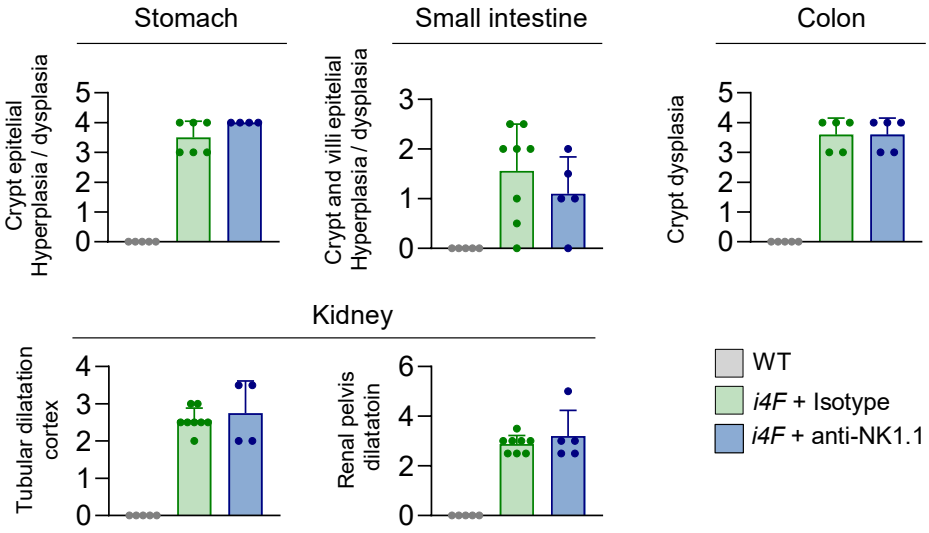

Figure 30 | Depletion of NK cells does not affect reprogramming efficiency in stomach, small intestine, colon and kidney. Histological score of alterations induced by reprogramming in WT and *i4F* mice after anti-NK1.1 or isotype control antibody administration at days -1, 3 and 5 of doxycycline treatment (1 mg/ml) (*n*= 5 for WT, *n*=6 for *i4F* with isotype control and *n*=5 for *i4F* with anti-NK1.1). Note: stomach and tubular dilatation in the kidney cortex of one *i4F* animal treated with anti-NK1.1 could not be scored because the tissue extracted for quantification was too small.

2.5. NK1.1^{+} cell depletion promotes teratoma formation

To further test the role of NK cells during *in vivo* reprogramming, we shifted to a different experimental model previously reported in our lab, based on the delivery of the four Yamanaka factors using adeno-associated viruses (AAV) (Senís *et al.*, 2018). In particular,

WT mice were inoculated with a mixture of AAV8 viruses (a kind gift from Dr. Dirk Grimm, DKFZ, Germany), which exhibit high tropism for the liver (Zincarelli *et al.*, 2008), carrying each of the four Yamanaka factors and GFP, and this resulted in GFP$^+$ teratomas in the liver (**Figure 31A**). It is important to clarify that in this model, we are not directly measuring tissue dysplasia as a readout of partial reprogramming (as we did for the pancreas) but teratoma formation, which is a readout of full reprogramming. In line with the negative role of NK cells during *in vivo* reprogramming, mice in which NK1.1$^+$ cells were depleted developed teratomas significantly earlier than mice with NK cells (**Figure 31B**). We conclude from this experiment that NK cells are a limiting factor for the process of reprogramming. It is tempting to speculate that NK cells may act by eliminating hepatic

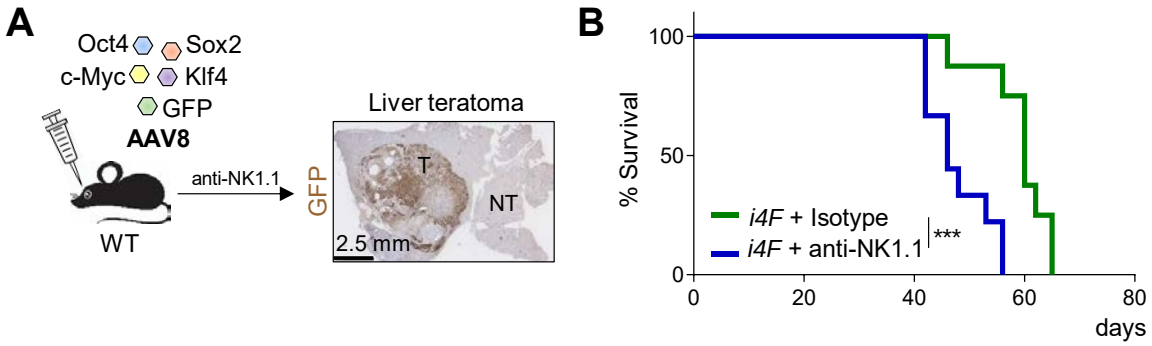

Figure 31 | NK1.1$^+$ cell depletion enables full reprogramming and promotes teratoma formation. A. WT mice were retroorbitally injected with scAAV8 SFFV-hCO-O/K/S/M. A scAAV8 vector encoding GFP was additionally added as tracer. Anti-NK1.1 or isotype control antibodies were injected intraperitoneally once a week until liver teratomas were palpable. T = teratoma; NT = non-teratoma. **B.** Survival curve upon teratoma formation in the liver. Data pooled from two independent experiments (n=9). Graph represents mean ± SD; ***p<0.001 and statistical significance was evaluated using log-rank (Mantel-Cox) test.

2.6. Depletion of NK1.1$^+$ cells allows the survival of highly plastic pancreatic cells

To further investigate the role of NK cells as a barrier for reprogramming, we wondered if the absence or presence of NK cells in the context of OSKM expression impacts the emergence of cells with stem/progenitor properties. To evaluate this, we used an *ex vivo* system based on pancreatic organoids (Clevers, 2016). We first reprogrammed mice for 7 days, while treating them with isotype control or anti-NK1.1$^+$ antibodies (**Figure 32A**). Of note, *i4F* mice treated with anti-NK1.1 presented higher amylase in serum and lost more weight than those treated with isotype control (**Figures 32B and 32C**). In these settings,

we prepared single cell pancreatic suspensions, and an equal number of cells per condition were embedded in Matrigel. All organoids grew as homogeneous, hollow spheres composed of a single-layer epithelium as previously described (Huch, Bonfanti, *et al.*, 2013). At day 5 post-embedding, we found that organoids originating from anti-NK1.1-treated animals were significantly larger than the ones derived from *i4F* mice treated with isotype control and, at day 8, the size difference was evident macroscopically (**Figure 33D**). This result demonstrates that the absence of NK cells allows the emergence of cells with high stem/progenitor capacity, as determined by their capacity to form bigger organoids.

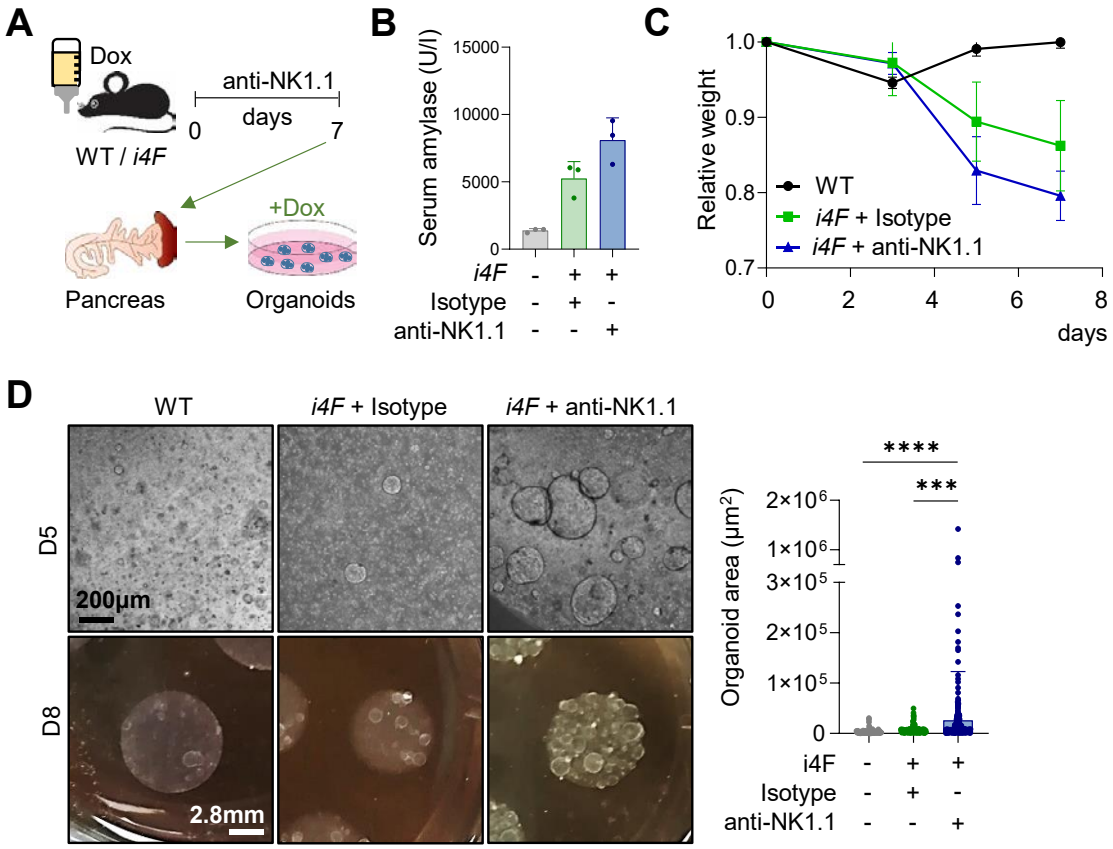

Figure 32 | NK1.1^{+} cell depletion promotes the survival of pancreatic cells with high plasticity. A. Mice were treated with doxycycline (dox) and anti-NK1.1 or isotype control antibodies for 7 days. Pancreata were dissociated to the single cell level and the same number of cells ($3x10^5$) were embedded in Matrigel. **B**. Amylase levels in serum at day 7 and (**C**) relative weight loss of WT and *i4F* (with isotype or anti-NK1.1 antibodies) mice. Graphs represent mean ± SD; and statistical significance was evaluated using two-tailed Student's t-test. **D.** Representative images at day 5 (D5) and day 8 (D8) after seeding (left), and quantification of organoids size at D10 (right) (each dot represents one organoid from 3 biological replicates. A total 10 images were measured per sample)**.** Graph represents mean ± SD; ***p<0.001, ****p<0.0001 and statistical significance was evaluated using two-tailed Student's t-test.

2.7. Dysplasia generated upon NK1.1^{+} cell depletion is reversible

It has been previously established that the *in vivo* effects of short periods of OSKM induction are reversible in the sense that tissues recover their original histology after cessation of doxycycline and do not develop teratomas (Ohnishi *et al.*, 2014; Ocampo *et al.*, 2016). As previously shown, the dysplastic foci generated in the absence of NK cells contain cells with a potent stem/progenitor state. Considering this, we wondered if the dysplastic foci formed in the absence of NK cells were also reversible. We administered doxycycline for 7 days to *i4F* mice treated with or without NK1.1 antibody, and we let the pancreas to recover for 7 more days (**Figure 33A**). We observed that pancreata of both *i4F* and anti-NK1.1-treated *i4F* mice recovered their normal histology (**Figure 33B**). To check whether they indeed underwent reprogramming during the 7 days of OSKM induction, we checked amylase and urea levels in serum (**Figure 33C**). Of note, amylase levels were higher in anti-NK1.1-treated mice compared to isotype control-treated mice, indicating a higher degree of reprogramming in these animals. After 7 days of doxycycline withdrawal, amylase and urea levels in both groups decreased to their normal basal state, correlating with the results observed at histological level. Therefore, the dysplastic foci originated upon NK cell depletion can be eliminated or reversed after a short pulse of OSKM induction.

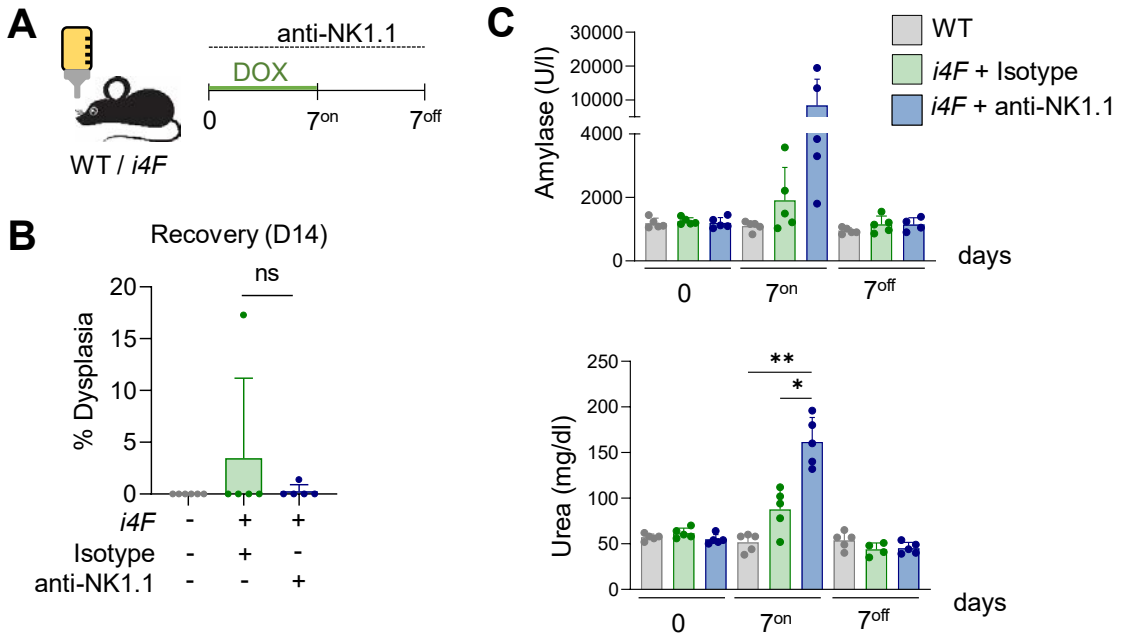

Figure 33 | NK1.1^{+} cell depletion induces reversible focal areas of dysplastic cells. A. Doxycycline (dox) was administrated in water for 7 days (7^{on}) and removed for 7 more days (7^{off}). Reprogrammable mice were injected with isotype control or anti-NK1.1 antibody during the 14 days of the experiment. **B.** Pancreatic dysplasia quantification after 1 week of reprogramming (7^{on}) and 1 week of recovery (7^{off}) (n=5). **C**. Amylase and urea levels in serum. Graphs represent mean ± SD; *p<0.05, **p<0.01 and statistical significance was evaluated using two-tailed Student's t-test.

2.8. Modulation of *in vivo* reprogramming by other cell types of the innate immune system: macrophages, MDSCs and neutrophils

Finally, we evaluated two other cell populations from the innate immune system that also infiltrate the pancreas during reprogramming, namely, macrophages and $Gr1^+$ cells, the latter including neutrophils and myeloid-derived suppressive cells (MDSCs). Clodronate-mediated depletion of phagocytic cells (**Figures 34A and 34B**) failed to significantly modify the reprogramming process (**Figure 34C**). To deplete $Gr1^+$ cells, we used the anti-Gr1 antibody (clone RB6-8C5) that recognizes the antigenic markers Ly6G and Ly6C. $Gr1^+$ cells include neutrophils ($CD11b^+Ly6G^{hi}$), and MDSCs. Of note, MDSCs are generally divided into mononucleated-MDSCs or M-MDSCs ($CD11b^+Ly6G^-Ly6C^{hi}$) and polymorphonucleated-MDSCs or PMN-MDSCs ($CD11b^+Ly6G^+Ly6C^{low}$) (Gabrilovich and Nagaraj, 2009) (**Figure 34D**). Interestingly, anti-Gr1 treatment strongly reduced reprogramming in the pancreas (**Figure 34E**). Considering that neutrophils and MDSCs suppress the activity of NK cells in different contexts, such as cancer (Bruno *et al.*, 2019; Li *et al.*, 2020; Sun *et al.*, 2020; Zalfa and Paust, 2021), these results are consistent with a scenario where NK cells eliminate cells undergoing reprogramming and, at the same time, NK cells are negatively regulated by infiltrating $Gr1^+$ cells.

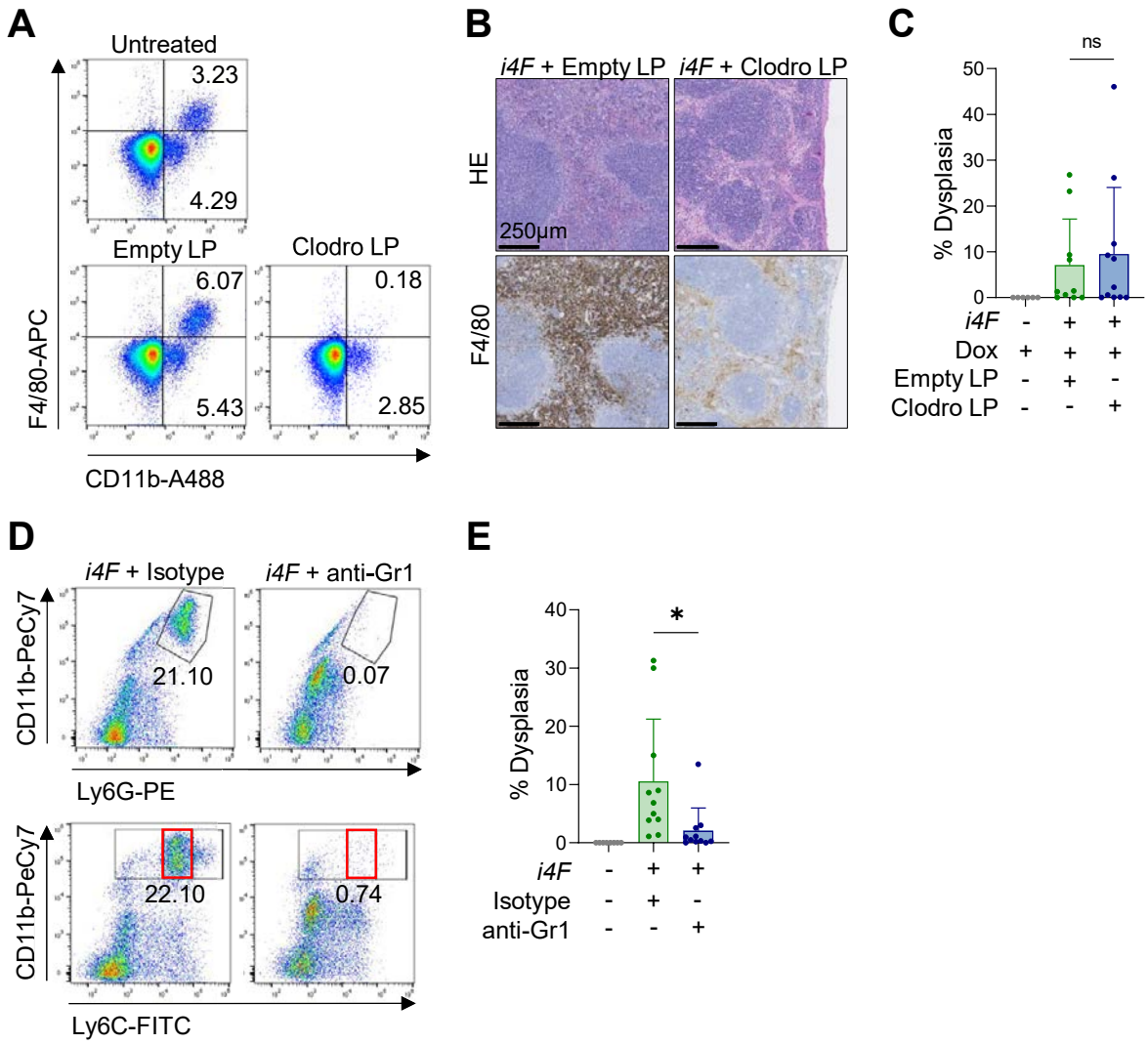

Figure 34 | Macrophage and Gr1$^+$ cells depletion during *in vivo* reprogramming. A. Cytometry quantification of F4/80 and CD11b double positive populations in blood 16 hours after intraperitoneally liposomes (LP) administration at day 3 of reprogramming. Gated in DAPI$^-$/CD45$^+$ cells. **B**. Immunohistochemistry of HE and F4/80 in the spleen of mice treated with doxycycline and empty or clodronate LP for 7 days. **C**. Dysplasia quantification in the pancreas of mice reprogrammed with empty or clodronate LP for 7 days (n=6 for WT, n=10 for empty LP and n=11 for clodronate LP group). **D**. Representative cytometry quantification of Ly6C and CD11b, or Ly6G and CD11b populations in blood at day 5 of reprogramming. Gated in DAPI$^-$/CD45$^+$ cells. **E**. Dysplasia quantification in the pancreas of mice reprogrammed for 7 days with either anti-Gr1 or isotype control. Gated in DAPI$^-$ cells (n=8 for WT and n=11 for *i4F* and anti-Gr1 groups). Graphs represent mean ± SD; *p<0.05 and statistical significance was evaluated using two-tailed Student's t-test.

2.9. T cells limit *in vivo* reprogramming

Additionally, we investigated whether the adaptive immune system modulates the efficiency of reprogramming. To that aim, we first analyzed T cell infiltration, marked by the membrane receptor CD3, in pancreata undergoing reprogramming (days 0, 3, 6, 9 and 12). Whereas $CD3^+$ T cells were mostly within the lumen of blood vessels at days 0 and 3, they started to infiltrate within dysplastic regions at later time points (**Figure 35A**). Moreover, the percentage of infiltrated $CD3^+$ T cells significantly correlated with the degree of dysplasia in pancreas at day 7 of reprogramming (**Figure 35B**). These results prompted us to hypothesize that T cells could have an active role in modulating the efficiency of reprogramming. To address this question, we depleted both $CD4^+$ helper T cells and $CD8^+$ cytotoxic T cells using two specific monoclonal antibodies during one week of reprogramming (**Figure 35C, 35D**). Histologically, the absence of $CD4^+$ and $CD8^+$ cells resulted in a trend, not statistically significant, towards increased pancreatic dysplasia (**Figure 35E**). As it is known that the adaptive immune response is initiated around one week after the initial damage (Julier *et al.*, 2017), we decided to repeat the experiment reprogramming the mice for 14 days instead. We administrated a low dose of doxycycline (0.2 mg/ml) to reduce the lethality of *i4F* mice under conditions of long treatment and high doses of doxycycline. In this setting, the degree of dysplasia upon $CD4^+$ and $CD8^+$ T cell depletion was significantly higher compared to *i4F* mice that received isotype control antibody (**Figure 35E**). This result suggests that, similarly to NK cells, T cells limit *in vivo* reprogramming.

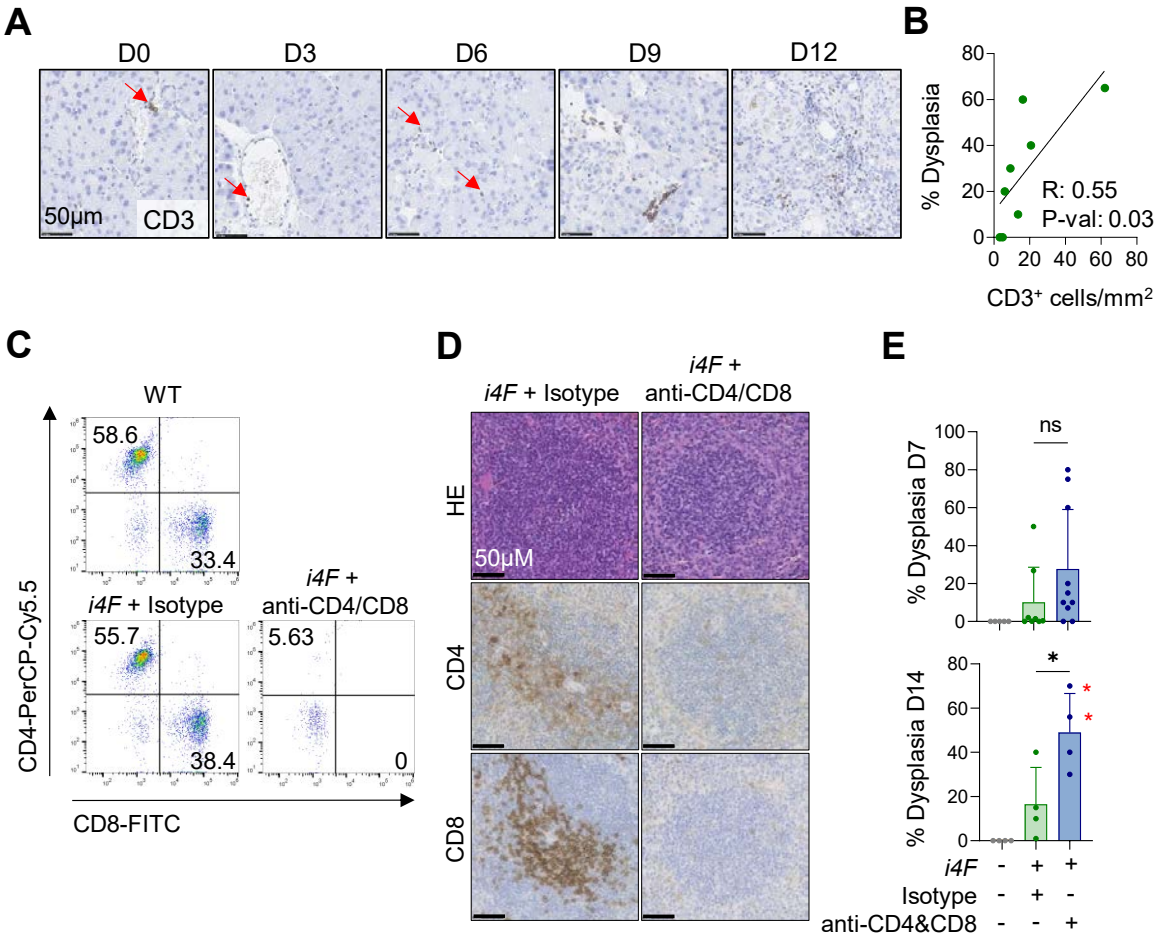

Figure 35 | T cell infiltrate the reprogrammed pancreas and limit *in vivo* reprogramming. **A**. Representative CD3 staining of reprogrammed pancreas at different time points (day, 0, 3, 6, 9 and 12) (*n*=3). **B**. Correlation between percentage of dysplastic pancreas and the percentage of $CD3^+$ cells infiltrating the pancreas at day 7 of reprogramming (*n*=7). Statistical significance was evaluated by simple lineal regression (p.val = 0.003) **C**. Cytometry quantification of $CD4^+$ and $CD8^+$ T cells populations in blood at day 3 of reprogramming. Gated in $DAPI^-/CD3^+$ cells. **D**. Serial sections of HE, CD4 and CD8-positive cells in the spleen of mice treated with isotype control or anti-CD4 and anti-CD8 antibodies at day 7. **E**. Percentage of dysplasia in the pancreas (upper graph) of WT mice (*n*=5), and *i4F* mice treated with isotype (*n*=8) or anti-CD4 and anti-CD8-depleting antibodies (*n*=10) for 7 days (injections at day -1 and 4 of the doxycycline (1 mg/ml) treatment) and percentage of dysplasia in the pancreas (lower graph) of mice treated with the same antibodies for 14 days (injections at day -1, 4 and 11 of the doxycycline (0.2 mg/ml) treatment) (*n*=4). Mice marked with (*) had to be sacrificed at day 11 due to ethical endpoint guidelines. Graphs represents mean ± SD; *$p<0.05$, and statistical significance was evaluated using two-tailed Student's t-test.

2.10. Immunopeptidome of *in vitro* reprogramming

The process of reprogramming involves the expression of genes that are normally silent in the genome, even at the thymus epithelial cells responsible for central tolerance. For this reason, it is conceivable that reprogramming may generate an adaptive immune response against self-antigens. In this regard, previous studies support the idea that iPSCs produce immunogenic epitopes that are recognized by the adaptive immune system (Kooreman *et al.*, 2018; Deuse *et al.*, 2019; Ouyang *et al.*, 2021). However, nothing is known about the early stages of reprogramming. Thus, we hypothesized that partially reprogrammed cells could already present immunogenic self-antigens to T cells. To address this question, we collaborated with the team led by Etienne Caron and Isabelle Sirois (University of Montreal, Canada). We used *in vitro* reprogramming of MEFs, as this approach offers the possibility to collect high number of cells for analysis. Thus, we reprogrammed WT and *i4F* MEFs in the presence of doxycycline for 5 days, when iPSCs colonies are not yet formed. Next, the group of Caron extracted and purified the peptides bound to the MHC-I haplotypes (H2-Db and H2-Kb) in the above-described MEFs undergoing partial reprogramming, and performed mass-spectrometry (MS). We first analysed the technical quality of the results. A total of 754 peptides in WT MEFs and 663 peptides in *i4F* MEFs were identified. Moreover, 79-85% of the identified peptides in both conditions were 8-12 mers long (mers = number of residues in the peptide), which is the size of the peptides that bind to MHC-I molecules. Overall, these numbers demonstrate a high quality isolation of peptides. The resulting 8-12 mers were further classified as weak, strong, or non-binders to MHC-I molecules according to the "eluted ligand" (EL) scores. EL scores reflect the likelihood of observing a given peptide in an eluted ligand experiment (Kovalchik *et al.*, 2020). Non-binders (NON-B) for both haplotypes are considered contaminations from peptides that are not associated to MHC-I. At present, we have focused on the strong binders (SB) for at least one of the two MHC-I haplotypes (H2-Kb/Db). In order to know whether there were specific peptides of the *i4F* MEFs condition, we next compared the WT and *i4F* peptides with peptides obtained from three more conditions (**Figure 37**):

1- Senescent MEFs previously treated with doxorubicin, a DNA damage agent, for 10 days (n=4).
2- WT MEFs maintained in culture for 10 days (n=4).
3- Nineteen tissues from adult male and female C57BL/6 mice (8-12 mers) (n=5-6) (Schuster *et al.*, 2018). Of note, we excluded peptides detected in testis due to the presence of germline-derived SCs in this tissue that could interfere with our objective (Liu *et al.*, 2009).

Venn diagrams represent merged peptides from the five different conditions above mentioned (**Figure 36**). Of note, senescent and WT (control) samples were processed at the same time as our samples of interest. In the case of the tissues from adult mice, they were previously reported by the group of Dr. Etienne Caron (Schuster *et al.*, 2018), but the protocol of peptide elution was performed in the same conditions and in the same facility as our samples of interest. Interestingly, there were eight peptides expressed exclusively in the reprogramming MEFs (**Figure 36**). These peptides were then compared with the reference proteome in order to decipher the proteins of origin (**Table 3**).

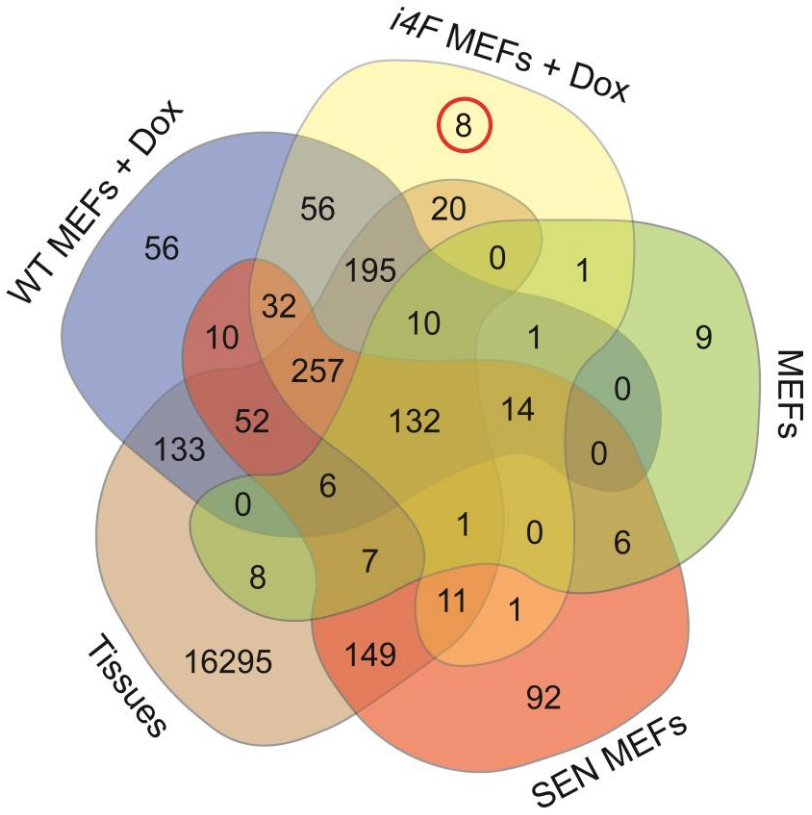

Figure 36 | Partially reprogrammed *i4F* MEFs present eight unique H2-Db/Kb-associated peptides. Venn diagram showing the overlap between high-confidence H2-Db/Kb-associated peptides identified from WT MEFs and *i4F* MEFs treated with doxycycline (dox) (1 µg/ml) for 5 days (*n*=3), senescent cells treated with doxorubicin (100 nM) for 10 days (SEN MEFs) (*n*=4), WT MEFs in culture for 10 days (MEFs) and heathy tissues from adult male and female C57BL/6 mice previously published (Schuster *et al.*, 2018), with exception of the testis (Tissues) (*n*=5-6).

As mentioned before, all the unique peptides were predicted to strongly bind at least one MHC-I haplotype (H2-Db or H2-Kb). The peptides corresponding to proteins ZFP870 and DHRS3 were strong binders to both haplotypes. Surprisingly, six out of eight peptides

belonged to proteins related to embryonic development or tumour progression: ZFP780, SMARCA5, RNF216, MYL12a, GBP (1/2a/2b/5) and DHRS3.

Overall, we can conclude that there are peptides presented in *i4F* MEFs that are not presented by WT MEFs (cultured in presence of absence of doxycycline), by senescent MEFs and by tissues coming from adult healthy mice. Reprogramming shares characteristics with embryonic and cancer cells, which could explain the MHC-I-mediated presentation of peptides overexpressed in cancer or embryogenesis in partially reprogrammed MEFs. We speculate that these peptides could be involved in the adaptive immune response elicited during partial reprogramming (**Figure 35**). This hypothesis is being addressed in ongoing experiments at the moment of writing this Thesis.

Peptide	Protein	Number of *i4F* samples	Binds H2-Db	Binds H2-Kb
SSFQFHNRM	ZFP870	1	SB	SB
RNYEYCRL	SMARCA5	1	NON-B	SB
AVFAFRAV	TBC1D19	2	NON-B	SB
TSYMYKGL	PLEKHH2	1	NON-B	SB
VNYDFGHMHV	RNF216	2	NON-B	SB
SMGKNPTDEYL	MYL12a	1	SB	NON-B
KSYLMNKL	GBP1/2a/2b/5	1	NON-B	SB
SAFAFMESL	DHRS3	1	SB	SB

Table 3 | Partially reprogrammed *i4F* MEFs express unique MHC-I-associated peptides. Eight peptides belonging to specific proteins were detected by mass spectrometry (MS) in at least one of the three *i4F* MEFs replicates reprogrammed for five days in the presence of doxycycline (1 µg/ml). All the peptides were detected as strong binders (SB) of one or both MHC-1 haplotypes (H2-Db and H2-Kb). Non-binders peptides are depicted as "NON-B".

PART 3. Interplay between vitamin B12 and *in vivo* reprogramming

In recent years, several studies have supported the idea that *in vitro* reprogramming is a process with unique metabolic requirements (Shyh-Chang, Daley and Cantley, 2013; Shiraki, Ogaki and Kume, 2014b). At the same time, it is known that the intestinal microbiota is an important and diverse source of metabolites in mammals (McCarville *et al.*, 2020). Indeed, mouse microbiota contributes to many aspects of physiology and disease (Durack and Lynch, 2019). Therefore, a member of our laboratory previously reasoned that manipulation of mouse microbiota could provide novel insight into metabolic requirements of *in vivo* reprogramming.

To interrogate whether microbial changes occur during *in vivo* reprogramming, bacterial DNA from stool samples was isolated at days 0 and 7 of doxycycline administration and metagenome sequencing was performed (Levy, Thaiss and Elinav, 2015). Interestingly, microbial gene modules related to biosynthesis and metabolism of cobalamin (vitamin B12) were significantly altered in *i4F* mice (data not shown). While some such genes were upregulated in *i4F* mice compared to WT, others were upregulated in WT mice compared to *i4F* mice, reflecting an imbalance in cobalamin metabolism.

3.1. *In vivo* and *in vitro* reprogramming is characterized by an increased demand of 1C metabolism

These changes in cobalamin metabolism in the microbiota prompted us to examine the levels of vitamin B12 in the serum of reprogrammed mice. Interestingly, we found that vitamin B12 levels were significantly reduced in *i4F* mice 7 days after doxycycline administration (**Figure 37**).

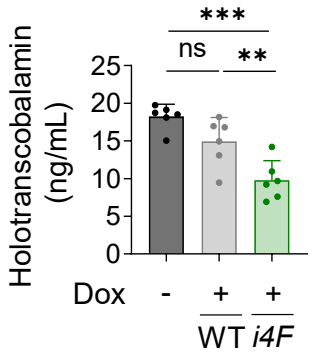

Figure 37 | *In vivo* reprogramming reduces the serum levels of vitamin B12. Levels of serum holotranscobalamin (available vitamin B12 to enter the cells) in untreated mice, and WT and *i4F* mice treated with doxycycline for 7 days (n=6). Graph represents mean ± SD; **p<0.01, ***p<0.001 by two-tailed Student's t-test.

To decipher the potential role of vitamin B12 during *in vivo* reprogramming, we examined serum metabolomics at different time points in *i4F* and WT mice treated with doxycycline. At day 7 of reprogramming, one of the most altered metabolic pathways in the serum of *i4F* mice was "glycine (Gly), serine (Ser), threonine (Thr) metabolism" (**Figure 38A**). These three amino acids (AAs), together with methionine (Met), feed the one-carbon (1C) metabolism. In particular, Thr is critical for *in vitro* iPSCs generation and for the maintenance of PSCs (Wang *et al.*, 2009; Shyh-Chang *et al.*, 2013; Shiraki, Ogaki and Kume, 2014a). Indeed, there was progressive reduction of four amino acids (Gly/Ser/Thr/Met) in the serum over the course of the 7 days of reprogramming (**Figure 38B**). Concretely, the abundance of Gly/Ser/Thr/Met reached their respective minima at day 4, and partially recovered at day 7 (**Figure 38B**). Importantly, similar changes (reduced Thr) have been reported in *in vitro* cultured PSCs (Wang *et al.*, 2009; Shyh-Chang *et al.*,

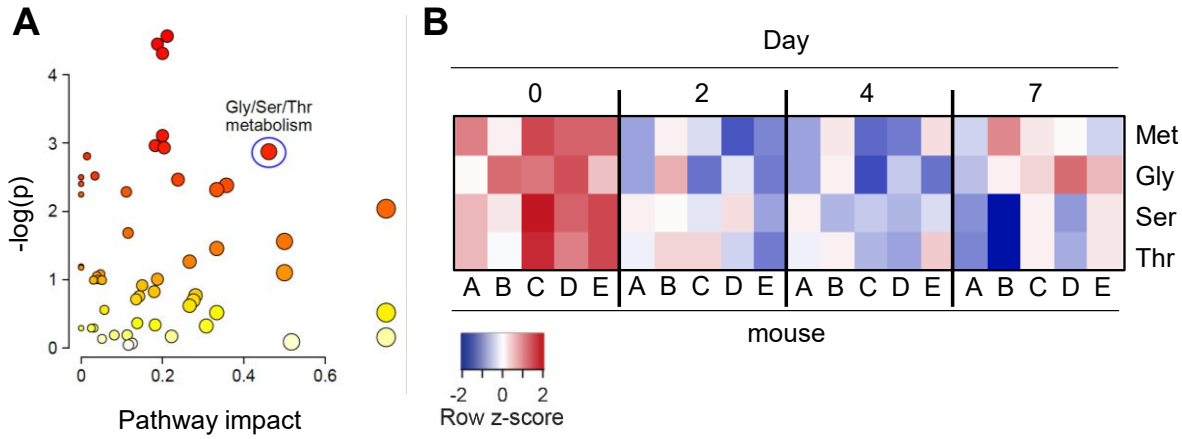

Figure 38 | *In vivo* reprogramming is characterized by an increased demand of 1C metabolism. A. Changes in serum metabolites during *in vivo* reprogramming. The metabolic pathway impact of annotated metabolites identified in the serum of *i4F* mice (*n*=5) at day 7 *versus* day 0 of doxycycline administration was calculated using MetaboAnalyst 5.0 (Pang *et al.*, 2021). This analysis ranks changes based on their enrichment analysis (white to red *p*-value gradient, being red the most significant); circle size indicates the relative contribution of the detected metabolites in its respective KEGG pathway. Pathway impact scores the centrality of the detected metabolites in the pathway. Gly/Ser/Thr metabolism (KEGG entry: map00260) is highlighted in a blue circle. **B**. Peak areas of methionine (Met), glycine (Gly), serine (Ser) and threonine (Thr) detected by MS on the indicated days (D0, 2, 4 and 7) of doxycycline (1 mg/ml) administration in the drinking water (*n*=5).

3.2. B12 supplementation improves *in vivo* and *in vitro* reprogramming

The reduced levels of vitamin B12 in the serum during reprogramming led us to hypothesize that B12 may be limiting for the process. To test this, we supplemented the drinking water of mice with vitamin B12 during 7 days of reprogramming. Remarkably, vitamin B12 significantly increased the percentage of dysplastic cells in the colon and the pancreas (**Figure 39**). Moreover, in the pancreas we observed a significant increase of $NANOG^+$ cells, indicating that vitamin B12 increases the frequency at which pluripotency is achieved (**Figure 39**). The results demonstrate that B12 levels are limiting for *in vivo* reprogramming, while vitamin B12 supplementation ameliorates the efficiency of the process.

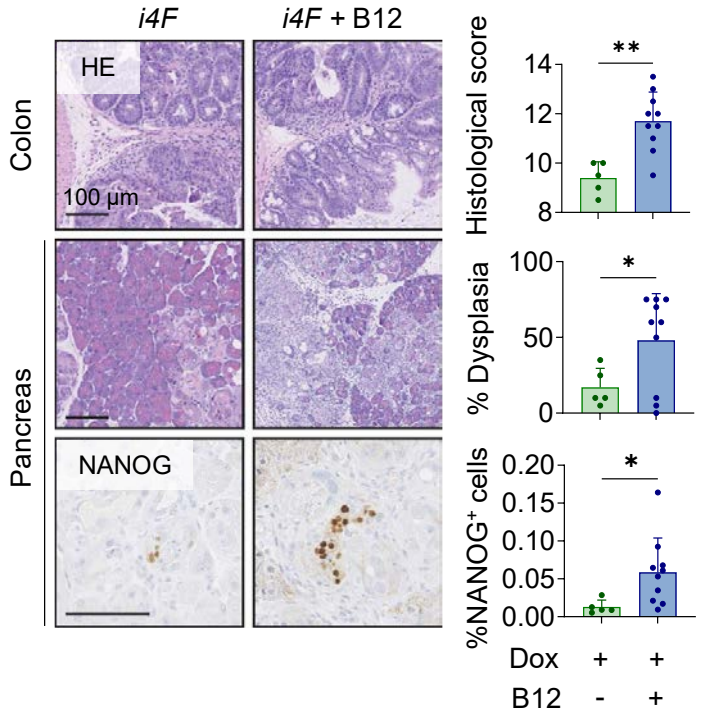

Figure 39 | Vitamin B12 supplementation increases the efficiency of *in vivo* reprogramming. *i4F* mice were treated with doxycycline (dox) (1 mg/ml) for 7 days with our without vitamin B12 supplementation (1.25 mg/l, together with dox in the drinking water). Representative HE images (left) and quantification (right) of reprogrammed colon and the pancreas, and NANOG staining (left) and quantification (right) of pancreas are shown. Colons were assigned a histologic score by a blinded pathologist according to the degree of dysplasia. For the pancreas, percentage of dysplasia and $NANOG^+$ cells was measured in a blinded way (n=5 for *i4F* and n=10 for *i4F* + B12). Graphs represent mean ± SD; *p<0.05, **p<0.001 by two-tailed Student's t-test.

We next wondered whether the effect of vitamin B12 on reprogramming could be recapitulated *in vitro*. Indeed, addition of vitamin B12 to *i4F* MEFs significantly increased

the efficiency of iPSC colony formation (**Figure 40B and 40C**). Similarly, addition of SAM, the methyl donor of the 1C metabolism, also significantly increased the formation of iPSC colonies. On the contrary, an inhibitor of the enzyme MAT2A, that converts methionine into SAM (**Figure 40A**), in combination with vitamin B12, blunted the effect that vitamin B12 had in promoting reprogramming, suggesting that the role that B12 has is directly related to SAM synthesis.

Overall, these results indicate a cell-autonomous role of vitamin B12 in reprogramming. Moreover, the increase in reprogramming efficiency upon vitamin B12 addition is mediated through MAT2A, which promotes the formation of SAM to provide methyl groups for methylation reactions.

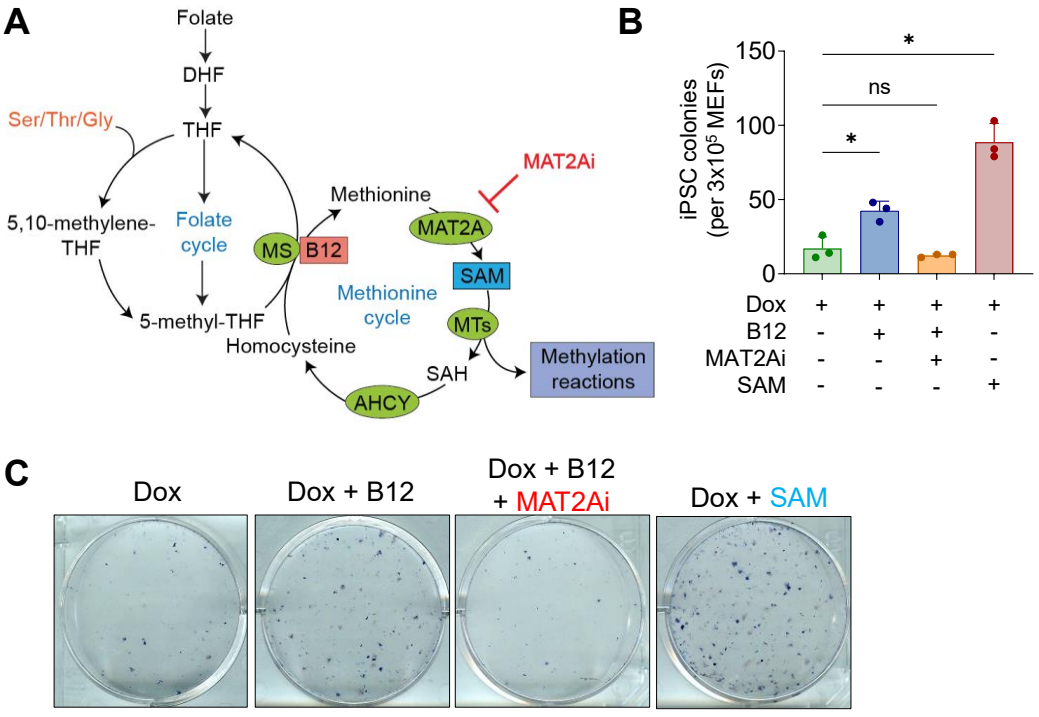

Figure 40 | Components of the 1C metabolism modulate the efficiency of *in vitro* reprogramming. A. Folate and methionine cycles, including the MAT2A inhibitor (MAT2Ai). **B**. Quantification of iPSC colonies and **C.** representative images of *i4F* MEFs reprogrammed in the presence of vitamin B12 (2μM), MAT2A inhibitor PF-9366 (2μM) and SAM (20μM) added directly into the iPSC media. Presence of iPSC colonies was scored by alkaline phosphatase staining. Each data point represents *i4F* MEFs generated from an independent embryo (n=3). Graphs represent mean ± SD; *p<0.05 by two-tailed Student's t-test.

Discussion

PART 1: OSKM-driven reprogramming as a model to study cellular dedifferentiation

Tissues of adult organisms are formed mostly by terminally differentiated cells that express specific transcriptional programs in order to perform precise functions within the tissue. Under homeostatic conditions, some tissues renovate their cells in a manner that depends on multipotent resident SCs. However, upon tissue damage, the microenvironment and signals caused by the injury can induce dedifferentiation in some cells, generating *de novo* multipotent progenitor cells (or facultative SCs) that repair the tissue. This method of tissue generation differs from that which operates in homeostasis. Examples of new cellular identities with SC-like features formed upon damage can be found in liver (Huch, Dorrell, *et al.*, 2013), small intestine (van Es *et al.*, 2012), lung (Tata *et al.*, 2013), stomach (Stange *et al.*, 2013), mammary gland (Chaffer *et al.*, 2011) and kidney (Chang-Panesso and Humphreys, 2017). At present, there is no evidence supporting that tissue maintenance during homeostasis or tissue repair upon injury rely on OSKM-driven cellular reprogramming. Nonetheless, cellular reprogramming using OSKM factors has been proposed as a powerful tool to dissect the events of cellular plasticity, as somatic cells become iPSCs through a process that also involves cellular dedifferentiation. Thus, in this thesis, we have used cellular reprogramming as a model to better understand cellular plasticity upon injury.

Long-term OSKM expression leads to teratoma formation (Abad *et al.*, 2013; Ohnishi *et al.*, 2014), while short-term expression induces cellular dedifferentiation without uncontrollable progression to full pluripotency (Ohnishi *et al.*, 2014; Ocampo *et al.*, 2016). *In vitro*, a short pulse of the Yamanaka factors was previously described to lead to the generation of dedifferentiated progenitor-like cells from MEFs without complete loss of cellular identity (*Thy1*) and without the upregulation of markers associated with intermediate reprogramming (*SSEA-1*) and pluripotency (*Nanog*) (Ocampo *et al.*, 2016). However, a detailed description of *in vivo* partial reprogramming based on markers is missing. In the first part of this thesis, we characterize this intermediate state of reprogramming using both histological and serological markers. First, we show that foci of acinar pancreatic cells undergo dysplasia and lose two key identity markers (CPA1 and PTF1a). This observation is in line with a study that demonstrated that short-term OSKM induction represses acinar cell enhancers (Shibata *et al.*, 2018). Some acinar cells acquire a ductal-like phenotype, which suggests a partial transdifferentiation or dedifferentiation, similar to what has been reported in caerulein-induced pancreatitis (Giroux and Rustgi, 2017). Other reprogrammed organs such as the colon and the stomach also lose epithelial markers, thus supporting the idea that there is multi-tissue cellular dedifferentitation in our *i4F* mouse model.

These histological markers are useful to determine the degree of reprogramming in post-mortem tissue analysis. However, there are currently no markers of partial reprogramming that can be measured in live mice. Here we describe for the first time serum markers that correlate with the degree of partial reprogramming. We first found significant upregulation of inflammatory cytokines (IL-15, IL-9, IL-6 and IFNγ) in the serum of *i4F* mice compared to WT mice, which implies the initiation of a systematic immune response, probably as result of the replicative stress and DNA damage produced upon OSKM expression (Ruiz *et al.*, 2015). Moreover, metabolomics analysis revealed the downregulation of four acyl-alkyl-phosphatidylcholines (Pcae18:1, Pcae20:1, Pcae20:2 and Pcae20:3) upon partial reprogramming. Among other functions, phosphatidylcholines inhibit the upregulation of the inflammatory cytokines, such as TNFα and IL-6, in various conditions (Ghyczy *et al.*, 2008; Tokés *et al.*, 2011; Jung *et al.*, 2013). Thus, their decrease in serum may contribute to the above-mentioned upregulation of IL-6 in serum. Whether phosphatydylcholines modulate the efficiency of *in vivo* reprogramming through IL-6 levels in blood would be an interesting avenue to explore. Additionally, we detected increased levels of urea in serum upon partial reprogramming. Urea is generated in the liver as a waste product of the digestion of proteins and its accumulation in blood generally corresponds to disruption of the kidney filtration system (Bigot *et al.*, 2017). This disruption could be the cause of increased urea levels in our *i4F* mice, as histological alterations in the kidney are detected upon partial reprogramming. Finally, we also validated amylase in our model as an enzyme that quantifies pancreatic damage. We have shown that accumulation of both urea and amylase is proportional to the amount of dysplasia observed in the pancreas and the kidney, respectively. Of all the detected cytokines, metabolites and enzymes that significantly changed in the first days of reprogramming, urea and amylase are easily measurable by commercial kits. Thus, we propose them as suitable markers for tracking the levels of partial reprogramming in live animals.

PART 2: The interplay between the immune system and *in vivo* reprogramming

NK cells are a barrier for cellular reprogramming

The process of reprogramming is typically inefficient, both *in vitro* and *in vivo* (Hanna *et al.*, 2009). This is due, at least in part, to the existence of multiple cell-autonomous barriers, such as tumour suppressors, chromatin regulators, transcription factors, signalling pathways and micro RNAs (Haridhasapavalan *et al.*, 2020; Arabacı *et al.*, 2021). Most of this knowledge comes from *in vitro* studies. In the context of *in vivo* reprogramming, however, little is known about whether the unexplored tissue microenvironment modulates the efficiency of reprogramming in a cell-extrinsic way.

In the second part of this thesis, we describe a considerable increase in immune infiltration in the pancreas upon partial reprogramming compared to WT mice. The infiltrating immune cell types are different from those ones in caerulein-induced pancreatitis, which suggests that *in vivo* partial reprogramming induces a specific immune response that different to general damage. We also report that NK cells target dysplastic cells during the first stages of OSKM reprogramming, as depletion of $NK1.1^{+}$ cell significantly improves the efficiency of the process, both in the pancreas and in the liver. Conversely, exogenous infusion of NK cells into *i4F* mice strongly reduces reprogramming in the pancreas. Regarding the mechanism of action, we show upregulation of NK-activating ligands during *in vivo* and *in vitro* partial reprogramming. In our *in vitro* co-culture system, blocking anti-NKG2D antibodies partially rescued the formation of iPSCs colonies. We conclude that NKG2D binding is an important process for the activation of NK cells during partial reprogramming. Our results do not exclude, however, the potential contribution of other stimulating receptors, such as LFA-1 (activated by ICAM-1) and DNAM-1 (stimulated by CD155 and CD122), to the negative effect of NK cells on reprogramming. Moreover, using the ATPase inhibitor ConA, we also demonstrate that NK cells kill target cells in a granule-dependent manner. *In vivo*, we show that infiltrating NK cells actively release lytic granules (CD107a), while upregulating inhibitory receptors (NKG2A), possibly as part of the acquisition of an exhausted phenotype (Ablamunits *et al.*, 2011; Sun *et al.*, 2017). It would be interesting to check whether blocking NKG2A with a specific antibody could avoid the proposed NK exhaustion, leading to a reduction of *in vivo* reprogramming efficiency in the pancreas. Another inhibitory receptor, Ly49C/I, significantly increases at day 3 and it returns to basal levels in the posterior days. A published study demonstrated that Ly49C/I is shed from the surface of infiltrating NK cells

in lung tumours (Shi *et al.*, 2018). In the future, we will check whether the same phenomenon also occurs during *in vivo* reprogramming.

Using an organoid assay, we have also proven that the absence of NK cells facilitates the growth of progenitor-like cells. In the near future, we will explore whether these NK-depleted organoids display better engraftment properties and improve tissue regeneration after injury. We are also planning to check whether they express markers of other pancreatic cell types, such as ductal cells or insulin-producing β-cells, which would imply *in vitro* multipotency. Finally, we have also shown that, upon doxycycline withdrawal, the pancreas of mice treated with anti-NK1.1 recovers homeostatic appearance. This result can have two possible, non-exclusive, interpretations: (1) the progenitor-like cells that survive in the absence of $NK1.1^+$ cells are able to differentiate again into acinar or other pancreatic cell types; or (2) these cells are eliminated by immune populations other than NK cells upon doxycycline withdrawal. Ohnishi *et al*. provided evidence of this first interpretation after labelling partial reprogrammed cells with bromodeoxyuridine (BrdU) for 4-7 days. BrdU-labelled cells were detected in normal-looking pancreatic and kidney tissues at day 14. This observation suggests that the proliferating cells caused by transient OSKM expression were, at least in part, integrated again into the tissue after doxycycline withdrawal (Ohnishi *et al.*, 2014).

Due to the lack of a commercial specific NK-depleting antibody, we have used anti-NK1.1 in our *in vivo* experiments. NK1.1 receptor has been suggested to have co-stimulatory functions in mouse (Tassi *et al.*, 2007) and, apart from NK cells, it is expressed in NKT cells (Sköld *et al.*, 2000), a T cell subpopulation (Assarsson *et al.*, 2000), and in some immature thymocytes (Kirkham and Carlyle, 2014). However, we consider that our interpretation that NK cells limit partial reprogramming is accurate for various reasons: (1) we performed *in vitro* co-culture experiments with isolated splenic NK cells previously primed with IL-2 and IL-15. Thus, the decrease in iPSC colony formation is exclusively produced by the cytotoxic activity of NK cells; (2) *In vivo* flow cytometry analysis of infiltrated NK cells (defined as $CD3^-/NK1.1^+$ cells) demonstrates that this cell type is activated and degranulates upon *in vivo* reprogramming; and (3) The *in vivo* adoptive transfer was done with isolated splenic NK cells. Therefore, the reduction in dysplasia and the absence of $NANOG^+$ cells in the pancreas of *i4F* mice that received NK cells compared to mice that received PBS is a result of the activity of NK cells. However, in the future, it would be appropriate to test more specific strategies to eliminate NK cells *in vivo* in order to validate our results. For instance, crossing our *i4F* mouse model with the transgenic mice generated by Dr. Eric Vivier, in which EGFP and diphtheria toxin receptor are expressed under the NKp46 promoter (Walzer *et al.*, 2007), would be a way to selectively deplete NK cells.

A limitation of our study is that the OSKM cassette is ubiquitously expressed in *i4F* mice. Thus, immune cells are also susceptible to reprogramming and, consequently, to dedifferentiation. In fact, circulating iPSCs in the bloodstream were found in our *i4F* mouse model, and it was shown that both hematopoietic and non-hematopietic cells can generate iPSCs (Abad *et al.*, 2013). We demonstrate that NK cells isolated from *i4F* mice reprogrammed for 5 days and incubated with doxycycline *in vitro* for 6 more days do not lose their cytotoxic capacity. In WT mice infected with OSKM-AAV-8 (a kind gift from Dr. Dirk Grimm, DKFZ, Germany), the absence of NK cells accelerates teratoma formation, a result that is in agreement with our findings in *i4F* mice. Moreover, we have tried to further validate our results in *i4F* mice transplanted with BM from WT mice. We are using the recently described antibody conditioning method, in which a combination of six antibodies depletes HSCs and immune lineages in the host and in this way it becomes amenable to grafting by transplanted HSCs (George *et al.*, 2019) (**Figure 43**). In parallel, we are generating a UBQ-creERT2;ROSA26-LSL-rtTA-IRES-eGFP;Neto2-tetO-OSKM mouse model in the lab, in which OSKM-expressing cells will be labelled with eGFP upon tamoxifen and doxycycline administration. UBQ-creERT2 can be replaced by any other tissue-specific creERT2 promoter. Thus, we will soon be able to express OSKM factors in specific cell types. Furthermore, this mouse model will allow us to determine whether NK cells directly target rtTA-expressing cells, labelled with eGFP, and whether these cells are proliferative or senescent.

Exploiting NK cell depletion as a tool to increase tissue regeneration via transient OSKM expression

Cellular reprogramming has been proposed as a potential strategy for regenerative medicine (Tabar and Studer, 2014; Trounson and DeWitt, 2016). Given the self-renewal and differentiation capacity of iPSCs, they are a suitable tool to obtain *in vitro* any desired cell type lost upon injury. However, full reprogramming raises several concerns for clinical applications, including the difficulty in obtaining homogenous populations with the desired state of maturation, possible genetic mutations induced during *in vitro* culture, the long time required to differentiate iPSCs into the desired cell type, and the difficulty in achieving efficient grafting. *In vivo* partial reprogramming also presents challenges, but it has the advantage of not requiring *in vitro* amplification and grafting. Moreover, it offers the possibility to unveil non-cell autonomous factors that can potentially increase the efficiency of the process. For instance, our lab described that OSKM-induced senescence promotes cellular plasticity during *in vivo* reprogramming in neighbouring non-senescent cells (Mosteiro *et al.*, 2016). Here we describe NK cells as a novel non-cellular autonomous

barrier for the process. It would be interesting to see whether NK cell depletion in combination with transient OSKM induction after injury improves tissue regeneration even more than in the presence of NK cells. In particular, we have recently set up an injury model of the colon (Dextran-Sulfate Sodium (DSS)-induced ulcers) where we have observed that transient activation of OSKM improves the repair of the colonic epithelium. We will soon test the effect of NK depletion in this model.

Finally, we demonstrate that NK cell depletion does not increase ADM lesions in acute pancreatitis, suggesting that NK cells are not a barrier for caerulein-induced dedifferentiation, but only for OSKM-induced dedifferentiation. In recent years, efforts have been channelled into trying to mimic OSKM-induced reprogramming in a gene-free setting. Thus, here we propose NK cell depletion as a possible factor that, in combination with other chemical compounds or biological factors, could contribute to the formation of an OSKM-free reprogramming system.

Involvement of other innate immune cell types in modulating cellular reprogramming efficiency

Our cytometry and scRNAseq data indicated that multiple leukocyte populations other than NK cells accumulate in the pancreas upon *in vivo* reprogramming. To study whether these cell types regulate OSKM-induced cellular dedifferentiation, we depleted them separately. Surprisingly, we did not detect any significant change in reprogramming efficiency when macrophages were depleted using clodronate liposomes. We surmise that this finding may reflect the presence of macrophage subpopulations with opposing effects on reprogramming, which is in line with the high heterogeneity and plasticity of these types of cells (Murray *et al.*, 2014; Guilliams and van de Laar, 2015).

In contrast to macrophages, depletion of MDSCs and neutrophils using an anti-Gr1 antibody significantly reduced *in vivo* reprogramming in the pancreas. It has been extensively described that MDSCs suppress the inflammatory functions of NK cells in different contexts, such as hepatitis C virus (HCV) infection (Celeste C. *et al.*, 2016), hepatocellular carcinoma (HCC) (Hoechst *et al.*, 2009), and other types of solid and haematological malignancies (Tumino *et al.*, 2021; Zalfa and Paust, 2021). Similarly, intra-tumoral MDSCs induce immune paralysis of $CD8^+$ T cells (Baumann *et al.*, 2020). Neutrophils also impair the cytotoxicity and infiltration capacity of NK cells in cancer (Spiegel *et al.*, 2016; Li *et al.*, 2020; Sun *et al.*, 2020) and suppress cytotoxic T cell-mediated immune responses (Murray *et al.*, 2014). Our data are therefore compatible with

a model in which $Gr1^+$ cells establish an immunosuppressive environment that counteracts the cytotoxic activities of NK and T cells against partially reprogrammed cells.

T cells limit *in vivo* partial reprogramming

In the second part of the thesis, we have also studied the role of the T cell-induced immune response during partial reprogramming. Two observations led us to hypothesize that T cells target cells undergoing reprogramming: (1) $CD3^+$ T cell infiltration positively correlates with the percentage of pancreatic dysplasia at day 7 of reprogramming and (2) elimination of $CD4^+$ and $CD8^+$ T cells increases the percentage of pancreatic dysplastic cells in *i4F* mice compared to their counterparts that have T cells. Of note, this difference is significant at day 14 of doxycycline administration, but not at day 7, thereby suggesting that the adaptive immune response is triggered mainly after one week of reprogramming.

T cells recognize as self-peptides those previously presented in the medulla of the thymus. These peptides derive from the degradation of proteins by the proteasome of thymic epithelial cells. However, it is now well established that under stress contexts, cells generate a fraction of prematurely terminated proteins that are processed by the proteasome in a manner that is different from non-stressed conditions. The result is the presentation of self-peptides that are normally not presented in the thymus and for which there is no tolerance (Yewdell and Hollý, 2020; Dersh, Hollý and Yewdell, 2021). Reprogramming induces replicative stress (Ruiz *et al.*, 2015), so we hypothesized that $CD8^+$ T cells target partial reprogrammed cells after recognizing immunogenic self-peptides in their MHC-I molecules. In collaboration with Dr. Etienne Caron (University of Montreal, Canada), we have isolated and sequenced peptides bound to MHC-I in fibroblasts undergoing reprogramming. In this manner, we have found 8 self-peptides expressed exclusively in these cells and not in senescent or control MEFs (treated with or without doxycycline). Moreover, they were not expressed in adult C57BL/6 mouse tissues (Schuster *et al.*, 2018). Of these peptides, six are normally upregulated during embryogenesis or cancer progression:

- ZFP870 (zinc finger protein 870) is a DNA-binding TF. Its human orthologue, ZNF670, is not expressed in homeostatic tissues and it is affiliated with long non-coding RNAs. It has been found to be significantly up-regulated in human breast cancer (Z. Chen *et al.*, 2021).
- SMARCA5 (SWI/SNF Related, Matrix.Associated, Actin-Dependent Regulator of Chromatin, Subfamily A, Member 5) is a chromatin remodeller. SMARCA5 maintains chromatin accessibility at promoters of haematopoiesis-related genes in

foetal hematopoietic stem and progenitor cells of zebrafish (Ding *et al.*, 2021) and mouse (Zikmund *et al.*, 2019). It is part of the common oocyte and ESC expression profiles (Assou *et al.*, 2009), and it has been implicated in zygotic genome activation (Alda-Catalinas *et al.*, 2020). SMARCA5 overexpression has also been related to proliferation in some types of cancer (Gigek *et al.*, 2011; Jin *et al.*, 2015).

- RNF216 (Ring finger protein 216) belongs to the RING family of E3 ubiquitin ligases and it plays a critical role in human gonadal development (Melnick *et al.*, 2019; Li *et al.*, 2021). Moreover, RNF216 enhances cell proliferation and its overexpression is correlated with colorectal cancer progression (Wang *et al.*, 2016).
- MYL12a (Myosin Light Chain 12A) is a non-sarcomeric myosin regulatory light chain and it is upregulated in methotrexate-induced senescence in human colon cancer cells (Dabrowska, Skoneczny and Rode, 2011)
- GBPs are guanylate-binding proteins. Several of them have been related to tumorigenesis: GBP2 in glioblastoma (Yu *et al.*, 2020) and pancreatic adenocarcinoma (B. Liu *et al.*, 2021), GBP1 in non-small lung adenocarcinoma (Song and Wei, 2020) and GBP5 in oral squamous cell carcinoma (P. Liu *et al.*, 2021).
- DHRS3 (short-chain retinaldehyde reductase) is expressed early in development and it prevents the formation of excessive retinoid acid during embryogenesis. *Dhrs3*-null embryos die late in gestation and display many cardiac and skeletal defects (Billings *et al.*, 2013).

It is known that reprogramming shares molecular features with both embryonic development and malignant cell transformation (Semi *et al.*, 2013; Friedmann-Morvinski and Verma, 2014; Zachary D Smith, Sindhu and Meissner, 2016; Pei *et al.*, 2019; Kim, 2020; Kishi *et al.*, 2021) Thus, it would not be surprising that peptides that form proteins normally expressed in both contexts are immunogenic in an healthy adult organism. The two other peptides detected belong to TBC1D19 (TBC1 Domain Family Member 19), which is a GTPase-activating protein, and PLEKHH2 (Pleckstrin Homology, MyTH4 and FERM Domain Containing H2), which is a membrane protein of unknown function.

Our immunopeptidome was obtained from comparing our MS spectra against a reference canonical proteome. However, there is a substantial fraction of peptides that cannot be assigned to annotated sequences, such as those that derive from introns, 3' and 5' UTRs, long and short non-coding RNAs, frameshifts of annotated genes, etc. (Murphy *et al.*, 2017). Non-canonical translation is specially enhanced by viral infections and other stressors (Prasad, Starck and Shastri, 2016; Starck *et al.*, 2016; Zanker *et al.*, 2019). Thus, it would be pertinent to perform non-canonical immunopeptidome in our model to get a greater insight into the complete T cell responses at the level of target peptides during

reprogramming. Moreover, of note, although we have focused on $CD8^+$ T cell-mediated response, $CD4^+$ T cells can also recognize peptides in the context of MHC-II after presentation by professional APCs (Hilligan and Ronchese, 2020). To decipher the specific role of each T lymphocyte subset during reprogramming, it would be interesting to deplete $CD4^+$ and $CD8^+$ T cells individually for 14 days.

In the near future, we will check whether our eight candidate peptides are immunogenic in an *in vivo* context. We are planning to immunize mice with subcutaneous injections of partially reprogrammed dying *i4F* MEFs and, after several rounds, we will isolate splenocytes and check their reactivity to these peptides. We are also planning to test our peptides as a vaccination strategy for cancer, as previously described using iPSCs as a vaccination for cancer protection (Kooreman *et al.*, 2018; Kishi *et al.*, 2021; Ouyang *et al.*, 2021).

PART 3: The interplay between *in vivo* reprogramming and one-carbon metabolism

Vitamin B12 is required for cellular reprogramming

In the third part of this thesis, we have identified vitamin B12 as a critical, cell-autonomous driver of cellular reprogramming. Indeed, vitamin B12 levels become limiting for reprogramming due to the high demand within the reprogramming tissues themselves. Accordingly, supplementation of the diet with B12 in drinking water increased reprogramming significantly in the pancreas and the colon.

The elevated demand for vitamin B12 is reflected in the reduction of vitamin B12 and metabolites of the 1C metabolism (Ser/Thr/Gly/Met) in the serum. Although our MS analysis did not generate data of the metabolite SAH, it would be interesting to determine whether its levels change upon reprogramming. If the SAM/SAH ratio were high, this would confirm that the cycle is constantly "running" in order to provide the cells with methyl groups. Similarly, levels of homocysteine were not provided by the MS analysis, but high levels of homocysteine in serum would be a good indicator of vitamin B12 deficiency (Vashi *et al.*, 2016). Moreover, in the future, it will be pertinent to do metabolic tracing of the 1C metabolism precursors (Ser/Thr/Gly) to validate whether their methyl groups are used for methylation reactions and even to trace where their carbon atoms are deposited (e.g. Histone modifications, DNA methylation, or protein methylation).

Mechanistically, it is known that insufficient 1C metabolism during *in vitro* reprogramming and the maintenance of ESCs leads to a loss of H3K4me3 (Ang *et al.*, 2011; Shyh-Chang *et al.*, 2013; Shiraki, Ogaki and Kume, 2014a). This epigenetic modification is characteristic of activated and bivalent promoters (Ang et al.,2011; Huang et al., 2016; Mikkelsen et al., 2007) and it is particularly sensitive to reductions in 1C metabolism (Shiraki et al., 2014; Shyh-Chang et al., 2013; Wang et al., 2009). In part, this is due to the fact that the methyl-transferases that catalyse H3K4 trimethylation present an affinity for SAM that is in the range of its intracellular concentration (Mentch and Locasale, 2016). Therefore, small variations in SAM cause changes in catalytic activity. Given this consideration, it would be interesting to examine the levels of H3K4me3 during *in vitro* and *in vivo* reprogramming, and to determine whether vitamin B12 supplementation modifies these levels. We hypothesize that vitamin B12 may be essential for achieving the H3K4me3 levels that are necessary to sustain changes in cellular identity. Finally, it would also be interesting to check whether other histone and DNA methylation marks change upon reprogramming, with and without vitamin B12 supplementation.

Due to the essential role of vitamin B12 in nucleic acid synthesis and methylation reactions, we speculate that vitamin B12 could also be involved in tissue repair. Thus, in the near future, we also plan to test whether vitamin B12 has a role in tissue damage and regeneration in different pathophysiological contexts.

Working model and its relevance

Partial cellular reprogramming recreates a similar situation to physiological damage, where cellular plasticity is acquired by cellular dedifferentiation. Some unsuccessful reprogramming trajectories lead to cellular senescence and apoptotic cell death. Here, we have first demonstrated that levels of amylase and urea in serum are indicative markers of the efficiency of *in vivo* reprogramming by ubiquitous OSKM induction. We have also identified NK and T cells as extrinsic barriers to the process. In contrast, MDSCs and neutrophils promote reprogramming. Abundant literature in several damage contexts supports the idea that MDSCs and neutrophils create an immunosuppressive environment that directly limits the cytotoxic activity of NK and T cells. Finally, we have provided evidence of vitamin B12 as a driver of reprogramming. Increased vitamin B12 demand starts midway during reprogramming, reaching its peak around day 4. This is reflected in reduction of metabolite precursors of the 1C metabolism (Ser/Thr/Gly) and Met at early time points in serum of mice undergoing reprogramming. At day 7, vitamin B12 levels in serum are significantly reduced (**Figure 41**).

The insights obtained in this thesis advance our current understanding of *in vivo* and *in vitro* reprogramming. The results presented here put forward the hypothesis that monoclonal antibodies targeting specific immune subsets, such as NK and T cells, and/or vitamin B12 administration could be deployed for the therapeutic enhancement of cellular plasticity in regenerative medicine.

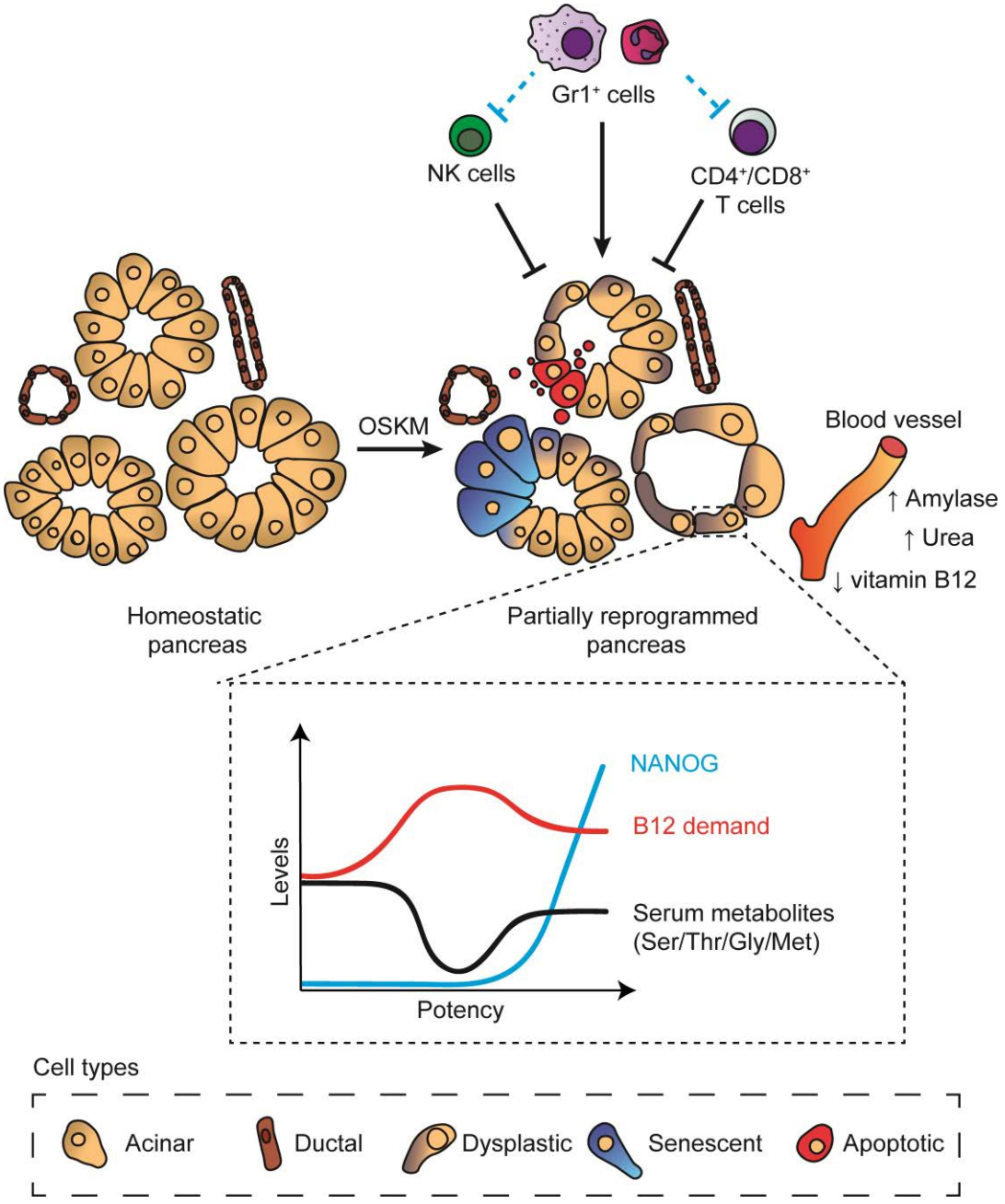

Figure 41 | Working model. Transient activation of the OSKM Yamanaka factors leads to pancreas dedifferentiation, reflected in the appearance of dysplastic foci. Other cellular fates, such as cellular senescence and apoptosis, occur in parallel. This scenario induces immune cell infiltration and consequent inflammation. NK and $CD4^+/CD8^+$ T cells recognize and limit reprogramming, while $Gr1^+$ cells, composed by MDSCs and neutrophils, favour the process, probably by inhibiting the cytotoxic activities of NK and T cells (blue dashed lines). In serum, amylase and urea levels increase proportionally to the degree of reprogramming. The temporal dynamics of reprogramming regarding vitamin B12 are depicted in a dashed square. Increased vitamin B12 demand begins early in reprogramming and peaks at day 4. This is reflected in a reduction of metabolites of the 1C metabolism (Ser/Thr/Gy/Met). Pluripotent $NANOG^+$ cells increase exponentially, reflecting the clonal expansion of individual successful reprogramming events.

Conclusions

PART 1

1. Dysplastic cells of partially reprogrammed *i4F* mice lose the expression of typical epithelial markers: CPA1 and PTF1a in the pancreas, and KRT19 in the colon and the stomach.
2. Pancreatic dysplastic cells acquire a ductal-like phenotype, as they start expressing KRT19, but lack canonical ductal markers, like HNF1β.
3. Upregulation of serum cytokines (IL-15, IL-9, IL-6 and IFNγ) upon partial reprogramming reflects a general inflammatory signature.
4. Serum amylase and urea are markers of the degree of partial reprogramming in *i4F* mice, as their levels in serum correlate with the percentage of dysplasia and hyperplasia in the pancreas and in the kidney, respectively.

PART 2

1. NK cells recognize NK-activating ligands in MEFs undergoing reprogramming and target them in a degranulation-dependent manner.
2. In mice, transient depletion of NK cells using a monoclonal anti-NK1.1 antibody significantly improves the efficiency of reprogramming, whereas NK cell adoptive transfer reduces it, thereby inferring that NK cells limit *in vivo* reprogramming.
3. Transient *in vivo* depletion of NK cells allows the generation of pancreatic cells with high organoid-formation capacity.
4. In mice, transient depletion of T lymphocytes using monoclonal antibodies significantly improves the efficiency of reprogramming after 14 days of OSKM-induction, thereby implying that T lymphocytes limit *in vivo* reprogramming.
5. Partially reprogrammed *i4F* MEFs express MHC-I-associated peptides that are not presented by WT MEFs (cultured in presence of absence of doxycycline), senescent MEFs and tissues coming from adult healthy mice.
6. *In vivo* transient depletion of MDSCs and neutrophils using an anti-Gr1 antibody significantly reduces the efficiency of reprogramming, inferring that these cell types promote *in vivo* reprogramming.

PART 3

1. *In vivo* reprogramming exhausts the supply of vitamin B12 to such an extent that the serum levels are significantly reduced.
2. Supplementation with vitamin B12 significantly improves the efficiency of *in vivo* and *in vitro* reprogramming.
3. Vitamin B12 has a cell-autonomous role in *in vitro* reprogramming.

References

Aasen, T. *et al.* (2008) 'Efficient and rapid generation of induced pluripotent stem cells from human keratinocytes', *Nature biotechnology*, 26(11), pp. 1276–1284. doi: 10.1038/NBT.1503.

Abad, M. *et al.* (2013) 'Reprogramming in vivo produces teratomas and iPS cells with totipotency features', *Nature*, 502(7471), pp. 340–345. doi: 10.1038/nature12586.

Abdool, K. *et al.* (2006) 'NK cells use NKG2D to recognize a mouse renal cancer (Renca), yet require intercellular adhesion molecule-1 expression on the tumor cells for optimal perforin-dependent effector function.', *Journal of immunology (Baltimore, Md. : 1950)*, 177(4), pp. 2575–2583. doi: 10.4049/jimmunol.177.4.2575.

Abel, A. M. *et al.* (2018) 'Natural Killer Cells: Development, Maturation, and Clinical Utilization', 9(August), pp. 1–23. doi: 10.3389/fimmu.2018.01869.

Ablamunits, V. *et al.* (2011) 'NKG2A is a marker for acquisition of regulatory function by human CD8+ T cells activated with anti-CD3 antibody', *European Journal of Immunology*, 41(7), pp. 1832–1842. doi: 10.1002/eji.201041258.

Abnave, P. and Ghigo, E. (2019) 'Role of the immune system in regeneration and its dynamic interplay with adult stem cells', *Seminars in Cell and Developmental Biology*, 87, pp. 160–168. doi: 10.1016/j.semcdb.2018.04.002.

Abubaker, K. *et al.* (2014) 'Inhibition of the JAK2/STAT3 pathway in ovarian cancer results in the loss of cancer stem cell-like characteristics and a reduced tumor burden', *BMC Cancer*, 14(1), pp. 1–22. doi: 10.1186/1471-2407-14-317.

Adams, E. J. *et al.* (2007) 'Structural elucidation of the m157 mouse cytomegalovirus ligand for Ly49 natural killer cell receptors.', *Proceedings of the National Academy of Sciences of the United States of America*, 104(24), pp. 10128–10133. doi: 10.1073/pnas.0703735104.

Aksoy, I. *et al.* (2014) 'Klf4 and Klf5 differentially inhibit mesoderm and endoderm differentiation in embryonic stem cells', *Nature Communications*, 5. doi: 10.1038/ncomms4719.

Alda-Catalinas, C. *et al.* (2020) 'A Single-Cell Transcriptomics CRISPR-Activation Screen Identifies Epigenetic Regulators of the Zygotic Genome Activation Program.', *Cell systems*, 11(1), pp. 25-41.e9. doi: 10.1016/j.cels.2020.06.004.

Allard-Chamard, H. *et al.* (2020) 'Interleukin-15 in autoimmunity.', *Cytokine*, 136, p. 155258. doi: 10.1016/j.cyto.2020.155258.

Alter, G., Malenfant, J. M. and Altfeld, M. (2004) 'CD107a as a functional marker for the identification of natural killer cell activity', *Journal of Immunological Methods*, 294(1–2), pp. 15–22. doi: 10.1016/j.jim.2004.08.008.

de Andrade, L. F., Smyth, M. J. and Martinet, L. (2014) 'DNAM-1 control of natural killer cells functions through nectin and nectin-like proteins.', *Immunology and cell biology*, 92(3), pp. 237–244. doi: 10.1038/icb.2013.95.

Ang, Y.-S. *et al.* (2011) 'Wdr5 mediates self-renewal and reprogramming via the embryonic stem cell core transcriptional network.', *Cell*, 145(2), pp. 183–197. doi: 10.1016/j.cell.2011.03.003.

Antonangeli, F. *et al.* (2016) 'Natural killer cell recognition of in vivo drug-induced senescent multiple myeloma cells', *OncoImmunology*, 5(10), pp. 1–11. doi: 10.1080/2162402X.2016.1218105.

Antonangeli, F. *et al.* (2019) 'Senescent cells: Living or dying is a matter of NK cells', *Journal of Leukocyte Biology*, 105(6), pp. 1275–1283. doi: 10.1002/JLB.MR0718-299R.

Aoi, T. *et al.* (2008) 'Generation of pluripotent stem cells from adult mouse liver and stomach cells', *Science (New York, N.Y.)*, 321(5889), pp. 699–702. doi: 10.1126/SCIENCE.1154884.

Arabacı, D. H. *et al.* (2021) 'Going up the hill: chromatin-based barriers to epigenetic reprogramming', *FEBS Journal*, 288(16), pp. 4798–4811. doi: 10.1111/febs.15628.

Arnold, K. *et al.* (2011) 'Sox2 + adult stem and progenitor cells are important for tissue regeneration and survival of mice', *Cell Stem Cell*, 9(4), pp. 317–329. doi: 10.1016/j.stem.2011.09.001.

Assarsson, E. *et al.* (2000) ' CD8 + T Cells Rapidly Acquire NK1.1 and NK Cell-Associated Molecules Upon Stimulation In Vitro and In Vivo ', *The Journal of Immunology*, 165(7), pp. 3673–3679. doi: 10.4049/jimmunol.165.7.3673.

Assou, S. *et al.* (2009) 'A gene expression signature shared by human mature oocytes and embryonic stem cells.', *BMC genomics*, 10, p. 10. doi: 10.1186/1471-2164-10-10.

Avilion, A. A. *et al.* (2003) 'Multipotent cell lineages in early mouse development depend on SOX2 function', *Genes and Development*, 17(1), pp. 126–140. doi: 10.1101/gad.224503.

Banito, A. *et al.* (2009) 'Senescence impairs successful reprogramming to pluripotent stem cells', *Genes and Development*, 23(18), pp. 2134–2139. doi: 10.1101/gad.1811609.

Bankhead, P. *et al.* (2017) 'QuPath: Open source software for digital pathology image analysis', *Scientific Reports*, 7(1), pp. 1–7. doi: 10.1038/s41598-017-17204-5.

Bareiss, P. M. *et al.* (2013) 'SOX2 expression associates with stem cell state in human ovarian carcinoma', *Cancer Research*, 73(17), pp. 5544–5555. doi: 10.1158/0008-

5472.CAN-12-4177.

Barker, N. *et al.* (2007) 'Identification of stem cells in small intestine and colon by marker gene Lgr5.', *Nature*, 449(7165), pp. 1003–1007. doi: 10.1038/nature06196.

Baron, M. *et al.* (2016) 'A Single-Cell Transcriptomic Map of the Human and Mouse Pancreas Reveals Inter- and Intra-cell Population Structure', *Cell Systems*, 3(4), pp. 346-360.e4. doi: 10.1016/j.cels.2016.08.011.

Bass, A. J. *et al.* (2009) 'SOX2 is an amplified lineage-survival oncogene in lung and esophageal squamous cell carcinomas', *Nature Genetics*, 41(11), pp. 1238–1242. doi: 10.1038/ng.465.

Baumann, T. *et al.* (2020) 'Regulatory myeloid cells paralyze T cells through cell–cell transfer of the metabolite methylglyoxal', *Nature Immunology*, 21(5), pp. 555–566. doi: 10.1038/s41590-020-0666-9.

Becht, E. *et al.* (2019) 'Dimensionality reduction for visualizing single-cell data using UMAP', *Nature Biotechnology*, 37(1), pp. 38–47. doi: 10.1038/nbt.4314.

Benabdallah, B. *et al.* (2019) 'Natural Killer Cells Prevent the Formation of Teratomas Derived From Human Induced Pluripotent Stem Cells', *Frontiers in Immunology*, 10, pp. 1–9. doi: 10.3389/fimmu.2019.02580.

Bendelac, A. *et al.* (1997) 'Mouse CD1-specific NK1 T cells: development, specificity, and function.', *Annual review of immunology*, 15, pp. 535–562. doi: 10.1146/annurev.immunol.15.1.535.

Benevento, M. *et al.* (2014) 'Proteome adaptation in cell reprogramming proceeds via distinct transcriptional networks', *Nature Communications*, 5. doi: 10.1038/ncomms6613.

Benjamini, Y. and Hochberg, Y. (1995) 'Controlling the False Discovery Rate: A Practical and Powerful Approach to Multiple Testing', *Journal of the Royal Statistical Society. Series B (Methodological)*, 57(1), pp. 289–300. Available at: http://www.jstor.org/stable/2346101.

Bernstein, B. E. *et al.* (2006) 'A bivalent chromatin structure marks key developmental genes in embryonic stem cells.', *Cell*, 125(2), pp. 315–326. doi: 10.1016/j.cell.2006.02.041.

Bigot, A. *et al.* (2017) 'Liver involvement in urea cycle disorders: a review of the literature.', *Journal of inherited metabolic disease*, 40(6), pp. 757–769. doi: 10.1007/s10545-017-0088-5.

Billings, S. E. *et al.* (2013) 'The retinaldehyde reductase DHRS3 is essential for preventing

the formation of excess retinoic acid during embryonic development.', *Federation of American Societies for Experimental Biology*, 27(12), pp. 4877–4889. doi: 10.1096/fj.13-227967.

Blaine, S. A. *et al.* (2010) 'Adult pancreatic acinar cells give rise to ducts but not endocrine cells in response to growth factor signaling.', *Development (Cambridge, England)*, 137(14), pp. 2289–2296. doi: 10.1242/dev.048421.

Blau, H. M., Chiu, C.-P. and Webster, C. (1983) 'Cytoplasmic activation of human nuclear genes in stable heterocaryons', *Cell*, 32(4), pp. 1171–1180. doi: 10.1016/0092-8674(83)90300-8.

Bourillot, P. Y. *et al.* (2009) 'Novel STAT3 target genes exert distinct roles in the inhibition of mesoderm and endoderm differentiation in cooperation with Nanog', *Stem Cells*, 27(8), pp. 1760–1771. doi: 10.1002/stem.110.

Brady, J. *et al.* (2004) 'IL-21 induces the functional maturation of murine NK cells.', *Journal of Immunology*, 172(4), pp. 2048–2058. doi: 10.4049/jimmunol.172.4.2048.

Brambrink, T. *et al.* (2008) 'Sequential expression of pluripotency markers during direct reprogramming of mouse somatic cells.', *Cell stem cell*, 2(2), pp. 151–9. doi: 10.1016/j.stem.2008.01.004.

Briggs, R. and King, T. J. (1952) 'Transplantation of Living Nuclei From Blastula Cells into Enucleated Frogs' Eggs.', *Proceedings of the National Academy of Sciences of the United States of America*, 38(5), pp. 455–463. doi: 10.1073/pnas.38.5.455.

Bruno, A. *et al.* (2019) 'Myeloid Derived Suppressor Cells Interactions With Natural Killer Cells and Pro-angiogenic Activities: Roles in Tumor Progression', *Frontiers in immunology*, 10(April), p. 771. doi: 10.3389/fimmu.2019.00771.

Bryceson, Y. T., Ljunggren, H.-G. and Long, E. O. (2009) 'Minimal requirement for induction of natural cytotoxicity and intersection of activation signals by inhibitory receptors.', *Blood*, 114(13), pp. 2657–2666. doi: 10.1182/blood-2009-01-201632.

Buganim, Y. *et al.* (2012) 'Single-cell expression analyses during cellular reprogramming reveal an early stochastic and a late hierarchic phase', *Cell*, 150(6), pp. 1209–1222. doi: 10.1016/j.cell.2012.08.023.

Bussian, T. J. *et al.* (2018) 'Clearance of senescent glial cells prevents tau-dependent pathology and cognitive decline.', *Nature*, 562(7728), pp. 578–582. doi: 10.1038/s41586-018-0543-y.

Campbell, K. *et al.* (1996) 'Sheep cloned by nuclear transfer from a cultured cell line', *Nature*, 380(6569), pp. 64–66. doi: 10.1038/380064A0.

Campisi, J. and d'Adda di Fagagna, F. (2007) 'Cellular senescence: when bad things happen to good cells.', *Nature reviews. Molecular cell biology*, 8(9), pp. 729–740. doi: 10.1038/nrm2233.

Carey, B. W. *et al.* (2009) 'Reprogramming of murine and human somatic cells using a single polycistronic vector', *Proceedings of the National Academy of Sciences of the United States of America*, 106(1), pp. 157–162. doi: 10.1073/pnas.0811426106.

Carlyle, J. R. *et al.* (2006) 'Molecular and genetic basis for strain-dependent NK1.1 alloreactivity of mouse NK cells.', *Journal of Immunology*, 176(12), pp. 7511–7524. doi: 10.4049/jimmunol.176.12.7511.

Cartwright, P. *et al.* (2005) 'LIF/STAT3 controls ES cell self-renewal and pluripotency by a Myc-dependent mechanism', *Development (Cambridge, England)*, 132(5), pp. 885–896. doi: 10.1242/DEV.01670.

Celeste C., G. *et al.* (2016) 'Hepatitis C Virus–Induced Myeloid-Derived Suppressor Cells Suppress NK Cell IFN-γ Production by Altering Cellular Metabolism via Arginase-1', pp. 2283–2292. doi: https://doi.org/10.4049/jimmunol.1501881.

Cerwenka, A., Baron, J. L. and Lanier, L. L. (2001) 'Ectopic expression of retinoic acid early inducible-1 gene (RAE-1) permits natural killer cell-mediated rejection of a MHC class I-bearing tumor in vivo.', *Proceedings of the National Academy of Sciences of the United States of America*, 98(20), pp. 11521–11526. doi: 10.1073/pnas.201238598.

Chaffer, C. L. *et al.* (2011) 'Normal and neoplastic nonstem cells can spontaneously convert to a stem-like state.', *Proceedings of the National Academy of Sciences of the United States of America*, 108(19), pp. 7950–7955. doi: 10.1073/pnas.1102454108.

Chakraborty, S., Kubatzky, K. F. and Mitra, D. K. (2019) 'An update on interleukin-9: From its cellular source and signal transduction to its role in immunopathogenesis', *International Journal of Molecular Sciences*, 20(9). doi: 10.3390/ijms20092113.

Chang-Panesso, M. and Humphreys, B. D. (2017) 'Cellular plasticity in kidney injury and repair', *Nature Reviews Nephrology*, 13(1), pp. 39–46. doi: 10.1038/nrneph.2016.169.

Chappell, J. *et al.* (2013) 'MYC/MAX control ERK signaling and pluripotency by regulation of dual-specificity phosphatases 2 and 7', *Genes & development*, 27(7), pp. 725–733. doi: 10.1101/GAD.211300.112.

Chen, Jiekai *et al.* (2013) 'H3K9 methylation is a barrier during somatic cell reprogramming into iPSCs.', *Nature genetics*, 45(1), pp. 34–42. doi: 10.1038/ng.2491.

Chen, Y. *et al.* (2021) 'Reversible reprogramming of cardiomyocytes to a fetal state drives adult heart regeneration in mice', *Science*, 1540(September), pp. 1537–1540.

Chen, Z. *et al.* (2021) 'Profiling of specific long non-coding RNA signatures identifies ST8SIA6-AS1 AS a novel target for breast cancer.', *The Journal of Gene Medicine*, 23(2), p. e3286. doi: 10.1002/jgm.3286.

Chera, S. *et al.* (2014) 'Diabetes recovery by age-dependent conversion of pancreatic δ-cells into insulin producers', *Nature*, 514(7253), pp. 503–507. doi: 10.1038/nature13633.

Chiche, A. *et al.* (2017) 'Injury-Induced Senescence Enables In Vivo Reprogramming in Skeletal Muscle', *Cell Stem Cell*, 20(3), pp. 407-414.e4. doi: 10.1016/j.stem.2016.11.020.

Childs, B. G. *et al.* (2016) 'Senescent intimal foam cells are deleterious at all stages of atherosclerosis.', *Science*, 354(6311), pp. 472–477. doi: 10.1126/science.aaf6659.

Chong, J. and Xia, J. (2020) 'Using MetaboAnalyst 4.0 for Metabolomics Data Analysis, Interpretation, and Integration with Other Omics Data.', *Methods in molecular biology (Clifton, N.J.)*, 2104, pp. 337–360. doi: 10.1007/978-1-0716-0239-3_17.

Cikes, M., Friberg Jr., S. and Klein, G. (1973) 'Progressive Loss of H-2 Antigens With Concomitant Increase of Cell-Surface Antigen(s) Determined by Moloney Leukemia Virus in Cultured Murine Lymphomas23', *JNCI: Journal of the National Cancer Institute*, 50(2), pp. 347–362. doi: 10.1093/jnci/50.2.347.

Clancy, J. L. *et al.* (2014) 'Small RNA changes en route to distinct cellular states of induced pluripotency', *Nature Communications*, 5. doi: 10.1038/ncomms6522.

Clevers, H. (2016) 'Modeling Development and Disease with Organoids', *Cell*, 165(7), pp. 1586–1597. doi: 10.1016/j.cell.2016.05.082.

Cohnen, A. *et al.* (2013) 'Surface CD107a/LAMP-1 protects natural killer cells from degranulation-associated damage.', *Blood*, 122(8), pp. 1411–1418. doi: 10.1182/blood-2012-07-441832.

Cressman, D. E. *et al.* (1996) 'Liver failure and defective hepatocyte regeneration in interleukin-6-deficient mice.', *Science (New York, N.Y.)*, 274(5291), pp. 1379–1383. doi: 10.1126/science.274.5291.1379.

Criscimanna, A. *et al.* (2011) 'Duct cells contribute to regeneration of endocrine and acinar cells following pancreatic damage in adult mice', *Gastroenterology*, 141(4), pp. 1451–1462. doi: 10.1053/j.gastro.2011.07.003.

Dabrowska, M., Skoneczny, M. and Rode, W. (2011) 'Functional gene expression profile underlying methotrexate-induced senescence in human colon cancer cells.', *Tumour biology: the journal of the International Society for Oncodevelopmental Biology and Medicine*, 32(5), pp. 965–976. doi: 10.1007/s13277-011-0198-x.

Davis, R., Weintraub, H. and Lassar, A. (1987) 'Expression of a single transfected cDNA converts fibroblasts to myoblasts', *Cell*, 51(6), pp. 987–1000. doi: 10.1016/0092-8674(87)90585-X.

Day, M. and Schultz, R. (2010) 'An Overview of the Immune System', *Veterinary Immunology*, 357, pp. 9–18. doi: 10.1201/b15224-2.

De-Lázaro, I. *et al.* (2014) 'Generation of induced pluripotent stem cells from virus-free in vivo reprogramming of BALB/c mouse liver cells', *Biomaterials*, 35(29), pp. 8312–8320. doi: 10.1016/j.biomaterials.2014.05.086.

Demols, A. *et al.* (2000) 'CD4(+)T cells play an important role in acute experimental pancreatitis in mice.', *Gastroenterology*, 118(3), pp. 582–590. doi: 10.1016/s0016-5085(00)70265-4.

Denzin, L. K. and Cresswell, P. (1995) 'HLA-DM induces clip dissociation from MHC class II αβ dimers and facilitates peptide loading', *Cell*, 82(1), pp. 155–165. doi: 10.1016/0092-8674(95)90061-6.

Dersh, D., Hollý, J. and Yewdell, J. W. (2021) 'A few good peptides: MHC class I-based cancer immunosurveillance and immunoevasion', *Nature Reviews Immunology*, 21(2), pp. 116–128. doi: 10.1038/s41577-020-0390-6.

Desai, B. M. *et al.* (2007) 'Preexisting pancreatic acinar cells contribute to acinar cell, but not islet beta cell, regeneration.', *The Journal of Clinical Investigation*, 117(4), pp. 971–977. doi: 10.1172/JCI29988.

van Deursen, J. M. (2014) 'The role of senescent cells in ageing.', *Nature*, 509(7501), pp. 439–446. doi: 10.1038/nature13193.

Deuse, T. *et al.* (2019) 'De novo mutations in mitochondrial DNA of iPSCs produce immunogenic neoepitopes in mice and humans', *Nature Biotechnology*, 37(10), pp. 1137–1144. doi: 10.1038/s41587-019-0227-7.

Diefenbach, A. *et al.* (2001) 'Rae1 and H60 ligands of the NKG2D receptor stimulate tumour immunity.', *Nature*, 413(6852), pp. 165–171. doi: 10.1038/35093109.

Dimitrijević, M. *et al.* (2016) 'Aging affects the responsiveness of rat peritoneal macrophages to GM-CSF and IL-4.', *Biogerontology*, 17(2), pp. 359–371. doi: 10.1007/s10522-015-9620-x.

Ding, Y. *et al.* (2021) 'Smarca5-mediated epigenetic programming facilitates fetal HSPC development in vertebrates.', *Blood*, 137(2), pp. 190–202. doi: 10.1182/blood.2020005219.

Doeser, M. C., Schöler, H. R. and Wu, G. (2018) 'Reduction of Fibrosis and Scar Formation

by Partial Reprogramming In Vivo', *Stem Cells*, 36(8), pp. 1216–1225. doi: 10.1002/stem.2842.

Dor, Y. *et al.* (2004) 'Adult pancreatic beta-cells are formed by self-duplication rather than stem-cell differentiation.', *Nature*, 429(6987), pp. 41–46. doi: 10.1038/nature02520.

Dressel, R. *et al.* (2008) 'The tumorigenicity of mouse embryonic stem cells and in vitro differentiated neuronal cells is controlled by the recipients' immune response', *PLoS ONE*, 3(7). doi: 10.1371/journal.pone.0002622.

Dressel, R. *et al.* (2009) 'Multipotent adult germ-line stem cells, like other pluripotent stem cells, can be killed by cytotoxic T lymphocytes despite low expression of major histocompatibility complex class I molecules', *Biology Direct*, 4, p. 31. doi: 10.1186/1745-6150-4-31.

Dressel, R. *et al.* (2010) 'Pluripotent stem cells are highly susceptible targets for syngeneic, allogeneic, and xenogeneic natural killer cells', *The FASEB Journal*, 24(7), pp. 2164–2177. doi: 10.1096/fj.09-134957.

Drukker, M. and Benvenisty, N. (2004) 'The immunogenicity of human embryonic stem-derived cells.', *Trends in biotechnology*, 22(3), pp. 136–141. doi: 10.1016/j.tibtech.2004.01.003.

Durack, J. and Lynch, S. V. (2019) 'The gut microbiome: Relationships with disease and opportunities for therapy', *Journal of Experimental Medicine*, 216(1), pp. 20–40. doi: 10.1084/jem.20180448.

Edel, M. J. *et al.* (2010) 'Rem2 GTPase maintains survival of human embryonic stem cells as well as enhancing reprogramming by regulating p53 and cyclin D1', *Genes and Development*, 24(6), pp. 561–573. doi: 10.1101/gad.1876710.

Egashira, M. *et al.* (2017) 'F4/80+ Macrophages Contribute to Clearance of Senescent Cells in the Mouse Postpartum Uterus.', *Endocrinology*, 158(7), pp. 2344–2353. doi: 10.1210/en.2016-1886.

Eminli, S. *et al.* (2008) 'Reprogramming of neural progenitor cells into induced pluripotent stem cells in the absence of exogenous Sox2 expression', *Stem cells*, 26(10), pp. 2467–2474. doi: 10.1634/STEMCELLS.2008-0317.

van Es, J. H. *et al.* (2012) 'Dll1+ secretory progenitor cells revert to stem cells upon crypt damage.', *Nature cell biology*, 14(10), pp. 1099–1104. doi: 10.1038/ncb2581.

Farr, J. N. *et al.* (2017) 'Targeting cellular senescence prevents age-related bone loss in mice.', *Nature medicine*, 23(9), pp. 1072–1079. doi: 10.1038/nm.4385.

Feng, B. *et al.* (2009) 'Reprogramming of fibroblasts into induced pluripotent stem cells

with orphan nuclear receptor Esrrb', *Nature Cell Biology*, 11(2), pp. 197–203. doi: 10.1038/ncb1827.

Feng, R. and Wen, J. (2015) 'Overview of the roles of Sox2 in stem cell and development', *Biological Chemistry*, 396(8), pp. 883–891. doi: 10.1515/hsz-2014-0317.

Fiore, P. F. *et al.* (2020) 'Interleukin-15 and cancer: some solved and many unsolved questions.', *Journal for immunotherapy of cancer*, 8(2). doi: 10.1136/jitc-2020-001428.

Folmes, C. D. L. *et al.* (2011) 'Somatic oxidative bioenergetics transitions into pluripotency-dependent glycolysis to facilitate nuclear reprogramming.', *Cell metabolism*, 14(2), pp. 264–271. doi: 10.1016/j.cmet.2011.06.011.

Frenzel, L. P. *et al.* (2009) 'Role of Natural-Killer Group 2 Member D Ligands and Intercellular Adhesion Molecule 1 in Natural Killer Cell-Mediated Lysis of Murine Embryonic Stem Cells and Embryonic Stem Cell-Derived Cardiomyocytes', *Stem Cells*, 27(2), pp. 307–316. doi: 10.1634/stemcells.2008-0528.

Friedmann-Morvinski, D. and Verma, I. M. (2014) 'Dedifferentiation and reprogramming: Origins of cancer stem cells', *EMBO Reports*, 15(3), pp. 244–253. doi: 10.1002/embr.201338254.

Frossard, J. L. *et al.* (1999) 'The role of intercellular adhesion molecule 1 and neutrophils in acute pancreatitis and pancreatitis-associated lung injury.', *Gastroenterology*, 116(3), pp. 694–701. doi: 10.1016/s0016-5085(99)70192-7.

Furse, S. and de Kroon, A. I. P. M. (2015) 'Phosphatidylcholine's functions beyond that of a membrane brick.', *Molecular membrane biology*, 32(4), pp. 117–119. doi: 10.3109/09687688.2015.1066894.

Gabrilovich, D. I. and Nagaraj, S. (2009) 'Myeloid-derived suppressor cells as regulators of the immune system', *Nature Reviews Immunology*, 9(3), pp. 162–174. doi: 10.1038/nri2506.

Garstka, M. A. *et al.* (2015) 'The first step of peptide selection in antigen presentation by MHC class I molecules', *Proceedings of the National Academy of Sciences of the United States of America*, 112(5), pp. 1505–1510. doi: 10.1073/pnas.1416543112.

Gasslander, T., Ihse, I. and Smeds, S. (1992) 'The importance of the centroacinar region in cerulein-induced mouse pancreatic growth.', *Scandinavian journal of gastroenterology*, 27(7), pp. 564–570. doi: 10.3109/00365529209000120.

Gasteiger, G. *et al.* (2013) 'IL-2-dependent tuning of NK cell sensitivity for target cells is controlled by regulatory T cells.', *The Journal of experimental medicine*, 210(6), pp. 1167–1178. doi: 10.1084/jem.20122462.

George, B. M. *et al.* (2019) 'Antibody Conditioning Enables MHC-Mismatched Hematopoietic Stem Cell Transplants and Organ Graft Tolerance', *Cell Stem Cell*, 25(2), pp. 185-192.e3. doi: 10.1016/j.stem.2019.05.018.

Geou-Yarh, L. *et al.* (2013) 'Liou, Macrophage-secreted cytokines drive pancreatic acinar-to-ductal metaplasia through NF-κB and MMPs.pdf', pp. 563–577.

Ghyczy, M. *et al.* (2008) 'Oral phosphatidylcholine pretreatment decreases ischemia-reperfusion-induced methane generation and the inflammatory response in the small intestine.', *Shock (Augusta, Ga.)*, 30(5), pp. 596–602. doi: 10.1097/SHK.0b013e31816f204a.

Gigek, C. O. *et al.* (2011) 'SMARCA5 methylation and expression in gastric cancer.', *Cancer investigation*, 29(2), pp. 162–166. doi: 10.3109/07357907.2010.543365.

Gilmour, K. C. *et al.* (2001) 'Defective expression of the interleukin-2/interleukin-15 receptor beta subunit leads to a natural killer cell-deficient form of severe combined immunodeficiency.', *Blood*, 98(3), pp. 877–879. doi: 10.1182/blood.v98.3.877.

Giroux, V. and Rustgi, A. K. (2017) 'Metaplasia: Tissue injury adaptation and a precursor to the dysplasia-cancer sequence', *Nature Reviews Cancer*, 17(10), pp. 594–604. doi: 10.1038/nrc.2017.68.

Golipour, A. *et al.* (2012) 'A late transition in somatic cell reprogramming requires regulators distinct from the pluripotency network', *Cell Stem Cell*, 11(6), pp. 769–782. doi: 10.1016/j.stem.2012.11.008.

Greder, L. V. *et al.* (2012) 'Brief report: Analysis of endogenous Oct4 activation during induced pluripotent stem cell reprogramming using an inducible Oct4 lineage label', *Stem Cells*, 30(11), pp. 2596–2601. doi: 10.1002/stem.1216.

Green, R. *et al.* (2017) 'Vitamin B12 deficiency', *Nature Reviews Disease Primers*, 3. doi: 10.1038/nrdp.2017.40.

Guerra, N. *et al.* (2008) 'NKG2D-deficient mice are defective in tumor surveillance in models of spontaneous malignancy.', *Immunity*, 28(4), pp. 571–580. doi: 10.1016/j.immuni.2008.02.016.

Guilliams, M. and van de Laar, L. (2015) 'A hitchhiker's guide to myeloid cell subsets: Practical implementation of a novel mononuclear phagocyte classification system', *Frontiers in Immunology*, 6(JUL), pp. 1–12. doi: 10.3389/fimmu.2015.00406.

Guo, H. *et al.* (1993) 'Therapeutic tumor-specific cell cycle block induced by methionine starvation in vivo.', *Cancer research*, 53(23), pp. 5676–5679.

Gurdon, J. B. (1962a) 'Adult frogs derived from the nuclei of single somatic cells.',

Developmental biology, 4, pp. 256–273. doi: 10.1016/0012-1606(62)90043-x.

Gurdon, J. B. (1962b) 'The developmental capacity of nuclei taken from intestinal epithelium cells of feeding tadpoles.', *Journal of embryology and experimental morphology*, 10, pp. 622–640.

Habtezion, A. (2016) 'Immune modulation in acute and chronic pancreatitis', *Curr. Opin. Gastroenterol.*, 31(5), pp. 395–9. doi: 10.1097/MOG.0000000000000195.

Hafemeister, C. and Satija, R. (2019) 'Normalization and variance stabilization of single-cell RNA-seq data using regularized negative binomial regression', *Genome Biology*, 20(1), pp. 1–15. doi: 10.1186/s13059-019-1874-1.

Hall, J. *et al.* (2009) 'Oct4 and LIF/Stat3 Additively Induce Krüppel Factors to Sustain Embryonic Stem Cell Self-Renewal', *Cell Stem Cell*, 5(6), pp. 597–609. doi: 10.1016/J.STEM.2009.11.003.

Han, J. *et al.* (2010) 'Tbx3 improves the germ-line competency of induced pluripotent stem cells', *Nature*, 463(7284), pp. 1096–1100. doi: 10.1038/nature08735.

Hanke, T. *et al.* (1999) 'Direct assessment of MHC class I binding by seven Ly49 inhibitory NK cell receptors.', *Immunity*, 11(1), pp. 67–77. doi: 10.1016/s1074-7613(00)80082-5.

Hanna, J. *et al.* (2008) 'Direct reprogramming of terminally differentiated mature B lymphocytes to pluripotency', *Cell*, 133(2), pp. 250–264. doi: 10.1016/J.CELL.2008.03.028.

Hanna, J. *et al.* (2009) 'Direct cell reprogramming is a stochastic process amenable to acceleration', *Nature*, 462(7273), pp. 595–601. doi: 10.1038/nature08592.

Hansson, J. *et al.* (2012) 'Highly coordinated proteome dynamics during reprogramming of somatic cells to pluripotency.', *Cell reports*, 2(6), pp. 1579–92. doi: 10.1016/j.celrep.2012.10.014.

Haridhasapavalan, K. K. *et al.* (2020) 'An Insight into Reprogramming Barriers to iPSC Generation', *Stem Cell Reviews and Reports*, 16(1), pp. 56–81. doi: 10.1007/s12015-019-09931-1.

Haurum, J. S. *et al.* (1999) 'Presentation of cytosolic glycosylated peptides by human class I major histocompatibility complex molecules in vivo', *Journal of Experimental Medicine*, 190(1), pp. 145–150. doi: 10.1084/jem.190.1.145.

Hayakawa, Y. *et al.* (2004) 'NK cell TRAIL eliminates immature dendritic cells in vivo and limits dendritic cell vaccination efficacy.', *Journal of immunology (Baltimore, Md. : 1950)*, 172(1), pp. 123–129. doi: 10.4049/jimmunol.172.1.123.

He, J. *et al.* (2014) 'Regeneration of liver after extreme hepatocyte loss occurs mainly via biliary transdifferentiation in zebrafish', *Gastroenterology*, 146(3), pp. 789-800.e8. doi: 10.1053/j.gastro.2013.11.045.

Herrera, P. L. (2000) 'Adult insulin- and glucagon-producing cells differentiate from two independent cell lineages.', *Development*, 127(11), pp. 2317–2322.

Hilligan, K. L. and Ronchese, F. (2020) 'Antigen presentation by dendritic cells and their instruction of CD4+ T helper cell responses.', *Cellular & molecular immunology*, 17(6), pp. 587–599. doi: 10.1038/s41423-020-0465-0.

Hishida, T. *et al.* (2011) 'Indefinite self-renewal of ESCs through Myc/Max transcriptional complex-independent mechanisms', *Cell stem cell*, 9(1), pp. 37–49. doi: 10.1016/J.STEM.2011.04.020.

Hochedlinger, K. *et al.* (2005) 'Ectopic expression of Oct-4 blocks progenitor-cell differentiation and causes dysplasia in epithelial tissues.', *Cell*, 121(3), pp. 465–77. doi: 10.1016/j.cell.2005.02.018.

Hoechst, B. *et al.* (2009) 'Myeloid derived suppressor cells inhibit natural killer cells in patients with hepatocellular carcinoma via the NKp30 receptor', *Hepatology*, 50(3), pp. 799–807. doi: 10.1002/hep.23054.

Hong, H. *et al.* (2009) 'Suppression of induced pluripotent stem cell generation by the p53-p21 pathway', *Nature*, 460(7259), pp. 1132–1135. doi: 10.1038/nature08235.

Hou, P. *et al.* (2013) 'Pluripotent stem cells induced from mouse somatic cells by small-molecule compounds', *Science*, 341(6146), pp. 651–654. doi: 10.1126/science.1239278.

Huang, P. *et al.* (2011) 'Induction of functional hepatocyte-like cells from mouse fibroblasts by defined factors', *Nature 2011 475:7356*, 475(7356), pp. 386–389. doi: 10.1038/nature10116.

Huch, M., Dorrell, C., *et al.* (2013) 'In vitro expansion of single Lgr5+ liver stem cells induced by Wnt-driven regeneration.', *Nature*, 494(7436), pp. 247–250. doi: 10.1038/nature11826.

Huch, M., Bonfanti, P., *et al.* (2013) 'Unlimited in vitro expansion of adult bi-potent pancreas progenitors through the Lgr5/R-spondin axis', *EMBO Journal*, 32(20), pp. 2708–2721. doi: 10.1038/emboj.2013.204.

Huntington, N. D. *et al.* (2007) 'NK cell maturation and peripheral homeostasis is associated with KLRG1 up-regulation.', *Journal of Immunology*, 178(8), pp. 4764–4770. doi: 10.4049/jimmunol.178.8.4764.

Huntington, N. D. (2017) ‘Regulation of Murine Natural Killer Cell Development’, 8, pp. 1–9. doi: 10.3389/fimmu.2017.00130.

Hussein, S. M. I. *et al.* (2014) ‘Genome-wide characterization of the routes to pluripotency.’, *Nature*, 516(7530), pp. 198–206. doi: 10.1038/nature14046.

Ieda, M. *et al.* (2010) ‘Direct reprogramming of fibroblasts into functional cardiomyocytes by defined factors’, *Cell*, 142(3), pp. 375–386. doi: 10.1016/J.CELL.2010.07.002.

Irvine, K. M. *et al.* (2014) ‘Senescent human hepatocytes express a unique secretory phenotype and promote macrophage migration.’, *World journal of gastroenterology*, 20(47), pp. 17851–17862. doi: 10.3748/wjg.v20.i47.17851.

Ito, M. *et al.* (2006) ‘Killer cell lectin-like receptor G1 binds three members of the classical cadherin family to inhibit NK cell cytotoxicity.’, *The Journal of experimental medicine*, 203(2), pp. 289–295. doi: 10.1084/jem.20051986.

Jaenisch, R. and Young, R. (2008) ‘Stem Cells, the Molecular Circuitry of Pluripotency and Nuclear Reprogramming’, *Cell*, 132(4), pp. 567–582. doi: 10.1016/j.cell.2008.01.015.

Jain, R. *et al.* (2010) ‘The use of Cytokeratin 19 (CK19) immunohistochemistry in lesions of the pancreas, gastrointestinal tract, and liver.’, *Applied immunohistochemistry & molecular morphology : AIMM*, 18(1), pp. 9–15. doi: 10.1097/PAI.0b013e3181ad36ea.

Jamieson, A. M. *et al.* (2004) ‘Turnover and proliferation of NK cells in steady state and lymphopenic conditions.’, *Journal of immunology (Baltimore, Md. : 1950)*, 172(2), pp. 864–870. doi: 10.4049/jimmunol.172.2.864.

Janeway, C. A. J. and Medzhitov, R. (2002) ‘Innate immune recognition.’, *Annual review of immunology*, 20, pp. 197–216. doi: 10.1146/annurev.immunol.20.083001.084359.

Jeon, H. *et al.* (2016) ‘Methionine deprivation suppresses triple-negative breast cancer metastasis in vitro and in vivo.’, *Oncotarget*, 7(41), pp. 67223–67234. doi: 10.18632/oncotarget.11615.

Jeon, O. H. *et al.* (2017) ‘Local clearance of senescent cells attenuates the development of post-traumatic osteoarthritis and creates a pro-regenerative environment.’, *Nature medicine*, 23(6), pp. 775–781. doi: 10.1038/nm.4324.

Jessen, K. R., Mirsky, R. and Arthur-Farraj, P. (2015) ‘The Role of Cell Plasticity in Tissue Repair: Adaptive Cellular Reprogramming’, *Developmental Cell*, 34(6), pp. 613–620. doi: 10.1016/j.devcel.2015.09.005.

Jewett, A., Man, Y. and Tseng, H. (2013) ‘Dual Functions of Natural Killer Cells in

Selection and Differentiation of Stem Cells; Role in Regulation of Inflammation and Regeneration of Tissues', *J Cancer*, 4(1), pp. 12–24. doi: 10.7150/jca.5519.

Jiang, J. *et al.* (2004) 'Disruption of cadherin/catenin expression, localization, and interactions during HgCl2-induced nephrotoxicity', *Toxicological Sciences*, 80(1), pp. 170–182. doi: 10.1093/toxsci/kfh143.

Jiang, J. *et al.* (2008) 'A core Klf circuitry regulates self-renewal of embryonic stem cells', *Nature cell biology*, 10(3), pp. 353–360. doi: 10.1038/NCB1698.

Jiao, Y. *et al.* (2016) 'Type 1 Innate Lymphoid Cell Biology: Lessons Learnt from Natural Killer Cells.', *Frontiers in immunology*, 7, p. 426. doi: 10.3389/fimmu.2016.00426.

Jin, Q. *et al.* (2015) 'Overexpression of SMARCA5 correlates with cell proliferation and migration in breast cancer.', *Tumour biology : the journal of the International Society for Oncodevelopmental Biology and Medicine*, 36(3), pp. 1895–1902. doi: 10.1007/s13277-014-2791-2.

Julier, Z. *et al.* (2017) 'Promoting tissue regeneration by modulating the immune system', *Acta Biomaterialia*, 53, pp. 13–28. doi: 10.1016/j.actbio.2017.01.056.

Jung, Y. Y. *et al.* (2013) 'Protective effect of phosphatidylcholine on lipopolysaccharide-induced acute inflammation in multiple organ injury', *Korean Journal of Physiology and Pharmacology*, 17(3), pp. 209–216. doi: 10.4196/kjpp.2013.17.3.209.

Kale, A. *et al.* (2020) 'Role of immune cells in the removal of deleterious senescent cells.', *Immunity & ageing : I & A*, 17, p. 16. doi: 10.1186/s12979-020-00187-9.

Kang, T.-W. *et al.* (2011) 'Senescence surveillance of pre-malignant hepatocytes limits liver cancer development.', *Nature*, 479(7374), pp. 547–551. doi: 10.1038/nature10599.

Kawamura, T. *et al.* (2009) 'Linking the p53 tumour suppressor pathway to somatic cell reprogramming', *Nature*, 460(7259), pp. 1140–1144. doi: 10.1038/nature08311.

Kehler, J. *et al.* (2004) 'Oct4 is required for primordial germ cell survival', *EMBO Reports*, 5(11), pp. 1078–1083. doi: 10.1038/sj.embor.7400279.

Kelly, C. J. *et al.* (2019) 'Oral vitamin B12 supplement is delivered to the distal gut, altering the corrinoid profile and selectively depleting Bacteroides in C57BL/6 mice.', *Gut microbes*, 10(6), pp. 654–662. doi: 10.1080/19490976.2019.1597667.

Kennedy, M. K. *et al.* (2000) 'Reversible defects in natural killer and memory CD8 T cell lineages in interleukin 15-deficient mice.', *The Journal of experimental medicine*, 191(5), pp. 771–780. doi: 10.1084/jem.191.5.771.

Kim, E. J. Y. *et al.* (2018) 'BAK/BAX-Mediated Apoptosis Is a Myc-Induced Roadblock

to Reprogramming', *Stem Cell Reports*, 10(2), pp. 331–338. doi: 10.1016/j.stemcr.2017.12.019.

Kim, J. (2020) 'Cellular reprogramming to model and study epigenetic alterations in cancer', *Stem Cell Research*, 49(October), p. 102062. doi: 10.1016/j.scr.2020.102062.

Kim, S. *et al.* (2002) 'In vivo developmental stages in murine natural killer cell maturation.', *Nature immunology*, 3(6), pp. 523–528. doi: 10.1038/ni796.

Kirkham, C. L. and Carlyle, J. R. (2014) 'Complexity and diversity of the NKR-P1: Clr (Klrb1: Clec2) recognition systems', *Frontiers in Immunology*, 5(JUN), pp. 1–16. doi: 10.3389/fimmu.2014.00214.

Kishi, M. *et al.* (2021) 'Evidence of Antitumor and Antimetastatic Potential of Induced Pluripotent Stem Cell-Based Vaccines in Cancer Immunotherapy', *Frontiers in Medicine*, 8(December), pp. 1–17. doi: 10.3389/fmed.2021.729018.

Klaewsongkram, J. *et al.* (2007) 'Krüppel-like factor 4 regulates B cell number and activation-induced B cell proliferation', *Journal of immunology (Baltimore, Md. : 1950)*, 179(7), pp. 4679–4684. doi: 10.4049/JIMMUNOL.179.7.4679.

Klein, L. *et al.* (2014) 'Positive and negative selection of the T cell repertoire: What thymocytes see (and don't see)', *Nature Reviews Immunology*, 14(6), pp. 377–391. doi: 10.1038/nri3667.

Koch, C. A., Jordan, C. E. and Platt, J. L. (2006) 'Complement-Dependent Control of Teratoma Formation by Embryonic Stem Cells', *The Journal of Immunology*, 177(7), pp. 4803–4809. doi: 10.4049/jimmunol.177.7.4803.

Koch, U. and Radtke, F. (2011) 'Mechanisms of T cell development and transformation', *Annual Review of Cell and Developmental Biology*, 27, pp. 539–562. doi: 10.1146/annurev-cellbio-092910-154008.

Koo, B. S. *et al.* (2015) 'Oct4 is a critical regulator of stemness in head and neck squamous carcinoma cells', *Oncogene*, 34(18), pp. 2317–2324. doi: 10.1038/onc.2014.174.

Kooreman, N. G. *et al.* (2018) 'Autologous iPSC-Based Vaccines Elicit Anti-tumor Responses In Vivo', *Cell Stem Cell*, 22(4), pp. 501-513.e7. doi: 10.1016/j.stem.2018.01.016.

Kovalchik, K. A. *et al.* (2020) 'Immunopeptidomics for Dummies: Detailed Experimental Protocols and Rapid, User-Friendly Visualization of MHC I and II Ligand Datasets with MhcVizPipe', *bioRxiv*, p. 2020.11.02.360958. doi: 10.1101/2020.11.02.360958.

Kragl, M. *et al.* (2009) 'Cells keep a memory of their tissue origin during axolotl limb regeneration', *Nature*, 460(7251), pp. 60–65. doi: 10.1038/nature08152.

Krizhanovsky, V. *et al.* (2008) 'Senescence of activated stellate cells limits liver fibrosis.', *Cell*, 134(4), pp. 657–667. doi: 10.1016/j.cell.2008.06.049.

Kubin, T. *et al.* (2011) 'Oncostatin M is a major mediator of cardiomyocyte dedifferentiation and remodeling.', *Cell stem cell*, 9(5), pp. 420–432. doi: 10.1016/j.stem.2011.08.013.

Kuleshov, M. V. *et al.* (2016) 'Enrichr: a comprehensive gene set enrichment analysis web server 2016 update', *Nucleic acids research*, 44(W1), pp. W90–W97. doi: 10.1093/nar/gkw377.

Kulessa, H., Frampton, J. and Graf, T. (1995) 'GATA-1 reprograms avian myelomonocytic cell lines into eosinophils, thromboblasts, and erythroblasts', *Genes & development*, 9(10), pp. 1250–1262. doi: 10.1101/GAD.9.10.1250.

Kumar, P. *et al.* (2013) 'IL-22 from conventional NK cells is epithelial regenerative and inflammation protective during influenza infection.', *Mucosal immunology*, 6(1), pp. 69–82. doi: 10.1038/mi.2012.49.

Kunath, T. *et al.* (2005) 'Imprinted X-inactivation in extra-embryonic endoderm cell lines from mouse blastocysts.', *Development*, 132(7), pp. 1649–1661. doi: 10.1242/dev.01715.

Kurita, M. *et al.* (2018) 'In vivo reprogramming of wound-resident cells generates skin epithelial tissue', *Nature*, 561(7722), pp. 243–270. doi: 10.1038/s41586-018-0477-4.

Kurotaki, D. *et al.* (2013) 'Essential role of the IRF8-KLF4 transcription factor cascade in murine monocyte differentiation', *Blood*, 121(10), p. 1839. doi: 10.1182/BLOOD-2012-06-437863.

Kuruvilla, J. *et al.* (2016) 'Krüppel-like Factor 4 Modulates Development of BMI1(+) Intestinal Stem Cell-Derived Lineage Following γ-Radiation-Induced Gut Injury in Mice', *Stem cell reports*, 6(6), pp. 815–824. doi: 10.1016/J.STEMCR.2016.04.014.

Kusaba, T. *et al.* (2014) 'Differentiated kidney epithelial cells repair injured proximal tubule', *Proceedings of the National Academy of Sciences*, 111(4), pp. 1527 LP – 1532. doi: 10.1073/pnas.1310653110.

Kylänpää, M. L., Repo, H. and Puolakkainen, P. A. (2010) 'Inflammation and immunosuppression in severe acute pancreatitis', *World Journal of Gastroenterology*, 16(23), pp. 2867–2872. doi: 10.3748/wjg.v16.i23.2867.

Lapasset, L. *et al.* (2011) 'Rejuvenating senescent and centenarian human cells by reprogramming through the pluripotent state', *Genes and Development*, 25(21), pp. 2248–2253. doi: 10.1101/gad.173922.111.

Lee, J. *et al.* (2012) 'Activation of innate immunity is required for efficient nuclear reprogramming', *Cell*, 151(3), pp. 547–558. doi: 10.1016/j.cell.2012.09.034.

Lee, M. Y. *et al.* (2020) 'Antigen processing and presentation in cancer immunotherapy', *Journal for immunotherapy of cancer*, 8(2), pp. 1–15. doi: 10.1136/jitc-2020-001111.

Leeson, T. S. and Leeson, R. (1986) 'Close association of centroacinar/ductular and insular cells in the rat pancreas.', *Histology and histopathology*, 1(1), pp. 33–42.

Leis, O. *et al.* (2012) 'Sox2 expression in breast tumours and activation in breast cancer stem cells', *Oncogene*, 31(11), pp. 1354–1365. doi: 10.1038/onc.2011.338.

Lengerke, C. *et al.* (2011) 'Expression of the embryonic stem cell marker SOX2 in early-stage breast carcinoma', *BMC Cancer*, 11(1), p. 42. doi: 10.1186/1471-2407-11-42.

Leung, C. Y. and Zernicka-Goetz, M. (2015) 'Mapping the journey from totipotency to lineage specification in the mouse embryo', *Current Opinion in Genetics and Development*, 34, pp. 71–76. doi: 10.1016/j.gde.2015.08.002.

Levy, M., Thaiss, C. A. and Elinav, E. (2015) 'Metagenomic cross-talk: the regulatory interplay between immunogenomics and the microbiome.', *Genome medicine*, 7, p. 120. doi: 10.1186/s13073-015-0249-9.

Li, D. *et al.* (2021) 'RNF216 regulates meiosis and PKA stability in the testes.', *FASEB journal : official publication of the Federation of American Societies for Experimental Biology*, 35(4), p. e21460. doi: 10.1096/fj.202002294RR.

Li, H. *et al.* (2009) 'The Ink4/Arf locus is a barrier for iPS cell reprogramming', *Nature*, 460(7259), pp. 1136–1139. doi: 10.1038/nature08290.

Li, P. *et al.* (2020) 'Dual roles of neutrophils in metastatic colonization are governed by the host NK cell status', *Nature Communications*, 11(1), pp. 1–14. doi: 10.1038/s41467-020-18125-0.

Liao, J. *et al.* (2009) 'Generation of induced pluripotent stem cell lines from adult rat cells', *Cell stem cell*, 4(1), pp. 11–15. doi: 10.1016/J.STEM.2008.11.013.

Lin, C. H. *et al.* (2009) 'Myc-regulated microRNAs attenuate embryonic stem cell differentiation', *EMBO Journal*, 28(20), pp. 3157–3170. doi: 10.1038/emboj.2009.254.

Lin, Z.-Q. *et al.* (2003) 'Essential involvement of IL-6 in the skin wound-healing process as evidenced by delayed wound healing in IL-6-deficient mice.', *Journal of leukocyte biology*, 73(6), pp. 713–721. doi: 10.1189/jlb.0802397.

Liu, B. *et al.* (2021) 'GBP2 as a potential prognostic biomarker in pancreatic adenocarcinoma.', *PeerJ*, 9, p. e11423. doi: 10.7717/peerj.11423.

Liu, C. F. *et al.* (2009) 'Stem cell potential of the mammalian gonad', *Frontiers in Bioscience - Elite*, 1 E(2), pp. 510–518. doi: 10.2741/e47.

Liu, H. *et al.* (2008) 'Generation of induced pluripotent stem cells from adult rhesus monkey fibroblasts', *Cell stem cell*, 3(6), pp. 587–590. doi: 10.1016/J.STEM.2008.10.014.

Liu, P. *et al.* (2018) 'CRISPR-Based Chromatin Remodeling of the Endogenous Oct4 or Sox2 Locus Enables Reprogramming to Pluripotency', *Cell Stem Cell*, 22(2), pp. 252-261.e4. doi: 10.1016/j.stem.2017.12.001.

Liu, P. *et al.* (2021) 'Clinical Significance and the Role of Guanylate-Binding Protein 5 in Oral Squamous Cell Carcinoma.', *Cancers*, 13(16). doi: 10.3390/cancers13164043.

Lodolce, J. P. *et al.* (1998) 'IL-15 receptor maintains lymphoid homeostasis by supporting lymphocyte homing and proliferation.', *Immunity*, 9(5), pp. 669–676. doi: 10.1016/s1074-7613(00)80664-0.

Long, E. O. (2007) 'Ready for prime time: NK cell priming by dendritic cells.', *Immunity*, 26(4), pp. 385–387. doi: 10.1016/j.immuni.2007.04.001.

Lu, L. *et al.* (2007) 'Regulation of activated CD4+ T cells by NK cells via the Qa-1-NKG2A inhibitory pathway.', *Immunity*, 26(5), pp. 593–604. doi: 10.1016/j.immuni.2007.03.017.

Lu, Y. *et al.* (2020) 'Reprogramming to recover youthful epigenetic information and restore vision', *Nature*, 588(7836), pp. 124–129. doi: 10.1038/s41586-020-2975-4.

Lucas, M. *et al.* (2007) 'Dendritic cells prime natural killer cells by trans-presenting interleukin 15.', *Immunity*, 26(4), pp. 503–517. doi: 10.1016/j.immuni.2007.03.006.

Luczynski, P. *et al.* (2016) 'Growing up in a Bubble: Using Germ-Free Animals to Assess the Influence of the Gut Microbiota on Brain and Behavior.', *The international journal of neuropsychopharmacology*, 19(8). doi: 10.1093/ijnp/pyw020.

Lujambio, A. *et al.* (2013) 'Non-cell-autonomous tumor suppression by p53', *Cell*, 153(2), pp. 449–460. doi: 10.1016/j.cell.2013.03.020.

Maghazachi, A. A. (2010) 'Role of chemokines in the biology of natural killer cells.', *Current topics in microbiology and immunology*, 341, pp. 37–58. doi: 10.1007/82_2010_20.

Maherali, N. *et al.* (2007) 'Directly Reprogrammed Fibroblasts Show Global Epigenetic Remodeling and Widespread Tissue Contribution', *Cell Stem Cell*, 1(1), pp. 55–70. doi: 10.1016/j.stem.2007.05.014.

Mahmoudi, S. *et al.* (2019) 'Heterogeneity in old fibroblasts is linked to variability in

reprogramming and wound healing', *Nature*, 574(7779), pp. 553–558. doi: 10.1038/s41586-019-1658-5.Heterogeneity.

Maier, S. *et al.* (2011) 'SOX2 amplification is a common event in squamous cell carcinomas of different organ sites', *Human Pathology*, 42(8), pp. 1078–1088. doi: 10.1016/j.humpath.2010.11.010.

Mandelboim, O. and Porgador, A. (2001) 'NKp46.', *The International Journal of Biochemistry & Cell Biology*, 33(12), pp. 1147–1150. doi: 10.1016/s1357-2725(01)00078-4.

Marión, R. M. *et al.* (2009) 'A p53-mediated DNA damage response limits reprogramming to ensure iPS cell genomic integrity', *Nature*, 460(7259), pp. 1149–1153. doi: 10.1038/nature08287.

Martín-Fontecha, A. *et al.* (2004) 'Induced recruitment of NK cells to lymph nodes provides IFN-gamma for T(H)1 priming.', *Nature immunology*, 5(12), pp. 1260–1265. doi: 10.1038/ni1138.

Martin, G. R. (1981) 'Isolation of a pluripotent cell line from early mouse embryos cultured in medium conditioned by teratocarcinoma stem cells', *Proceedings of the National Academy of Sciences of the United States of America*, 78(12), pp. 7634–7638. doi: 10.1073/PNAS.78.12.7634.

Masaki, T. *et al.* (2013) 'Reprogramming adult Schwann cells to stem cell-like cells by leprosy bacilli promotes dissemination of infection.', *Cell*, 152(1–2), pp. 51–67. doi: 10.1016/j.cell.2012.12.014.

Mathieu, J. *et al.* (2014) 'Hypoxia-inducible factors have distinct and stage-specific roles during reprogramming of human cells to pluripotency.', *Cell stem cell*, 14(5), pp. 592–605. doi: 10.1016/j.stem.2014.02.012.

Mayshar, Y. *et al.* (2010) 'Identification and classification of chromosomal aberrations in human induced pluripotent stem cells.', *Cell stem cell*, 7(4), pp. 521–531. doi: 10.1016/j.stem.2010.07.017.

McCarville, J. L. *et al.* (2020) 'Microbiota Metabolites in Health and Disease', *Annual Review of Immunology*, 38, pp. 147–170. doi: 10.1146/annurev-immunol-071219-125715.

McFarland-Mancini, M. M. *et al.* (2010) 'Differences in wound healing in mice with deficiency of IL-6 versus IL-6 receptor.', *Journal of immunology (Baltimore, Md. : 1950)*, 184(12), pp. 7219–7228. doi: 10.4049/jimmunol.0901929.

McKay, C., Imrie, C. W. and Baxter, J. N. (1996) 'Mononuclear phagocyte activation and acute pancreatitis.', *Scandinavian journal of gastroenterology. Supplement*, 219, pp.

32–36. doi: 10.3109/00365529609104997.

Melnick, A. F. *et al.* (2019) 'RNF216 is essential for spermatogenesis and male fertility.', *Biology of reproduction*, pp. 1132–1134. doi: 10.1093/biolre/ioz006.

Mews, P. *et al.* (2002) 'Pancreatic stellate cells respond to inflammatory cytokines: Potential role in chronic pancreatitis', *Gut*, 50(4), pp. 535–541. doi: 10.1136/gut.50.4.535.

Meyer, V. S. *et al.* (2009) 'Identification of natural MHC class II presented phosphopeptides and tumor-derived MHC class I phospholigands', *Journal of Proteome Research*, 8(7), pp. 3666–3674. doi: 10.1021/pr800937k.

Michael R., B. *et al.* (2002) 'The zinc-finger transcription factor Klf4 is required for terminal differentiation of goblet cells in the colon', *Development*, 129(11), pp. 2619–28.

Michalek, M. T. *et al.* (1993) 'A role for the ubiquitin-dependent proteolytic pathway in MHC class I-restricted antigen presentation.', *Nature*, 363(6429), pp. 552–554. doi: 10.1038/363552a0.

Mikkelsen, T. S. *et al.* (2008) 'Dissecting direct reprogramming through integrative genomic analysis', *Nature*, 454(7200), pp. 49–55. doi: 10.1038/nature07056.

Miller, D. M. *et al.* (2012) 'c-Myc and Cancer Metabolism', *Clin Cancer Res.*, 18(20), pp. 5546–5553. doi: 10.1158/1078-0432.CCR-12-0977.

Mohammed, F. *et al.* (2008) 'Phosphorylation-dependent interaction between antigenic peptides and MHC class I: A molecular basis for the presentation of transformed self', *Nature Immunology*, 9(11), pp. 1236–1243. doi: 10.1038/ni.1660.

Molfetta, R. *et al.* (2016a) 'Regulation of NKG2D Expression and Signaling by Endocytosis', *Trends in Immunology*, 37(11), pp. 790–802. doi: 10.1016/j.it.2016.08.015.

Molfetta, R. *et al.* (2016b) 'Regulation of NKG2D Expression and Signaling by Endocytosis', *Trends in Immunology*, 37(11), pp. 790–802. doi: 10.1016/j.it.2016.08.015.

Molfetta, R. *et al.* (2017) 'Regulation of NKG2D-Dependent NK Cell Functions : The Yin and the Yang of Receptor Endocytosis'. doi: 10.3390/ijms18081677.

Moretta, L. *et al.* (2006) 'Effector and regulatory events during natural killer-dendritic cell interactions.', *Immunological reviews*, 214, pp. 219–228. doi: 10.1111/j.1600-065X.2006.00450.x.

Moris, N., Pina, C. and Arias, A. M. (2016) 'Transition states and cell fate decisions in

epigenetic landscapes', *Nature Reviews Genetics 2016 17:11*, 17(11), pp. 693–703. doi: 10.1038/nrg.2016.98.

Morita, R. *et al.* (2021) 'Tracing the origin of hair follicle stem cells', *Nature*, 594(7864), pp. 547–552. doi: 10.1038/s41586-021-03638-5.

Mosteiro, L. *et al.* (2016) 'Tissue damage and senescence provide critical signals for cellular reprogramming in vivo', *Science*, 354(6315). doi: 10.1126/science.aaf4445.

Mosteiro, L. *et al.* (2018) 'Senescence promotes in vivo reprogramming through p16 INK4a and IL-6', *Aging Cell*, 17(2). doi: 10.1111/acel.12711.

Muñoz-Espín, D. and Serrano, M. (2014) 'Cellular senescence: From physiology to pathology', *Nature Reviews Molecular Cell Biology*, 15(7), pp. 482–496. doi: 10.1038/nrm3823.

Muñoz, D. P. *et al.* (2019) 'Targetable mechanisms driving immunoevasion of persistent senescent cells link chemotherapy-resistant cancer to aging', *JCI Insight*, 4(14), pp. 1–22. doi: 10.1172/jci.insight.124716.

Murphy, J. P. *et al.* (2017) 'MHC-I Ligand Discovery Using Targeted Database Searches of Mass Spectrometry Data: Implications for T-Cell Immunotherapies.', *Journal of proteome research*, 16(4), pp. 1806–1816. doi: 10.1021/acs.jproteome.6b00971.

Murray, P. J. *et al.* (2014) 'Experimental Guidelines', *Immunity.*, 41(1), pp. 14–20. doi: 10.1016/j.immuni.2014.06.008.Macrophage.

Musi, N. *et al.* (2018) 'Tau protein aggregation is associated with cellular senescence in the brain.', *Aging cell*, 17(6), p. e12840. doi: 10.1111/acel.12840.

Nagasao, J. *et al.* (2003) 'Centroacinar and intercalated duct cells as potential precursors of pancreatic endocrine cells in rats treated with streptozotocin.', *Annals of anatomy*, 185(3), pp. 211–216. doi: 10.1016/s0940-9602(03)80025-0.

Nechemia-Arbely, Y. *et al.* (2011) 'Early hepatocyte DNA synthetic response posthepatectomy is modulated by IL-6 trans-signaling and PI3K/AKT activation.', *Journal of hepatology*, 54(5), pp. 922–929. doi: 10.1016/j.jhep.2010.08.017.

Niwa, H. *et al.* (2005) 'Interaction between Oct3/4 and Cdx2 determines trophectoderm differentiation', *Cell*, 123(5), pp. 917–929. doi: 10.1016/j.cell.2005.08.040.

O'Malley, J. *et al.* (2013) 'High-resolution analysis with novel cell-surface markers identifies routes to iPS cells', *Nature*, 499(7456), pp. 88–91. doi: 10.1038/nature12243.

Ocampo, A. *et al.* (2016) 'In Vivo Amelioration of Age-Associated Hallmarks by Partial Reprogramming', *Cell*, 167(7), pp. 1719-1733.e12. doi: 10.1016/j.cell.2016.11.052.

Ohnishi, K. *et al.* (2014) 'Premature termination of reprogramming in vivo leads to cancer development through altered epigenetic regulation', *Cell*, 156(4), pp. 663–677. doi: 10.1016/j.cell.2014.01.005.

Ohnishi, S. *et al.* (2000) 'Developmental expression of the mouse gene coding for the Kruppel-like transcription factor KLF5', *Developmental Dynamics*, 217(4), pp. 421–429. doi: 10.1002/(SICI)1097-0177(200004)217:4<421::AID-DVDY9>3.0.CO;2-1.

Okubo, T., Clark, C. and Hogan, B. L. M. (2009) 'Cell Lineage Mapping of Taste Bud Cells and Keratinocytes in the Mouse Tongue and Soft Palate', *Stem Cells*, 27(2), pp. 442–450. doi: 10.1634/stemcells.2008-0611.

Onder, T. T. *et al.* (2012) 'Chromatin-modifying enzymes as modulators of reprogramming', *Nature*, 483(7391), pp. 598–602. doi: 10.1038/nature10953.

Ouyang, X. *et al.* (2021) 'Antitumor effects of iPSC-based cancer vaccine in pancreatic cancer', *Stem Cell Reports*, 16(6), pp. 1468–1477. doi: 10.1016/j.stemcr.2021.04.004.

Pan, F. C. *et al.* (2013) 'Spatiotemporal patterns of multipotentiality in Ptf1aexpressing cells during pancreas organogenesis and injuryinduced facultative restoration', *Development (Cambridge)*, 140(4), pp. 751–764. doi: 10.1242/dev.090159.

Pan, F. C. and Wright, C. (2011) 'Pancreas organogenesis: From bud to plexus to gland', *Developmental Dynamics*, 240(3), pp. 530–565. doi: 10.1002/dvdy.22584.

Pang, Z. *et al.* (2021) 'MetaboAnalyst 5.0: Narrowing the gap between raw spectra and functional insights', *Nucleic Acids Research*, 49(W1), pp. W388–W396. doi: 10.1093/nar/gkab382.

Panopoulos, A. D. *et al.* (2012) 'The metabolome of induced pluripotent stem cells reveals metabolic changes occurring in somatic cell reprogramming', *Cell Research*, 22(1), pp. 168–177. doi: 10.1038/cr.2011.177.

Parisi, S. *et al.* (2008) 'Klf5 is involved in self-renewal of mouse embryonic stem cells', *Journal of Cell Science*, 121(16), pp. 2629–2634. doi: 10.1242/jcs.027599.

Park, K. S. *et al.* (2006) 'Transdifferentiation of ciliated cells during repair of the respiratory epithelium', *American Journal of Respiratory Cell and Molecular Biology*, 34(2), pp. 151–157. doi: 10.1165/rcmb.2005-0332OC.

Pei, D. *et al.* (2019) 'Mesenchymal–epithelial transition in development and reprogramming', *Nature Cell Biology*, 21(1), pp. 44–53. doi: 10.1038/s41556-018-0195-z.

Peng, H. and Tian, Z. (2017) 'Diversity of tissue-resident NK cells.', *Seminars in immunology*, 31, pp. 3–10. doi: 10.1016/j.smim.2017.07.006.

Pereira, B. I. *et al.* (2019) 'Senescent cells evade immune clearance via HLA-E-mediated NK and CD8+ T cell inhibition', *Nature Communications*, 10(1). doi: 10.1038/s41467-019-10335-5.

Pesce, M. and Schöler, H. R. (2001) 'Oct-4: Gatekeeper in the Beginnings of Mammalian Development', *Stem Cells*, 19, pp. 271–278.

Petrus-Reurer, S. *et al.* (2021) 'Immunological considerations and challenges for regenerative cellular therapies', *Communications biology*, 4(1), p. 798. doi: 10.1038/s42003-021-02237-4.

Pham, D. L. *et al.* (2013) 'SOX2 expression and prognostic significance in ovarian carcinoma', *International Journal of Gynecological Pathology*, 32(4), pp. 358–367. doi: 10.1097/PGP.0b013e31826a642b.

Poirson-Bichat, F. *et al.* (1997) 'Methionine deprivation and methionine analogs inhibit cell proliferation and growth of human xenografted gliomas.', *Life sciences*, 60(12), pp. 919–931. doi: 10.1016/s0024-3205(96)00672-8.

Polo, J. M. *et al.* (2012) 'A molecular roadmap of reprogramming somatic cells into iPS cells', *Cell*, 151(7), pp. 1617–1632. doi: 10.1016/j.cell.2012.11.039.

Poss, K. D., Wilson, L. G. and Keating, M. T. (2002) 'Heart regeneration in zebrafish', *Science*, 298(5601), pp. 2188–2190. doi: 10.1126/science.1077857.

Prajapati, K. *et al.* (2018) 'Functions of NKG2D in CD8+ T cells: an opportunity for immunotherapy', *Cellular and Molecular Immunology*, 15(5), pp. 470–479. doi: 10.1038/cmi.2017.161.

Prasad, S., Starck, S. R. and Shastri, N. (2016) 'Presentation of Cryptic Peptides by MHC Class I Is Enhanced by Inflammatory Stimuli.', *Journal of Immunology*, 197(8), pp. 2981–2991. doi: 10.4049/jimmunol.1502045.

Prévot, P.-P. *et al.* (2012) 'Role of the ductal transcription factors HNF6 and Sox9 in pancreatic acinar-to-ductal metaplasia.', *Gut*, 61(12), pp. 1723–1732. doi: 10.1136/gutjnl-2011-300266.

Qin, S. *et al.* (2011) 'Dysregulation of Kruppel-like factor 4 during brain development leads to hydrocephalus in mice', *Proceedings of the National Academy of Sciences*, 108(52), pp. 21117–21121. doi: 10.1073/PNAS.1112351109.

Quatrini, L. *et al.* (2015) 'Ubiquitin-dependent endocytosis of NKG2D-DAP10 receptor complexes activates signaling and functions in human NK cells', *Science Signaling*, 8(400), pp. 1–11. doi: 10.1126/scisignal.aab2724.

Que, J. *et al.* (2009) 'Multiple roles for Sox2 in the developing and adult mouse trachea',

Development, 136(11), pp. 1899–1907. doi: 10.1242/dev.034629.

Quinlan, J. D. (2014) 'Acute pancreatitis', *American Family Physician*, 90(9), pp. 632–639. doi: 10.5005/jp/books/13118_50.

Rais, Y. *et al.* (2013) 'Deterministic direct reprogramming of somatic cells to pluripotency.', *Nature*, 502(7469), pp. 65–70. doi: 10.1038/nature12587.

Rasmussen, M. A. *et al.* (2014) 'Transient p53 suppression increases reprogramming of human fibroblasts without affecting apoptosis and DNA damage', *Stem Cell Reports*, 3(3), pp. 404–413. doi: 10.1016/j.stemcr.2014.07.006.

Raulet, D. H. and Guerra, N. (2009) 'Oncogenic stress sensed by the immune system: role of natural killer cell receptors.', *Nature reviews. Immunology*, 9(8), pp. 568–580. doi: 10.1038/nri2604.

Raya, A. *et al.* (2003) 'Activation of Notch signaling pathway precedes heart regeneration in zebrafish', *Proceedings of the National Academy of Sciences of the United States of America*, 100(SUPPL. 1), pp. 11889–11895. doi: 10.1073/pnas.1834204100.

Ritschka, B. *et al.* (2017) 'The senescence-associated secretory phenotype induces cellular plasticity and tissue regeneration.', *Genes & development*, 31(2), pp. 172–183. doi: 10.1101/gad.290635.116.

Rock, K. L. *et al.* (1994) 'Inhibitors of the proteasome block the degradation of most cell proteins and the generation of peptides presented on MHC class I molecules.', *Cell*, 78(5), pp. 761–771. doi: 10.1016/s0092-8674(94)90462-6.

Rock, K. L., Reits, E. and Neefjes, J. (2016) 'Present Yourself! By MHC Class I and MHC Class II Molecules', *Trends in Immunology*, 37(11), pp. 724–737. doi: 10.1016/j.it.2016.08.010.

Rompianesi, G. *et al.* (2017) 'Serum amylase and lipase and urinary trypsinogen and amylase for diagnosis of acute pancreatitis.', *The Cochrane database of systematic reviews*, 4(4), p. CD012010. doi: 10.1002/14651858.CD012010.pub2.

Rovira, M. *et al.* (2010) 'Isolation and characterization of centroacinar/terminal ductal progenitor cells in adult mouse pancreas', *Proceedings of the National Academy of Sciences of the United States of America*, 107(1), pp. 75–80. doi: 10.1073/pnas.0912589107.

Rowland, B. and Peeper, D. (2006) 'KLF4, p21 and context-dependent opposing forces in cancer', *Nature reviews. Cancer*, 6(1), pp. 11–23. doi: 10.1038/NRC1780.

Ruairi, F., Sjaak Van Der, S. and Patrick J., M. (2005) 'Embryonic stem cells: Understanding their history, cell biology and signalling', *Advanced Drug Delivery*

Reviews, 57(13 SPEC. ISS.), pp. 1894–1903. doi: 10.1016/j.addr.2005.08.002.

Ruiz, S. *et al.* (2015) 'Limiting replication stress during somatic cell reprogramming reduces genomic instability in induced pluripotent stem cells', *Nature Communications*, 6, pp. 1–8. doi: 10.1038/ncomms9036.

Saeki, K. *et al.* (2012) 'CCL2-induced migration and SOCS3-mediated activation of macrophages are involved in cerulein-induced pancreatitis in mice.', *Gastroenterology*, 142(4), pp. 1010-1020.e9. doi: 10.1053/j.gastro.2011.12.054.

Sagiv, A. *et al.* (2016) 'NKG2D ligands mediate immunosurveillance of senescent cells', *Aging*, 8(2), pp. 328–344. doi: 10.18632/aging.100897.

Samavarchi-Tehrani, P. *et al.* (2010) 'Functional genomics reveals a BMP-Driven mesenchymal-to-Epithelial transition in the initiation of somatic cell reprogramming', *Cell Stem Cell*, 7(1), pp. 64–77. doi: 10.1016/j.stem.2010.04.015.

Sarkar, T. J. *et al.* (2020) 'Transient non-integrative expression of nuclear reprogramming factors promotes multifaceted amelioration of aging in human cells.', *Nature communications*, 11(1), p. 1545. doi: 10.1038/s41467-020-15174-3.

Schenkel, A. R., Kingry, L. C. and Slayden, R. A. (2013) 'The Ly49 gene family. A brief guide to the nomenclature, genetics, and role in intracellular infection', *Frontiers in immunology*, 4, pp. 1–8. doi: 10.3389/fimmu.2013.00090.

Schiebinger, G. *et al.* (2017) 'Reconstruction of developmental landscapes by optimal-transport analysis of single-cell gene expression sheds light on cellular reprogramming.', *Doi.Org*, p. 191056. doi: 10.1101/191056.

Schoenborn, J. R. and Wilson, C. B. (2007) 'Regulation of interferon-gamma during innate and adaptive immune responses.', *Advances in immunology*, 96, pp. 41–101. doi: 10.1016/S0065-2776(07)96002-2.

Schröck, A. *et al.* (2013) 'Sex Determining Region Y-Box 2 (SOX2) Amplification Is an Independent Indicator of Disease Recurrence in Sinonasal Cancer', *PLoS ONE*, 8(3). doi: 10.1371/journal.pone.0059201.

Schröck, A. *et al.* (2014) 'Expression and role of the embryonic protein SOX2 in head and neck squamous cell carcinoma', *Carcinogenesis*, 35(7), pp. 1636–1642. doi: 10.1093/carcin/bgu094.

Schuster, H. *et al.* (2018) 'Data Descriptor: A tissue-based draft map of the murine MHC class I immunopeptidome', *Scientific Data*, 5, pp. 1–11. doi: 10.1038/sdata.2018.157.

Schwarz, B. A. *et al.* (2018) 'Prospective Isolation of Poised iPSC Intermediates Reveals Principles of Cellular Reprogramming', *Cell Stem Cell*, 23(2), pp. 289-305.e5. doi:

10.1016/j.stem.2018.06.013.

Scoville, S. D., Freud, A. G. and Caligiuri, M. A. (2017) 'Modeling Human Natural Killer Cell Development in the Era of Innate Lymphoid Cells.', *Frontiers in immunology*, 8, p. 360. doi: 10.3389/fimmu.2017.00360.

Segura, E. and Amigorena, S. (2015) *Cross-presentation in Mouse and Human Dendritic Cells*, *Advances in Immunology*. Elsevier Inc. doi: 10.1016/bs.ai.2015.03.002.

Seita, J. and Weissman, I. L. (2010) 'Hematopoietic stem cell: self-renewal versus differentiation.', *Wiley interdisciplinary reviews. Systems biology and medicine*, 2(6), pp. 640–653. doi: 10.1002/wsbm.86.

Sekiya, S. and Suzuki, A. (2014) 'Hepatocytes, rather than cholangiocytes, can be the major source of primitive ductules in the chronically injured mouse liver', *American Journal of Pathology*, 184(5), pp. 1468–1478. doi: 10.1016/j.ajpath.2014.01.005.

Semi, K. *et al.* (2013) 'Cellular reprogramming and cancer development.', *International journal of cancer*, 132(6), pp. 1240–1248. doi: 10.1002/ijc.27963.

Senís, E. *et al.* (2018) 'AAVvector-mediated in vivo reprogramming into pluripotency', *Nature Communications*, 9(1), pp. 1–14. doi: 10.1038/s41467-018-05059-x.

Serrano, M. *et al.* (1997) 'Oncogenic ras provokes premature cell senescence associated with accumulation of p53 and p16(INK4a)', *Cell*, 88(5), pp. 593–602. doi: 10.1016/S0092-8674(00)81902-9.

Shahbazi, M. N. and Zernicka-Goetz, M. (2018) 'Deconstructing and reconstructing the mouse and human early embryo', *Nature Cell Biology*, 20(8), pp. 878–887. doi: 10.1038/s41556-018-0144-x.

Shi, L. *et al.* (2018) 'Modulation of NKG2D, NKp46, and Ly49C/I facilitates natural killer cell-mediated control of lung cancer', *Proceedings of the National Academy of Sciences of the United States of America*, 115(46), pp. 11808–11813. doi: 10.1073/pnas.1804931115.

Shibata, H. *et al.* (2018) 'In vivo reprogramming drives Kras-induced cancer development', *Nature Communications*, 9(1), pp. 1–7. doi: 10.1038/s41467-018-04449-5.

Shiraki, N., Ogaki, S. and Kume, S. (2014a) 'Profiling of embryonic stem cell differentiation.', *The review of diabetic studies: RDS*, 11(1), pp. 102–114. doi: 10.1900/RDS.2014.11.102.

Shiraki, N., Ogaki, S. and Kume, S. (2014b) 'Profiling of embryonic stem cell differentiation.', *The review of diabetic studies : RDS*, 11(1), pp. 102–114. doi: 10.1900/RDS.2014.11.102.

Shyh-Chang, N. *et al.* (2013) 'Influence of threonine metabolism on S-adenosylmethionine and histone methylation.', *Science (New York, N.Y.)*, 339(6116), pp. 222–226. doi: 10.1126/science.1226603.

Shyh-Chang, N., Daley, G. Q. and Cantley, L. C. (2013) 'Stem cell metabolism in tissue development and aging', *Development (Cambridge)*, 140(12), pp. 2535–2547. doi: 10.1242/dev.091777.

Sköld, M. *et al.* (2000) 'CD1d-specific NK1.1+ T cells with a transgenic variant TCR.', *Journal of Immunology*, 165(1), pp. 168–174. doi: 10.4049/jimmunol.165.1.168.

Smith, H. J. (1966) 'Antigeneicity of carcinogen-induced and spontaneous tumours in inbred mice', *British Journal of Cancer*, 20(4), pp. 831–837. doi: 10.1038/bjc.1966.95.

Smith, K. N., Singh, A. M. and Dalton, S. (2010) 'Myc represses primitive endoderm differentiation in pluripotent stem cells', *Cell stem cell*, 7(3), p. 343. doi: 10.1016/J.STEM.2010.06.023.

Smith, Z. D. *et al.* (2010) 'Dynamic single-cell imaging of direct reprogramming reveals an early specifying event', *Nature Biotechnology*, 28(5), pp. 521–526. doi: 10.1038/nbt.1632.

Smith, Zachary D, Sindhu, C. and Meissner, A. (2016) 'Molecular features of cellular reprogramming and development.', *Nature reviews. Molecular cell biology*, 17(3), pp. 139–154. doi: 10.1038/nrm.2016.6.

Smith, Zachary D., Sindhu, C. and Meissner, A. (2016) 'Molecular features of cellular reprogramming and development', *Nature Reviews Molecular Cell Biology*, 17(3), pp. 139–154. doi: 10.1038/nrm.2016.6.

Smyth, M. J., Cretney, E., *et al.* (2005) 'Activation of NK cell cytotoxicity.', *Molecular immunology*, 42(4), pp. 501–510. doi: 10.1016/j.molimm.2004.07.034.

Smyth, M. J., Swann, J., *et al.* (2005) 'NKG2D function protects the host from tumor initiation.', *The Journal of experimental medicine*, 202(5), pp. 583–588. doi: 10.1084/jem.20050994.

Snippert, H. J. and Clevers, H. (2011) 'Tracking adult stem cells', *EMBO reports*, 12(2), pp. 113–122. doi: 10.1038/EMBOR.2010.216.

Song, J. and Wei, Q.-Y. (2020) 'GBP1 promotes non-small cell lung carcinoma malignancy and chemoresistance via activating the Wnt/β-catenin signaling pathway.', *European review for medical and pharmacological sciences*, 24(13), p. 7221. doi: 10.26355/eurrev_202007_21872.

Soriani, A. *et al.* (2009) 'ATM-ATR-dependent up-regulation of DNAM-1 and NKG2D

ligands on multiple myeloma cells by therapeutic agents results in enhanced NK-cell susceptibility and is associated with a senescent phenotype.', *Blood*, 113(15), pp. 3503–3511. doi: 10.1182/blood-2008-08-173914.

Soufi, A., Donahue, G. and Zaret, K. S. (2012) 'Facilitators and impediments of the pluripotency reprogramming factors' initial engagement with the genome', *Cell*, 151(5), pp. 994–1004. doi: 10.1016/j.cell.2012.09.045.

Spiegel, A. *et al.* (2016) 'Neutrophils suppress intraluminal NK cell-mediated tumor cell clearance and enhance extravasation of disseminated carcinoma cells', *Cancer Discovery*, 6(6), pp. 630–649. doi: 10.1158/2159-8290.CD-15-1157.

Sridharan, R. *et al.* (2009) 'Role of the Murine Reprogramming Factors in the Induction of Pluripotency', *Cell*, 136(2), pp. 364–377. doi: 10.1016/j.cell.2009.01.001.

Stadtfeld, M., Maherali, N., *et al.* (2008) 'Defining Molecular Cornerstones during Fibroblast to iPS Cell Reprogramming in Mouse', *Cell Stem Cell*, 2(3), pp. 230–240. doi: 10.1016/j.stem.2008.02.001.

Stadtfeld, M., Nagaya, M., *et al.* (2008) 'Induced pluripotent stem cells generated without viral integration.', *Science (New York, N.Y.)*, 322(5903), pp. 945–9. doi: 10.1126/science.1162494.

Stadtfeld, M., Brennand, K. and Hochedlinger, K. (2008) 'Reprogramming of pancreatic beta cells into induced pluripotent stem cells', *Current biology : CB*, 18(12), pp. 890–894. doi: 10.1016/J.CUB.2008.05.010.

Stange, D. E. *et al.* (2013) 'Differentiated Troy+ chief cells act as reserve stem cells to generate all lineages of the stomach epithelium.', *Cell*, 155(2), pp. 357–368. doi: 10.1016/j.cell.2013.09.008.

Starck, S. R. *et al.* (2016) 'Translation from the 5' untranslated region shapes the integrated stress response.', *Science (New York, N.Y.)*, 351(6272), p. aad3867. doi: 10.1126/science.aad3867.

Di Stefano, B. *et al.* (2014) 'C/EBPα poises B cells for rapid reprogramming into induced pluripotent stem cells.', *Nature*, 506(7487), pp. 235–239. doi: 10.1038/nature12885.

Storz, P. (2017) 'Acinar cell plasticity and development of pancreatic ductal adenocarcinoma', *Nature Reviews Gastroenterology and Hepatology*, 14(5), pp. 296–304. doi: 10.1038/nrgastro.2017.12.

Strekalova, E. *et al.* (2015) 'Methionine Deprivation Induces a Targetable Vulnerability in Triple-Negative Breast Cancer Cells by Enhancing TRAIL Receptor-2 Expression.', *Clinical Cancer Research*, 21(12), pp. 2780–2791. doi: 10.1158/1078-0432.CCR-14-2792.

Strobel, O. *et al.* (2007) 'In vivo lineage tracing defines the role of acinar-to-ductal transdifferentiation in inflammatory ductal metaplasia.', *Gastroenterology*, 133(6), pp. 1999–2009. doi: 10.1053/j.gastro.2007.09.009.

Subramanian, A. *et al.* (2005) 'Gene set enrichment analysis: A knowledge-based approach for interpreting genome-wide expression profiles', *Proceedings of the National Academy of Sciences of the United States of America*, 102(43), pp. 15545–15550. doi: 10.1073/pnas.0506580102.

Sun, C. *et al.* (2017) 'High NKG2A expression contributes to NK cell exhaustion and predicts a poor prognosis of patients with liver cancer', *OncoImmunology*, 6(1), pp. 1–12. doi: 10.1080/2162402X.2016.1264562.

Sun, J. C., Beilke, J. N. and Lanier, L. L. (2010) 'Immune memory redefined: characterizing the longevity of natural killer cells.', *Immunological reviews*, 236, pp. 83–94. doi: 10.1111/j.1600-065X.2010.00900.x.

Sun, R. *et al.* (2020) 'Tumor-associated neutrophils suppress antitumor immunity of NK cells through the PD-L1/PD-1 axis', *Translational Oncology*, 13(10), pp. 1–9. doi: 10.1016/j.tranon.2020.100825.

Suri, A., Lovitch, S. B. and Unanue, E. R. (2006) 'The wide diversity and complexity of peptides bound to class II MHC molecules', *Current Opinion in Immunology*, 18(1), pp. 70–77. doi: 10.1016/j.coi.2005.11.002.

Swamynathan, S., Davis, J. and Piatigorsky, J. (2008) 'Identification of candidate Klf4 target genes reveals the molecular basis of the diverse regulatory roles of Klf4 in the mouse cornea', *Investigative ophthalmology & visual science*, 49(8), pp. 3360–3370. doi: 10.1167/IOVS.08-1811.

Sze, K., Lee, W. and Lui, W. (2008) 'Expression of CLMP, a novel tight junction protein, is mediated via the interaction of GATA with the Kruppel family proteins, KLF4 and Sp1, in mouse TM4 Sertoli cells', *Journal of cellular physiology*, 214(2), pp. 334–344. doi: 10.1002/JCP.21201.

Tabar, V. and Studer, L. (2014) 'Pluripotent stem cells in regenerative medicine: challenges and recent progress.', *Nature reviews. Genetics*, 15(2), pp. 82–92. doi: 10.1038/nrg3563.

Tada, M. *et al.* (2001) 'Nuclear reprogramming of somatic cells by in vitro hybridization with ES cells', *Current biology : CB*, 11(19), pp. 1553–1558. doi: 10.1016/S0960-9822(01)00459-6.

Tada, S. *et al.* (1997) 'Embryonic germ cells induce epigenetic reprogramming of somatic nucleus in hybrid cells', *EMBO Journal*, 16(21), pp. 6510–6520. doi: 10.1093/emboj/16.21.6510.

Takahashi, H. *et al.* (2012) 'Age-dependent reduction of the PI3K regulatory subunit p85α suppresses pancreatic acinar cell proliferation.', *Aging cell*, 11(2), pp. 305–314. doi: 10.1111/j.1474-9726.2011.00787.x.

Takahashi, K. *et al.* (2007) 'Induction of Pluripotent Stem Cells from Adult Human Fibroblasts by Defined Factors', *Cell*, 131(5), pp. 861–872. doi: 10.1016/j.cell.2007.11.019.

Takahashi, K. and Yamanaka, S. (2006) 'Induction of pluripotent stem cells from mouse embryonic and adult fibroblast cultures by defined factors', *Cell*, 126(4), pp. 663–676. doi: 10.1016/J.CELL.2006.07.024.

Talmasov, D. *et al.* (2015) 'Krüppel-like factor 4 is a radioprotective factor for the intestine following γ-radiation-induced gut injury in mice', *American journal of Physiology-Gastrointestinal and liver physiology*, 308(2), pp. G121–G138. doi: 10.1152/AJPGI.00080.2014.

Tanabe, K. *et al.* (2013) 'Maturation, not initiation, is the major roadblock during reprogramming toward pluripotency from human fibroblasts', *Proceedings of the National Academy of Sciences of the United States of America*, 110(30), pp. 12172–12179. doi: 10.1073/pnas.1310291110.

Tanaka, S. *et al.* (1998) 'Promotion of trophoblast stem cell proliferation by FGF4.', *Science*, 282(5396), pp. 2072–2075. doi: 10.1126/science.282.5396.2072.

Taranova, O. V. *et al.* (2006) 'SOX2 is a dose-dependent regulator of retinal neural progenitor competence', *Genes & Development*, 20(9), pp. 1187–1202. doi: 10.1101/GAD.1407906.

Tassi, I. *et al.* (2007) 'p110gamma and p110delta phosphoinositide 3-kinase signaling pathways synergize to control development and functions of murine NK cells.', *Immunity*, 27(2), pp. 214–227. doi: 10.1016/j.immuni.2007.07.014.

Tata, P. R. *et al.* (2013) 'Dedifferentiation of committed epithelial cells into stem cells in vivo', *Nature*, 503(7475), pp. 218–223. doi: 10.1038/nature12777.

Teta, M. *et al.* (2005) 'Very slow turnover of beta-cells in aged adult mice.', *Diabetes*, 54(9), pp. 2557–2567. doi: 10.2337/diabetes.54.9.2557.

Teta, M. *et al.* (2007) 'Growth and regeneration of adult beta cells does not involve specialized progenitors.', *Developmental cell*, 12(5), pp. 817–826. doi: 10.1016/j.devcel.2007.04.011.

Thorel, F. *et al.* (2010) 'Conversion of adult pancreatic α-cells to b-cells after extreme b-cell loss', *Nature*, 464(7292), pp. 1149–1154. doi: 10.1038/nature08894.

Tokés, T. *et al.* (2011) 'Protective effects of a phosphatidylcholine-enriched diet in lipopolysaccharide-induced experimental neuroinflammation in the rat.', *Shock*, 36(5), pp. 458–465. doi: 10.1097/SHK.0b013e31822f36b0.

Tomioka, M. *et al.* (2002) 'Identification of Sox-2 regulatory region which is under the control of Oct-3/4-Sox-2 complex', *Nucleic Acids Research*, 30(14), pp. 3202–3213. doi: 10.1093/nar/gkf435.

Tompkins, D. H. *et al.* (2009) 'Sox2 Is Required for Maintenance and Differentiation of Bronchiolar Clara, Ciliated, and Goblet Cells', *PLOS ONE*, 4(12), p. e8248. doi: 10.1371/JOURNAL.PONE.0008248.

Tonge, P. D. *et al.* (2014) 'Divergent reprogramming routes lead to alternative stem-cell states', *Nature*, 516(7530), pp. 192–197. doi: 10.1038/nature14047.

Tran, K. A. *et al.* (2019) 'Defining Reprogramming Checkpoints from Single-Cell Analyses of Induced Pluripotency.', *Cell reports*, 27(6), pp. 1726-1741.e5. doi: 10.1016/j.celrep.2019.04.056.

Treede, I. *et al.* (2007) 'Anti-inflammatory effects of phosphatidylcholine.', *The Journal of biological chemistry*, 282(37), pp. 27155–27164. doi: 10.1074/jbc.M704408200.

Trounson, A. and DeWitt, N. D. (2016) 'Pluripotent stem cells progressing to the clinic.', *Nature reviews. Molecular cell biology*, 17(3), pp. 194–200. doi: 10.1038/nrm.2016.10.

Tumino, N. *et al.* (2021) 'Interaction Between MDSC and NK Cells in Solid and Hematological Malignancies: Impact on HSCT', *Frontiers in Immunology*, 12, pp. 1–10. doi: 10.3389/fimmu.2021.638841.

van Tuyn, J. *et al.* (2017) 'Oncogene-Expressing Senescent Melanocytes Up-Regulate MHC Class II, a Candidate Melanoma Suppressor Function.', *The Journal of investigative dermatology*, 137(10), pp. 2197–2207. doi: 10.1016/j.jid.2017.05.030.

Ubil, E. *et al.* (2014) 'Mesenchymal-endothelial transition contributes to cardiac neovascularization.', *Nature*, 514(7524), pp. 585–590. doi: 10.1038/nature13839.

Ulmer, J. B., Donnelly, J. J. and Liu, M. A. (1994) 'Presentation of an exogenous antigen by major histocompatibility complex class I molecules.', *European journal of immunology*, 24(7), pp. 1590–1596. doi: 10.1002/eji.1830240721.

Utikal, J. *et al.* (2009) 'Immortalization eliminates a roadblock during cellular reprogramming into iPS cells', *Nature*, 460(7259), pp. 1145–1148. doi: 10.1038/nature08285.

Vashi, P. *et al.* (2016) 'Methylmalonic acid and homocysteine as indicators of Vitamin B-

12 deficiency in cancer', *PLoS ONE*, 11(1), pp. 1–13. doi: 10.1371/journal.pone.0147843.

Veglia, F., Perego, M. and Gabrilovich, D. (2018) 'Myeloid-derived suppressor cells coming of age review-article', *Nature Immunology*, 19(2), pp. 108–119. doi: 10.1038/s41590-017-0022-x.

Vicari, A. P. and Zlotnik, A. (1996) 'Mouse NK1.1+ T cells: a new family of T cells.', *Immunology today*, 17(2), pp. 71–76. doi: 10.1016/0167-5699(96)80582-2.

Vierbuchen, T. *et al.* (2010) 'Direct conversion of fibroblasts to functional neurons by defined factors', *Nature*, 463(7284), pp. 1035–1041. doi: 10.1038/NATURE08797.

Viltard, M. *et al.* (2019) 'The metabolomic signature of extreme longevity: naked mole rats versus mice.', *Aging*, 11(14), pp. 4783–4800. doi: 10.18632/aging.102116.

Vivier, E. *et al.* (2011) 'Innate or adaptive immunity? The example of natural killer cells.', *Science*, 331(6013), pp. 44–49. doi: 10.1126/science.1198687.

Vivier, E. *et al.* (2018) 'Innate Lymphoid Cells: 10 Years On.', *Cell*, 174(5), pp. 1054–1066. doi: 10.1016/j.cell.2018.07.017.

Waddington, C. H. (1957) 'The strategy of the genes: A discussion of some aspects of theoretical biology', *The Strategy of the Genes: A Discussion of Some Aspects of Theoretical Biology*, pp. 1–262.

Wahl, G. M. and Spike, B. T. (2017) 'Cell state plasticity, stem cells, EMT, and the generation of intra-tumoral heterogeneity', *Breast Cancer*, 3(1), pp. 1–12. doi: 10.1038/s41523-017-0012-z.

Walker, A. E. (2018) 'The Adult Pancreas in Trauma and Disease', *Academic Forensic Pathology*, 8(2), pp. 192–218. doi: 10.1177/1925362118781612.

Walzer, T. *et al.* (2007) 'Identification, activation, and selective in vivo ablation of mouse NK cells via NKp46.', *Proceedings of the National Academy of Sciences of the United States of America*, 104(9), pp. 3384–3389. doi: 10.1073/pnas.0609692104.

Wang, G. *et al.* (2013) 'Critical regulation of miR-200/ZEB2 pathway in Oct4/Sox2-induced mesenchymal-to-epithelial transition and induced pluripotent stem cell generation.', *Proceedings of the National Academy of Sciences of the United States of America*, 110(8), pp. 2858–2863. doi: 10.1073/pnas.1212769110.

Wang, H. *et al.* (2016) 'RNF216 contributes to proliferation and migration of colorectal cancer via suppressing BECN1-dependent autophagy.', *Oncotarget*, 7(32), pp. 51174–51183. doi: 10.18632/oncotarget.9433.

Wang, J. *et al.* (2009) 'Dependence of mouse embryonic stem cells on threonine

catabolism.', *Science*, 325(5939), pp. 435–439. doi: 10.1126/science.1173288.

Wang, J. *et al.* (2019) 'Core gut bacteria analysis of healthy mice', *Frontiers in Microbiology*, 10, pp. 1–14. doi: 10.3389/fmicb.2019.00887.

Wang, T. *et al.* (2011) 'The histone demethylases Jhdm1a/1b enhance somatic cell reprogramming in a vitamin-C-dependent manner', *Cell Stem Cell*, 9(6), pp. 575–587. doi: 10.1016/j.stem.2011.10.005.

Wang, W. *et al.* (2015) 'NK cell-mediated antibody-dependent cellular cytotoxicity in cancer immunotherapy', *Frontiers in Immunology*, 6. doi: 10.3389/fimmu.2015.00368.

Wang, X. (2019) 'Stem cells in tissues, organoids, and cancers', *Cellular and Molecular Life Sciences*, 76(20), pp. 4043–4070. doi: 10.1007/s00018-019-03199-x.

Wang, Z. *et al.* (2019) 'Methionine is a metabolic dependency of tumor-initiating cells.', *Nature medicine*, 25(5), pp. 825–837. doi: 10.1038/s41591-019-0423-5.

Watanabe, H. *et al.* (2005) 'Aging is associated with decreased pancreatic acinar cell regeneration and phosphatidylinositol 3-kinase/Akt activation.', *Gastroenterology*, 128(5), pp. 1391–1404. doi: 10.1053/j.gastro.2005.03.016.

Westphalen, C. B. *et al.* (2016) 'Dclk1 defines quiescent pancreatic progenitors that promote injury-induced regeneration and tumorigenesis', *Cell Stem Cell*, 18(4), pp. 441–455. doi: 10.1016/j.stem.2016.03.016.Dclk1.

Whitcomb, D. C. and Lowe, M. E. (2007) 'Human pancreatic digestive enzymes.', *Digestive diseases and sciences*, 52(1), pp. 1–17. doi: 10.1007/s10620-006-9589-z.

Wollny, D. *et al.* (2016) 'Single-Cell Analysis Uncovers Clonal Acinar Cell Heterogeneity in the Adult Pancreas', *Developmental Cell*, 39(3), pp. 289–301. doi: 10.1016/j.devcel.2016.10.002.

Worringer, K. A. *et al.* (2014) 'let-7/LIN41 pathway regulates reprogramming to hiPSCs-CSC2013.pdf', *Cell Stem Cell*, 14(1), pp. 40–52. doi: 10.1016/j.stem.2013.11.001.The.

Wu, X. *et al.* (2021) 'NKG2D Engagement Alone Is Sufficient to Activate Cytokine-Induced Killer Cells While 2B4 Only Provides Limited Coactivation', *Frontiers in Immunology*, 12(October), pp. 1–12. doi: 10.3389/fimmu.2021.731767.

Xie, H. *et al.* (2004) 'Stepwise reprogramming of B cells into macrophages', *Cell*, 117(5), pp. 663–676. doi: 10.1016/S0092-8674(04)00419-2.

Xue, W. *et al.* (2007) 'Senescence and tumour clearance is triggered by p53 restoration in murine liver carcinomas.', *Nature*, 445(7128), pp. 656–660. doi: 10.1038/nature05529.

Yamanaka, Y. *et al.* (2006) 'Cell and molecular regulation of the mouse blastocyst', *Developmental Dynamics*, 235(9), pp. 2301–2314. doi: 10.1002/dvdy.20844.

Yanger, K. *et al.* (2013) 'Robust cellular reprogramming occurs spontaneously during liver regeneration', *Genes and Development*, 27(7), pp. 719–724. doi: 10.1101/gad.207803.112.

Yewdell, J. W. and Hollý, J. (2020) 'DRiPs get molecular.', *Current opinion in immunology*, 64, pp. 130–136. doi: 10.1016/j.coi.2020.05.009.

Yilmazer, A. *et al.* (2013) 'In Vivo Cell Reprogramming towards Pluripotency by Virus-Free Overexpression of Defined Factors', *PLoS ONE*, 8(1). doi: 10.1371/journal.pone.0054754.

Yin, Y. *et al.* (2019) 'The FBXW2–MSX2–SOX2 axis regulates stem cell property and drug resistance of cancer cells', *Proceedings of the National Academy of Sciences of the United States of America*, 116(41), pp. 20528–20538. doi: 10.1073/pnas.1905973116.

Yokoyama, W. M. and Plougastel, B. F. M. (2003) 'Immune functions encoded by the natural killer gene complex.', *Nature reviews. Immunology*, 3(4), pp. 304–316. doi: 10.1038/nri1055.

Yoneda, O. *et al.* (2000) 'Fractalkine-mediated endothelial cell injury by NK cells.', *Journal of immunology (Baltimore, Md.: 1950)*, 164(8), pp. 4055–4062. doi: 10.4049/jimmunol.164.8.4055.

Yoon, H. *et al.* (2005) 'Krüppel-like factor 4 prevents centrosome amplification following gamma-irradiation-induced DNA damage', *Oncogene*, 24(25), pp. 4017–4025. doi: 10.1038/SJ.ONC.1208576.

Yoon, H. and Yang, V. (2004) 'Requirement of Krüppel-like factor 4 in preventing entry into mitosis following DNA damage', *The Journal of biological chemistry*, 279(6), pp. 5035–5041. doi: 10.1074/JBC.M307631200.

Yoshida, T. *et al.* (2010) 'Smooth and cardiac muscle-selective knock-out of Kruppel-like factor 4 causes postnatal death and growth retardation', *The Journal of biological chemistry*, 285(27), pp. 21175–21184. doi: 10.1074/JBC.M110.112482.

Young, M. D. and Behjati, S. (2020) 'SoupX removes ambient RNA contamination from droplet-based single-cell RNA sequencing data', *GigaScience*, 9(12), pp. 1–10. doi: 10.1093/gigascience/giaa151.

Yu, S. *et al.* (2020) 'GBP2 enhances glioblastoma invasion through Stat3/fibronectin pathway.', *Oncogene*, 39(27), pp. 5042–5055. doi: 10.1038/s41388-020-1348-7.

Zalfa, C. and Paust, S. (2021) 'Natural Killer Cell Interactions With Myeloid Derived Suppressor Cells in the Tumor Microenvironment and Implications for Cancer Immunotherapy', *Frontiers in Immunology*, 12(May). doi: 10.3389/fimmu.2021.633205.

Zanker, D. J. *et al.* (2019) 'Influenza A Virus Infection Induces Viral and Cellular Defective Ribosomal Products Encoded by Alternative Reading Frames.', *Journal of Immunology*, 202(12), pp. 3370–3380. doi: 10.4049/jimmunol.1900070.

Zappia, L. and Oshlack, A. (2018) 'Clustering trees: a visualization for evaluating clusterings at multiple resolutions', *GigaScience*, 7(7), pp. 1–9. doi: 10.1093/gigascience/giy083.

Zarling, A. L. *et al.* (2000) 'Phosphorylated peptides are naturally processed and presented by major histocompatibility complex class I molecules in vivo.', *The Journal of experimental medicine*, 192(12), pp. 1755–1762. doi: 10.1084/jem.192.12.1755.

Zeromski, J. *et al.* (2011) 'NK cells prevalence, subsets and function in viral hepatitis C.', *Archivum immunologiae et therapiae experimentalis*, 59(6), pp. 449–455. doi: 10.1007/s00005-011-0145-y.

Zhang, C. *et al.* (2005) 'Opposing effect of IFNgamma and IFNalpha on expression of NKG2 receptors: negative regulation of IFNgamma on NK cells.', *International immunopharmacology*, 5(6), pp. 1057–1067. doi: 10.1016/j.intimp.2005.02.003.

Zhang, C. *et al.* (2019) 'NKG2A is a NK cell exhaustion checkpoint for HCV persistence', *Nature Communications*, 10(1). doi: 10.1038/s41467-019-09212-y.

Zhang, P. *et al.* (2010) 'Kruppel-like Factor 4 (Klf4) Prevents Embryonic Stem (ES) Cell Differentiation by Regulating Nanog Gene Expression', *Journal of Biological Chemistry*, 285(12), pp. 9180–9189. doi: 10.1074/JBC.M109.077958.

Zhang, Y. and Huang, B. (2017) 'The Development and Diversity of ILCs, NK Cells and Their Relevance in Health and Diseases.', *Advances in experimental medicine and biology*, 1024, pp. 225–244. doi: 10.1007/978-981-10-5987-2_11.

Zhao, Y. *et al.* (2015) 'A XEN-like State Bridges Somatic Cells to Pluripotency during Chemical Reprogramming', *Cell*, 163(7), pp. 1678–1691. doi: 10.1016/j.cell.2015.11.017.

Zhao, Yang *et al.* (2008) 'Two Supporting Factors Greatly Improve the Efficiency of Human iPSC Generation', *Cell Stem Cell*, 3(5), pp. 475–479. doi: 10.1016/j.stem.2008.10.002.

Zheng, L. *et al.* (2013) 'Role of immune cells and immune-based therapies in pancreatitis and pancreatic ductal adenocarcinoma.', *Gastroenterology*, 144(6), pp. 1230–1240.

doi: 10.1053/j.gastro.2012.12.042.

Zhongwei, L. *et al.* (2012) 'BMP4 Signaling Acts via Dual-Specificity Phosphatase 9 to Control ERK Activity in Mouse Embryonic Stem Cells', *Cell Stem Cell*, 10(2), pp. 171–182. doi: 10.1016/J.STEM.2011.12.016.

Zhou, Q. *et al.* (2008) 'In vivo reprogramming of adult pancreatic exocrine cells to beta-cells', *Nature*, 455(7213), pp. 627–632. doi: 10.1038/NATURE07314.

Zhou, Z. *et al.* (2020) 'Granzyme A from cytotoxic lymphocytes cleaves GSDMB to trigger pyroptosis in target cells', *Science*, 368(6494). doi: 10.1126/science.aaz7548.

Zikmund, T. *et al.* (2019) 'ISWI ATPase Smarca5 Regulates Differentiation of Thymocytes Undergoing β-Selection.', *Journal of immunology (Baltimore, Md. : 1950)*, 202(12), pp. 3434–3446. doi: 10.4049/jimmunol.1801684.

Zincarelli, C. *et al.* (2008) 'Analysis of AAV serotypes 1-9 mediated gene expression and tropism in mice after systemic injection', *Molecular Therapy*, 16(6), pp. 1073–1080. doi: 10.1038/mt.2008.76.

Manuscripts directly related to this PhD Thesis:

Under revision:

1- **Natural killer cells are an extrinsic barrier for *in vivo* reprogramming**

Elena Melendez, Dafni Chondronasiou, Lluc Mosteiro, Jaime Martínez de Villarreal, Cian Lynch, Dirk Grimm, Francisco X. Real, José Alcamí, Núria Climent, Federico Pietrocola, Manuel Serrano

In preparation:

1- **Vitamin B12 is a limiting metabolite for *in vivo* reprogramming**

Marta Kovatcheva, Elena Melendez, Dafni Chondronasiou, Federico Pietrocola, Raquel Bernad, Adria Caballe, Alexandra Junza, Camille Stephan- Otto Attolini, Neus Prats, Sylvere Durand, Oscar Yanes, Guido Kroemer, Manuel Serrano

2- **Deciphering *in vivo* reprogramming using single cell transcriptomics**

Dafni Chondronasiu, Jaime Martínez, Elena Melendez, Natalia del Pozo, Miguel Lafarga, Neus Prats, Franisco X. Real, Manuel Serrano

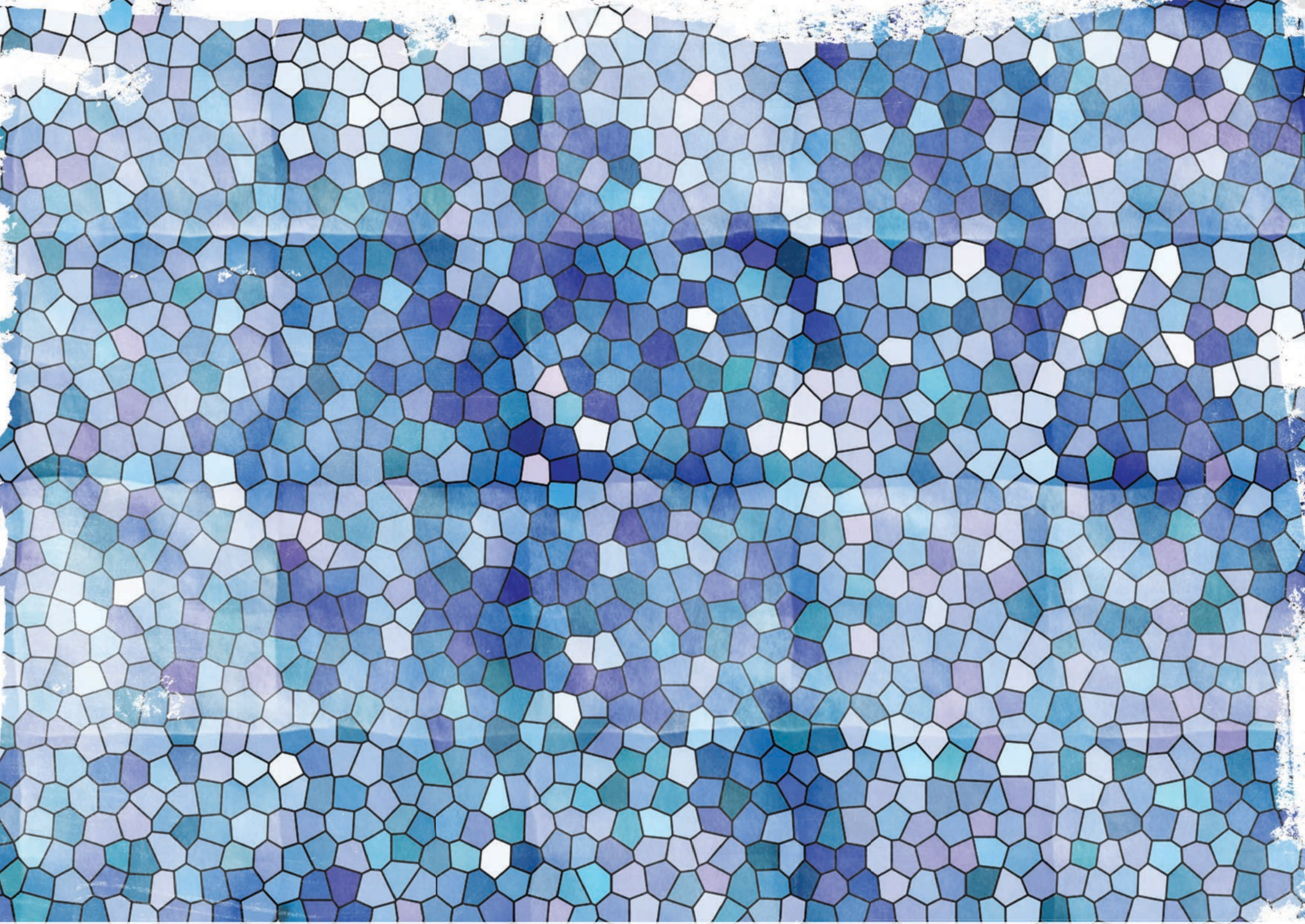

ELENA MELÉNDEZ ESTEBAN

2022

DOCTORAL THESIS